Polycomb-like 2 (Mtf2/Pcl2) is required for epigenetic regulation of hematopoiesis

Janet L. Manias Rothberg

This thesis is submitted to the Faculty of Graduate and Postdoctoral Studies as a partial fulfillment of the Ph.D. program in Cellular & Molecular Medicine.

Department of Cellular and Molecular Medicine
Faculty of Medicine
University of Ottawa
Ottawa, Ontario
Canada

Abstract

Polycomb proteins are epigenetic regulators that are critical in mediating gene repression at critical stages during development. Core and accessory proteins make up the Polycomb Repressive Complex 2 (PRC2), which is responsible for trimethylation of lysine 27 on histone 3 (H3K27me3), leading to maintenance of chromatin compaction and sustained gene repression. Classically, Polycomb accessory proteins are often thought of as having minor roles in fine-tuning the repressive action of PRC2. Their actions have often been attributed to chromatin recognition, targeting to specific loci and enhancing methyltransferase activity. In our previous work in mouse embryonic stem cells (ESCs), we showed that Polycomb-like 2 (Mtf2/Pcl2) is critical for PRC2-mediated regulation of stem cell self-renewal through feed-forward control of the pluripotency network. In moving beyond the ESC model system, we sought to interrogate the role of Mtf2 in vivo by creating a gene-targeted knockout mouse model. Surprisingly, we discovered a tissue-specific role for Mtf2 in controlling erythroid maturation and hematopoietic stem cell self-renewal. Via its regulation of other PRC2 members, Mtf2 is critical for global H3K27me3 methylation at promoter-proximal sites in developing erythroblasts. Thus, Mtf2 is required for proper maturation of erythroblasts. Loss of Mtf2 also reduces HSC self-renewal leading to stem cell pool exhaustion. Additionally, misregulation of Mtf2 in leukemia models contributes to massive leukemic blast expansion at the expense of leukemic stem cell self-renewal. In the developing hematopoietic system, Mtf2 functions as a core complex member, controlling epigenetic regulation of self-renewal and maturation of both stem and committed cells.

Authorization

Images originally published in “PCL2 modulates gene regulatory networks controlling self-renewal and commitment in embryonic stem cells” by Walker E, Manias JL, Chang WY and Stanford WL (Cell Cycle 2011 Jan; 10(1): 45-51) and are reprinted here with kind permission of Taylor and Francis Publishing under the Creative Commons Attribution License.

Table of Contents

Abstract		ii
Authorization		iii
List of Tables		viiI
List of Figures		ix
List of Abbreviations		xi
Acknowledgements		xiv
Chapter 1 – Introduction		**1**
1.1	Epigenetic regulation of stem cell fate decisions	2
1.2	Polycomb Proteins as Transcriptional Repressors	3
	1.2.1 Polycomb Repressive Complexes 1 & 2	4
	1.2.2 Targeting Polycomb proteins to genetic loci	7
	1.2.2.1 Polycomb Response Elements	7
1.3	PRC2 accessory proteins	8
	1.3.1 AEBP2	9
	1.3.2 JARID2	11
	1.3.3 Polycomblike proteins	11
1.4	Targeting of Accessory proteins to DNA	14
1.5	The role of Mtf2 in embryonic stem cells	15
1.6	The role of Mtf2 *in vivo*	18
1.7	Mammalian hematopoiesis	18
	1.7.1 Mammalian erythropoiesis	22
1.8	Cell Cycle and Hematopoiesis	25
1.9	Polycomb proteins in hematopoietic development and disease	26
	1.9.1 PRC1 and hematopoietic development	26
	1.9.2 PRC2 and hematopoietic development	27
	1.9.3 The role of PcG proteins in cancer	28
1.10	Leukemia	29
	1.10.1 Acute Myeloid Leukemia	29

1.10.2 Chronic Myeloid Leukemia 30
1.10.3 Pre-leukemic events 31
1.10.4 Modeling leukemia using the Friend Virus as a two-stage model of leukemia 31
1.11 Approaches to uncovering function of novel proteins 35
1.11.1 Using gene regulatory networks to interrogate function of novel proteins 35
1.11.2 A reductionist approach to discovering gene function 37
1.12 Rationale and Approach 38
1.13 Hypothesis and Aims 39
1.13.1 Overarching hypothesis 39
1.13.2 Specific Aims 39

Chapter 2 –
Mtf2/Pcl2 controls PRC2-mediated epigenetic regulation of hematopoiesis 40
Author Contributions 41
Abstract 43
Introduction 44
Results 47
Mtf2 null mice die in utero from a block in definitive erythropoiesis 47
Mtf2 is necessary for erythroid maturation in a cell-intrinsic manner 51
Mtf2 is required for HSC self-renewal 57
Mtf2 regulates core PRC2 members in the hematopoietic system 60
Mtf2 regulates promoter-proximal H3K27me3 in erythroblasts 64
Mtf2 controls gene regulatory networks critical for hematopoietic function 66
Reduced expression of Mtf2 contributes to blast expansion in a model of erythroleukemia 73

Discussion 76
Materials and Methods 84
Generation of Mice and Embryonic Analysis 84
Flow Cytometry 85
Capillary Electrophoresis Immunodetection 86
Lentiviral production of Mtf2 shRNA 87
Lentiviral-mediated Mtf2 knockdown of mouse bone marrow cells 87
RNA-seq and ChIP-seq 88
Bone Marrow Transplants and Analysis 90
Friend Virus 90
Statistics 91
Study Approval 91
Acknowledgements 92
List of Supplementary Tables 101

Chapter 3 - Discussion and Future Directions 102
3.1 Thesis Summary and Major Findings 103
3.2 Studying Mtf2 in a constitutive gene-targeted mouse model 104
3.3 The changing role of Polycomb accessory proteins 106
3.4 Using a systems biology approach to define the role of Mtf2 in development 109
3.5 Implications for normal hematopoietic stem-cell development 111
3.6 The role of Mtf2 in hematological diseases 112
3.7 Future studies 114
3.7.1 Mtf2 regulating cell cycle control in HSCs 115
3.7.2 Identifying the role of Mtf2 in disease to improve diagnosis and therapies 120
3.8 Conclusions 122

References **124**

Appendix A. Additional data, methods and results 153

Appendix B. Janet Rothberg CV 159

List of Tables

Table S1. Genes that lose H3K27me3 in Mtf2 null erythroblasts 158

Table S2. Genes contained in the Mtf2-PRC2 gene regulatory network 99

Table S3. Gene expression changes during erythroblast differentiation 99

Table S4. Hematological measurements in wild-type and *Mtf2*$^{+/-}$ mice 99

Table S5. Primers used for genotyping, qPCR and ChIP-qPCR analysis 99

List of Figures

Figure 1.1	Polycomb-mediated gene repression	6
Figure 1.2	Core and accessory proteins function together as the Polycomb Repressive Complex 2	10
Figure 1.3	Comparison of various isoforms of Mtf2	13
Figure 1.4	MTF2-PRC2-JARID2 gene regulatory network during early differentiation	17
Figure 1.5	Hierarchical structure of mammalian hematopoiesis	21
Figure 1.6	Expression of key regulators of erythropoiesis	24
Figure 1.7	A schematic of the two-stage model of leukemia using the Friend Erythroleukemia virus	34
Figure 1.8	Integration of systems level data to create gene regulatory networks	36
Figure 1.9	Flow chart of project integration	39
Figure 2.1	*Mtf2*$^{-/-}$ die at e15.5 due to severe anemia	49
Figure 2.2	Mtf2 is required for normal erythroid differentiation	52
Figure 2.3	Mtf2 deficiency causes a cell-intrinsic erythroid differentiation defect	55
Figure 2.4	Mtf2 is required for self-renewal of HSCs	59
Figure 2.5	Mtf2 regulates core PRC2 protein levels and promoter-proximal H3K27me3 in erythroblasts	62
Figure 2.6	Mtf2-PRC2 hematopoietic gene regulatory networks regulate erythroid maturation and HSC self-renewal	69
Figure 2.7	Misregulation of Mtf2 alters the progression of erythroleukemia	75
Figure 2.8	A model of Mtf2-PRC2 in hematopoiesis.	77
Fig S2.1	Mtf2 expression in the mouse hematopoietic system	93
Fig S2.2	Morphology of wild-type and *Mtf2*$^{-/-}$ fetal liver and peripheral	

	blood erythroblasts	94
Fig S2.3	Knockdown of Mtf2 in adult lineage-depleted mouse bone marrow also reduces core PRC2 proteins and methylation levels	95 96
Fig S2.4	H3K27me3 binding in wild-type erythroblasts correlates well with publicly available data	97
Fig S2.5	Genes associated with Mtf2 binding in erythroid cells show little overlap with Mtf2 and PRC2 targets in ESCs	98
Fig S2.6	A Mtf2-PRC2 GRN controls chromatin modifiers and cell cycle regulators during erythroid differentiation	99
Fig S2.7	*Mtf2*$^{+/-}$ mice have normal recovery kinetics after induction of cytopenia	100
Figure A1	Reduced Mtf2 levels in other models of leukemia also leads to progenitor cell expansion	153
Figure A2	Isolated single *Mtf2*$^{+/-}$ HSCs have a reduced time to 1st cell division compared to wild-type LT-HSCs	154
Figure A3	Overexpression of p57 can partially rescue the erythroid differentiation defect seen in *Mtf2*$^{-/-}$ erythroblasts	155
Figure A4	Genes without promoter-proximal H3K27me3 marks in Mtf2-deficient erythroblasts are related to the DNA damage and repair pathways	156

List of Abbreviations

5FU	5-fluorouracil
AGM	aorta-gonadal-mesonephros
AML	acute myeloid leukemia
BasoE	basophilic erythroblast
BFU-E	burst forming-unit, erythroid
BM	bone marrow
CFSE	carboxyfluorescein diacetate succinimidyl ester
CDKs	cyclin-dependent kinases
CFU	colony forming unit
CFU-E	colony forming unit-erythroid
CFU-G	colony forming unit-granulocyte
CFU-GEMM	colony forming unit-granulocyte, erythrocyte, macrophage, megakaryocyte
CFU-GM	colony forming unit-granulocyte, macrophage
CFU-M	colony forming unit-macrophage
ChIP	chromatin immunoprecipitation
CKIs	cyclin-dependent kinase inhibitors
CLP	common lymphoid progenitor
CML	chronic myeloid leukemia
CMP	common myeloid progenitor
Epo	erythropoietin
EryA	BM-derived basophilic erythroblast
EryB	BM-derived polychromatic erythroblast
EryC	BM-derived orthochromatic erythroblasts
EryD	definitive erythrocytes
EryP	primitive erythrocytes
ESC	embryonic stem cell
FL	fetal liver

F-MuLV	Friend murine leukemia virus
FV	Friend Virus
GMP	granulocyte-macrophage progenitor
GRN	gene regulatory network
GO	gene ontology
H2AK119ub1	ubiquitination on lysine 119 of histone 2A
H3K27me3	trimethylation on lysine 27 of histone 3
H3K36me3	trimethylation on lysine 36 of histone 3
HMTase	histone methyltransferase
Hox	homeotic
HSC	hematopoietic stem cell
HSPCs	hematopoietic stem and progenitor cells
LSC	leukemic stem cell
LSK	lineage$^-$Sca1$^+$cKit$^+$
LT-HSC	long-term repopulating hematopoietic stem cell (LSK CD48$^-$CD150$^+$)
mESCs	mouse embryonic stem cells
MEP	megakaryocyte-erythroid progenitor
MLL	mixed lineage leukemia gene
Mtf2/Pcl2	Polycomb-like 2
OrthoE	orthophilic erythroblast
PcG	Polycomb protein
Pcl	Polycomblike
PHD	plant homeodomain
PolyE	polychromatophilic erythroblast
PRC1	Polycomb Repressive Complex 1
PRC2	Polycomb Repressive Complex 2
PRE	Polycomb Response Element
ProE	pro-erythroblast
RBC	red blood cell

SSPV-P	spleen focus forming virus, polycythemia (SFFV-P)
ST-HSC	short-term repopulating hematopoietic stem cell (LSK $CD48^{-}CD150^{-}$)
TFs	transcription factors
TSS	transcriptional start site
YS	yolk sac

Acknowledgements

I would not be who I am today without the contribution of so many important people in my life.

First, a heartfelt thank you to my supervisors Dr. Bill Stanford and Dr. Caryn Ito. From the beginning, Bill took me under his wing and helped me develop as an independent scientist. Together Bill and Caryn have always welcomed me with open arms and have taught me many lessons about what it means to be a great scientist, mentor and manager. Thank you also for their support in allowing me to pursue interests outside of bench work – while this may have occasionally taken me away from the lab, the opportunities provided and the skills I have learned have help me become a better scientist.

Thank you to all our collaborators who made progress on this project possible. I would like to thank all of our collaborators at the Ottawa Hospital Research Institute including members of the Stem Core Facility, the Flow Cytometry Facility and the Ottawa Bioinformatics Core Facility without whom this work would not be possible. Special thanks also to the staff at the University of Ottawa Animal Care and Veterinary Services whose collective knowledge helps our research advance by leaps and bounds. Thank you to my advisory committee members Dr. David Allan, Dr. Marjorie Brand and Dr. Rashmi Kothary for their insightful discussions, helpful advice and constant support on the project. Thank you to my thesis advisory panel for taking the time to evaluate this thesis and participate in the defense examination. A grateful thank you for the financial support of the OHRI, the University of Ottawa and scholarships through the

Ontario Graduate Scholarship program and the Canadian Institute for Health Research who made it possible to complete the work presented herein.

To the members of the Stanford lab, past and present: I have had the luck and pleasure to be able to work with not one, but many amazing groups of people. My short time at the University of Toronto created bonds with fellow trainees (SK, PC, DL and JK) that have withstood time and distance. Establishment of the lab at the OHRI, literally from the unpacking of the first boxes, helped forge a unique group of misfits that can blend science and fun. Together, we have shared countless stories and experiences inside and outside of the lab. Thanks to Hari and Hani for their continued work on the project. Special thanks to the SK, ZC, LJ, RC, SD and CD - both physically and mentally, you have been my home away from home, and instrumental in keeping my sanity and a smile on my face.

Last, but never least, an incredible thanks to my parents Louise and Sergio, my grandmother Nina, my in-laws Shelley and Norman, my family (Paul, Sabrina, Brandon, Christina, Giacomo, Matteo and Isabella) and those considered 'practically family', for your love, support and patience. Thanks to Stefanie and Daniel who opened up their home and hotel room with open arms. To my amazing husband Joel – whose unwavering support, love, positive outlook, and realism make each day not only possible, but more enjoyable than the last. Together Team Rothberg- along with a little help from Jinx- will always be unstoppable.

Chapter 1

Introduction

1.1 Epigenetic regulation of stem cell fate decisions

Stem cells are unique cells found both in the embryo and in adult tissue that retain the capability to both self-renew and differentiate into various cell types. Signals from the environment can trigger cell fate decisions and lead to differentiation. Responses to these signals arise from both hard-coded information within the nucleotide structure of DNA within the cell and access to this genetic information. Covalent modifications to DNA that do not compromise the underlying nucleotide sequence, generally termed ‘epigenetics’, can regulate DNA accessibility. A modern definition of epigenetics states that: “An epigenetic trait is a stably heritable phenotype resulting from changes in a chromosome without alterations in the DNA sequence.” (Berger, Kouzarides et al. 2009). Modifications of DNA or histone proteins are examples of inherited epigenetic modifications that can play a major role in stem cell fate decisions. Various lysine residues of multiple histone proteins can be modified via addition of an acetyl group, a ubiquitin molecule or multiple methyl groups. The presence of epigenetic modifications to histone proteins can recruit or antagonize other proteins, resulting in changes in gene expression and, ultimately, cell fate decisions.

1.2 Polycomb Proteins as Transcriptional Repressors

Polycomb group (PcG) proteins are a family of highly conserved transcriptional regulators responsible for depositing epigenetic modifications on histones. Histone modifications controlled by PcG proteins are dynamically regulated during development (Ringrose and Paro 2004, Ringrose and Paro 2007, Christophersen and Helin 2010), as stem cells differentiate into various committed progeny. Histone modifications are also stably maintained in differentiated cells by PcG proteins (first described by (Struhl and Akam 1985)), providing epigenetic memory and preventing spurious differentiation in fully committed cells.

The first Polycomb protein *Pc* was described in *Drosophila melanogaster* (Lewis 1978) as a critical negative regulator of homeotic genes that determine body patterning. Following this discovery, a collection of Polycomb genes were described as transcriptional repressors of homeotic genes, including many described in more detail below. In addition to suppression of homeotic genes, enhancer genes were also identified which promoted the expression of homeotic genes. One of the first genes from this group of genetic activators was the trithorax (*trx*) gene (Ingham 1985), described as a gene required for maintaining appropriate levels of the Antennapedia and bithorax complex proteins, which regulate body segmentation. The antagonistic action of Polycomb and enhancer function of trithorax genes at homeotic targets that was first described in Drosophila (Kennison and Tamkun 1988) is conserved among many species including mammals (Hanson, Hess et al. 1999).

1.2.1 Polycomb Repressive Complexes 1 & 2

PcG proteins belong to one of two main complexes: Polycomb Repressive Complex 1 (PRC1) or Polycomb Repressive Complex 2 (Figure 1.1). Mammalian canonical PRC1 contains a core group of proteins including members of the Cbx, RING, Pcgf and Phc families. In the classic model of action, Cbx recognizes the repressive H3K27me3 mark deposited by PRC2 and RING-domain proteins, such Ring1a/Ring1b, (Satijn and Otte 1999) mono-ubiquitinates lysine 119 on histone 2A (H2AK119ub1), compacting chromatin and further repressing downstream target genes (Wang, Wang et al. 2004). Recent evidence has identified multiple non-canonical PRC1 complexes which lack a Cbx protein but contain a Rybp/Yap2 protein and can deposit the H2AK119ub1 mark independent of PRC2-mediated H3K27me3 recruitment (Leeb, Pasini et al. 2010, Gao, Zhang et al. 2012, Morey, Pascual et al. 2012, Tavares, Dimitrova et al. 2012, Morey, Aloia et al. 2013). PRC1 variants can also recruit PRC2 via deposition of H2AK119ub1 (Blackledge, Farcas et al. 2014). Multiple isoforms of Cbx, Pcgf and Phc proteins, along with other protein interactions, create a structurally diverse group of PRC1 subtypes, each with a unique set of targets and actions.

The Polycomb Repressive Complex 2 (PRC2) contains core proteins Ezh1/2, Suz12, and Eed (Faust, Schumacher et al. 1995, O'Carroll, Erhardt et al. 2001, Kuzmichev, Nishioka et al. 2002, Pasini, Bracken et al. 2004). Ezh1/2 is a SET-containing protein with histone methyltransferase (HMTase) activity that can mono-, di- and tri-methylate histone 3 at lysine 27 (Muller, Hart et al. 2002, Lund and van Lohuizen 2004). These modifications require the binding of Suz12 and Eed, and there has been evidence

for the important role of PRC2 accessory proteins in maintaining these repressive marks at particular loci (Cao, Wang et al. 2002, Czermin, Melfi et al. 2002). Ezh1/2, Suz12 and Eed are present in 1:1:1 ratio (Smits, Jansen et al. 2013) in PRC2 and are necessary and sufficient for HMTase activity. Ezh1 and Ezh2 are mutually exclusive within a complex, but play complementary roles in different tissues (for example, in the hematopoietic system, discussed below). Suz12 is required for complex stability (Cao and Zhang 2004) and knockdown of Suz12 in mouse embryonic stem cells (mESCs) leads to a post-translational loss of Ezh2 and Eed (Pasini, Bracken et al. 2004). PRC2 action also relies on interactions with the histone binding proteins Rbbp4/7, which are not necessary for Ezh2 enzymatic function but likely aid in PRC2 targeting to histones (Nekrasov, Wild et al. 2005, Nowak, Alfieri et al. 2011).

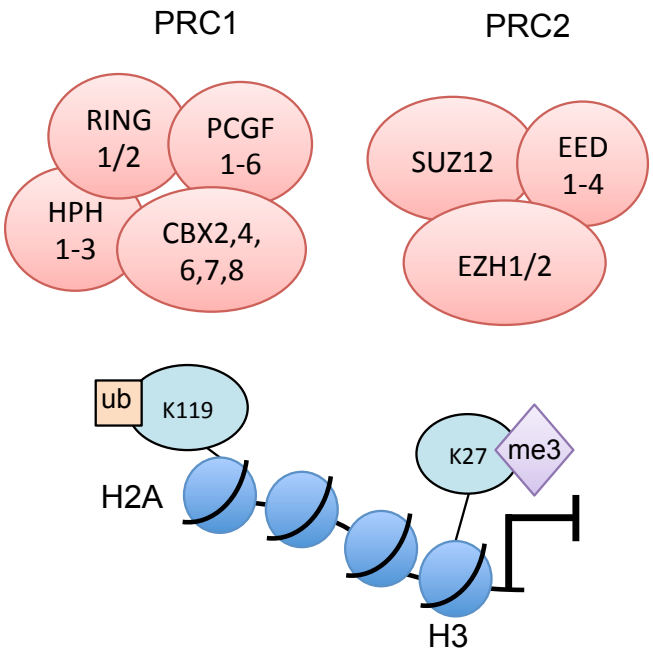

Figure 1.1. Polycomb-mediated gene repression. *Polycomb-mediated gene repression is a result of coordinated actions of Polycomb Repressive Complexes 1 & 2 (PRC1 and PRC2). In a classic model of PRC recruitment to chromatin, PRC2 deposits H3K27me3 marks on compacted chromatin and propagates and spreads the H3K27me3 repressive mark via that action of its enzymatic subunit Ezh1/2. PRC1 is recruited to H3K27me3 marked chromatin where it can mono-ubiquitinate lysine 119 on histone 2A (H2AK119ub1) further enhancing gene repression. Non-canonical PRC1 complexes can also act independently of PRC2.*

1.2.2 Targeting Polycomb proteins to genetic loci

Although first identified as regulating homeotic (Hox) genes, more recent evidence has described the wide-reaching nature of Polycomb proteins. Chromatin-immunoprecipitation combined with microarray (ChIP-chip) or next generation sequencing (ChIP-seq) has been used to identify global targets of various Polycomb proteins in mammalian embryonic stem cells, both human and mouse (Boyer, Plath et al. 2006, Bracken, Dietrich et al. 2006). Genome-wide occupancy studies on core PRC2 proteins have identified many critical transcription factors (TFs) as targets of Polycomb proteins. Genes that are re-expressed as cells differentiate lose PcG occupancy, while others that remain silenced continue to be bound by PcG proteins. PRC2 mediated gene regulation is known to play critical roles in cell differentiation, proliferation, and epigenetic inheritance (Boyer, Plath et al. 2006, Bracken, Dietrich et al. 2006, Surface, Thornton et al. 2010, Margueron and Reinberg 2011, Aloia, Di Stefano et al. 2013).

1.2.2.1 Polycomb Response Elements

In Drosophila, PcG complexes are recruited to specific DNA elements known as Polycomb Repressive Elements (PREs) to silence neighbouring promoters (Fauvarque and Dura 1993, Simon, Chiang et al. 1993). A third PcG complex, PhoRC, exists in Drosophila and contains multiple PcG and trithorax group (TrxG) proteins with DNA binding capabilities. Clustered pairs of DNA-binding consensus motifs for multiple proteins within the PhoRC complex, such as Pleiohomeotic (PHO), GAGA factor (GAF) and Zeste (Z), define invertebrate PREs (Ringrose, Rehmsmeier et al. 2003). The PhoRC

complex along with PRC1 and PRC2 are all recruited to PREs although the precise mechanism of recruitment is still poorly understood.

Many members of the PhoRC complex, including Zeste, GAF and Pipsqueak have no mammalian counterpart, making the existence of PREs in mammals questionable. An ortholog of PHO, Yin Yang 1 (YY1) is found in mammals, but since the PHO-binding sequence alone is not enough to predict a PRE sequence, the lack of consensus sequence for PREs has hindered their identification in mammals. Recently, putative PRE sites have been identified in mice (Sing, Pannell et al. 2009) and humans (Woo, Kharchenko et al. 2010) that contain multiple YY1 binding sites. Although these recent papers open up the possibility that PRE-like domains exist within the mammalian genome and function to recruit PRC1/2, it has also been suggested that a combinatorial action of proteins within the PhoRC complex are necessary for PcG recruitment to PREs and that YY1 alone may not be able to recruit mammalian PcG (Kahn, Stenberg et al. 2014).

1.3 PRC2 accessory proteins

Along with core proteins Ezh1/2, Suz12 and Eed, many studies have identified PRC2 accessory proteins, including members of the Polycomb-like (Pcl) family, Jarid2, Rbbp46/48, Aebp2, esPRC2p48 (Zhang, Jones et al. 2011) and two recently-discovered mammalian proteins, C17orf96 and C10orf12 (Smits, Jansen et al. 2013, Vizan, Beringer et al. 2015) (Figure 1.2). Accessory proteins such as Jarid2 and Mtf2 were thought to be non-essential components of the PRC2. Knockout of core proteins Ezh2, Suz12 and Eed

results in embryonic lethality at early gastrulation stage (Faust, Schumacher et al. 1995, O'Carroll, Erhardt et al. 2001, Pasini, Bracken et al. 2004, Montgomery, Yee et al. 2005). HMTase activity of PRC2 both *in vitro* and *in vivo* requires, at minimum, Suz12, Ezh2 and Eed (Cao, Wang et al. 2002) making them critical components of the PRC2. In contrast, deletion of PRC2 accessory proteins in ESCs allows for complex formation and varying levels of H3K27me3 deposition (discussed in more detail below). Although these proteins are not required for PRC2 function, they have been discovered to associate with PRC2 core proteins by mass spectrometry at sub-stoichiometric ratios and may provide stability to the complex, or have a role in recruitment to target loci.

1.3.1 AEBP2

Aepb2 (Adipocyte Enhancer-Binding Protein 2), a zinc-finger protein, was identified by mass spectrometry in purified HMTase activity-containing complex that also contained Ezh2, Eed, Suz12 and Rbbp4 (Cao, Wang et al. 2002). Using deletion mutants it was shown that AEBP2 associates with Rbbp4 and Suz12 *in vitro* and, while not necessary for PRC2 complex formation or activity, it significantly increases the HMTase activity of the complex (Cao and Zhang 2004). Homozygous deletion of Aebp2 is embryonic lethal and heterozygous gene trap mice display neural crest defects (Kim, Kang et al. 2011). The exact targets of Aebp2 are not known and its role in PRC2-mediated activity *in vivo* is not well understood.

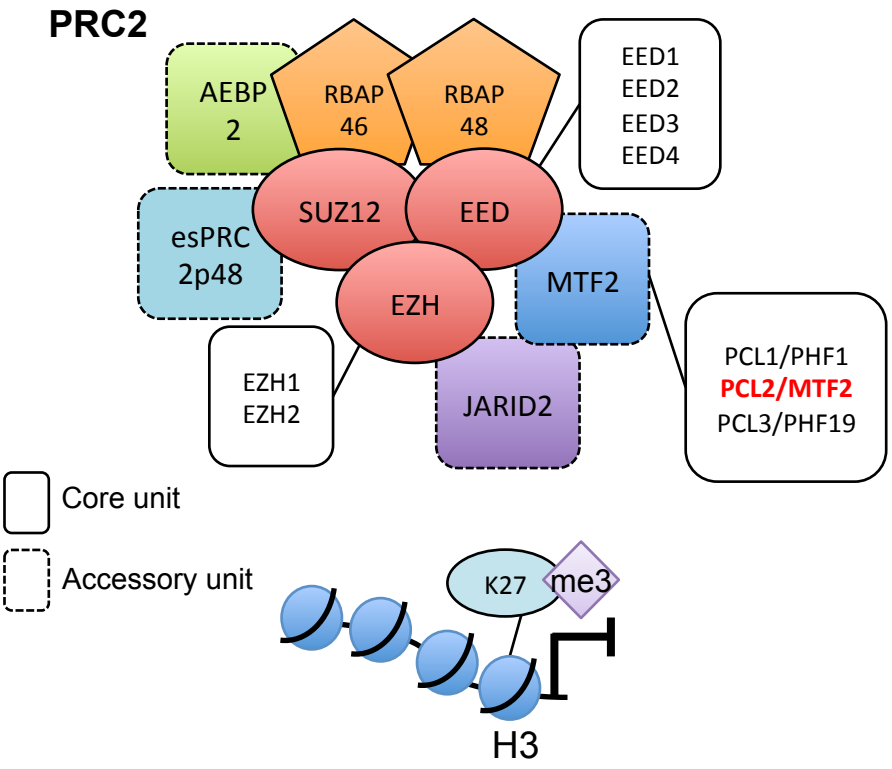

Figure 1.2. Core and accessory proteins function together as the Polycomb Repressive Complex 2. *Core proteins Ezh2, Suz12 and Eed are necessary for PRC2 function. Multiple isoforms of each protein can produce unique PRC2 species that may have unique functions. (Adapted from (Sauvageau and Sauvageau 2010)).*

1.3.2 JARID2

Jarid2 is a well studied PRC2 accessory protein and part of the JUMONJI family of histone demethylases. Jarid2 is not enzymatically active (Klose, Kallin et al. 2006, Shen, Kim et al. 2009) but contains DNA-binding domains which suggest it may have a role in PRC2 targeting and recruitment. Studies on Jarid2 function in ESCs provided evidence that Jarid2 is necessary for ESCs differentiation and that depletion of Jarid2 reduces PRC2 binding at target sites (Peng, Valouev et al. 2009, Shen, Kim et al. 2009, Landeira, Sauer et al. 2010, Li, Margueron et al. 2010, Pasini, Cloos et al. 2010). Beyond its role in ESCs, Jarid2 has also been implicated in muscle cell (Londhe and Davie 2013) and epidermal cell differentiation (Mejetta, Morey et al. 2011). Conflicting evidence has been unable to resolve whether Jarid2 inhibits (Peng, Valouev et al. 2009, Shen, Kim et al. 2009) or enhances (Li, Margueron et al. 2010, Pasini, Cloos et al. 2010) PRC2-mediated HMTase activity. Also, Jarid2 appears to be contained in PRC2 complexes devoid of Polycomblike accessory proteins and Jarid2 and Polycomblike may be mutally exclusive (Peng, Valouev et al. 2009, Landeira, Sauer et al. 2010, Li, Margueron et al. 2010), many aspects regarding the role of Jarid2 in cell differentiation and the mechanism of Jarid-dependent targeting of PRC2 still remain unanswered.

1.3.3 Polycomblike proteins

Polycomblike (*pcl*) was identified in a mutant genetic screen in Drosophila, based on its mutant phenotype similarity to Polycomb (*pc*) mutants (Duncan 1982). Like Polycomb, *Pcl* is a transcriptional repressor also involved in controlling body patterning

in flies (Duncan 1982), and it is required for recruitment and optimal HMTase activity of Enhancer of zeste, E(z) (Nekrasov, Klymenko et al. 2007, Savla, Benes et al. 2008). Polycomblike proteins all contain TUDOR domains and DNA-binding domains, and are potential candidates for recruitment of PRC2 to target sites. There are three mammalian homologs of *pcl*: Phf1 (also known as Pcl1), Phf19 (also known as Pcl3), and Mtf2 (also known as Pcl2).

Phf1 is a PRC2-accessory protein that occupies the same targets as PRC2 core components, including Hox genes. Depletion of Phf1 reduces PRC2 occupancy and it was reported that Phf1 modulates HMTase activity of PRC2 (Cao, Wang et al. 2008, Sarma, Margueron et al. 2008). Recently, Phf1 has been implicated in stabilizing p53 and promoting cell quiescence, via a chromatin-independent function (Brien, Healy et al. 2015). Further study will be necessary to interrogate the PRC2-dependent and independent roles of Phf1 in development and disease.

Phf19 was identified in humans as a PRC2 accessory protein, associating in PRC2 complexes that lack Jarid2. Genome-wide binding of Phf19 matches PRC2-binding profiles and reduction in Phf19 reduces Suz12 and H3K27me3 binding (Boulay, Rosnoblet et al. 2011, Hunkapiller, Shen et al. 2012). Overexpression of various isoforms of Phf19 has been found in human cancers (Wang, Robertson et al. 2004) and Phf19 has been linked to regulation of growth in cancer cell lines (Ghislin, Deshayes et al. 2012).

Three isoforms of Mtf2 exist, each containing two plant homeodomain (PHD) zinc finger-binding domains, which suggest its role in PRC2 targeting. The two longer forms also include a TUDOR domain, which can interact with trimethylated lysines

(Friberg, Oddone et al. 2010) (Figure 1.3). Mtf2 functions, in part, by targeting the PRC2 complex to particular loci via its DNA-binding domains and it was shown that the second PHD domain is necessary for targeting to particular loci, including Xist (Casanova, Preissner et al. 2011). Reduction in Mtf2 in mESCs does not affect global levels of H3K27me3, but levels are reduced at a subset of targets (Walker, Chang et al. 2010).

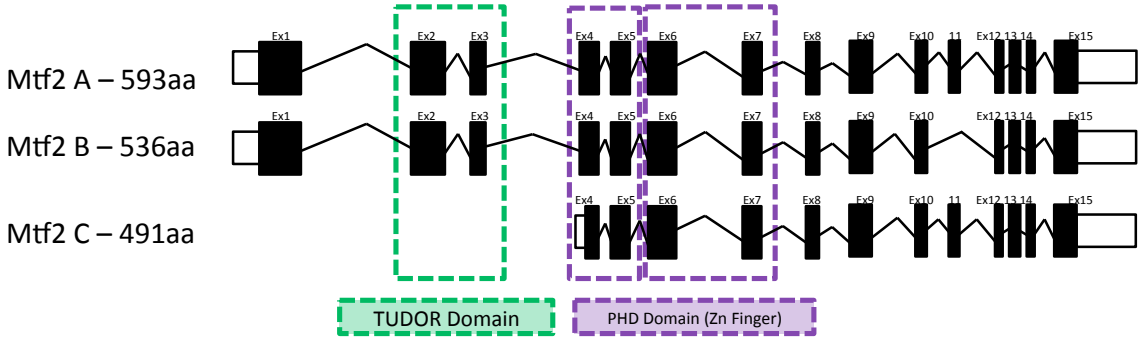

Figure 1.3 Comparison of various isoforms of Mtf2. *Mtf2 is produced as three different isoforms, including a truncated version lacking a TUDOR domain and a version with an alternative splice of exon 11. Two zinc finger (PHD) domains may provide DNA-binding capabilities. Figure adopted from {Walker, 2011 #1001}.*

1.4 Targeting of Accessory proteins to DNA

PRC2 accessory proteins such as Jarid2 and Phf1/Mtf2/Phf19 contain DNA-binding domains and many groups have interrogated genome-wide binding profiles from these proteins to identify a consensus-binding motif. ChIP-sequencing data from Phf19/Pcl3 binding in mESCs failed to identify a consensus sequence, revealing that Phf19/Pcl3 binding is focused at CpG-rich regions (Hunkapiller, Shen et al. 2012). This binding preference is similar to that of Jarid2 (Peng, Valouev et al. 2009, Landeira, Sauer et al. 2010, Li, Margueron et al. 2010) and other PRC2 proteins (Ku, Koche et al. 2008). A lack of specific-sequencing binding of PRC2 accessory proteins and failure to identify widespread mammalian PREs illustrate the difficulty in determining how PRC2 recruitment to target loci in mammals occurs.

Polycomblike proteins may also have a unique role in recruitment of PRC2. The aromatic ring formed by the TUDOR domain in Phf1 and Phf19 proteins binds with high affinity to H3K36me3 (Cai, Rothbart et al. 2013), a mark laid down by TrxG proteins at active chromatin. This interaction is critical for deposition and spreading of PRC2-mediated H3K27me3 into active areas marked by H3K36me3 (Musselman, Avvakumov et al. 2012, Ballare, Castellano et al. 2013, Cai, Rothbart et al. 2013).

While targets of the PRC2 complex have been identified using chromatin immunoprecipitation (ChIP) studies (Ku, Koche et al. 2008), core PRC2 proteins do not have DNA-binding capability and the mechanism for recruitment of PRC2 proteins to target loci remains unknown. PRC2 accessory proteins Jarid2 and members of the Pcl family contain DNA-binding domains (Kim, Kraus et al. 2003, Walker, Ohishi et al. 2007)

and are likely candidates for this role. Analysis of our *Mtf2* knockdown mESCs showed that while global levels of H3K27me3 are maintained, there is a significant decrease in that methylation mark at a particular subset of targets (Walker, Chang et al. 2010). Additionally, these targets also showed reduced binding of core PRC2 proteins, suggesting the role of MTF2 may be in the recruitment or stabilization of the complex at particular targets (Walker, Manias et al. 2011).

1.5 The role of Mtf2 in embryonic stem cells

PcG proteins along with transcription factors, RNA binding proteins, microRNAs and other histone modifiers make up complex gene regulatory networks (GRNs) governing gene expression and cellular identity. Previous work from our lab drafted transcriptional networks during the initial stages of mESC differentiation. By probing ESC regulatory networks, we identified key regulators of pluripotency and differentiation. Based on this work, our lab identified Polycomb-like 2 (Mtf2, also referred to as Pcl2), as a critical regulator of embryonic stem cell fate (Walker, Ohishi et al. 2007). *In vitro* experiments were performed to further elucidate the role of MTF2 in mESCs, and its role within the gene regulatory network (Figure 1.4). Using shRNA knockdown studies, it was shown that a decrease in MTF2 maintains mESCs in an undifferentiated state and enhances cell proliferation (Walker, Chang et al. 2010). Our lab and others have shown that mammalian MTF2 associates with core PRC2 complex members through co-immunoprecipitation and mass spectrometry studies (Shen, Kim et al. 2009, Li, Margueron et al. 2010, Walker, Chang et al. 2010). In mESCs, MTF2 associates with a

subset of PRC2 targets, including genes important during differentiation, like Tbx3, Klf4 and Foxd3. Through prediction and testing of our mESC GRN, it was determined that MTF2 acts on the pluripotency network to regulate ESC fate through a feed-forward loop (Walker, Chang et al. 2010).

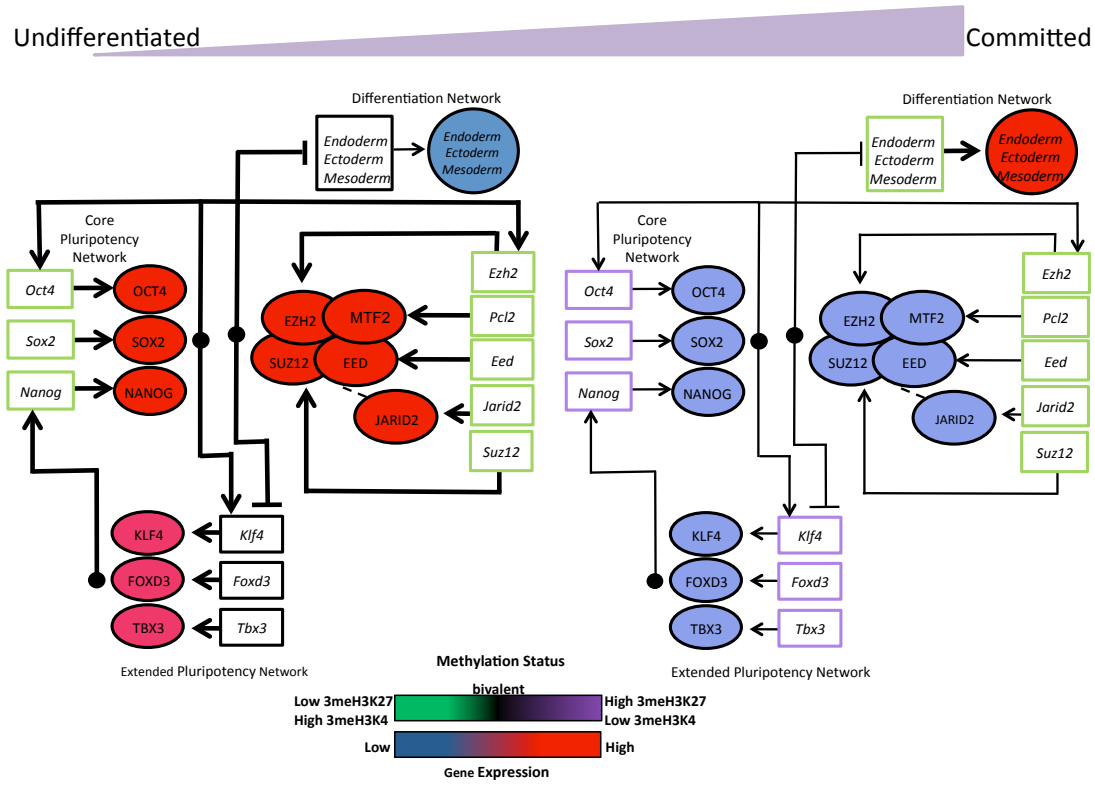

Figure 1.4 MTF2-PRC2-JARID2 gene regulatory network during early differentiation. *In ESCs, promoters of PRC2 genes, including Mtf2 and Jarid2, contain the H3K4me3 methylation mark and genes are highly expressed. PRC2 represses bivalent-marked members of the extended pluripotency network, Klf4, Foxd3 and Tbx3 which then act to induce transcription of the core pluripotency network (Oct4, Sox2, Nanog) via feed-forward mechanisms. High expression of the core and extended pluripotency network, along with PRC2 repression of developmental genes, maintains ESC self-renewal and pluripotency. During differentiation, the downregulation of Oct4, Sox2 and Nanog leads to the decreased expression of Klf4, Tbx3, Foxd3 and PRC2 genes, and collapse of the pluripotency network. Developmental genes previously poised for activation, are now de-repressed due to the decreased expression of PRC2. Loss of 3meH3K27 and increased expression of differentiation genes allows cells to become committed to various lineages. Methylation states are reflected in colour of gene boxes. For simplicity, gene expression levels are represented as protein expression levels, although this may not always reflect the true case. Dashed lines indicate potential interactions. (Adapted from (Walker, Manias et al. 2011))*

1.6 The role of Mtf2 *in vivo*

Various animal models, beginning with Drosophila Pcl mutants, have been used to elucidate the role of Mtf2 *in vivo*. Mtf2 plays an important role in embryonic patterning in the chick (Wang, Yu et al. 2004) via regulation of sonic hedgehog (*Shh*). A gene trap knockout of *Mtf2* (Wang, He et al. 2007), described a mouse with a variety of phenotypes, most prominently skeletal abnormalities. These skeletal transformations were recently confirmed in a second gene trap knockout model of *Mtf2* (Li, Isono et al. 2011) and attributed to changes in *Hox* gene expression and cell cycle regulator genes such as Cdkn2a, known targets of the MTF2-PRC2 complex. Previously in our lab we generated a hypomorphic *Mtf2* gene trap mutant mouse, which displayed pleiotropic defects, including absence of subcutaneous fat, situs inversus, hair cycling defects, severe growth impairment, and death by 3 months of age (Stanford Lab, unpublished). One of the most interesting findings was superficial lymph node enlargement, bordering on lymphoma. Differences seen in these mouse models of Mtf2 highlight the need for more *in vivo* studies to pinpoint the precise role of Mtf2 in normal and disease conditions.

1.7 Mammalian hematopoiesis

Hematopoiesis involves the coordinated regulation of cell growth and differentiation during development to populate all cell types of the blood system. Establishment of the hematopoietic stem cell (HSC) capable of both long-term self-renewal and differentiation is essential for continued hematopoiesis during the life of

the animal. In times of stress, disease or injury, HSCs can exit quiescence, re-entering the cell cycle, proliferate and differentiate into erythroid, lymphoid and myeloid lineages.

Early in mouse development, around embryonic day 7-7.5 (e7.0-7.5), mesoderm progenitors in the extraembryonic yolk sac (YS) differentiate into the hemangioblast, forming blood islands that differentiate to primitive erythroblasts. This transient first wave, or "primitive" hematopoiesis produces erythroblasts and macrophages with a limited lifespan, incapable of long-term self-renewal. The production of these cells is none-the-less critical to provide oxygen to developing tissues. At this point, the first expression of hematopoietic genes such as Lmo2 and Scl are detected in the yolk sac. Maturing erythroid cells express GATA1 in the yolk sac, and by day e8.5-9, have entered embryonic circulation. A common model of mammalian hematopoiesis suggests that cells that first began in the YS, can then travel through the circulation to colonize other sites of hematopoiesis. Cells derived from the YS alone are not able to convey long term reconstitution of adult recipients (Yoder and Hiatt 1997, Yoder, Hiatt et al. 1997), but can when cultured with stromal cells from the aorta-gonadal-mesonephros (AGM) region (Matsuoka, 2001). In the mouse, the first definitive HSCs, emerge from the dorsal aortic endothelium in the AGM between e10-11(Boisset, van Cappellen et al. 2010). In zebrafish and chick development, HSCs emerge via cell remodeling and not cell division (Bertrand, Chi et al. 2010, Kissa and Herbomel 2010). HSC development in an mESC *in vitro* model system is also not associated with asymmetric division (Eilken, Nishikawa et al. 2009), but the exact mechanism of HSC budding *in vivo* is still unclear. HSCs then

colonize the AGM, along with the placenta, vitelline and umbilical arteries and begin to produce multi-potent precursors capable of self-renewal and differentiation. These HSCs are capable of long-term self-renewal and multilineage differentiation and can repopulate adult mice. They are characterized by expression of cell surface markers CD45, Sca1, c-kit, CD34, and transcription factors Runx, SCL and Gata2 (Sanchez, Holmes et al. 1996, Sanchez, Bockamp et al. 2001, North, de Bruijn et al. 2002, Ling, Ottersbach et al. 2004). This secondary, or "definitive" wave of hematopoiesis produces early HSCs that, along with precursors from the yolk sac, can then colonize the fetal liver. By e11, the fetal liver becomes the primary site for hematopoiesis in the developing embryo. Just prior to birth of the mouse fetus, HSCs colonize the bone marrow. Up to three weeks after birth, HSCs in the bone marrow have similar properties to those found in the fetal liver. At 4 weeks post-birth, there is an abrupt, developmental switch, including an up-regulation of Ezh2, and HSCs gain unique self-renewal and differentiation properties that remain throughout adulthood (Bowie, Kent, et al., 2007). HSCs within the bone marrow provide a constant pool of cells from all blood lineages throughout the lifetime of the mouse. Differentiation of HSCs follows a hierarchical pattern where cells become more lineage restricted in order to finally produce erythrocytes, megakaryocytes, platelets, myeloid cells and lymphocytes (Figure 1.5).

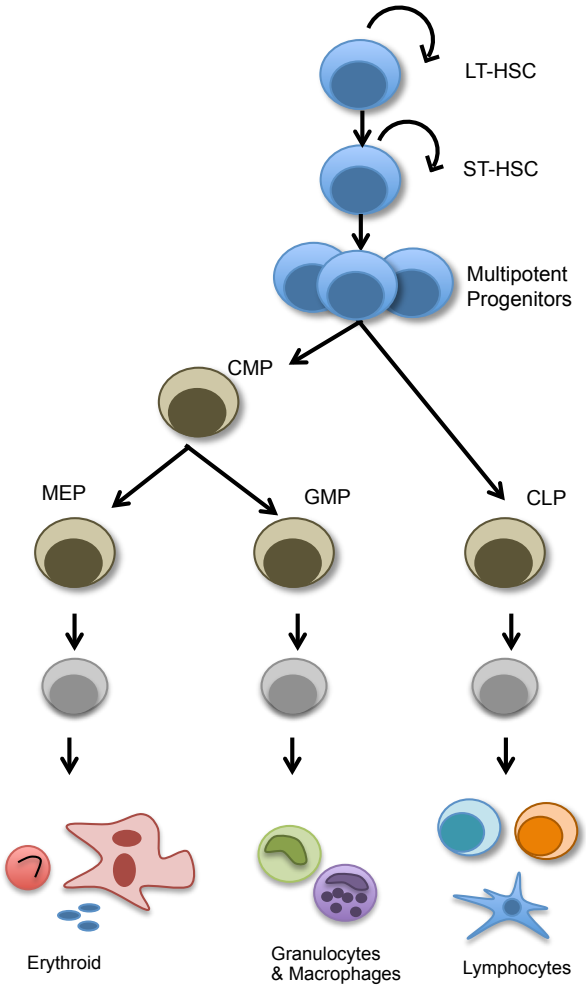

Figure 1.5. Hierarchical structure of mammalian hematopoiesis*. Mammalian hematopoiesis is a multi-step hierarchical process where self-renewing multi-potent stem cells sequentially differentiate into various multi-potent progenitors, which then specialize to form each of the progeny of the blood and the immune system. Long-term hematopoietic stem cell (LT-HSC), short-term hematopoietic stem cell (ST-HSC), common myeloid progenitor (CMP), megakaryocyte-erythroid progenitor (MEP), granulocyte-macrophage progenitor (GMP), common lymphoid progenitor (CLP).*

1.7.1 Mammalian erythropoiesis

The process of erythropoiesis is a key step in hematopoietic development and forms the circulating red blood cells that are able to carry essential oxygen throughout the body. In mammals, during early development (mouse age at e6.5), mesoderm precursors in the yolk sac begin differentiating into primitive erythrocytes (EryP) (Palis, Robertson et al. 1999, Palis and Yoder 2001). EryP cells differentiate in close proximity to endothelial cells, although the concept of a bipotent progenitor that gives rise to both of these cells, termed the "hemangioblast" is not clear to happen *in vivo* (Xiong 2008, Padron-Barthe, Temino et al. 2014). These large cells (Palis, Robertson et al. 1999), which express the fetal and embryonic forms of haemoglobin (translated from the alpha globin genes and beta globin gene cluster, epsilon) (Kingsley, Malik et al. 2006), cease cell division at e12.5 then are released into circulation where they complete the enucleation process during e12.5 and e17.5 (Kingsley, Malik et al. 2004). These EryP cells are critical for supporting the developing embryos and exist in circulation even up to several days after birth (Kingsley, Malik et al. 2004, Fraser, Isern et al. 2007).

A second wave of erythropoiesis (termed "definitive erythropoiesis") begins in the fetal liver as HSCs differentiate into multipotent progenitors then MEPs to form burst-forming unit erythroid (BFU-E), the first erythroid-restricted progenitor cells. BFU-Es mature through distinct stages, sequentially, from the colony-forming unit erythroid (CFU-E), proerythroblast (ProE) to basophilic (BasoE), polychromatophilic (PolyE), and orthochromatic (OrthoE) erythroblast stages. During these cell divisions there is expansion of the erythroid pool, and an accumulation of hemoglobin. Final stages of

maturation involve a reduction in the RNA content, nuclear pyknosis and eventual enucleation, a process unique to mammalian erythropoiesis. The enucleation process creates reticulocytes, which contain hemoglobin (Geiduschek and Singer 1979, Koury, Koury et al. 1989, Lee, Gimm et al. 2004, Liu, Mohandas et al. 2011) and pyrenocytes (McGrath, Kingsley et al. 2008), which are rapidly ingested by macrophages (Yoshida, Kawane et al. 2005). The final stage of erythrocyte maturation involves autophagy and exocytosis of cytoplasmic organelles in the reticulocyte to form mature red blood cells (Waugh, Mantalaris et al. 2001, Griffiths, Kupzig et al. 2012).

Isolation of distinct erythroid cell stages has become possible using traditional flow cytometry and multi-spectral imaging flow cytometry based on the expression of cell surface markers such as CD71 and Ter119, which fluctuate during erythroid maturation (McGrath, Bushnell et al. 2008, Pop, Shearstone et al. 2010, Koulnis, Pop et al. 2011). Additionally, a variety of transcription factors are critical for erythroid maturation, including Gata1, Klf1, Tal1, Lmo2, Ldb1, Myb and decreased or ectopic expression of these transcription factors can result in defects in erythroid development (Warren, Colledge et al. 1994, Robb, Lyons et al. 1995, Shivdasani and Orkin 1995, Tsang, Fujiwara et al. 1998, Isern, Fraser et al. 2010, Li, Lee et al. 2010) (Figure 1.6).

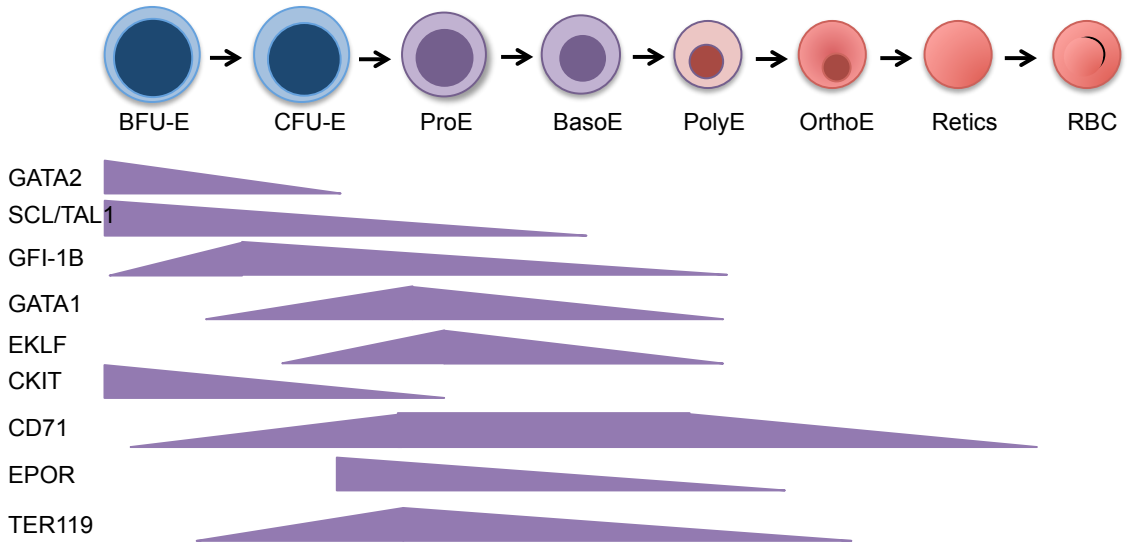

Figure 1.6. Expression of key regulators of erythropoiesis. *During mammalian erythropoiesis, megakaryocyte-erythroid progenitors differentiate through a series of erythroid progenitor stages, finally expressing hemoglobin and extruding their nucleus, forming oxygen-transporting red blood cells (RBCs). Expression levels of many transcription factors (SCL/TAL1, GATA1/2) and cell surface proteins (EPOR, Ter119) vary during the erythroid maturation process and are shown in purple bars. (burst forming unit-erythoid, BFU-E; colony forming unit-erythroid, CFU-E; proerythroblast, ProE; basophilic erythroblast, BasoE; polychromatophilic erythroblast, PolyE; orthochromatic erythroblasts, OrthoE; reticulocytes, Retics).*

1.8 Cell Cycle and Hematopoiesis

Hematopoiesis is a well-regulated biological process that is very active in early development, but continues throughout the life of an organism. HSCs balance self-renewal and differentiation to provide replacement cells within various blood lineages while maintaining a relatively constant pool of stem cells (Giebel and Bruns 2008). HSCs within the fetal liver of the developing embryo turn over rapidly, with 95-100% of HSCs cycling and a cell cycle transit time of 10-14h (Bowie, McKnight et al. 2006, Nygren, Bryder et al. 2006). In contrast, the majority of HSC in the adult bone marrow are quiescent, residing in G_0 phase in homeostatic conditions (Bradford, Williams et al. 1997). Here, only about 5% of cells are actively cycling (Cheshier, Morrison et al. 1999, Bowie, McKnight et al. 2006, Kiel, He et al. 2007), with transit times similar to fetal HSCs (Nygren, Bryder et al. 2006). Exogenous signals trigger cell cycle re-entry and cells can differentiate into multi potent progenitors, and ultimately cells of various blood lineages. A small fraction of HSCs are dormant, dividing very infrequently (estimated to be only dividing 5 times during the life of one mouse) (Wilson, Laurenti et al. 2008). These dormant HSCs can become activated under stress conditions, providing a pool of stem cells available for repair after injury.

Progression through the cell cycle is dependent on a host of cyclins and cyclin-dependent kinases (CDKs), which are further regulated by cyclin-dependent kinase inhibitors (CKIs). Transit through G_1 phase is regulated by Cyclin D-CDK4/6 that is then followed by Cyclin E-CDK2 activation in late G_1. Double knockout of CDK4/6 or triple knockout of Cyclin 1/2/3 leads to embryonic lethality and severe defect in

erythropoiesis (Malumbres, Sotillo et al. 2004). Overexpression of CDK6 was recently reported to regulate HSC self-renewal by reducing G_0 transit time (Benveniste, Frelin et al. 2010, Laurenti, Frelin et al. 2015). CDK6 is differentially expressed in ST-HSCs compared to LT-HSCs and may be responsible for heterogeneity in cycling. Single knockout of many components of the cell cycle results in a mild phenotype, indicating redundancy amongst cell cycle proteins or dosage-dependent effects. Knockout of many members of the INK4 family of CKIs, classical PcG targets, also affect hematopoietic development. Knockout of $p16^{INK4a}$ (Cdkn2a) leads to HSC defects with stress or aging (Serrano, Lee et al. 1996, Janzen, Hake et al. 2006), while knockout of $p18^{INK4c}$ (Cdkn2c) increases HSC self-renewal (Yuan, Shen et al. 2004, Yu, Alder et al. 2006). Reduction in CKI from the CIP/KIP family such as $p21^{CIP}$ (Cdkn1a) (Cheng 2000) and $p57^{KIP2}$ (Cdkn1c), leads to exhaustion of HSC activity or reduction in HSC quiescence (Matsumoto, Takeishi et al. 2011), respectively. Regulation of transcription factors such as HOX genes, c-myb, and GATA2 can all affect hematopoietic cell cycling and HSC function (Persons, Allay et al. 1999, Antonchuk, Sauvageau et al. 2001, Malaterre, Carpinelli et al. 2007). Regulation of cell cycle-related proteins and transcription factors by PcG proteins can significantly affect hematopoietic development.

1.9 Polycomb proteins in hematopoietic development and disease

1.9.1 PRC1 and hematopoietic development

In the hematopoietic system, Polycomb proteins play fundamental roles in cell fate decisions and differentiation programs. Bmi-1 maintains HSC self-renewal and loss

of Bmi-1 leads to profound anemia in young mice (van der Lugt, Domen et al. 1994, Park, Qian et al. 2003). Other PRC1 members have also been implicated in erythroid differentiation and loss of Cbx4/MPc2 (Alkema, Jacobs et al. 1997) or L3mbtl3/MBT1 (Arai and Miyazaki 2005) leads to anemia during late stages of embryogenesis. PRC1 proteins Pcgf2/Mel18 (Akasaka, Tsuji et al. 1997), Phc1/Rae28 (Ohta, Sawada et al. 2002), and Ring1B (Cales, Roman-Trufero et al. 2008) are also critical for hematopoietic development. Core components of PRC2 also have significant roles in regulating hematopoiesis and recent studies have demonstrated that various PRC2 core components are differentially regulated during hematopoietic ontogeny (Xie, Xu et al. 2014).

1.9.2 PRC1 and hematopoietic development

Mutant mouse models have helped gain insight into the role of PRC2 components in the hematopoietic development. Reduction in Suz12, via an ENU-induced hypomorphic mutation results in mice with increased HSC activity (Majewski, Blewitt et al. 2008). In a more recent study, conditional knockout of Suz12 in the hematopoietic system led to exhaustion of the HSC pool (Lee, Miller et al. 2015). Together these studies show that Suz12 is critical in normal HSC development and function but that its role is dose-dependent.

Conditional ablation in hematopoietic cells demonstrated that Ezh2 plays a critical role in early B cell development (Su, Basavaraj et al. 2003) and maintenance of fetal HSCs (Mochizuki-Kashio, Mishima et al. 2011). Loss of Ezh2 causes self-renewal and

differentiation defects in fetal liver (FL) HSCs leading to anemia. This role for Ezh2 is stage-specific as Ezh2 is dispensable in adult HSCs via compensatory Ezh1 function (Mochizuki-Kashio, Mishima et al. 2011). Loss of Jarid2 leads to hematopoietic defects including defective definitive erythropoiesis as well as cardiac and neural defects during embryonic development (Takeuchi, Yamazaki et al. 1995, Motoyama, Kitajima et al. 1997, Jung, Mysliwiec et al. 2005). In the hematopoietic system, loss of Jarid2 by shRNA knockdown in transplanted mouse and human HSCs increases the number and function of HSPCs (Kinkel, Galeev et al. 2015). Thus, the coordinated efforts of both PRC1 and PRC2 proteins are needed for epigenetic regulation of genes critical for hematopoietic development.

1.9.3 The role of PcG proteins in cancer

Many different lines of evidence point to how genetic and epigenetic changes, including histone modifications, have been associated with disease progression, particularly in cancer. DNA hypomethylation and promoter histone hypermethylation have been associated with the initiation and progression of various tumors (Taby and Issa 2010). Since PRC2 proteins are involved in many essential cell processes, tightly controlled expression is essential and misexpression of PRC2 has been associated with neoplasia. Over- or under-expression of PRC2 proteins caused by multiple sources including gene mutations or changes in methylation, can contribute to cancer initiation and progression (Bracken and Helin 2009, Gieni and Hendzel 2009, Sauvageau and Sauvageau 2010, Lin, Chen et al. 2011). In many reports, over-expression of PcG

proteins such as Bmi1, Ezh2 and Suz12, have been associated with multiple forms of cancer, including leukemias and lymphomas, suggesting a role for PcG proteins as oncogenes (reviewed in (Sauvageau and Sauvageau 2010)). In other instances, loss of heterozygosity of PcG proteins is also associated with cancer progression (Tokimasa, Ohta et al. 2001). Loss-of-function mutations in *SUZ12*, *EZH2* and *EED* have been identified in T cell acute lymphoblastic leukemia (Ntziachristos, Tsirigos et al. 2012, Zhang, Mortazavi et al. 2012) and gain-of-function mutations in EZH2 has been identified in lymphomas (Bracken, Pasini et al. 2003). Recently, documented cases of mutations or truncations within PcG proteins, including Ezh2 have been linked to leukemia, highlighting the role of PcG proteins as both oncogenes and tumor suppressors (Ernst, Chase et al. 2010, Nikoloski, Langemeijer et al. 2010).

1.10 Leukemia

Leukaemia can be thought of as a misregulation of hematopoiesis that results in aberrant cell differentiation and excess proliferation. Acute leukemias also display an accumulation of immature undifferentiated cells termed 'blasts'. Leukaemias can manifest as acute or chronic and affect either the myeloid or lymphoid lineage, diagnosed depending on which branch of hematopoietic differentiation is affected.

1.10.1 Acute Myeloid Leukemia

Acute myeloid leukaemia (AML) results from aberrant myeloid differentiation and an uncontrolled proliferation of myeloid progenitors. In the search to describe the

underlying etiology of AML, mutations in a few genes, such as DNMT3A, FLT3, RUNX1, TP53, IDH2 (Cancer Genome Atlas Research 2013), have been positively associated with the disease. A “multi hit” model has been proposed for AML where multiple mutations act synergistically to create the disease where neither could alone (Gilliland and Griffin 2002). Chromosomal translocations that result in fusion proteins and gene activation are often behind the evolution of AML. Translocations of the mixed lineage leukaemia gene (MLL) account for the majority of pediatric leukemias and approximately 10% of adult AML (Aplan 2006, Muntean, Tan et al. 2010). MLL-AF9 is an example of a fusion protein that can be used to study leukemic progression in the mouse and interrogate the pathology and treatment of AML (Monroe, Jo et al. 2011).

1.10.2 Chronic Myeloid Leukemia

Myeloid leukemia can also present itself as a chronic disease, with a chronic (asymptomatic) phase, an accelerated phase and a blast crisis phase (Faderl, Talpaz et al. 1999). In chronic myeloid leukemia, the disease arises from a genetic crossover event between chromosomes 9 & 11, resulting in a fusion of the BCR and ABL genes. This product (also known as the Philadelphia chromosome from the city in which it‘s translocation was first identified) produces a fusion protein (BCR-ABL) that results in a hyperactivity to normal growth regulators. This aberrant signalling leads to uncontrolled cell division, leading to a sustained leukemia (Knuutila, 1994; Melo, 1996).

Modeling leukemia *in vitro* and using animal models has become possible with the discovery of gene mutations or fusion proteins that drive leukemic initiation and

progression. Expression of the MLL-AF9 fusion oncoprotein or the BCR-ABL oncoprotein in mice models enables controlled, mechanistic studies of the pathophysiology of leukemia.

1.10.3 Pre-leukemic events

Recent evidence has also pointed to a host of other mutations linked to AML that do not convey transformation on their own, but may predispose the cell to a second mutation. The concept of a "pre-leukemic state" in which one or more cell properties are affected by mutation, has been around since the late 1980s (Fialkow, Singer et al. 1987) and provides evidence for a multi-step development of leukemia. Increased genomic instability, increased cell cycle, inappropriate DNA damage repair mechanisms and increased self-renewal programs all define pre-leukemic HSCs. Identifying regulators of key processes specifically within HSCs will help us understand which genes are critical for proper maintenance of hematopoiesis and which genes may be candidates for preventing pre-leukemic changes within cells.

1.10.4 Modeling leukemia using the Friend Virus as a two-stage model of leukemia

An experimental model of leukemia was first described in 1957 using the spleen-focus forming Friend virus (Friend, 1957). Various forms of the Friend virus can induce erythroleukemia in susceptible mice through a multi-stage process (Tambourin, Wendling et al. 1981) (Figure 1.7). Here we will focus on data surrounding the FV-P virus model, which is a complex of the spleen focus forming virus, polycythemia (SFFV-P) and

the Friend murine leukemia virus (F-MuLV). First, infected erythroid progenitors (BFU-E, CFU-E) undergo massive expansion and lose their dependence on erythropoietin (Epo) for growth (Liao and Axelrad 1975, Peschle, Migliaccio et al. 1980). These initial events are dependent on the gp55 glycoprotein, encoded by the SFFV-P virus, binding and activating the erythropoietin receptor (EpoR) and recruitment of the short form of the stem-cell-kinase receptor (sf-Stk) (Ruscetti and Wolff 1984, Mager and Bernstein 1985, Chung, Wolff et al. 1989, Li, D'Andrea et al. 1990, Zon, Moreau et al. 1992, Nishigaki, Thompson et al. 2001, Zhang, Randall et al. 2006). Together, activation of signalling pathways through EpoR and sf-Stk by gp55 derails normal proliferation and differentiation of erythroblasts. The increased number of erythroid progenitors then become targets for re-infection by the virus, and after an incubation period of 3-4 weeks, malignant clones emerge. During the second stage of infection, further molecular events are responsible for oncogenic transformation. FV-P transformed clones can be transplanted into susceptible mice and propagate leukemia in a new host (Tambourin and Wendling 1975, Wendling, Moreau-Gachelin et al. 1981). Outgrowth of these transformed cells can be propagated in liquid culture and can be encouraged through terminal differentiation by dimethyl sulfoxide (Friend, Scher et al. 1971). During transformation, the FV-P virus preferentially inserts within the Sfpi1/PU.1 gene, inducing its constitutive activity (Moreau-Gachelin, Tavitian et al. 1988, Paul, Schuetze et al. 1989). Activation of *sfpi1* works in conjunction with activated signalling by gp55 to induce transformation (Longmore and Lodish 1991, Quang, Wessely et al. 1997). Mutations within p53 have also been classically associated with FV-P induced leukemic

clones (Mowat, Cheng et al. 1985, Ben David, Prideaux et al. 1988), but evidence suggests that p53 mutations are not absolutely required for transformation to leukemic stem cells within this model (Hegde, Hankey et al. 2012).

The multi-stage etiology of the Friend erythroleukemia virus also provides a model to study common types of human leukemia that also arise from a multi-step process. Progression of the Friend virus begins as a proliferative disease followed by transformation of blasts, which can propagate disease in a new host. These two stages are very similar to the progression of AML, and it has been proposed that Friend erythroleukemia can be used to study the "two-hit" model of AML and interrogate the cooperation of mutations in disease progression (Moreau-Gachelin 2006, Moreau-Gachelin 2008).

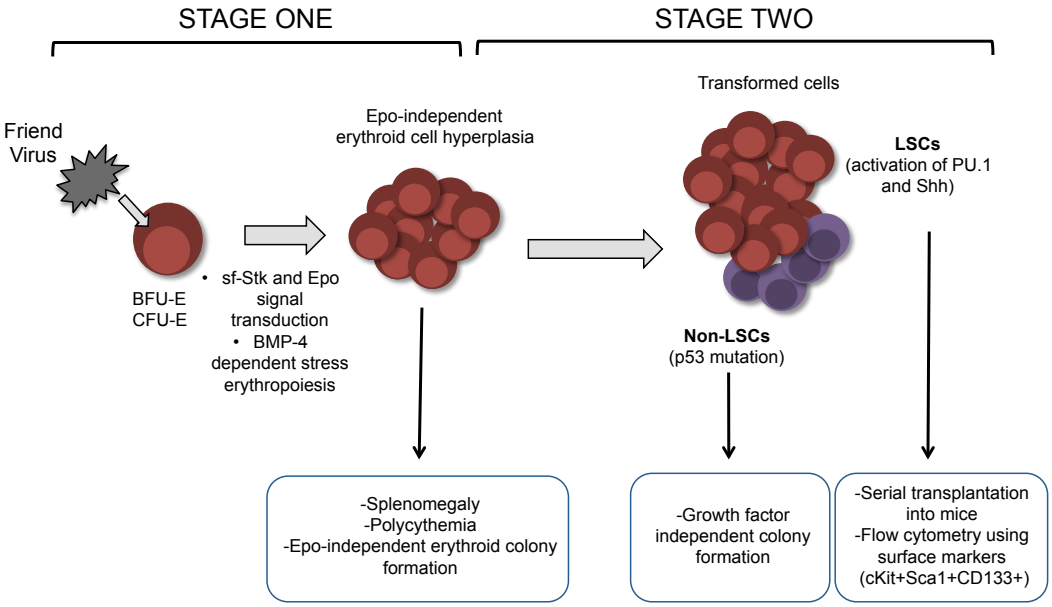

Figure 1.7. A schematic of the two-stage model of leukemia using the Friend Erythroleukemia virus. *Erythroid progenitors are initial targets of infection by the Friend virus that leads to massive cell expansion and growth factor-independence. Cells in the expanded progenitor pool become targets for re-infection, leading to development of transformed leukemic stem cells and other cells prone to p53-loss (Adapted from (Cmarik and Ruscetti 2010)).*

1.11 Approaches to uncovering function of novel proteins

1.11.1 Using gene regulatory networks to interrogate function of novel proteins

Discovering the function of a novel protein can often be a painstaking process when experiments are designed to capture only a few potential outcomes. Taking an integrative, systems biology approach to protein interactions can provide a more holistic view into what roles a novel protein may hold. Many groups have integrated data from transcriptomics, promoter occupancy (Boyer, Plath et al. 2006, Ivanova, Dobrin et al. 2006, Walker, Ohishi et al. 2007) and chromatin structure (Mikkelsen, Ku et al. 2007) to generate examples of gene regulatory networks in ESCs. Layering in new levels of data, including translational data (Sampath, Pritchard et al. 2008), non-coding RNAs (Khalil, Guttman et al. 2009) and even computational modeling, allow for a more comprehensive understanding of regulatory networks (Figure 1.8). Most importantly, gene regulatory networks can be used to extract regulatory modules, such as feedback and feed-forward loops, to interrogate mechanisms of interactions between key nodes within the network (Walker and Stanford 2009).

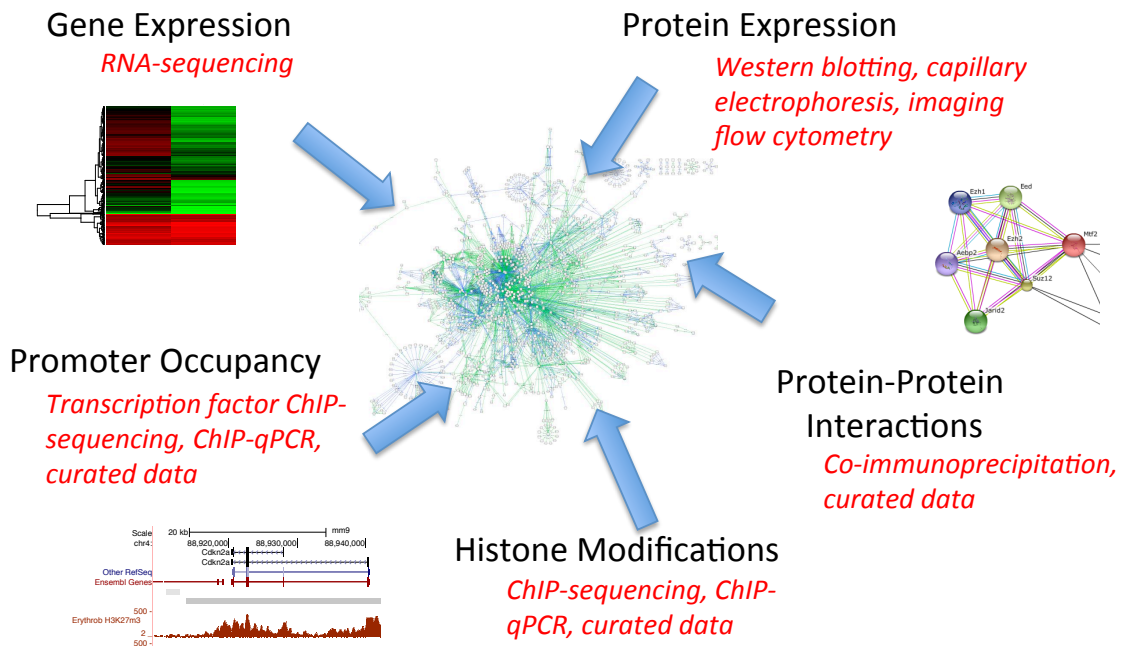

Figure 1.8. Integration of systems level data to create gene regulatory networks. *Multiple levels of data, including transcriptomics, promoter occupancy, histone binding patterns and protein expression can be integrated to form a comprehensive gene regulatory network. Examples of assays used to generate each type of data are reported in red. Manipulation of nodes within the network can be used to test the strength of the data and generate hypotheses.*

1.11.2 A reductionist approach to discovering gene function

With human health and disease in mind, ground-breaking work in *Drosophila* and zebrafish demands reproduction in the mammalian system. Fully defining the role of a novel protein *in vivo* can often be most obvious using a reductionist approach. Knockout mouse models have provided an excellent way of defining roles for genes in tissue development and pathology. Large-scale screens have been carried out using gene trapping approaches. In this model, promoterless reporter vectors with splice acceptor sites are introduced into ESCs and randomly insert throughout the genome (Gossler, Joyner et al. 1989, Friedrich and Soriano 1991). After phenotypic screens are established, candidate cell lines with unique phenotype can be further analyzed and location of the gene trap can be determined (Skarnes, Auerbach et al. 1992). Traps that insert within a coding gene often result in reduction in gene expression via frame shift mutation and presence of a premature stop codon within the cassette. These trapped ESCs can then be used to generate chimeric mice and, with selective breeding, can produce knockout mice. Hence, gene trapping can provide insightful information about protein function *in vivo* and has been widely used throughout, including the creation of thousands of trapped ES lines by multinational consortiums available to the public for further study (Stanford, Cohn et al. 2001, Nord, Chang et al. 2006, Rosen, Schick et al. 2015). This technology has proved useful, but is not without its limitations. Because of the random nature of the trap insertion, this type of forward genetic screen is time consuming and labour intensive. Additionally, the location of the insertion can often produce hypomorphic mutations when alternatively spliced gene products still remain.

Designing targeted cassettes to create loss of function mutations has expanded our knowledge of protein function. Methods of gene targeting have been used extensively to create constitutive and conditional knockout mice to interrogate gene function during development or disease (Skarnes, Rosen et al. 2011). By adding homologous arms to a reporter cassette, strategies can be used to create null mutations or isolate particular isoforms of genes or include or exclude particular protein domains to ask increasingly complex biological questions.

1.12 Rationale and Approach

Following the work of Walker, et al. (Walker, Chang et al. 2010), many questions regarding the function of Mtf2 were still outstanding. As PcG proteins have a role in controlling Hox genes during early development, studying their function in an embryonic stem cell model system has proven highly useful. Being an *in vitro* model system though, it does have limited interpretation with respect to other organ systems. Outside of the ESC, PcG proteins also play a role in homeostasis and disease states. To uncover the role(s) of Mtf2 in development and homeostasis, we used a gene-targeting approach (Figure 1.9). Through work described here, we uncovered a novel role for Mtf2 in the hematopoietic system. This data has generated a preclinical model where the role of Mtf2 can be more fully elucidated, including in the context of disease. The resulting analysis has spurred many future avenues of research, including those that can be translated to a better understanding of AML and potential therapies.

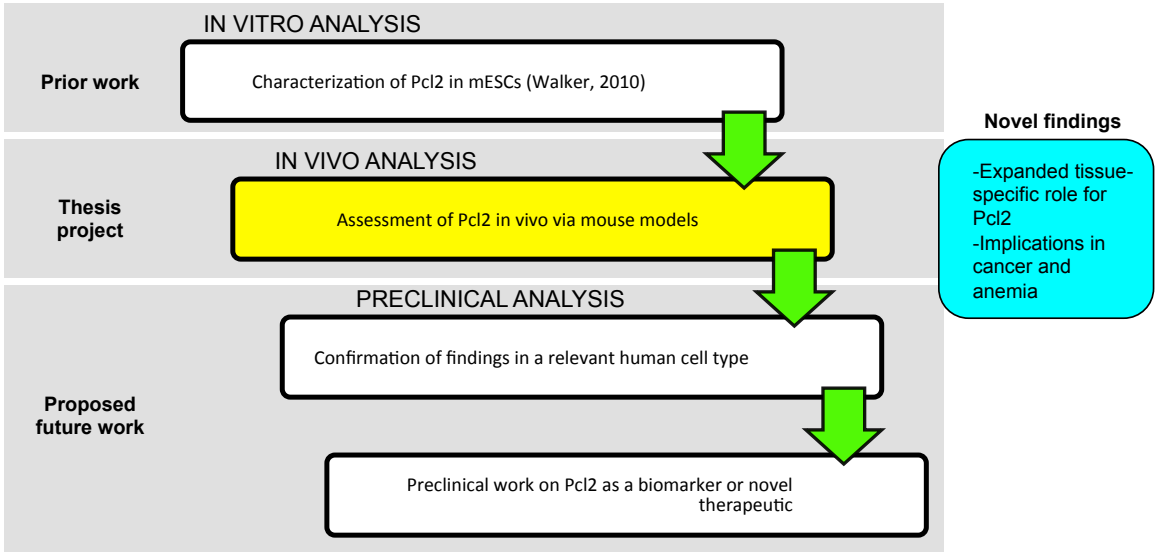

Figure 1.9 Flow chart of project integration. *The goal of this project was to build upon knowledge of Mtf2 within the mESC model system and to interrogate the effects of Mtf2 in vivo.*

1.13 Hypothesis and Aims

1.13.1 Overarching hypothesis:

Polycomb-like 2 (Pcl2/Mtf2) is required for epigenetic regulation of hematopoietic development.

1.13.2 Specific Aims:

Aim 1: Analyze the role of Mtf2 in embryonic hematopoietic development using a $Mtf2^{-/-}$ mouse model.

Aim 2: Identify a hematopoietic-specific Mtf2-PRC2 gene regulatory network.

Aim 3: Determine whether misregulation of Mtf2 affects leukemia progression.

Chapter 2

Janet L. Manias Rothberg, Harinad B. Maganti, Christopher J. Porter, Gareth A. Palidwor, R. Matthew Tanner, Hani Jrade, Robert F. Paulson, Theodore J. Perkins, Caryn Ito, William L. Stanford. **Mtf2/Pcl2 controls PRC2-mediated epigenetic regulation of hematopoiesis.** 2016, (in preparation).

A**uthor contributions:** JMR, along with CI and WLS, conceptualized experiments. JMR conducted all experiments, except for *in vitro* knockdown (Figure S2.3), analyzed data and prepared figures. Original gene targeted chimeras were generated by the Centre for Phenogenomics (Toronto). JMR maintained all mouse colonies and performed breeding and genotyping. HBM and HJ performed *in vitro* knockdown experiments (Figure S2.3) and optimized ChIP protocol. RMT, CJP, GAP and TJP performed initial bioinformatic analyses. RFP provided reagents for the Friend leukemia experiments and helped interpret data. JMR, in collaboration with CI and WLS, wrote and prepared the manuscript. All authors assisted in editing the manuscript.

Mtf2/Pcl2 controls PRC2-mediated epigenetic regulation of hematopoiesis

Janet L. Manias Rothberg[1,2,3], Harinad B. Maganti[1,2,4], Christopher J. Porter[5], Gareth A. Palidwor[5], R. Matthew Tanner[1,2,3], Hani Jrade[1,2,3], Robert F. Paulson[6], Theodore J. Perkins[1,4,5], Caryn Ito[1,3*], William L. Stanford[1,2,3,4*]

[1]The Sprott Center for Stem Cell Research, Regenerative Medicine Program, Ottawa Hospital Research Institute, Ottawa, ON, Canada K1H 8L6;

[2]Ottawa Institute of Systems Biology, Ottawa, Ontario, Canada;

[3]Department of Cellular and Molecular Medicine, University of Ottawa, Ottawa, Ontario, Canada; [4]Department of Biochemistry, Microbiology and Immunology, University of Ottawa, Ottawa, Ontario, Canada;

[5]Ottawa Bioinformatics Core Facility, The Sprott Center for Stem Cell Research, Ottawa Hospital Research Institute, Ottawa, ON, Canada K1H 8L6;

[6]Department of Veterinary and Biomedical Sciences, Pennsylvania State University, University Park, Pennsylvania 16802, USA

Abstract

In ESCs, Polycomb accessory proteins, such as the Drosophila ortholog Polycomb-like (Pcl), play substoichiometric roles to recruit the Polycomb repressive complexes (PRC) to a subset of genomic loci or increase enzymatic activity. Mtf2 (Pcl2) regulates ESC self-renewal and differentiation by recruiting PRC2 to specific pluripotent and developmental genes, fulfilling the function of a Polycomb accessory protein. To understand its impact on development *in vivo*, we generated gene targeted Mtf2 null mice, which die at e15.5 exhibiting growth defects and severe anemia. Mtf2 is required cell autonomously for definitive erythroid development and HSC self-renewal. Surprisingly, unlike its accessory function in ESCs, Mtf2 plays a role similar to that of a core PRC2 member in the hematopoietic system. Unexpectedly, Mtf2 null erythroblasts exhibit decreased levels of core PRC2 proteins and a global loss of H3K27me3 at promoter-proximal regions, uncovering a novel region-specific activity for an accessory protein. As a result, gene regulatory networks controlling transcription, differentiation and proliferation are de-repressed in the absence of Mtf2, leading to defective erythrocyte maturation and a block in HSC self-renewal. In a model of leukemia, Mtf2 haploinsufficiency leads to an expansion of leukemic blasts. Collectively, these findings place Mtf2 as a critical epigenetic regulator of hematopoiesis through its control of canonical PRC2 activity, while refining our understanding of Polycomb accessory proteins.

Introduction

The Polycomb Repressive Complex 2 (PRC2) proteins, including core and accessory family members, repress gene transcription via methylation of lysine 27 of histone 3 (H3K27me3). Accessory proteins such as Jarid2, Rbbp4/7, Aebp2 and members of the Polycomb-like (Pcl) family associate with core PRC2 members (Ezh2/Ezh1, Suz12 and Eed) in a combinatorial fashion that is poorly understood.

Analysis of PRC2 accessory proteins in mammalian ESCs has provided some evidence for their role in early development. PRC2 accessory proteins are defined by their association with the PRC2 complex and act to "fine-tune" H3K27me3-mediated repression via targeting of PRC2 to specific genomic loci or enhancing methylation. For example, Rbbp4 and Rbbp7 have a strong affinity for histones H3 and H4 and may contribute to PRC2 recruitment to target sites (Nekrasov, Wild et al. 2005, Nowak, Alfieri et al. 2011, Schmitges, Prusty et al. 2011). Aebp2 often co-purifies with the PRC2 in ESCs (Cao and Zhang 2004, Peng, Valouev et al. 2009, Shen, Kim et al. 2009, Li, Margueron et al. 2010) and is important in PRC2 targeting (Kim, Kang et al. 2009) or for enzymatic activity of the complex (Cao and Zhang 2004), although its molecular role is unclear. Jarid2, one of the most well-studied PRC2 accessory proteins, associates with core PRC2 complex members, stabilizes PRC2 at particular loci and is necessary for ESC differentiation (Peng, Valouev et al. 2009, Shen, Kim et al. 2009, Landeira, Sauer et al. 2010, Pasini, Cloos et al. 2010). Although the core PRC2 proteins are required for the stability of the PRC2 multimeric complex, none encode DNA binding domains. Jarid2 and

the *polycomb-like* (*Pcl*) accessory proteins contain DNA-binding domains which confer their role in PRC2 targeting and stability at target sites (Peng, Valouev et al. 2009, Shen, Kim et al. 2009, Landeira, Sauer et al. 2010, Li, Margueron et al. 2010, Pasini, Cloos et al. 2010, Walker, Chang et al. 2010, Casanova, Preissner et al. 2011, Walker, Manias et al. 2011). While the role of accessory proteins has been investigated in ESCs, for most of these accessory proteins, it is unclear whether their function is maintained *in vivo*.

In Drosophila, *pcl* is required for high levels of H3K27me3 by the PRC2 (Nekrasov, Klymenko et al. 2007), leading to gene repression. Mammalian *pcl* homologs Phf1 (also known as Pcl1), Mtf2 (Pcl2) and Phf19 (Pcl3) have been defined as PRC2 accessory proteins in ESCs (Sarma, Margueron et al. 2008, Walker, Chang et al. 2010, Hunkapiller, Shen et al. 2012). Phf19 helps recruit PRC2 to particular gene loci critical for early development (Hunkapiller, Shen et al. 2012). Phf1 is also associated with the PRC2 complex and plays a role in enhancing PRC2-mediated methylation (Sarma, Margueron et al. 2008). Mtf2 co-immunoprecipitates with core PRC2 complex members and co-elutes with multi-protein PRC2 complexes both in ESCs and hematopoietic cells (Shen, Kim et al. 2009, Walker, Chang et al. 2010, Xu, Shao et al. 2015). In ESCs, Mtf2 is required to repress the extended pluripotency network, thereby enabling ESCs to respond to extrinsic differentiation stimuli (Walker, Chang et al. 2010). Knockdown of Mtf2 in ESCs led to reduced H3K27me3 levels at Mtf2 target loci but did not affect global H3K27me3 levels (Walker, Chang et al. 2010). In another study, reduced levels of Mtf2 in ESCs depleted PRC2 occupancy at target genes but had little effect on H3K27me3 levels (Casanova, Preissner et al. 2011). Manipulating expression of Mtf2 did

not affect the expression level of core PRC2 complex members (Casanova, Preissner et al. 2011, Walker, Manias et al. 2011), supporting its role as a PRC2 accessory protein in ESCs. Despite recent advances in understanding the role of PRC2 accessory proteins, including Mtf2, their contribution to PRC2 function and their role in global and/or targeted H3K27me3 levels *in vivo* is not well understood.

In addition to their critical role in early development, core PRC2 proteins also function in homeostasis of many adult tissues. While recent studies have provided insight into the function of various PRC2 accessory proteins in ESCs, their roles in tissue homeostasis and disease are largely unknown. Here, using a variety of approaches, we demonstrate that Mtf2 is required cell autonomously for definitive erythroid development and HSC self-renewal via modulation of PRC2-mediated epigenetic repression. Unlike in ESCs, Mtf2 is required for genome-wide H3K27me3 deposition specifically at promoter-proximal regions within the erythroid lineage. Moreover, reduced Mtf2 expression leads to expansion of leukemic blasts and increased leukemic burden in the Friend virus erythroleukemia model. Surprisingly, Mtf2 deficiency also results in reduced levels of other PRC2 proteins. Together, these data demonstrate that Mtf2 is required for PRC2-mediated epigenetic regulation of hematopoiesis. Moreover, these findings refine our understanding of PRC2 associated proteins, indicating they can function similarly to core PRC2 proteins and regulate complex stability in a tissue-specific manner.

Results

Mtf2 null mice die in utero from a block in definitive erythropoiesis

Mtf2 is expressed highly in ESCs; however, our bioinformatic analysis of mouse tissue microarrays (Zhang, Morris et al. 2004) determined that *Mtf2* has a more restricted pattern in the adult, with higher expression in hematopoietic organs, such as the bone marrow, thymus and spleen. Using intracellular flow cytometry, we assessed Mtf2 protein abundance in various hematopoietic lineages isolated from bone marrow (BM) and observed that Mtf2 expression is high in long- and short-term HSCs (LT-HSCs and ST-HSCs, respectively), progenitors (LSK cells) and various stages of erythroblast development (indicated by CD71 and/or Ter119 expression; Figure S2.1A-C). In erythroblasts, Mtf2 expression is modulated during the cell cycle with highest expression observed during the S and G2/M phases (Figure S2.1D).

Previous work addressing the role of Mtf2 *in vivo* was limited to gene trap mutants that display variable phenotypes. Interruption of Mtf2 between the 4^{th} and 5^{th} exon produces viable mice with skeletal abnormalities (Wang, He et al. 2007). A second mutant strain, using mixed background gene-trapped ESCs, phenocopied the skeletal defects observed previously but also led to early post-natal lethality (Li, Isono et al. 2011). Since gene trap mutations are often hypomorphic (Stanford, Cohn et al. 2001) and to maintain strain fidelity which has also led to variable phenotypes with other Polycomb mutants (Motoyama, Kitajima et al. 1997, Kitajima, Kojima et al. 1999), we chose to generate Mtf2 null (*Mtf2*$^{-/-}$) mice in the *C57BL/6* background using gene

targeted ESCs (Figure 2.1A,B). In contrast to the gene trap alleles, no homozygous gene targeted mice were present at parturition; thus, embryos were analyzed at different developmental stages. *Mtf2*$^{-/-}$ mice die at e15.5, displaying growth defects, hemorrhage, and severe anemia (Figure 2.1C-E). Embryos also display skeletal alterations including fusion of vertebrae and ectopic ribs, as observed in the gene trap mutants (unpublished observations). Based both on gross pathology of the *Mtf2*$^{-/-}$ mice and the expression pattern of Mtf2 in adult erythroblasts (Figure S2.1), we further investigated erythroid development in the *Mtf2*$^{-/-}$ mice at e14.5, prior to death. At this embryonic stage, the fetal liver is the central site of hematopoietic development. Fetal liver (FL) cellularity was significantly reduced in *Mtf2*$^{-/-}$ e14.5 embryos (30.9±1.88 x10^6 cells per embryo compared to 64.7±8.95 x10^6 cells in wild-type embryos, p=0.013), although FL size as a percentage of body weight was not affected (Figure 2.1F). Peripheral blood smears from *Mtf2*$^{-/-}$ embryos showed fewer enucleated mature red blood cells and more nucleated, large primitive erythroblasts compared to *Mtf2*$^{+/+}$ controls (Figure 2.1G). Hematocrits were also dramatically reduced in *Mtf2*$^{-/-}$ embryos compared with their wild-type littermates (Figure 2.1H).

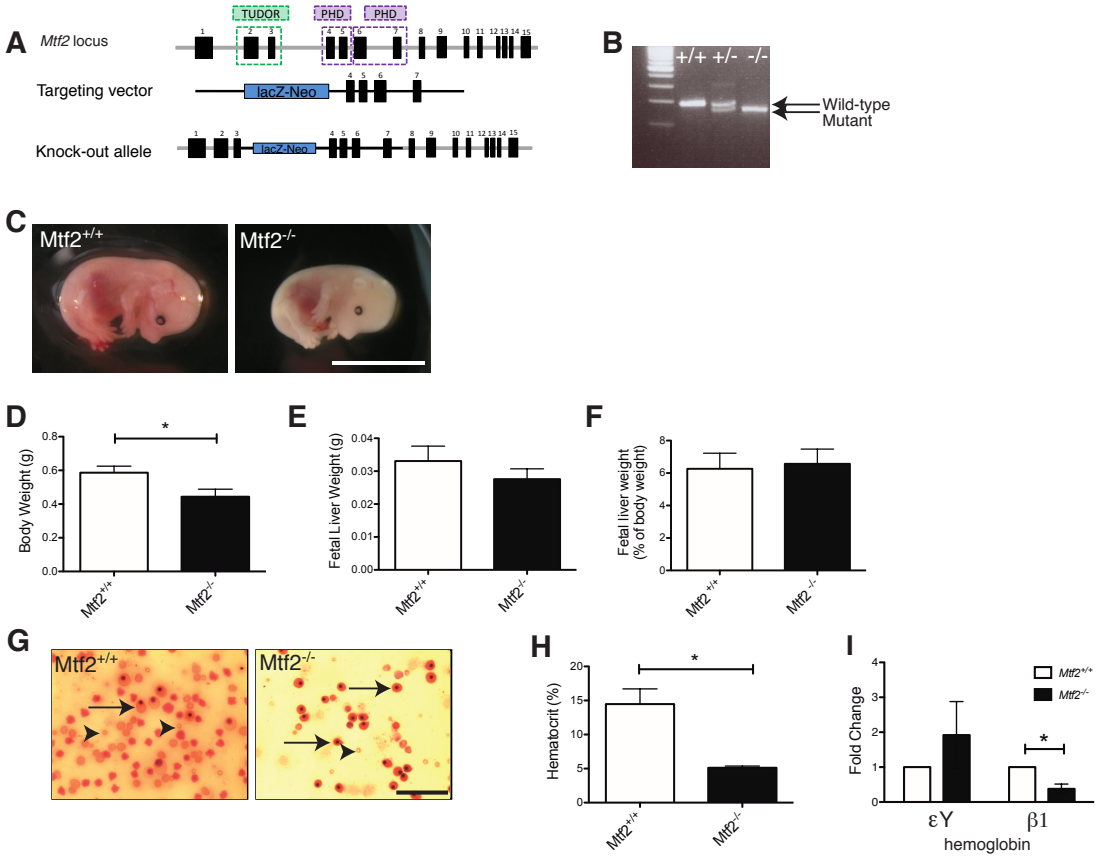

Figure 2.1. *Mtf2*$^{-/-}$ mice die at e15.5 due to severe anemia. (**A**) Schematic of the gene targeted ESCs used to create Mtf2 knockout mice. Mtf2 protein domains (Tudor, PHD) are indicated. (**B**) A PCR-based genotyping strategy was used to identify homozygous mutants. (**C**) *Mtf2*$^{-/-}$ embryos display anemia, growth defects, hemorrhage and die at e15.5. (**D**) e15.5 *Mtf2*$^{-/-}$ embryos are significantly smaller than their wild-type littermates but have (**E-F**) normal fetal liver (FL) weight as a measure of body size. (**G**) Peripheral blood taken from e15.5 *Mtf2*$^{-/-}$ embryos has fewer cells than wild-type littermates and very few enucleated red blood cells (arrowheads). The cells that do remain are large nucleated erythroid precursors (arrows). (**H**) Null embryos have a lower hematocrit and (**I**) fail to express adult b1 hemoglobin transcript at the appropriate level. All data is shown as mean ± SEM, n=3, *p<0.05.

Transcript of adult β1 hemoglobin, which is normally expressed by maturing red blood cells at this stage of development, was reduced in *Mtf2*$^{-/-}$ embryos while embryonic globin (eY) expression was maintained (Figure 2.1I).

To discern which stage of erythroid development was blocked in *Mtf2*$^{-/-}$ cells, we used cell surface markers CD71 and Ter119 to track erythroid maturation in the FL (Koulnis, Pop et al. 2011). We identified a delay in erythroblast differentiation, with an increased number of Ter119$^{-/lo}$ *Mtf2*$^{-/-}$ cells (erythroid stages S0-S2) and fewer Ter119^{high} (stage S3) *Mtf2*$^{-/-}$ cells (Figure 2.2A-B). Despite alterations in cell number between genotypes within fetal erythroid sub-populations S2 and S3, cell morphology between genotypes was unaltered, as assessed by imaging flow cytometry (Figure S2.2A-B). Similar to our observations in the FL, we observed increased numbers of pro-erythroblasts (Ter119^{lo}, Thiazole Orange^{hi}) cells in the peripheral blood of e14.5 *Mtf2*$^{-/-}$ embryos. *Mtf2*$^{-/-}$ Ter119^{hi} Thiazole Orange^{hi} cells that remained in the peripheral blood are more immature than their wild-type counter parts, as indicated by larger size and more centrally located nuclei (Figure S2.2C). There is also a reduction in the number of reticulocytes and mature red blood cells in *Mtf2*$^{-/-}$ e14.5 peripheral blood (0.7% Ter119^{-} DNA^{-} cells versus 1.89% in wild-type), supporting our qualitative observations in blood smears (Figure 2.1G). Together, these observations demonstrate that Mtf2 plays a critical role in erythroid maturation.

Mtf2 is necessary for erythroid maturation in a cell-intrinsic manner

As we found that Mtf2 is expressed in various hematopoietic progenitors (Figure S2.1), we assessed the impact of Mtf2 deficiency on the differentiation potential of progenitors using *in vitro* colony forming unit (CFU) assays. Consistent with the above findings, *Mtf2*$^{-/-}$ embryos contained fewer erythroid progenitors (CFU-E) but more multipotent clonogenic progenitors (CFU-granulocyte, erythrocyte, monocyte, megakaryocyte; or CFU-GEMM) than wild-type embryos, further demonstrating a block in erythroid differentiation potential (Figure 2.2C-D). To address the mechanism underlying the observed erythroblast maturation defect, we first assessed whether cell cycle and apoptosis was normal in *Mtf2*$^{-/-}$ erythroblasts. No increase in Annexin V staining was detected in either *Mtf2*$^{-/-}$ Ter119^{-} or Ter119^{+} cells (Figure 2.2E-F), therefore the reduction in *Mtf2*$^{-/-}$ mature erythroblasts seen in the FL is not due to enhanced apoptosis. *Mtf2*$^{-/-}$ Ter119^{lo} erythroblasts displayed increased cycling with a higher percentage of cells in S phase and a reduced number of cells in G_0/G_1 phase compared to wild-type erythroblasts (Figure 2.2G, Figure S2.2D). Increased proliferation in these erythroblast progenitors may contribute to their differentiation defect, as erythroid maturation is linked to cell cycle exit (Clark, Doyle et al. 2004). Collectively, these data illustrate that Mtf2 is necessary for normal definitive erythropoietic differentiation.

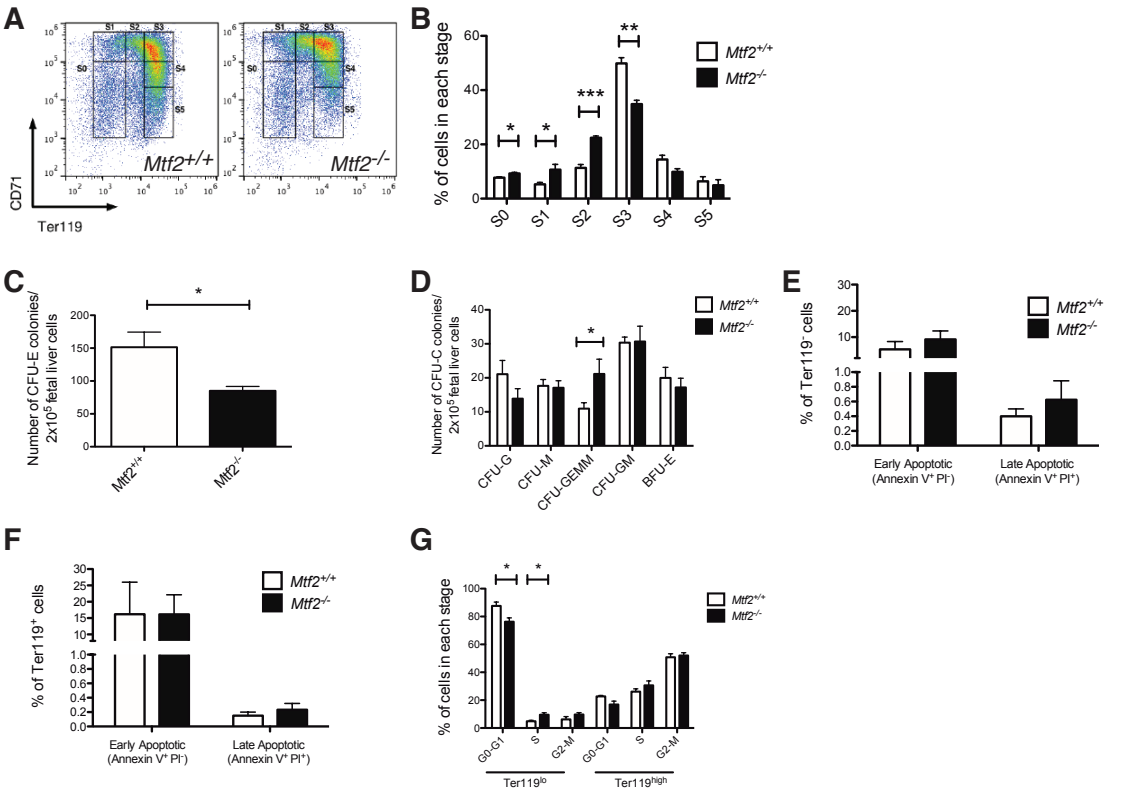

Figure 2.2. Mtf2 is required for normal erythroid differentiation. (**A-B**) *Mtf2*$^{-/-}$ FL cells have increased number of pro-erythroblasts (stages S0-S2) and fewer CD71^{+}Ter119^{+} erythroblasts (stage S3) as determined by flow cytometry analysis. (**C-D**) FL cells from *Mtf2*$^{-/-}$ embryos contain fewer erythroid progenitors (colony forming unit-erythroid, CFU-E) but have higher numbers of multipotent clonogenic progenitors (colony forming unit-granulocyte, erythrocyte, macrophage, megakaryocyte, CFU-GEMM). CFU-G, colony forming unit-granulocyte; CFU-M, colony forming unit-macrophage; CFU-GM, colony forming unit-granulocyte, macrophage; BFU-E, burst forming-unit, erythroid. Data is shown as number of colonies per 2x10^{5} FL cells plated, mean ± SEM for n=4 mice, in

triplicate. (**E**) Ter119^{-} FL cell or (**F**) Ter119^{+} from *Mtf2*$^{-/-}$ embryos do not show an increase in early or late-stage apoptosis, based on Annexin V staining, compared to wild-type littermates. (**G**) A higher number of *Mtf2*$^{-/-}$ Ter119^{lo} pro-erythroblasts are found in S-phase and fewer in G_0/G_1 phase compared to wild-type littermates indicating a defect in cell cycling. Data is shown as mean ± SEM, n=3, *p<0.05, **p<0.01, ***p<0.001.

In our constitutive Mtf2 knockout mouse model, Mtf2 is deleted both in developing hematopoietic cells and in supporting stromal cells of the fetal liver; therefore, we tested whether the role of Mtf2 in erythroid development could be due to the microenvironment, as has been previously attributed to the role of Jarid2 in erythroid maturation (Takeuchi, Yamazaki et al. 1995, Motoyama, Kitajima et al. 1997). Using competitive repopulation (Figure 2.3A), we observed that *Mtf2*$^{-/-}$ and wild-type FL cells were equally capable of homing to the BM 17 hours after injection (Figure 2.3B). Additionally, the contribution of donor derived (CD45.2^{+}) cells in the peripheral blood up to 16 weeks following primary transplant was comparable between genotypes (Figure 2.3C). Strikingly, analysis of erythroprogenitors demonstrated that *Mtf2*$^{-/-}$ donor-derived cells were also defective in erythroid maturation with an accumulation of pro-erythroblasts (ProE) and late basophilic (EryB) erythroblasts (Figure 2.3D). This erythroid maturation delay is similar to that observed in the Mtf2 null embryos and not due to a defect in the FL microenvironment. These data demonstrate that Mtf2, unlike Jarid2, plays a cell-intrinsic role in erythroblast maturation that is not limited to fetal development.

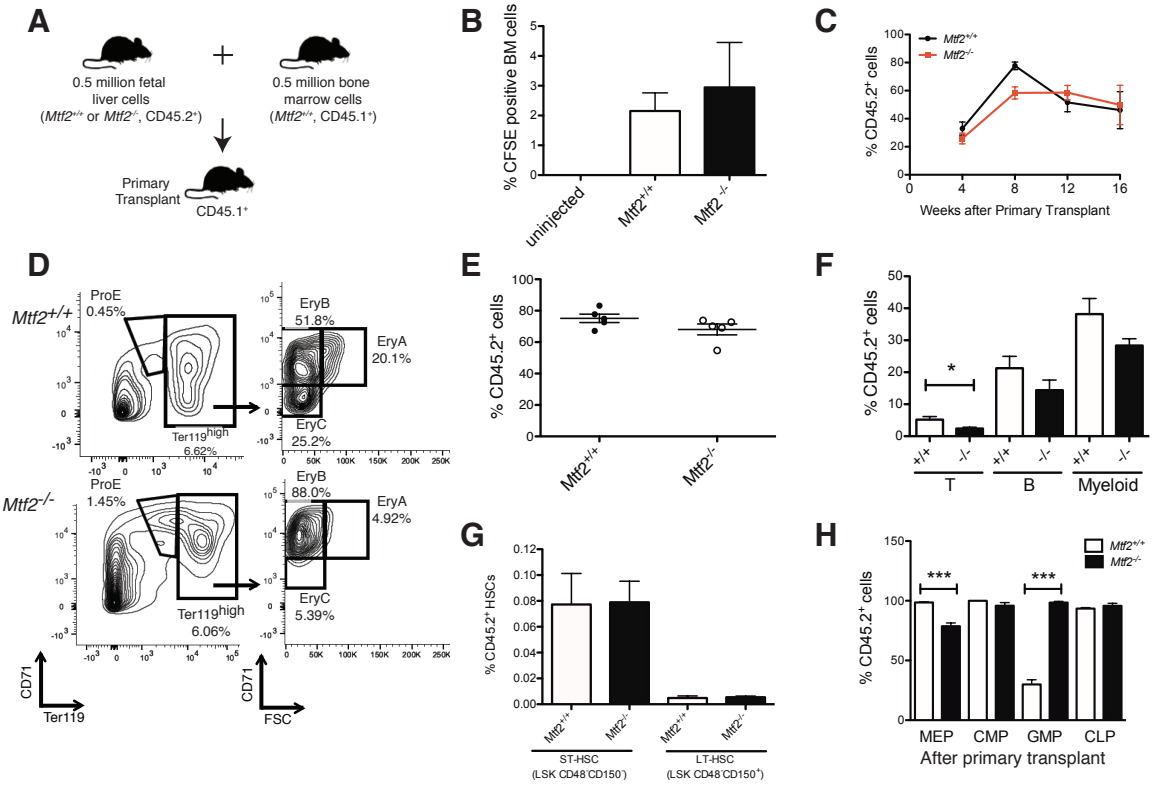

Figure 2.3. Mtf2 deficiency causes a cell-intrinsic erythroid differentiation defect. (**A**) Schematic showing primary repopulation experiments using donor wild-type and *Mtf2*$^{-/-}$ e14.5 FL cells. (**B**) *Mtf2*$^{-/-}$ cells are just as efficient as wild-type cells in homing to the BM 17 hours after tail vein injection. (**C**) The percentage of CD45.2^{+} donor derived cells in the peripheral blood of recipient animals is similar when either wild-type or *Mtf2*$^{-/-}$ FL donor cells are injected. (**D**) Erythroid defects observed in *Mtf2*$^{-/-}$ FL are cell-intrinsic and recapitulated in recipient mice. More *Mtf2*$^{-/-}$ FL donor-derived pro-erythroblasts (ProE), and fewer mature erythroblasts (EryC) were observed compared to *Mtf2*$^{+/+}$ FL donor

cells. (**E**) Total contribution of donor cells in the recipient bone marrow sixteen weeks after transplant, is similar between wild-type and *Mtf2*$^{-/-}$, although fewer *Mtf2*$^{-/-}$ donor T cells (CD4^{+} and/or CD8^{+}) were observed (F). (**G**) No difference is seen in donor-derived short-term and long-term HSCs from either genotype. (**H**) Analysis of various progenitor groups showed the proportion of MEPs derived from *Mtf2*$^{-/-}$ FL cells are significantly reduced in BM after primary transplant while the fraction of GMPs is increased.

Mtf2 is required for HSC self-renewal

Since Mtf2 expression is high in HSCs and progenitors (Figure S2.1), deficiency of Mtf2 in donor FL cells may affect the differentiation into other hematopoietic lineages. Analysis of BM 16 weeks post-transplant demonstrated decreased numbers of *Mtf2*$^{-/-}$ donor derived T cells but no change in donor derived *Mtf2*$^{-/-}$ cells of myeloid or B lineages (Figure 2.3E-F). No difference was observed in the percentage of donor-derived ST-HSCs and LT-HSCs, regardless of donor genotype (Figure 2.3G). *Mtf2*$^{-/-}$ MEPs were significantly decreased in BM 16 weeks post-transplant, while the number of GMPs was increased (Figure 2.3H). Thus, Mtf2 functions to direct cell fate decisions in a lineage-specific manner.

HSC cell fate decisions are highly regulated to ensure lifelong production of hematopoietic lineages, while maintaining a pool of HSCs. To assess the role of Mtf2 in HSC self-renewal, we performed secondary bone marrow transplants (Figure 2.4A). Surprisingly, unlike in primary transplants where total number of donor-derived cells was similar between genotypes, in secondary transplants, total *Mtf2*$^{-/-}$ donor derived cells and erythrocytes in the peripheral blood were appreciably decreased at 8 and 16 weeks post-secondary transplantation (Figure 2.4B,C). This marked difference in repopulation potential demonstrates that Mtf2 regulates the HSC pool and loss of Mtf2 results in stem cell exhaustion. Indeed, *Mtf2*$^{-/-}$ donor-derived short-term and long-term HSCs were also decreased in secondary transplants (Figure 2.4D). Within the significantly decreased *Mtf2*$^{-/-}$ donor cell population in secondary recipients, the

proportion of CMPs, MEPs and GMPs derived from *Mtf2*$^{-/-}$ cells was similar to BM of recipients engrafted with *Mtf2*$^{+/+}$ cells 16 weeks post-secondary transplantation (Figure 2.4E). Interestingly, the fraction of CLPs derived from *Mtf2*$^{-/-}$ cells was significantly increased in the BM following secondary transplant, indicating a role for Mtf2 regulating myeloid and lymphoid commitment (Figure 2.4E).

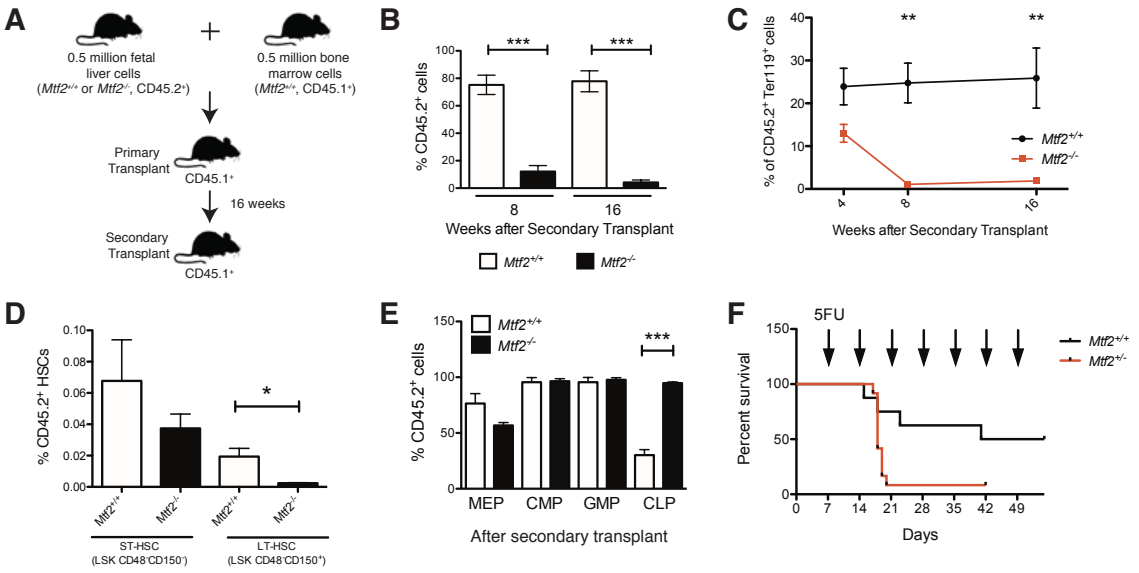

Figure 2.4. Mtf2 is required for self-renewal of HSCs. (**A**) Schematic of secondary reconstitution experiments. (**B**) In secondary transplants, *Mtf2*$^{-/-}$ cells have significantly decreased repopulation potential, demonstrating a requirement of Mtf2 in HSC self-renewal. At 8 and 16 weeks post-transplantation, the numbers of *Mtf2*$^{-/-}$ donor cells are significantly reduced in peripheral blood. (**C**) *Mtf2*$^{-/-}$ donor-derived Ter119^{+} erythroblasts are also greatly reduced in peripheral blood of secondary recipients. (**D**) *Mtf2*$^{-/-}$-derived short-term and long-term HSCs (LSK CD48^{-}CD150^{-} and LSK CD48^{-}CD150^{+}, respectively) were decreased in recipient bone marrow, 16 weeks post-secondary transplant. (**E**) Analysis of various progenitor groups in BM of secondary transplant recipients after 16 weeks indicates the fraction of donor-derived MEPs and GMPs is similar to wild-type but a large increase in the fraction of donor-derived CLPs is observed with *Mtf2*$^{-/-}$ donors. (**F**) *Mtf2*$^{+/-}$ adult mice receiving serial injection of 5FU (120mg/kg, arrows) have a higher

mortality rate than their wild-type littermates (p=0.0267) *p<0.05, **p<0.01, ***p<0.001.

Since the *Mtf2*$^{-/-}$ mice are non-viable and therefore transplants using adult mouse bone marrow lacking Mtf2 are not available, we sought to test HSC self-renewal in *Mtf2*$^{+/-}$ adult mice using serial injections of 5-fluorouracil (5FU), a chemotherapeutic that targets cycling cells (Cheng 2000, Santaguida, Schepers et al. 2009). Assessing hematocrit levels, *Mtf2*$^{+/-}$ adult mice responded normally to a single injection of 5FU (150mg/kg body weight) (Figure S2.8B). Thus, weekly injections of 5FU were delivered to eliminate cycling cells and drive quiescent HSCs into division at a dosage that allowed long-term viability of wild-type mice (Figure 2.4F) (Anderson, Berberovic et al. 2012). *Mtf2*$^{+/-}$ mice showed a dramatic decline in survival after just 2 doses (p<0.0267, Figure 2.4F). Together, the transplant and 5FU data suggest that Mtf2 is required for HSC self-renewal.

Mtf2 regulates core PRC2 members in the hematopoietic system

In ESCs, Mtf2 has been identified as a PRC2 accessory protein as it associates with PRC2 core proteins but does not regulate their expression (Walker, Chang et al. 2010, Casanova, Preissner et al. 2011, Li, Isono et al. 2011). We used *Mtf2*$^{-/-}$ erythroblasts to determine whether Mtf2 regulates the expression of other PRC2 family members. Confirming a null mutation, negligible *Mtf2* transcript was detected in *Mtf2*$^{-/-}$ erythroblasts (p<0.01, Figure 2.5A). At the RNA level, expression of PRC2 family members *Ezh2* and *Suz12* was not significantly affected by Mtf2 deletion; however,

Jarid2 expression was downregulated by approximately 50% in *Mtf2*$^{-/-}$ pro-erythroblasts (p=0.028, Figure 2.5A). We also assessed protein abundance of PRC2 components in sorted primary erythroblasts from individual embryos using capillary electrophoresis immunodetection, enabling protein analysis in very low cell numbers (O'Neill, Bhamidipati et al. 2006, Fan, Deb-Basu et al. 2009). As expected, Mtf2 protein is not detectable in *Mtf2*$^{-/-}$ cells (Figure 2.5B) and there is little change in Ezh1 expression between genotypes, consistent with the low levels of Ezh1 expression during fetal development (Mochizuki-Kashio, Mishima et al. 2011). Surprisingly, Ezh2 and Jarid2 protein levels were significantly decreased in *Mtf2*$^{-/-}$ cells (Figure 2.5B). Technical challenges with Suz12 antibodies prevented assessment by capillary electrophoresis. To confirm this analysis and gain insight into the role of Mtf2 in the adult hematopoietic system, lentiviral-mediated knockdown of Mtf2 in lineage-negative adult mouse bone marrow cells was performed, which resulted in a concomitant decrease in Suz12, Ezh2, and Ezh1 abundance (p<0.001, Figure S2.3A-D). The reduction in PRC2 core proteins indicates that Mtf2 is required for stability of the PRC2 or post-transcriptional regulation of PRC2 protein components in hematopoietic cells, a role more akin to a PRC2 core protein than an accessory protein.

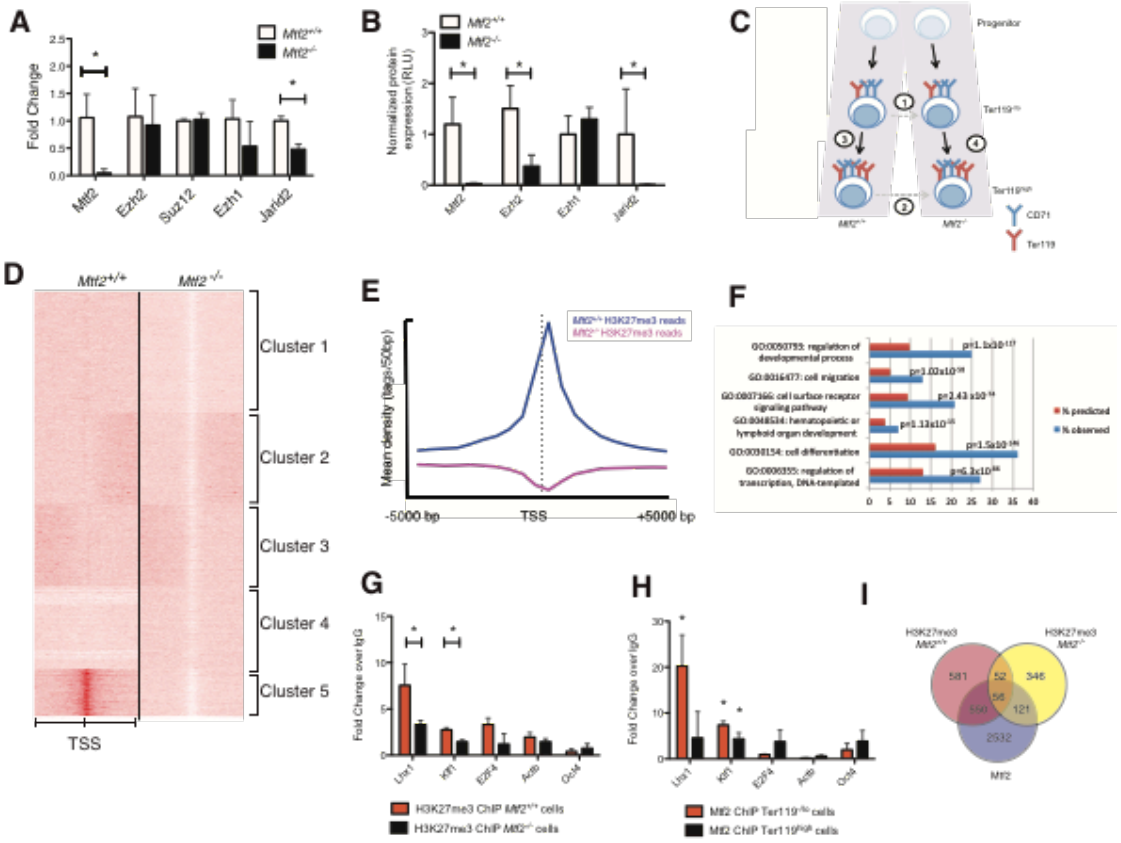

Figure 2.5. Mtf2 regulates core PRC2 protein levels and promoter-proximal H3K27me3 in erythroblasts. (**A**) Transcript expression of PRC2 complex members misregulated in *Mtf2*$^{-/-}$ pro-erythroblasts by qPCR. Levels core PRC2 members Suz12 and Ezh2 are not changed upon knockout of Mtf2. (**B**) Protein expression analysis by capillary electrophoresis in CD45^{+} FL cells shows down-regulation of Ezh2 and Jarid2 in *Mtf2*$^{-/-}$ mice (n=3-7 mice, shown as mean area under the curve ± SEM, normalized to expression in wild-type animals). *p<0.05. (**C**) Schematic of cell types used in RNA-seq and ChIP-seq analyses. Comparisons in gene expression are indicated by numbers and combined with Mtf2 ChIP and changes in H3K27me3 to identify a GRN controlled by the Mtf2/PRC2

axis. (**D**) *k*-mean clustering identifies patterns of H3K27me3 enrichment in primary erythroblasts. Globally, a loss of enrichment centered around transcriptional start sites (TSS) is seen in cells lacking Mtf2. (**E**) H3K27me3 ChIP-seq reads density is plotted within 5kb of the TSS within one cluster of approximately 2400 genes (Cluster 5). In these genes, H3K27me3 binding is specifically reduced immediately around the TSS in Mtf2-null erythroblasts. (**F**) Within Cluster 5, we observe an overrepresentation of genes associated with gene ontology terms for transcription, differentiation and hematopoietic development. (**G**) ChIP-qPCR validation of H3K27me3 levels in wild-type and *Mtf2*$^{-/-}$ erythroblasts, including Lhx1 and Klf1, which lose promoter methylation in the absence of Mtf2. (**H**) Some genes that have lost H3K27me3 in *Mtf2*$^{-/-}$ erythroblasts are also targets of Mtf2 itself, as indicated by Mtf2 ChIP-seq and validation by ChIP-qPCR in wild-type and Mtf2-null erythroblasts. ChIP-qPCR data is shown as mean ± SEM, n=3, normalized to IgG control. *$p<0.05$ **(I)** Overlap of genes associated with binding sites identified by ChIP-seq. 1131 genes have lost H3K27me3 marks upon misregulation of Mtf2/PRC2 and 550 of those targets also show Mtf2 binding.

While reduction of Mtf2 in ESCs affected H3K27me3 levels at particular loci, it did not result in changes in global levels of H3K27me3 (Walker, Chang et al. 2010). Unexpectedly, we observe a global decrease in total H3K27me3 levels upon knockdown of Mtf2 in bone marrow cells ($p<0.001$, Figure S2.3E), suggesting that Mtf2 deficiency, in part through its control of PRC2 core protein levels, results in the loss of PRC2-mediated epigenetic repression.

Mtf2 regulates promoter-proximal H3K27me3 in erythroblasts

To understand the effect of reduced global levels of H3K27me3 at genome resolution, we next analyzed H3K27me3 profiles by ChIP-seq as a functional consequence of Mtf2 deficiency. We performed H3K27me3 ChIP in cells from two distinct stages of erythropoiesis (Figure 2.5C), FL-derived $CD71^{+}Ter119^{-/lo}$ (stage S1&S2) pro-erythroblasts and $CD71^{+}Ter119^{high}$ (stage S3) erythroblasts from *Mtf2*$^{-/-}$ and wild-type e14.5 embryos. We chose these two fractions of cells since they flank the block in erythroid development we observe in Mtf2 deficient mice (Figure 2.2A-B).

To characterize the binding patterns of H3K27me3 within our wild-type and knockout erythroblasts, we used unsupervised *k-means* clustering to group genes with similar methylation patterns. In wild-type erythroblasts, we observe H3K27me3 binding across promoter regions and gene bodies. To corroborate our findings, we sampled publicly available H3K27me3 binding from $Ter119^{+}$ primary erythroblasts (ENCODE)(Consortium 2007) at a read-depth similar to our sequencing and observed a

very similar enrichment pattern as our wild-type erythroblasts (Figure S2.4A-B). Additionally the majority of genes associated with peaks identified in our wild-type cells overlap with publicly available data (Figure S2.4C), providing confidence that our results are comparable to published data. Next, we compared our H3K27me3 ChIP-seq enrichment patterns from *Mtf2*$^{+/+}$ erythroblasts to *Mtf2*$^{-/-}$ erythroblasts. By visualizing read density over an area 5kb up and downstream from the transcriptional start site (TSS) of each gene, and normalizing read depth between samples, we observe that Mtf2-null cells display a genome-wide loss of H3K27me3 specifically around the TSS (Figure 2.5D). This is even more evident by choosing one cluster (Cluster 5) and plotting read density within 5kb of the TSS (Figure 2.5E), clearly demonstrating specific loss of H3K27me3 at promoter-proximal regions. Over multiple iterations of clustering, we identified 2404 genes to have very strong H3K27me3 binding at the promoter region of wild-type erythroblasts, which is virtually eliminated in erythroblasts lacking Mtf2 (Table S1). This group of 2404 genes is highly enriched for master regulators of many biological processes including members of the Hox, Wnt, Gata and Lhx families. Genes from this group are strongly associated with regulation of transcription, cell differentiation and hematopoietic development (Figure 2.5F). Loss of H3K27me3 in *Mtf2*$^{-/-}$ erythroblasts at particular targets was confirmed by ChIP-qPCR (Figure 2.5G).

Mtf2 recruits PRC2 to chromatin; therefore, we analyzed Mtf2-chromatin interactions using ChIP-seq, followed by ChIP-qPCR validation to determine direct targets of Mtf2 in erythroid cells (Figure 2.5H). Over 72% of genes harboring H3K27me3 marks in wild-type cells had reduced H3K27me3 in *Mtf2*$^{-/-}$ pro-erythroblasts and half of

these genes were bound by Mtf2 at this stage of development (Figure 2.5I). Interestingly, genes associated with Mtf2 binding peaks in $CD71^{+}Ter119^{-/lo}$ pro-erythroblasts or $CD71^{+}Ter119^{high}$ erythroblasts show very little overlap with Mtf2 or other PRC2 binding profiles in ESCs (Peng, Valouev et al. 2009, Walker, Chang et al. 2010, Hunkapiller, Shen et al. 2012) (Figure S2.5A-D), demonstrating that it is critical to study transcription factor or chromatin remodeler binding in a tissue-specific context. *De novo* motif analysis of Mtf2 promoter occupancy in ESCs (Stanford lab, unpublished data) or erythroblasts (Figure S2.6) failed to reveal a consensus-binding motif. GC-rich binding regions are enriched in Jarid2 and Phf19 binding sites in mESCs but a specific binding motif has not been reported. Together this suggests that PRC2 binding through accessory proteins may be loosely defined for the purpose of acting on different targets in different cell types. Recognizing that ChIP-seq only provides a snapshot of transcription factor binding, we classified genes that lost H3K27me3 in Mtf2 null cells as "Mtf2-PRC2 targets", although not necessarily direct Mtf2 targets, and used this data as a first step in mapping the molecular mechanisms behind the hematopoietic defects observed in Mtf2 null mice.

Mtf2 controls gene regulatory networks critical for hematopoietic function

To assess the impact of Mtf2 deficiency upon transcriptional regulation of erythropoiesis, we used RNA-seq profiling of fetal liver erythroprogenitors from the same stages outlined for our ChIP-seq studies (Figure 2.5C). More than 1200 genes were significantly misregulated (p<0.05, Benjamini-Hochberg corrected) in $CD71^{+}Ter119^{-/lo}$

Mtf2$^{-/-}$ pro-erythroblasts compared to wild-type pro-erythroblasts (Figure 2.5C, comparison 1). Since these changes in gene expression occur prior to the block in erythroid development, they likely represent manifestation of early changes in hematopoietic progenitors that contribute to the defect in erythroid maturation. Of the most significantly regulated genes (p<0.01), nearly all (739/751) were upregulated in *Mtf2*$^{-/-}$ pro-erythroblasts, consistent with the role of Mtf2 as a transcriptional repressor. While fewer e14.5 *Mtf2*$^{-/-}$ fetal liver cells develop to the CD71^{+}Ter119^{high} erythroblast stage compared to their wild-type counterparts (34.9±1.4% versus 49.9±2.1%), the cells that do express CD71^{+}Ter119^{high} differ significantly between genotypes, with over 2200 genes differentially expressed in *Mtf2*$^{-/-}$ CD71^{+}Ter119^{high} cells (Figure 2.5C, comparison 2). Functional analysis of transcriptomic data from early and late erythroid precursors indicates that Mtf2 deficiency results in misregulation of apoptosis, protein transport, stress response, and immune response transcriptional networks in addition to expected hematopoietic development networks (Figure 2.6A). Further analysis of genes related to apoptosis revealed approximately equal numbers of pro- and anti-apoptotic genes that were significantly upregulated in *Mtf2*$^{-/-}$ pro-erythroblasts and erythroblasts. This, taken together with our observations that apoptosis levels are not changed in Mtf2-null erythroblasts (Figure 2.2F-G), suggests that lack of Mtf2 does not lead to overt change in levels of apoptosis in erythroprogenitors. Similarly, we observed no difference in apoptosis in stem and progenitor cells (LSK) from *Mtf2*$^{-/-}$ mice (Figure 2.6B).

We also considered the possibility of Mtf2 directly controlling expression of other PRC2 proteins. Interestingly, despite a reduction in expression level of Jarid2, we

did not detect any PRC2 components in our Mtf2 ChIP-seq analysis, suggesting transcriptional control of Jarid2 is not directly controlled by Mtf2.

To model the effects of Mtf2 on erythroblast maturation, we integrated our RNA-seq, Mtf2 ChIP-seq and H3K27me3 ChIP-seq data to draft a gene regulatory network (GRN) controlled by Mtf2-PRC2. We also integrated known targets of key transcription factors *Gata1, Gata2, Tal1, Lmo2, Gfi1b, Fli1, Klf1,* and *Sfpi1* in erythroblasts or hematopoietic progenitors (Kassouf, Hughes et al. 2010, Knezevic, Bee et al. 2011, Pilon, Ajay et al. 2011, Wontakal, Guo et al. 2011, Wu, Cheng et al. 2011) to place our data in context of known regulatory modules controlled by master transcriptional regulators. We first drafted a GRN that describes epigenetic alterations and transcriptional changes in genes during early erythroid development using data from our $CD71^{+}Ter119^{-/lo}$ cells (Figure 2.6C). This GRN encodes 78 genes (Table S2), and is significantly enriched for genes associated with gene ontology terms for cell differentiation and gene transcription (Figure 2.6D). Of particular interest to our system are developmental regulators such as *Gata2*, *Gfi1*, *Pbx1*, and *Prox1* (Figure S2.4D, Table S2). H3K27me3 is lost at each of these genes via dysregulation of the Mtf2/PRC2 axis, and some, like *Reln* and *Hdac9* are also direct Mtf2 targets.

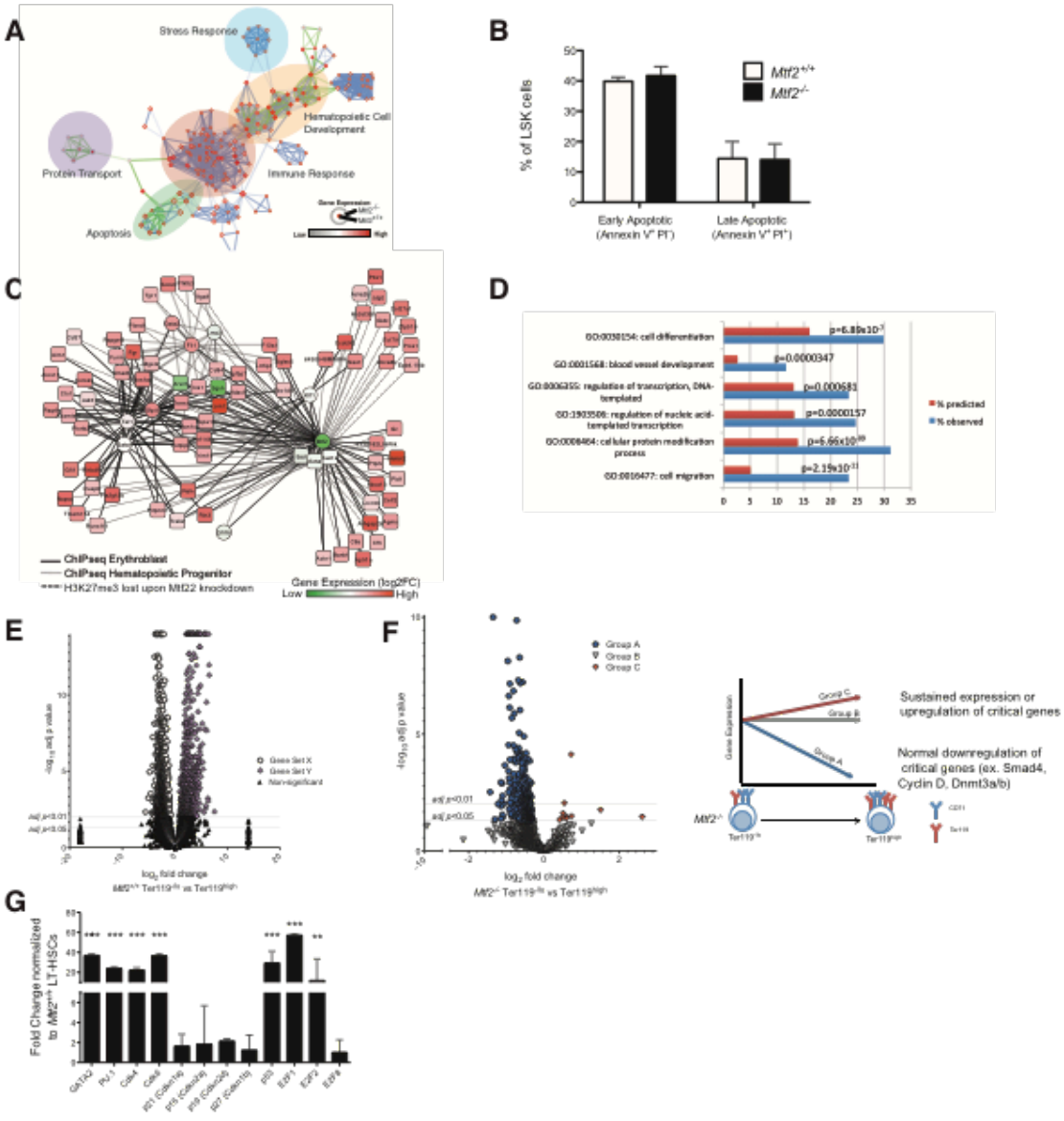

Figure 2.6. Mtf2-PRC2 hematopoietic gene regulatory networks regulate erythroid maturation and HSC self-renewal. (**A**) Enrichment map analysis using ontology terms of gene sets commonly misregulated in *Mtf2*$^{-/-}$erythroblasts shows many dysregulated genes are associated with immune response, apoptosis and HSC differentiation. (**B**) *Mtf2*$^{-/-}$ stem and progenitor cells (LSK) cells do not show an increase in early or late-

stage apoptosis, based on Annexin V staining, compared to wild-type littermates. (**C**) A gene regulatory network depicting genes regulated by PRC2 via loss of H3K27me3 (dotted lines) or by both loss of H3K27me3 and direct Mtf2 binding (solid lines). Gene expression in *Mtf2*$^{-/-}$ Ter119$^{-/lo}$ pro-erythroblasts is shown as node color. Binding of other key transcription factors in erythroblasts (solid lines) or hematopoietic progenitors (hatched lines) are included. (**D**) Mtf2-PRC2 controls genes associated with transcription, migration and cell differentiation. (**E**) During wild-type differentiation from CD71^{+}Ter119$^{-/lo}$ erythroblasts to CD71^{+}Ter119^{high} erythroblasts, the expression of some genes are significantly upregulated (Gene Set Y, purple diamonds) while others are repressed (Gene Set X, white circles). Black triangles indicate expression changes below significance threshold of p<0.05. (**F**) Genes normally repressed during erythroblast differentiation are not properly regulated in Mtf2-deficient cells. Examining expression of Gene Set X in *Mtf2*$^{-/-}$ cells, a minor fraction of genes is downregulated as in wild-type cells (Group A, blue circles). The majority of genes in Gene Set X are either not significantly regulated upon loss of Mtf2-PRC2 (Group B, grey triangles) or significantly upregulated (Group C, red diamonds), indicating a loss of epigenetic repression. (**G**) Using the erythroid GRN to identify nodes controlled by Mtf2, we tested expression of these nodes in *Mtf2*$^{-/-}$ HSCs. LT-HSCs (LSK CD48^{-}CD150^{+}) isolated from *Mtf2*$^{+/+}$ and *Mtf2*$^{-/-}$ e14.5 FL show upregulation of master transcription factors such as Gata2, PU.1 and many cell cycle regulators. Data is shown as mean ± SEM, n=3, *p<0.05, **p<0.01, ***p<0.001.

As wild-type erythroblasts mature from the S2 ($CD71^{+}Ter11^{-/lo}$) to S3 stage ($CD71^{+}Ter119^{high}$), many cell fate determinants including cell cycle regulators (e.g., Cdk6 and Cyclin D) and epigenetic modulators (e.g., Dnmt3a/b, Jmjc1d) are transcriptionally repressed (Figure 2.6E, Gene Set X, white circles), while other genes involved in metabolism, heme biosynthesis and coagulation are upregulated (Figure 2.6E, Gene Set Y, purple diamonds). In Mtf2 deficient erythroblasts, only a minor fraction of genes were downregulated as in wild-type cells (Figure 2.6F, Group A). However, approximately 85% of genes within Set X (including *Cdk4, Cdk6*, *Stat5a*, *Stat5b*, *Atm*, *p53*, *Bak, Casp3* and *Dnmt3b*) were either unchanged (Figure 2.6F, Group B) or were significantly de-repressed in *Mtf2*$^{-/-}$ erythroblast differentiation (Figure 2.6F, Group C; Table S3). Integrating genes with abnormal expression (Groups B & C) with our known Mtf2 targets (from our Mtf2 ChIP data and loss of H3K27me3) we define a group of genes that is not appropriately downregulated during late erythroblast differentiation. This GRN of over 100 genes includes epigenetic regulators (Dnmt3a/b, Jmjc1d) and cell cycle regulators (Cyclin D) (Figure S2.7A). Loss of Mtf2-PRC2 and subsequent downstream misregulation of other epigenetic regulators and cell cycle modulators within the Mtf2-PRC2 GRN, including components of the Cyclin D-Cdk4/6-Rb pathway, could affect cycling and result in observed phenotypes in our *Mtf2*$^{-/-}$ erythroblasts and HSCs. We observed upregulation of cell cycle regulators such as E2F2 and p21 (Cdkn1a), confirmed by qPCR, in *Mtf2*$^{-/-}$ erythroblasts (Figure S2.7B). Together, these data implicate Mtf2 in controlling erythroid differentiation both through H3K27me3-mediated repression by

the PRC2 and through secondary effects stemming from misregulation of PRC2 direct targets.

As GRNs are modular by design (Alon 2007, Walker and Stanford 2009), drafting the Mtf2-PRC2 GRN of erythroblasts also allows us to identify regulatory modules that potentially regulate HSC self-renewal. Based on our erythroblast GRN, we hypothesized that loss of epigenetic regulation of cell cycle and developmental regulators also underlies defective HSC self-renewal. To test this hypothesis, we isolated enriched LT-HSCs by FACS from wild-type and *Mtf2*$^{-/-}$ e14.5 FL and assessed mRNA expression of these candidate genes by qPCR. Consistent with our model, we observed increased expression of transcriptional regulators *Gata2* and *PU.1* in *Mtf2*$^{-/-}$ LT-HSCs (Figure 2.6G). While we observed little overexpression of Cdkn family members, cell cycle regulators including *Cdk4, Cdk6, p53, E2F1* and *E2F2* were highly overexpressed in *Mtf2*$^{-/-}$ LT-HSCs (Figure 2.6G). Expression of other members of the E2F family such as *E2F8* remained comparable to wild-type HSCs. The overexpression of many members of the cell cycle pathway, including *Cdk4*, *Cdk6,* and *E2F1*, promote decreased HSC quiescence or increased progression through the cell cycle (Saito, Helin et al. 1995, Gala, Marreiros et al. 2001, Matushansky, Radparvar et al. 2003, Laurenti, Frelin et al. 2015, Mende, Kuchen et al. 2015) and may underlie the HSC exhaustion phenotype and sensitivity to repeated 5FU doses observed in our *Mtf2*$^{-/-}$ mice.

Reduced expression of Mtf2 contributes to blast expansion in a model of erythroleukemia

De-repression of the Mtf2-PRC2 GRN in Mtf2 deficient erythroblasts led to a loss of promoter proximal H3K27me3 in a set of genes involved in cancer (KEGG pathway mmu05200: Pathways in cancer, Bonferroni correction: 1.98 $x10^{-17}$) including upregulation of oncogenes and cell cycle regulators. Therefore, we investigated the effect of reduced Mtf2 expression in cancer development using the Friend virus (FV) erythroleukemia model (Subramanian, Hegde et al. 2008, Hegde, Hankey et al. 2012). The two-stages of Friend Virus infection – first the proliferation of splenic erythropoietin (Epo)-independent erythroid progenitors (BFU-Es) followed by the secondary development of transformed clones - provides an excellent model of other hematological malignancies, such as acute myeloid leukemia (AML), that are thought to arise from a two-hit model (Moreau-Gachelin 2006). This well-defined leukemia model also allows us to quantify changes in pre-leukemic progenitors and transformed cells, providing insight into both stages of disease progression.

Heterozygous *Mtf2*$^{+/-}$ adult mice did not display any overt changes in hematological, including erythroid, parameters compared to wild-type adult mice (Table S4) and stressing the mice by induction of hemolytic anemia via a single injection of phenylhydrazine did not affect hematocrit recovery kinetics, suggesting adult *Mtf2*$^{+/-}$ mice have normal extramedullary hematopoiesis (Figure S2.8A). Additionally, isolated splenocytes from wild-type or *Mtf2*$^{+/-}$ mice produce the same number of BFU-E colonies (Figure 2.7A). Therefore, we reasoned that *Mtf2*$^{+/-}$ mice represent an appropriate model

to assess the impact of reduced Mtf2 expression on leukemic progression. Two weeks following infection with FV, *Mtf2*$^{+/-}$ mice exhibited increased numbers of Epo-independent BFU-E colonies compared to wild-type controls (Figure 2.7A). This suggests that Mtf2 regulates the formation and expansion of preleukemic progenitors during the first stage of FV infection. As expected, all mice developed polycythemia and splenomegaly; however, at 4 weeks post-infection, hematocrits were higher and spleen size significantly larger in the *Mtf2*$^{+/-}$ mice (Figure 2.7B-D) and some infected heterozygous *Mtf2*$^{+/-}$ mice died due to splenic hemorrhage ($p<0.03$, Figure 2.7E). Splenocytes were isolated and numbers of leukemic stem cells (LSCs) and transformed progenitors were analyzed by flow cytometry and colony assays, respectively. Although the frequency of virus-transformed LSCs (cKit^{+}Sca1^{+}CD133^{+}) was not significantly different between heterozygous *Mtf2*$^{+/-}$ and wild-type spleens (1.03±0.27% and 0.84±0.19%, respectively), *Mtf2*$^{+/-}$ splenocytes formed more growth factor independent transformed CFU-FV, which are functionally similar to blast cells as they do not differentiate (Figure 2.7F). Together, these data suggest that decreased Mtf2 expression causes increased formation of preleukemic progenitors that are the targets of FV infection leading to expansion of blast cells. Additionally, misregulation of the Mtf2-PRC2 axis, as described above, could lead to changes in cell cycling, allowing *Mtf2*$^{+/-}$ splenocytes to accumulate more p53 mutations. This is consistent with the increased number of CFU-FV colonies observed in Mtf2 deficient mice leading to a more aggressive leukemia. Taken together, Mtf2, through control of the PRC2 complex,

governs gene regulatory networks critical for hematopoietic development and homeostasis.

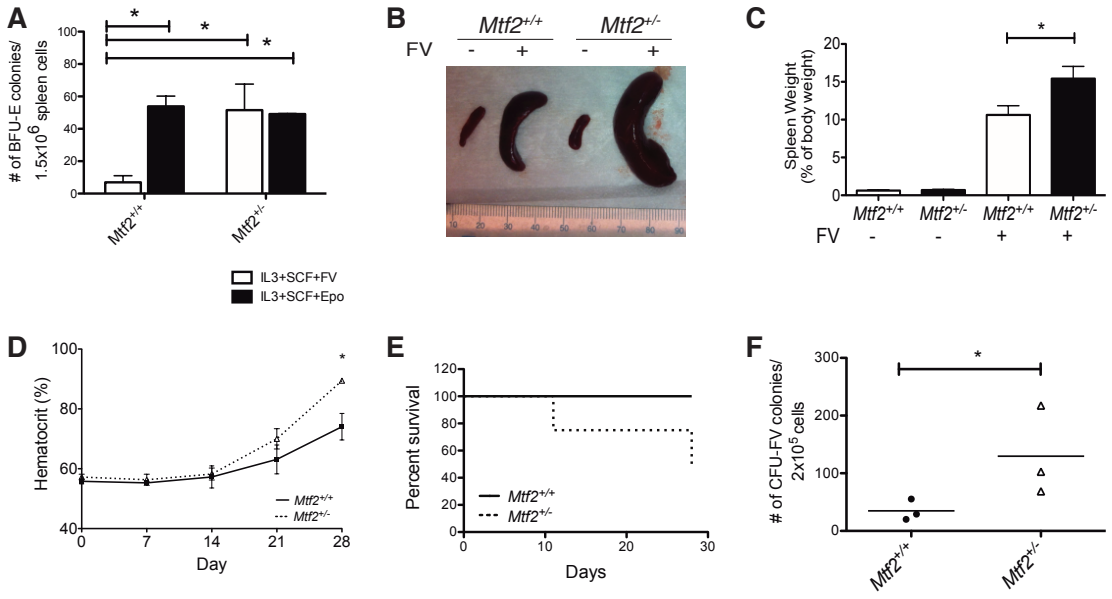

Figure 2.7. Misregulation of Mtf2 alters the progression of erythroleukemia. (**A**) In a Friend virus model of erythroleukemia, adult *Mtf2*$^{+/-}$ mice display greater numbers of BFU-E colonies arising from infected splenocytes after 14 days of infection. FV-infected *Mtf2*$^{+/-}$ mice have exacerbated effects including (**B-C**) increased splenomegaly, and (**D**) increased polycythemia at 4 weeks post-infection. (**E**) FV-infected *Mtf2*$^{+/-}$ mice also have increased mortality, compared to wild-type littermates infected with virus (p=0.03). (**F**) 2x10^5 splenocytes from mice infected with Friend virus were cultured in methylcellulose media without exogenous growth factors. *Mtf2*$^{+/-}$ mice infected with Friend virus form an increased number of growth-factor independent colonies (n=3 in duplicate). Together these data indicate an increase in the number of progenitor cells transformed by the virus. *p<0.05.

Discussion

Using a systems genetics approach, we uncovered a unique and fundamental role for Mtf2 in erythrocyte differentiation and HSC self-renewal via PRC2-mediated epigenetic repression of differentiation and proliferation programs (Figure 2.8). For the first time, we have discovered that PRC-related proteins may control cell fate by functioning as an accessory protein in one cell type, but a core PRC member in another. We have shown that a PRC2 protein other than a core protein is required for normal abundance of other PRC2 proteins and is required for region-specific methylation (in this case, promoter proximal H3K27me3 as opposed to gene bodies or telomeric regions). Furthermore, the regulation of Ezh2, Suz12 and H3K27me3 by Mtf2 was not previously observed in ESCs, demonstrating distinct functional roles by Mtf2 in two different cell lineages in which it regulates cell fate decisions.

Core PRC2 proteins Eed, Suz12 and Ezh2 are required for PRC2 stability such that the loss of any of the core proteins results in post-transcriptional loss of the PRC2 (Pasini, Bracken et al. 2004, Montgomery, Yee et al. 2005, Fiskus, Pranpat et al. 2006). In contrast, individual PRC2 accessory proteins by definition are not required for complex stability and function. Surprisingly we found that, as in *Suz12*$^{-/-}$ mice (Pasini, Bracken et al. 2007, Lee, Miller et al. 2015), knockout of Mtf2 reduced protein expression of both Ezh2 and Jarid2 within the fetal liver hematopoietic cells, redefining the role of Mtf2 as a core-like PRC2 protein in hematopoiesis.

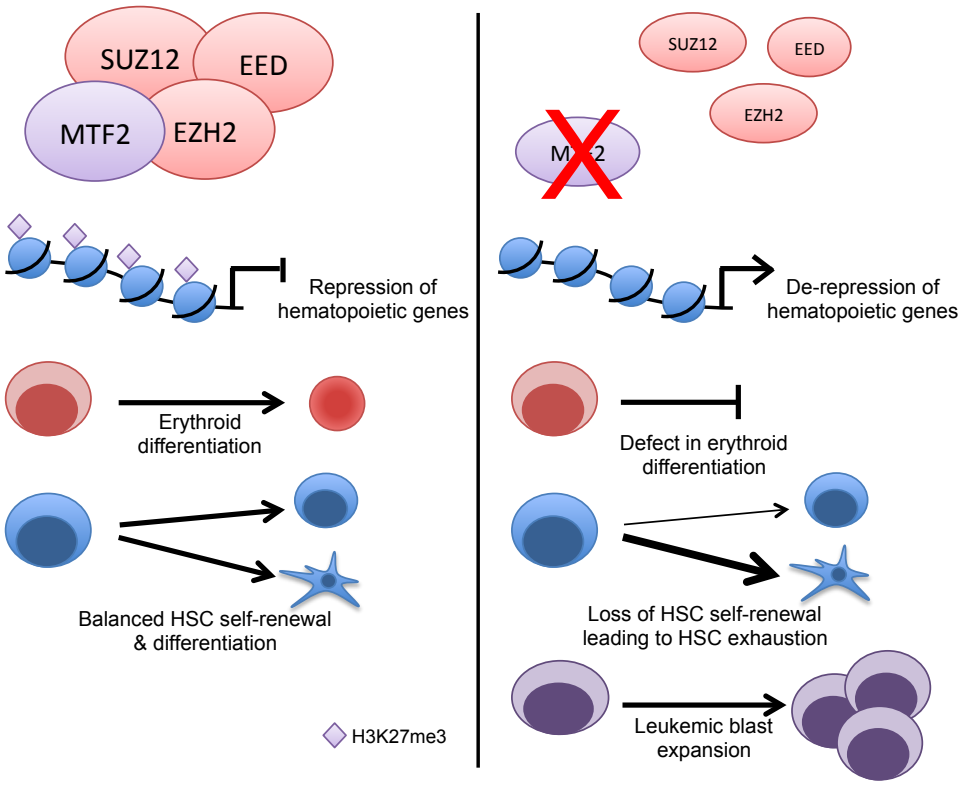

Figure 2.8. A model of Mtf2-PRC2 in hematopoiesis. Mtf2 regulates erythroid differentiation and HSC self-renewal via its interaction with the PRC2 complex. Loss of Mtf2 (right) leads to reduced levels of core PRC2 proteins, global loss of H3K27me3 and de-repression of key transcription factors that control erythroid maturation, HSC self-renewal and proliferation.

Supporting our results in primary Mtf2 null cells is the observed downregulation of core PRC2 proteins and H3K27me3 levels after knockdown of Mtf2 in mouse HSPCs. As homologs of Ezh each play unique roles in embryonic and adult hematopoietic tissue (Mochizuki-Kashio, Mishima et al. 2011), our data demonstrate that Mtf2 regulates both Ezh homologs, Ezh2 in fetal liver-derived erythroblasts and Ezh1 in adult bone marrow cells. Regulation of core complex members has not been observed for other PRC2 accessory proteins such as Jarid2 and this unique role of Mtf2 places it as a PRC2 essential member in the hematopoietic system.

Another unique feature we uncovered for Mtf2 is its cell-intrinsic role in hematopoietic development. While core components of PRC2 have significant roles in regulating hematopoiesis (Su, Basavaraj et al. 2003, Majewski, Blewitt et al. 2008, Mochizuki-Kashio, Mishima et al. 2011, Kinkel, Galeev et al. 2015), little is known about the role of PRC2 accessory proteins in hematopoietic development. Knockout of Jarid2 (Takeuchi, Yamazaki et al. 1995) leads to anemia during late stage embryonic development, although this effect was strain dependent (Motoyama, Kitajima et al. 1997, Kitajima, Kojima et al. 1999). Moreover, the effects of Jarid2 on erythroid development were attributed to a microenvironment defect since mice repopulated with Jarid2 mutant cells demonstrated normal erythropoiesis. Recently, depletion of Jarid2 in hematopoietic stem and progenitor cells (HSPCs) was shown to enhance repopulation capacity in primary transplants (Kinkel, Galeev et al. 2015). In contrast to Jarid2, Mtf2 is required cell-intrinsically for erythropoiesis as the erythroid differentiation defects observed in Mtf2 null embryos were recapitulated in

transplanted mice. This further supports a role for Mtf2 as an indispensable PRC2 component within the hematopoietic system.

In ESCs, Mtf2 recruits the PRC2 to a subset of PRC2 target loci, resulting in higher H3K27me3 at those loci (Walker, Chang et al. 2010, Casanova, Preissner et al. 2011). Once we determined that Mtf2 was required for erythroid development and self-renewal of HSCs, we predicted that Mtf2 would function to target PRC2 to only a subset of PRC2 targets and would play a sub-stoichiometric role in the PRC2. Unexpectedly, however, we show widespread loss of H3K27me3 at promoter-proximal regions in *Mtf2*$^{-/-}$ erythroblasts. Presence of the H3K27me3 mark relies on balance between deposition by Ezh2 and removal by Utx/Jmj3; therefore, the overexpression of the histone demethylase Kdm6a (Utx) could theoretically lead to the observed loss of H3K27me3, although at least in ESCs Utx and Ezh2 share only a small subset of targets (Wang, 2010). However, Utx transcript levels are normal in *Mtf2*$^{-/-}$ erythroblasts and HSCs; thus, the loss of epigenetic regulation observed in the hematopoietic lineages of Mtf2 null cells is likely due directly to Mtf2-mediated loss of PRC2. Histone methylation at promoter regions has often been associated with bivalent genes and loss of H3K27me3 is associated with gene activation. H3K27me3 levels at transcriptional start sites are therefore critical for proper gene regulation. In addition to H3K27me3-mediated repression, transcriptional regulation relies on multiple levels of epigenetic modifications of both histones and DNA. Since erythroid cells rapidly lose genome-wide DNA methylation as they differentiate (Shearstone, Pop et al. 2011), they may be more sensitive to changes in histone methylation as a means to regulate gene repression. The

relationship between DNA methylation and H3K27me3 recruitment is still poorly understood but loss of DNA methylation in ESCs leads to widespread re-distribution of H3K27me3 patterns (Reddington, Perricone et al. 2013) and sites of *de novo* H3K27me3 recruitment (Lynch, Smith et al. 2012) resulting in gene expression changes. Perturbations in PRC2-mediated epigenetic repression via Mtf2 may result in more profound effects in erythroblasts as they rely less on DNA methylation as a method of gene silencing during differentiation. Both the variable expression of epigenetic modulators across cell types along with the limited overlap of Mtf2/PRC2 occupancy in mouse ESCs and hematopoietic cells (Fig S2.5) demonstrate that the GRNs maintained by epigenetic complexes such as Mtf2-PRC2 are context dependent and need to be studied in a tissue-specific manner.

We used a systems genetics approach to analyze the function of Mtf2-PRC2, combining gene targeting, cellular phenotyping and molecular phenotyping using RNA-seq, Mtf2 ChIP-seq and H3K27me3 ChIP-seq at two developmental stages of erythroid development. We hypothesize that genes differentially expressed between Mtf2 wild-type and null Ter119$^{-/lo}$ pro-erythroblasts are composed of genes critical to early erythroid differentiation including genes important in cell adhesion (*Reln*) and embryonic organ development (*Gata2, Gfi1*). Previous studies have described roles for each of these genes in early embryonic development. For example, Reelin (*Reln*) negatively regulates erythroid development and *Reln*$^{-/-}$ mice have increased erythroid differentiation (Chu, Lee et al. 2014). *Gfi1* has been shown to regulate erythroid maturation via repression of Id2 (Kim, Klarmann et al. 2014). Downregulation of *Gata2* is

normally required for erythroid differentiation (Ikonomi, Rivera et al. 2000) but it remains highly expressed during *Mtf2*$^{-/-}$ erythroid maturation. With *Gata2* expression remaining high, target genes may continue to be bound by GATA2 not allowing GATA1 occupation. This important "factor switching" is critical for hematopoietic development (Suzuki, Kobayashi-Osaki et al. 2013) and has recently been shown to be implicated in proper PRC2 expression during erythropoiesis (Xu, Shao et al. 2015). Together, misregulation of multiple nodes of Mtf2 GRN in Ter119$^{-/lo}$ pro-erythroblasts, including overexpression of *Reln, Gfi1* and *Gata2*, may underlie the defective erythroid maturation phenotype observed in *Mtf2*$^{-/-}$ animals. We also analyzed our transcriptomic data as a time course, concentrating on genes that are not properly repressed during Mtf2-deficient erythroblast differentiation. Using Gene Ontology analysis, we identified misregulated genes involved in transcription, translation, cell cycle regulation (for example *Cdk4*, *Cdk6*) and pro- and anti-apoptosis (*Bcl family, Bak*). Together with our findings that *Mtf2*$^{-/-}$ erythroblasts and HSCs do not have increased Annexin V staining, the phenotypes we observe in *Mtf2*$^{-/-}$ animals are not due to apoptosis, but rather changes in cell cycle and differentiation. Master transcription factors and cell cycle regulators are known targets of canonical PRC2 repression, again highlighting how Mtf2 plays an indispensible core protein-like role in regulating PRC2-mediated H3K27me3 deposition at promoter-proximal regions in hematopoietic cells.

Competitive repopulation experiments suggest that Mtf2 is required for HSC self-renewal. Thus, we used our draft erythroid Mtf2-PRC2 GRN to elucidate the molecular pathways that underlie the self-renewal defect in Mtf2 deficient HSCs. Many genes

identified in our erythroid GRN, were upregulated in primary LT-HSCs isolated from *Mtf2*$^{-/-}$ mice and are known regulators of hematopoietic differentiation. For example, *Gata2* regulates the expansion and function of HSCs in a dose-dependent manner (Ling, Ottersbach et al. 2004). PU.1/Sfpi1 is also critical for HSC self-renewal and differentiation. While PU.1 expression is necessary for HSC self-renewal (Arinobu, Mizuno et al. 2007), expression of PU.1 is low in HSCs and increases as cells differentiate to a multi-potent progenitor stage (Iwasaki, Somoza et al. 2005). Upregulation of PU.1 in *Mtf2*$^{-/-}$ LT-HSC could contribute to defective self-renewal. As well, precise control of cell cycle regulators in HSCs is critical for both maintenance of quiescence during homeostasis and periods of rapid expansion after stress. For instance, altered expression of *Cdk4*, *Cdk6* or *p53* has significant effects on HSC activity (Malumbres, Sotillo et al. 2004, Dumble, Moore et al. 2007). Exogenous expression of Cdk6 in leukemic cells promotes continued cell cycling, even in the presence of cell cycle inhibitors. Recently, overexpression of CDK6 in human HSCs has been shown to control exit from quiescence (Laurenti, Frelin et al. 2015). Misregulation of multiple inputs of the cell cycle pathway may underlie an enhanced exit from quiescence or increase cycling in our *Mtf2*$^{-/-}$ HSCs and can contribute to the HSC exhaustion phenotype observed. In LT-HSCs deficient in Mtf2, perturbations in large gene networks regulated by PRC2 may result in non-significant changes in common cell cycle regulators like Cdkn2a and 2b. Our observation of high levels of Cdk4, Cdk6 and members of the E2F family suggests regulation of certain cell cycle genes within our Mtf2-PRC2 GRN

underlies the defects observed in both erythroid maturation and HSC self-renewal in Mtf2 deficient mice.

Dysregulation of genes controlling cell cycle progression often drive altered response to anti-growth signals or contribute to the gain of limitless replicative potential, two of the well-described hallmarks of cancer (Hanahan and Weinberg 2000, Hanahan and Weinberg 2011). While previous studies have concentrated on the role of core PRC2 complex member in cancer progression (Visser, Gunster et al. 2001, Ernst, Chase et al. 2010, Morin, Johnson et al. 2010, Nikoloski, Langemeijer et al. 2010, Brecqueville, Cervera et al. 2011, Sasaki, Imaizumi et al. 2011, Neff, Sinha et al. 2012, Tanaka, Miyagi et al. 2012, Beguelin, Popovic et al. 2013), little is known about the role of PRC2 accessory proteins during oncogenic progression. Since our data shows Mtf2 functions in both stem and progenitor cells, we use the Friend virus erythroleukemia model to study the role of Mtf2 in cancer progression as it is well-defined model of leukemia that allows quantification of both affected stem and progenitor cells and provides a good model for other two-hit hematopoietic malignancies, like AML. We demonstrate that, upon infection with FV, reduced Mtf2 expression leads to a massive polyclonal erythroid expansion, resulting in increased morbidity and mortality. We do not observe increased leukemic stem cell self-renewal in our *Mtf2*$^{+/-}$ virus-infected mice but surprisingly detect more transformed cells that have been associated with loss of p53 (Hegde, Hankey et al. 2012). The role of Mtf2 to repress leukemic blast expansion provides insight into the tumor suppressor function of the PRC2.

Tightly regulated epigenetic control of gene expression is critical for coordinated development. Here, for the first time we demonstrate a unique role for Mtf2 in erythroid development, HSC self-renewal and leukemic progression. Collectively, our data illustrate how Mtf2 functions as a critical PRC2 component in the hematopoietic system and through its control of PRC2 components, regulates PRC2-mediated promoter-proximal H3K27me3 epigenetic regulation of multiple gene networks that are essential for hematopoietic development and function.

Materials and Methods

Generation of Mice and Embryonic Analysis

Gene targeted mouse C57Bl/6 ESCs were obtained through EUCOMM and were aggregated with CD1 blastocysts to form chimeras. Germline transmission was confirmed using PCR-based genotyping (primers listed in Table S5) and all future breeding was done on the C57Bl6/J strain to maintain this background. Peripheral blood analysis on embryos was completed as described (Masuoka and Townes 2002). Blood smears were stained with Wright-Giemsa. For Mtf2 expression in developing tissues, wild-type and Mtf2-null mice at various embryonic stages of development were fixed in 4% PFA and paraffin-embedded. Immunofluorescence was performed on 4um sections of paraffin embedded embryos via overnight incubation with antibody against Mtf2 (also known as M96, Genway). Microscopy was performed using a Zeiss Inverted LSM510 microscope. For CFU analysis, $2x10^5$ fetal liver cells were isolated and plated in

methylcellulose media containing growth factors (Stem Cell Technologies), and colonies were enumerated after 12 days of growth.

Flow Cytometry

For flow cytometric analyses, samples were first subject to red blood cell lysis and stained with antibodies directed against lineage markers. Mouse peripheral blood, fetal liver or bone marrow was stained with antibodies directed against CD4 (Clone GK1.5), CD8 (53-6.7), CD11b (M1/70), CD71 (R17217), Ter119 (TER119), B220 (RA3-6B2), and Gr1 (RB6-8C5) for lineage analysis. To distinguish donor-derived cells during transplantation, samples were also stained with anti-CD45.2 (104). For mouse stem and progenitor cell analysis, mouse BM and FL cells were first incubated with purified antibodies against CD3 (17A2), CD4, CD5 (53-7.3), CD8, CD11b, Ter119, and B220 then depleted using Sheep Anti-Rat Dynabeads (LifeTech), except CD11b was excluded in FL analysis. Lineage-depleted samples were then stained with antibodies against cKit (2B8), Sca1 (D7), CD34 (RAM34), CD16/CD32 (93), CD127 (A7R34), CD48 (HM48-1) and CD150 (mShad150). For cell cycle analysis, pregnant dams (e14.5) were injected with BrdU (1mg by i.p) and embryos were harvested 2 hrs later. Cells were fixed in ice-cold ethanol, treated with 1.5M HCl for 30min then stained with an antibody against BrdU (Millipore) and a fluorescently-conjugated secondary antibody. Cells were stained with propidium iodide (Sigma) to assess cell cycle state. For erythroblast morphology analysis, cells were stained with antibodies against Ter119 and CD71 as above, and with Hoechst (LifeTech) and Thiazole Orange (Sigma) for nucleic acid detection. Cells were

analyzed using the ImageStream imaging flow cytometer (Amnis) and classified based on parameters outlined in (McGrath, Bushnell et al. 2008). Size measurements were based on area of brightfield images and cells with centrally located nuclei were determined based on delta XY centroid measurements (Konstantinidis, Pushkaran et al. 2014).

Capillary Electrophoresis Immunodetection

Hematopoietic cells were isolated from e14.5 mouse FL and enriched by $CD45^+$ selection using immunomagnetic selection with anti-CD45 (eBioscience) and Sheep Anti-Rat Dynabeads (Life Tech). Cells were lysed in Bicine/CHAPS buffer with DMSO and protease inhibitors (Protein Simple). Lysates were prepared according to instructions for the NanoPro 1000 and protein was quantified using the Bradford assay. Lysate containing 0.1mg of protein was combined with a G2 ampholyte mixture (pH 3-10, Protein Simple) containing fluorescent standards and charge-based separation was performed within glass capillaries using the NanoPro 1000 system (Protein Simple). After UV cross-linking, samples were probed with antibodies for Mtf2 (Genway, 1:50), Jarid2 (Aviva, 1:50), Ezh2 (Active Motif 1:50), Ezh1 (Abcam 1:50), followed by secondary HRP antibodies (Protein Simple, 1:100) and detection by chemiluminescence. Peaks associated with specific protein expression were manually identified and area under the curve was calculated and normalized to a loading control (Hsp70). Duplicate technical replicates were performed for each biological sample (n=3-7 mice).

Lentivirus production of Mtf2 shRNA

293T cells were co-transfected with lentiviral plasmids pMD2G, pPAX2 and pGIPZ containing the shRNA of interest using polyethylenimine (see table below). The supernatant containing the virus was collected 48 and 72 hours post transfection. The virus was concentrated through ultracentrifugation and was stored at -80C.

	shRNA Sequence
Mtf2 shRNA Clone 3	TAATGTATGTCATAAGCTC
Mtf2 shRNA Clone 7	TTGGCTTTATGTCCATCCT
Scrambled shRNA	GTTACACGATATGTTATCA

Lentiviral-mediated Mtf2 knockdown of mouse bone marrow cells

Adult mouse bone marrow was isolated and lineage-depleted to enrich for stem and progenitor cells (Stem Cell Technologies). Cells were maintained in IMDM media containing bovine serum albumin, insulin, and transferrin (Stem Cell Technologies), 1% PenStrep (Life Tech), SCF (50ng/mL), TPO (10ng/mL), Flt3 (10ng/mL), IL6 (10ng/mL). Growth factors were purchased from Peprotech. On Day 1 of infection, cells were incubated with polybrene (6mg/ml) for 2 hours at 37°C, then combined with viral supernatants containing either a GFP-tagged Mtf2 shRNA clones or a scrambled shRNA control (ThermoFisher). Cells were spun down at 400g for 20 minutes, then maintained at 37°C. On Day 2, infection was repeated. Cells were grown for 3 days using a fed-batch culture system, then sorted for high GFP-expression. Sorted cells were fixed in 4% PFA, permeabilized with 0.3% Triton and stained for Mtf2 (Genway), Ezh2 (Cell Signaling),

Suz12 (Millipore), or H3K27me3 (Millipore) and appropriate secondary antibodies. Protein expression was determined by flow cytometry compared with an isotype-only control. Data analysis compared mean fluorescent intensity values using a ratio paired t-test.

RNA-seq and ChIP-seq

FL cells from e14.5 *Mtf2*$^{+/+}$ and *Mtf2*$^{-/-}$ mice were isolated and CD71^{+}Ter119$^{-/lo}$ and CD71^{+}Ter119^{high} fractions were sorted directly into lysis buffer using a MoFlo sorter. For RNA-seq, RNA was isolated (Arcturus PicoPure Kit, LifeTech) and rDNase treated (Qiagen). Quality of RNA was determined using a Bioanalyzer. Library preparation was performed using 150ng of high-quality RNA (TruSeq Library Prep Kit, Illumina), and sequencing on a HiSeq 2000 (Illumina). TopHat v1.4.1 and Cuffdiff v1.3.0 (Trapnell, Roberts et al. 2012) were used to map reads to a reference mouse genome assembly (mm9) and determine expression differences against the Ensembl release 67 gene model. Significant fold changes were determined using Benjamini-Hochberg corrected *p* value of 0.05. Raw RNA-seq data is available in GEO (Accession # - to be completed upon acceptance). Data was analyzed using gProfiler bioinformatics tool for functional annotation (Reimand, Kull et al. 2007, Reimand, Arak et al. 2011) and Cytoscape with Enrichment Map plugin for visualization (Merico, Isserlin et al. 2010, Merico, Isserlin et al. 2011). RNA-seq targets were validated by qPCR after RNA was converted to cDNA using Superscript II (LifeTech). Raw RNA-seq data is available in GEO (Accession # - to be completed upon acceptance).

For ChIP-seq, sorted cells were crosslinked with 1% formaldehyde for 10 minutes at room temperature. Samples were sheared using a Covaris sonicator until DNA reached a final size of 75-700bp. 10ug of antibody (anti-Mtf2, Genway; anti-H3K27me3, Millipore) was bound to pre-blocked Protein A magnetic beads (Millipore), combined with sonicated DNA and incubated overnight. After incubation, beads were collected and DNA-antibody complexes were eluted at 65^{o}C. Crosslinks were reversed overnight at 65^{o}C. Samples were treated with Proteinase K and RNase A and DNA was purified using phenol-chloroform. 500,000 cells per sample were used for both immunoprecipiation and control (IgG, SantaCruz). For sequencing, 10 ug of DNA was used for amplification and library preparation (Diagenode Microplex Library Preparation Kit). DNA was analyzed for quality, quantity and size using a Bioanalyzer and digital PCR. Libraries were used for sequencing on a HiSeq 2000 (Illumina). Bowtie v2.2.3 (Langmead and Salzberg 2012) and MACS 1.3.7 (Zhang, Liu et al. 2008) were used for alignments and peak calling, respectively. Gene annotations and peak profile analysis were completed using PAVIS (Huang, Loganantharaj et al. 2013) and GREAT (McLean, Bristor et al. 2010). The gProfiler bioinformatics tool was used for functional annotation with a Benjamini-Hochberg FDR correction test, unless indicated (Reimand, Kull et al. 2007, Reimand, Arak et al. 2011). Repeated *k*-means clustering analysis of methylation occupancy was completed using seqMINER (Ye, Krebs et al. 2011). Validation of ChIP-seq targets was completed by ChIP-qPCR. All qPCR analysis was completed on a Roche Light Cycler 480 using Sybr Green MasterMix (Roche) and 0.1mM primers. Primer sequences are listed in Table S5.

Bone Marrow Transplants and Analysis

For homing experiments, $5x10^6$ FL cells from *Mtf2*$^{-/-}$ or wild-type e14.5 embryos were isolated and labeled with carboxyfluorescein diacetate succinimidyl ester (CFSE) (5mM/mL, Molecular Probes) and 5 x 10^6 washed cells were injected via tail vein into lethally irradiated *B6.SJL-Ptprca Pep3b/BoyJ* (CD45.1$^+$) mice (Jackson Labs). BM was harvested 17hrs later and assessed for CFSE fluorescence. For primary competitive transplants, $0.5x10^6$ million FL cells from either *Mtf2*$^{-/-}$ or wild-type e14.5 embryos (CD45.2$^+$) were combined with $0.5x10^6$ BM cells from adult CD45.1$^+$ mice and injected via tail vein into lethally irradiated CD45.1$^+$ mice. Peripheral blood was assessed by flow cytometry at various time points up to 4 months post-transplantation. For secondary transplants, $5x10^6$ cells were isolated from BM of primary transplant recipients and injected via tail vein into lethally irradiated CD45.1$^+$ mice.

Friend Virus

Pcl2$^{+/-}$ mice were backcrossed onto a BALB/c background to produce *Pcl2*$^{+/-}$ mice lacking the Fv2 gene, leading to susceptibility of the Friend virus. Mice (5-8 weeks of age) were injected with murine Friend virus at saturating doses via tail vein injection. Hematocrits were determined weekly by saphenous leg bleed. For BFU-E experiments, mice were sacrificed at 2 weeks post-infection and splenocytes collected and seeded in Methocult (Stem Cell Technologies) containing IL3 (2.5ng/ml) + SCF (100ng/ml). Uninfected cells were plated in the same media with the addition of Epo (3U/ml). Cells were seeded at a

density of $1.5x10^6$ cells per well in triplicate and scored for benzidine positive colony formation after 8 days. For all other experiments, mice were sacrificed at 4 weeks post-infection, and splenocytes collected. Flow cytometry was performed using antibodies cKit (2B8), Sca1 (D7) and CD133 (13A4) (eBioscience). For colony-forming assays, splenocytes were seeded at $2x10^5$ cells/ml in Methocult without growth factors (Stem Cell Technologies). After 12 days, growth-factor independent colonies were enumerated.

Statistics

All data were expressed as mean ± SEM. Data was analyzed using Prism 5.0 (GraphPad Software). Statistical significance of differences was measured by 2-tailed Student's t test. A p value < 0.05 was used as a cut-off to indicate statistical significance.

Study Approval

All animal experiments were conducted with the approval of the University of Ottawa Animal Care Committee, in accordance with the Canadian Council on Animal Care Standards and the Province of Ontario's Animals for Research Act. Hematological parameters were measured using a HEMAVET 950 (Drew Scientific) on peripheral blood collected from the saphenous vein of 6 and 8 week old animals. For specific studies mentioned, mice were injected with either a single dose of phenylhydrazine (PHZ, Sigma, 120mg/kg body weight), a single dose of 5-fluorouracil (5FU, Sigma Aldrich, 150mg/kg body weight) or repeated doses of 5FU (120mg/kg) every 7 days.

Acknowledgments

We thank the OHRI Stem Core Facility for their assistance with FACS and sequencing and M Brand, J Dilworth, and D Picketts for critical reading. Chimeras were generated by the Toronto Centre for Phenogenomics. JMR, HBM, CI and WLS designed the study and interpreted the results. This work was supported by operating grants from the Canadian Cancer Society Research Institute, the Cancer Research Society, and the Canadian Institutes of Health Research to WLS and CI. RFP is supported by National Institutes of Health (grant R01DK080040), an American Society of Hematology Bridge Grant and the USDA National Institute of Food and Agriculture Hatch Project #4736. JMR was supported by from Ontario Graduate Scholarship and a CIHR Banting and Best CGS Doctoral Research Award and WLS was supported by a Tier 1 Canada Research Chair in Integrative Stem Cell Biology. The authors have declared that no conflict of interest exists. Sequencing data can be found in GEO (Accession # GSE72286 and GSE72287).

Supplementary Figures

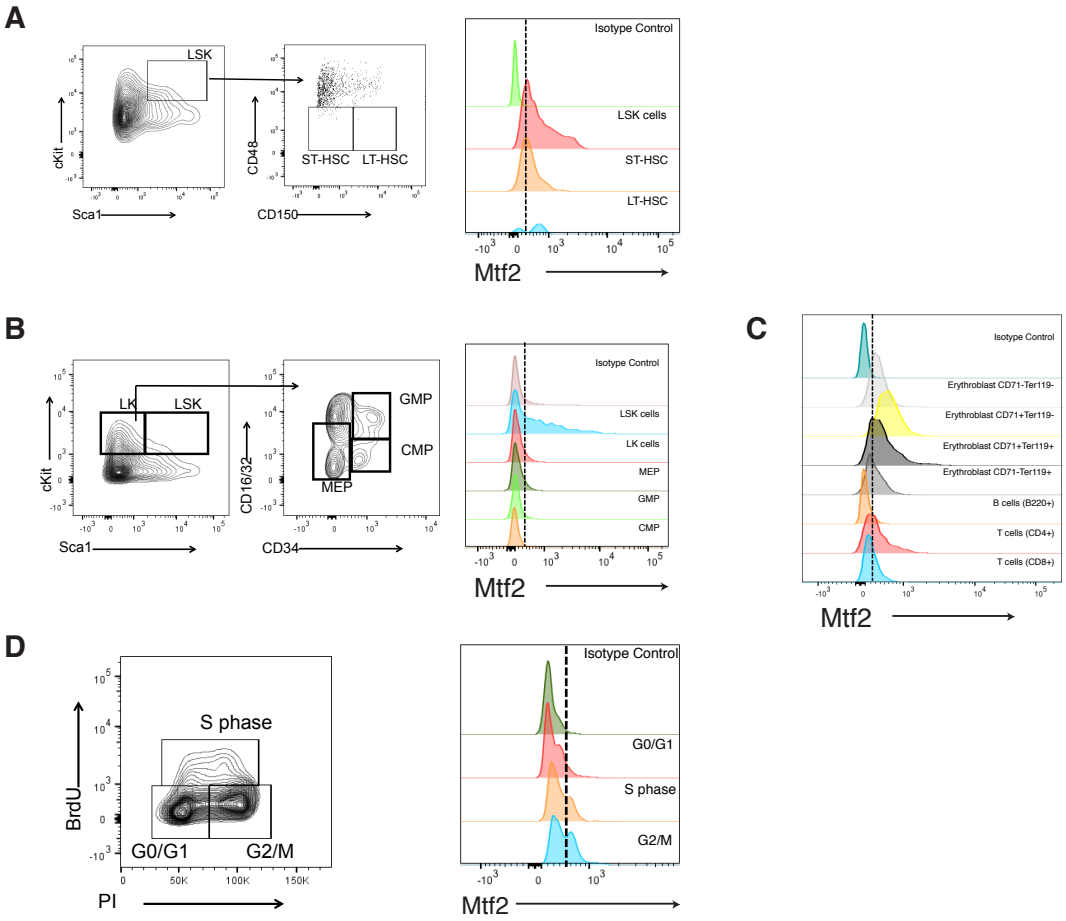

Figure S2.1. Mtf2 expression in the mouse hematopoietic system. (A) Mtf2 protein expression is high in LSK stem and progenitor cells, including ST-HSC and LT-HSCs. Dotted lines indicate level of isotype control. (B-C) Mtf2 protein expression was analyzed in progenitor and mature hematopoietic lineages by flow cytometry. A representative gating strategy is shown for progenitor analysis. Mtf2 expression is generally low in mature cells (B cells, T cells) and more restricted progenitors such as MEP, GMP, CMPs. (LK, lineage$^-$cKit$^+$). In mature cells, Mtf2 protein levels are highest in erythroid progenitors (CD71$^+$ and/or Ter119$^+$) (n=3). (D) In CD71$^+$ Ter119$^+$erythroid progenitors, Mtf2 expression is also regulated during the cell cycle, with highest expression seen in during S and G_2/M phase, based on BrdU/PI staining.

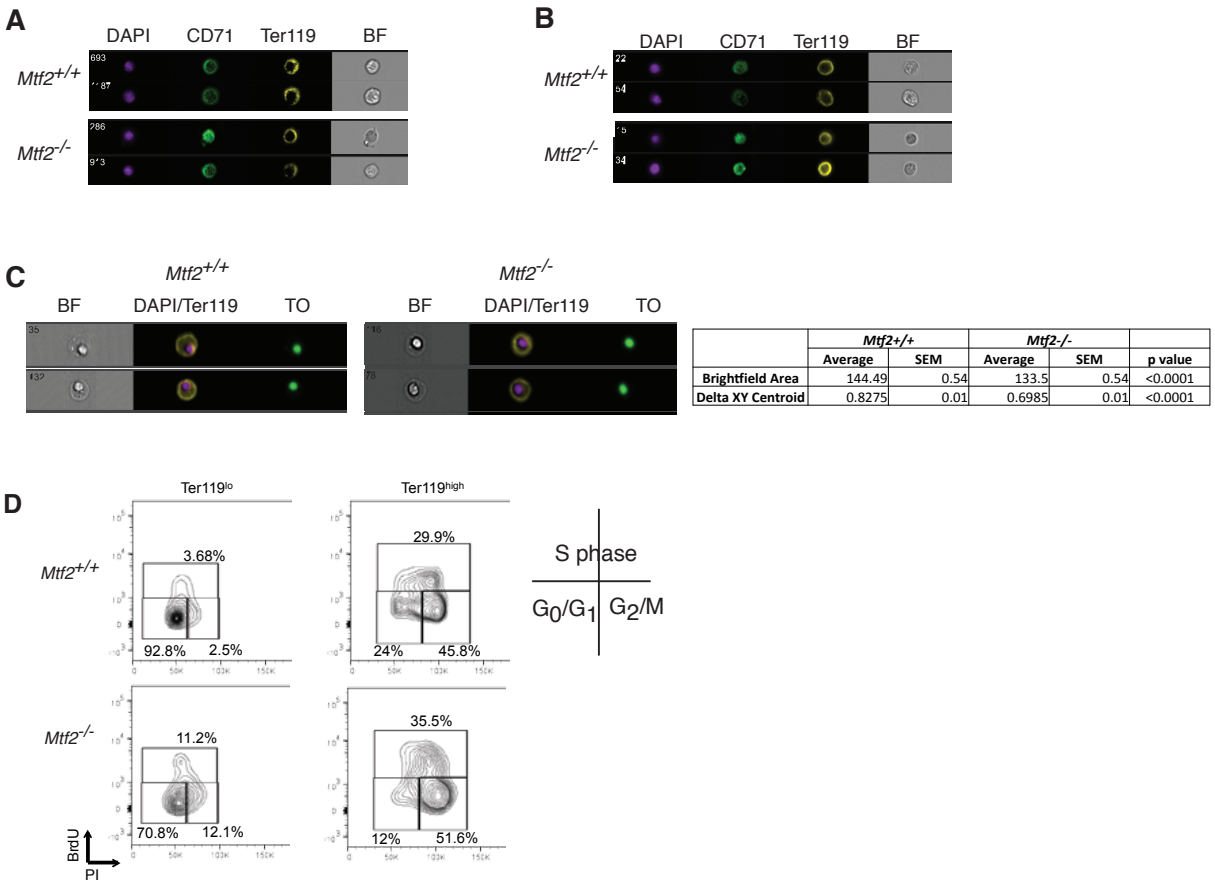

	Mtf2+/+		Mtf2-/-		
	Average	SEM	Average	SEM	p value
Brightfield Area	144.49	0.54	133.5	0.54	<0.0001
Delta XY Centroid	0.8275	0.01	0.6985	0.01	<0.0001

Figure S2.2. Morphology of wild-type and *Mtf2*$^{-/-}$ fetal liver and peripheral blood erythrocytes. (A) Fetal liver from e14.5 wild-type and *Mtf2*$^{-/-}$ embryos were isolated and stained for markers of erythrocyte development (CD71, Ter119). Using imaging flow cytometry, we can see that cells from either genotype within the S2 and S3 populations of erythroblasts (A and B, respectively), have similar morphology. (C) Representative pictures from imaging flow cytometry on *Mtf2*$^{-/-}$ e14.5 peripheral blood. *Mtf2*$^{-/-}$ Ter119^{hi} cells that are present are larger (Brightfield area) with more centrally located nuclei (lower delta XY centroid values) than their wild-type counterparts. (D) Representative cell cycle profiles of wild-type and *Mtf2*$^{-/-}$ Ter119^{lo} and Ter119^{hi} fetal liver erythroblasts was assessed using BrdU and PI staining. In the Ter119^{lo} fraction, there are fewer *Mtf2*$^{-/-}$ cells in G_0/G_1 and more in S phase, compared to wild-type cells.

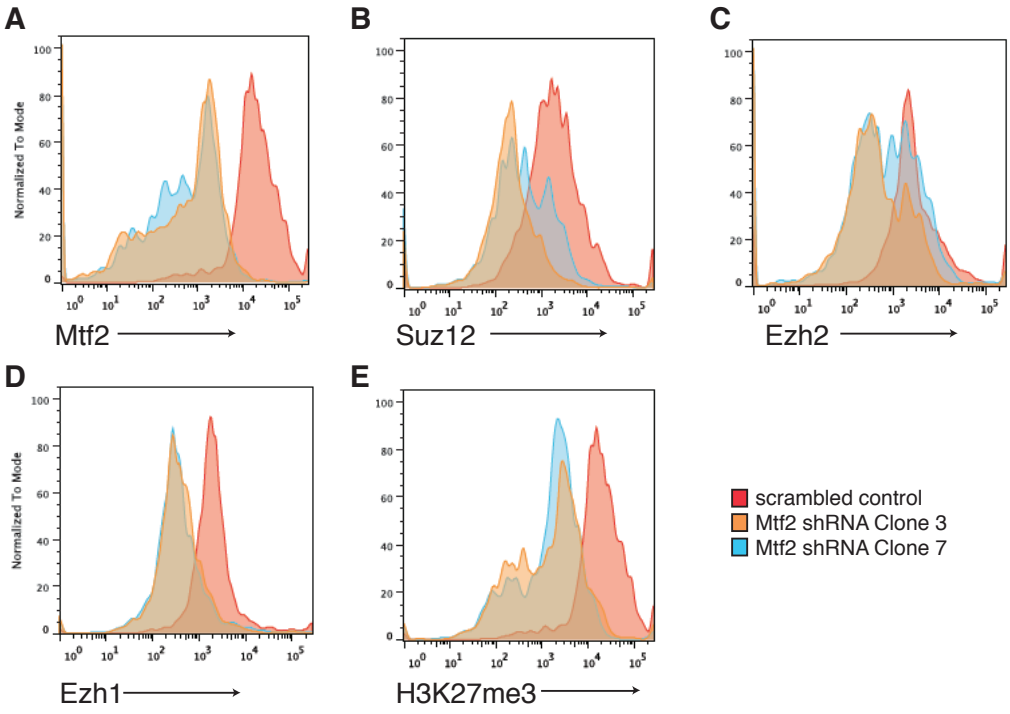

Figure S2.3. Knockdown of Mtf2 in adult lineage-depleted mouse bone marrow also reduces core PRC2 proteins and methylation levels. (A) Mtf2 levels are reduced after lentiviral-mediated knockdown using two different shRNA clones. Mtf2 levels cells transduced with a scrambled shRNA control vector are shown for comparison. (B-E) Upon knockdown of Mtf2, levels of Suz12 (B), Ezh2 (C), Ezh1 (D) and H3K27me3 (C) are also reduced. ($p<0.001$)

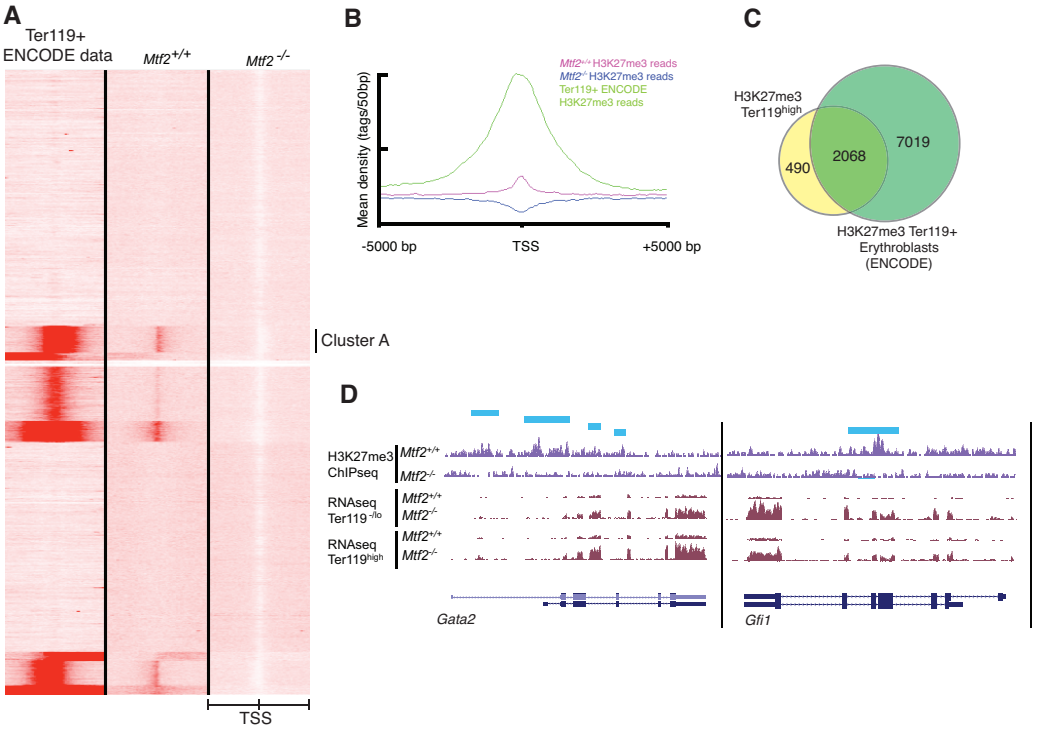

Figure S2.4. H3K27me3 binding in wild-type erythroblasts correlates well with publicly available data. (A) Using publicly available H3K27me3 binding in Ter119^{+} erythroblasts (from ENCODE) and sampling at a similar read depth, we observe very similar enrichment patterns between published data and our wild-type cells. *k*-means clustering (using seqMINER program) was used to visualize H3K27me3 enrichment patterns across all genes. A heatmap of enrichment densities are centered around the transcriptional start site of each gene and span +/- 5kb. (B) Plotting read density within 5kb of the TSS for genes contained within Cluster A (indicated in panel A), we observe as similar enrichment pattern, at a lower read depth, in our wild-type cells compared to Ter119^{+} erythroblast data from ENCODE. (C) Annotated genes associated with peak H3K27me3 binding in wild-type Ter119^{high} erythroblasts also overlaps well with published data from Ter119^{+} erythroblasts. Number of genes annotated with H3K27me3 peaks called by MACS 1.3.7 are shown. (D) Examples of traces from our H3K27me3 ChIP-seq and RNA-seq from wild-type and *Mtf2*$^{-/-}$ cells at *Gata2* and *Gfi1* loci. ChIP-seq peaks called by MACS 1.3.7 are indicated by blue bars.

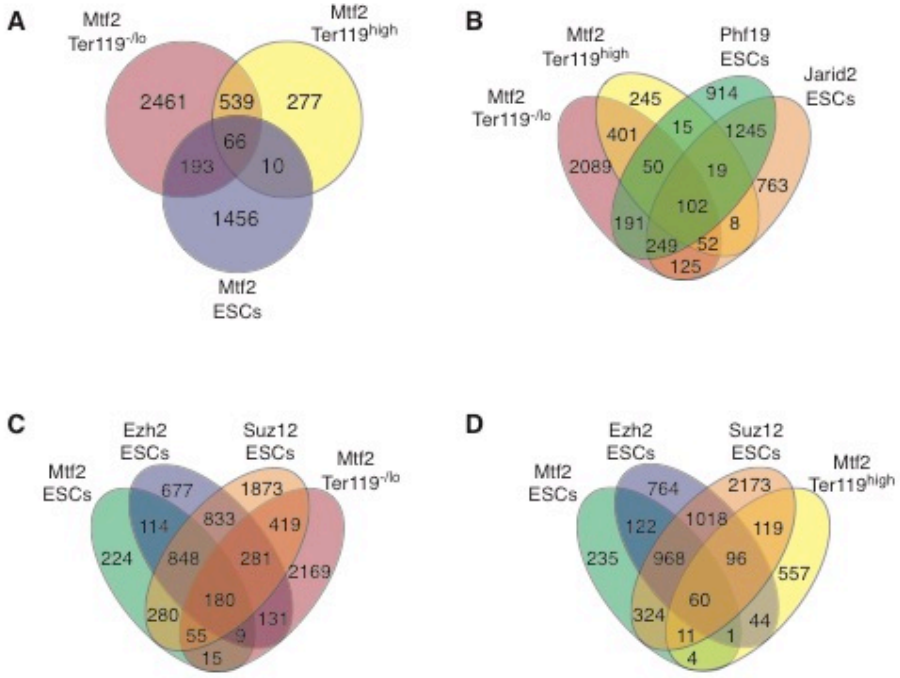

Figure S2.5. Genes associated with Mtf2 binding in erythroid cells show little overlap with Mtf2 and PRC2 targets in ESCs. (A) Mtf2 targets determined by ChIP-seq are distinct from Mtf2 targets identified in ESCs. (B-D) Targets of PRC2 members identified in ESCs show little overlap with Mtf2 targets identified in primary erythroid cells. (ChIP-seq data from ESCs: Mtf2 data (Walker, Chang et al. 2010), Ezh2 & Jarid2 data (Peng, Valouev et al. 2009), Suz12 & Phf19 data (Hunkapiller, Shen et al. 2012)).

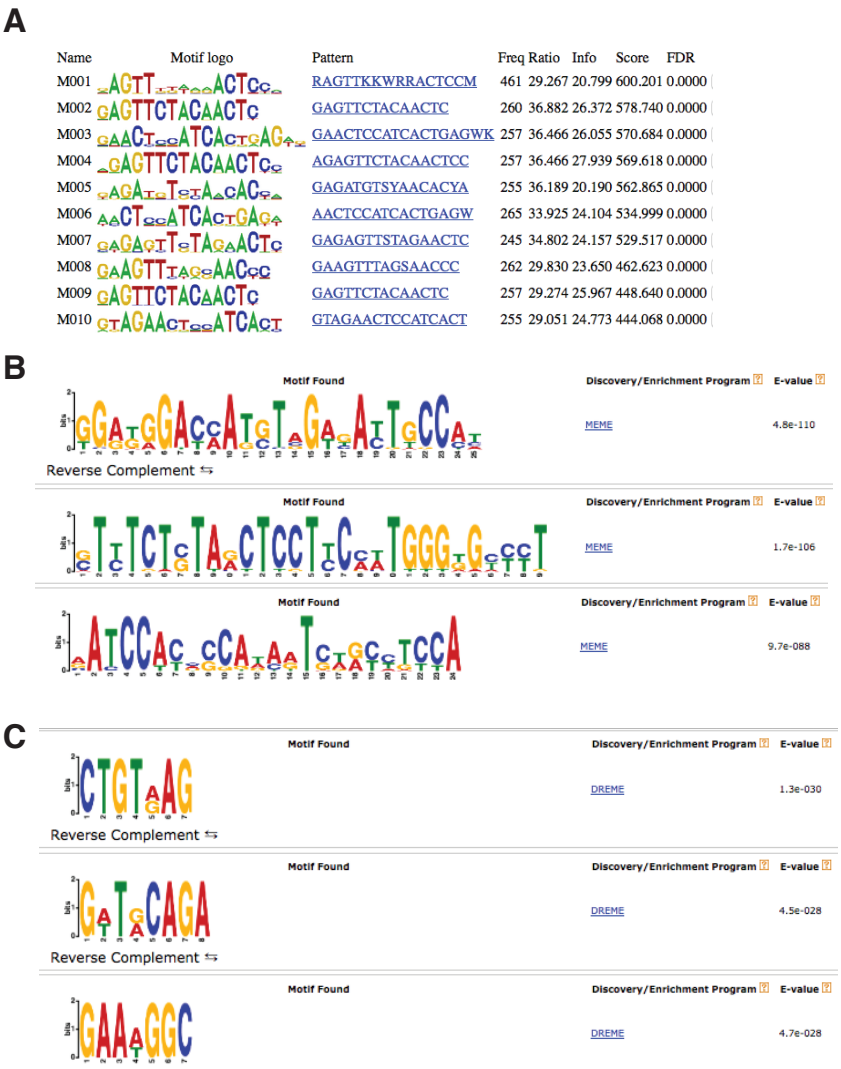

Figure S2.6. *de novo* motif analysis using Mtf2 promoter occupancy data in erythroblasts failed to find a consensus motif. Peaks identified from Mtf2 ChIP data in erythroblasts were used to search for a consensus DNA-binding motif. We took a rigorous approach by using multiple de novo motif-finding algorithms, under the assumption that a true consensus motif will be realized by multiple programs, despite differences in algorithms used. Examples of consensus motifs found from Mtf2 occupancy data using (A) CisFinder, (B) MEME and (C) DREME programs. While each program did provide a list of potential motifs and the position weight matrix of each one, no similarities were found between results. Additionally MEME and DREME failed to find any centrally located motifs (a common feature usually associating with the strongest portion of each peak) or motifs associated with any known transcription factors (based on data from the JASPAR database).

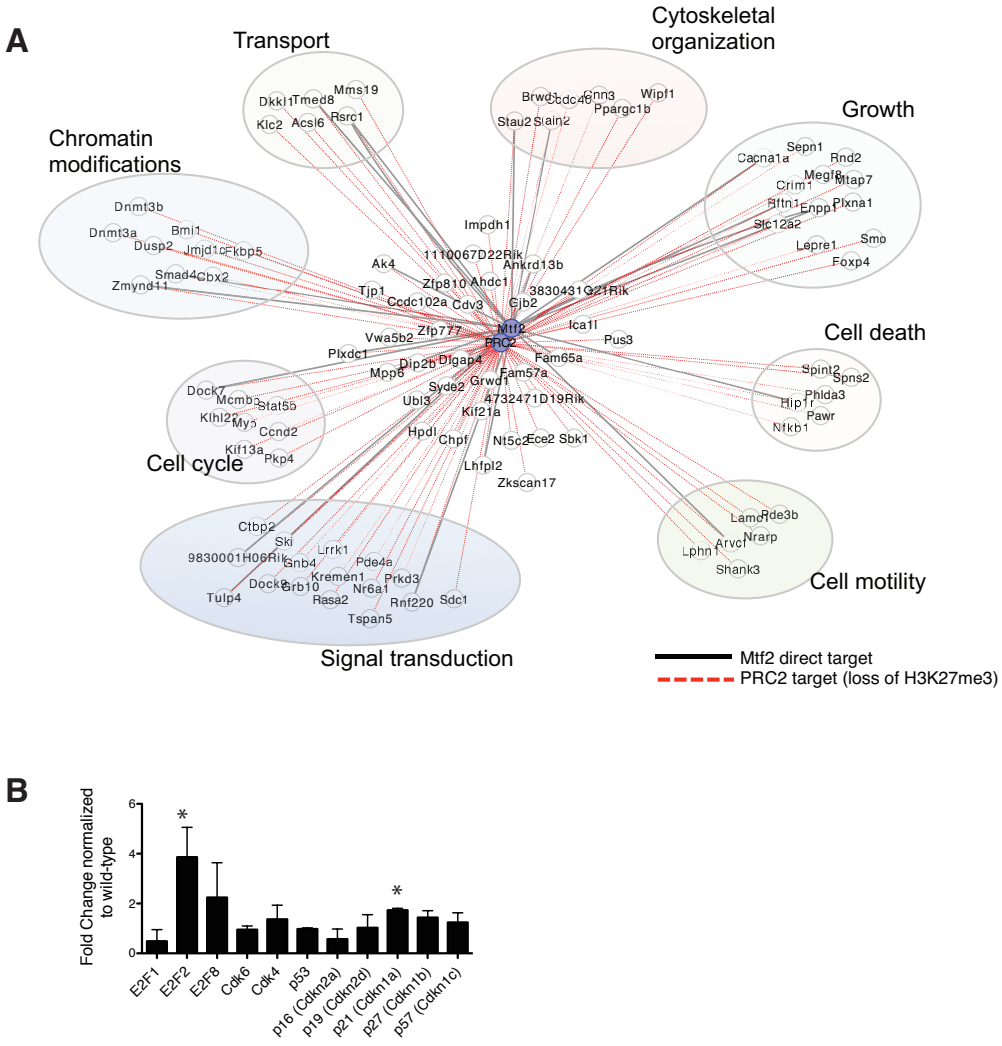

Figure S2.7. An Mtf2-PRC2 GRN controls chromatin modifiers and cell cycle regulators during erythroid differentiation. (A) Genes misregulated during *Mtf2*$^{-/-}$ erythroblast differentiation (Figure 2.6F, Group B & C) which are also Mtf2-PRC2 targets are associated with chromatin modifications, cell cycle and other critical cell processes. The GRN includes genes that are direct targets of Mtf2 in erythroid cells (solid lines) and those that have lost H3K27me3 (defined as PRC2 targets, dotted lines). (B) Validation of RNA-seq data by qPCR in *Mtf2*$^{-/-}$ erythroblasts shows upregulation of regulators of the cell cycle including E2F2 and p21 (Cdkn1a). Data is shown as mean ± SEM, n=3, *p<0.05, **p<0.01, ***p<0.001.

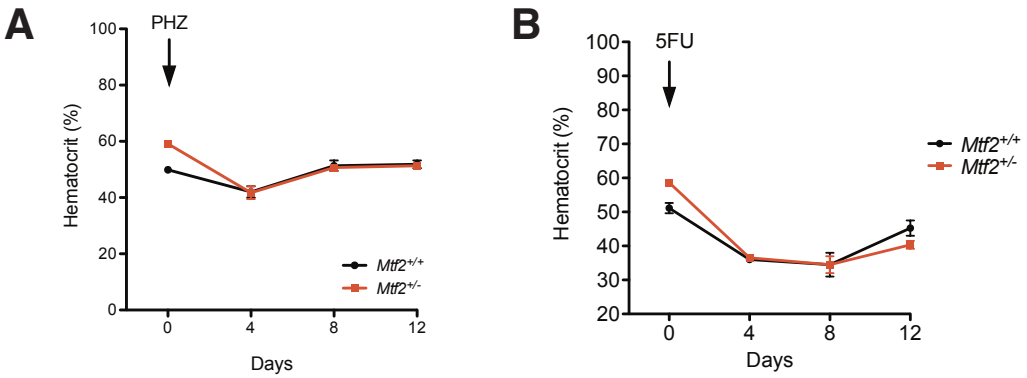

Figure S2.8. *Mtf2*$^{+/-}$ mice have normal recovery kinetics after induction of cytopenia. (A) Adult wild-type and *Mtf2*$^{+/-}$ mice were injected with a single dose of phenylhydrazine (120mg/kg body weight) on Day 0 and hematocrit levels were tracked over 12 days. *Mtf2*$^{+/-}$ mice had similar hematocrit recovery kinetics as wild-type mice in the 12 days following injection. (B) Adult wild-type and *Mtf2*$^{+/-}$ mice were injected with a single dose of 5FU (150mg/kg body weight) on Day 0 and hematocrit levels were tracked over 12 days. *Mtf2*$^{+/-}$ mice had similar hematocrit levels as wild-type cells in the 12 days following injection.

List of Supplementary Tables (provided in .zip file)

Table S1. Genes identified as losing H3K27me3 in Mtf2-null erythroblasts.

Table S2. Genes contained in the Mtf2-PRC2 gene regulatory network.

Table S3. Gene expression changes during erythroblast differentiation.

Table S4. Hematological measurements in wild-type and *Mtf2*$^{+/-}$ mice.

Table S5. Primers used for genotyping, qPCR and ChIP-qPCR analysis.

Chapter 3

Discussion and Future Directions

3.1 Thesis Summary and Major Findings

The Stanford lab identified the importance of Mtf2 in stem cell fate by GRN analysis in mESCs (Walker, 2007); the decision to study the role of Mtf2 in mESCs was made in part by our analysis of tissue microarrays that identified Mtf2 as being highly expressed *in utero* as well as in hematopoietic tissues within the adult. Because the Stanford lab had identified a critical role of Mtf2 in regulating self-renewal and commitment in mESCs (Walker, 2010), together with the tissue arrays data, I undertook this project to determine the role of Polycomb-like 2 *in vivo* and test our hypothesis that Mtf2 plays a similar role in the hematopoietic system as it does in mESCs. My thesis revealed an indispensible role of Mtf2 in hematopoietic development and regulation and a previously unrecognized, wider role for Polycomb accessory proteins. Using complementary approaches, including mouse models of disease, molecular and cellular biology, next generation sequencing technologies ChIP-seq and RNA-seq, and bioinformatics, I have taken a systems approach to investigate the role of Mtf2 outside of the ESC model system. Collectively, these data have expanded the role of Mtf2 beyond a canonical Polycomb accessory protein and has also opened many avenues of future research, including pre-clinical studies of Mtf2 as a potential biomarker or therapeutic target in leukemia.

The major findings outlined in this thesis place Mtf2 as a critical regulator of hematopoietic development. We show that the loss of Mtf2 results in the post-

transcriptional reduction of core PRC2 proteins and genome-wide promoter proximal loss of H3K27me3. The downstream effect of this loss of methylation perturbs Mtf2-PRC2 gene regulatory networks leading to a defect in erythroid differentiation, loss of HSC self-renewal and an expansion of progenitor cells in a model of leukemia. These results reveal unique control of hematopoietic development by Mtf2, something not originally predicted by its role in ESCs. Our data highlights a tissue-specific role for this Polycomb protein, and advances its role from an accessory protein in ESCs to a core-like member of the PRC2 in the hematopoietic system.

3.2 Studying Mtf2 in a constitutive gene-targeted mouse model

Previous work addressing the role of Mtf2 *in vivo* had been limited to gene trap mutants that display variable phenotypes. Interruption of Mtf2 between the 4^{th} and 5^{th} exon produces viable mice with skeletal abnormalities (Wang, He et al. 2007). A second mutant strain, using mixed background gene-trapped ESCs, phenocopied the skeletal phenotype seen previously but also led to early post-natal lethality (Li, Isono et al. 2011). Additionally, using a polyA trap Mtf2 model developed in the Stanford lab, we observed pre- and post-natal lethality and pleiotropic defects (Stanford Lab, unpublished data). Breeding difficulties led to a loss of the mouse strain, but not before we observed other developmental defects, including situs inversus, and a hair cycling defect suggestive of a role in hair follicle stem cells. In addition, pathological analysis of neonatal mice showed enlarged lymph nodes bordering on lymphoma, suggesting a role for Mtf2 in hematopoiesis. Since gene trap mutants can often be hypomorphic

(Stanford, Cohn et al. 2001), and to maintain strain fidelity which has also led to variable phenotypes with other Polycomb mutants (Motoyama, Kitajima et al. 1997, Kitajima, Kojima et al. 1999), we chose to generate Mtf2 null (*Mtf2*$^{-/-}$) mice in a C57BL/6J background using gene targeted ESCs.

While our gene-targeted Mtf2 knockout mouse model provides an excellent model to study the role of Mtf2 during early stage development *in vivo*, it is not without its drawbacks. Because the Mtf2 null mutation leads to embryonic lethality, the role of Mtf2 in non-hematopoietic adult tissues has not been assessed. In addition, if Mtf2 plays a role in the hematopoietic niche, including the fetal liver, the niche could contribute to the hematopoietic phenotype. I demonstrated that the erythroid maturation defect in Mtf2-deficient embryos is cell-intrinsic, as it is recapitulated in competitive reconstitution experiments, where supporting wild-type recipient bone marrow stromal cells have normal Mtf2 expression. Defining components of the BM niche and mapping interactions between hematopoietic cells and the stromal microenvironment have become the subject of many recent studies (Mendez-Ferrer, Michurina et al. 2010, Ding, Saunders et al. 2012, Ding and Morrison 2013, Greenbaum, Hsu et al. 2013). In the context of diseases such as myelodysplasia or leukemia, these interactions may be critical and studies have shown a reciprocal relationship where alterations in the BM niche may influence disease development and malignant cells can alter the BM niche (Medyouf, Mossner et al. 2014).

Other Polycomb proteins have roles in the BM niche, displaying both hematopoietic cell-autonomous and non-autonomous phenotypes. Bmi1 plays a cell-intrinsic role in HSC self-renewal (Park, Qian et al. 2003); in addition, the BM microenvironment of Bmi1$^{-/-}$ mice does not support HSC function (Iwama, Oguro et al. 2004). The role for Jarid2 in erythroid maturation has been attributed to microenvironmental defects in certain mouse strains rather than a cell-intrinsic defect (Takeuchi, Yamazaki et al. 1995, Motoyama, Kitajima et al. 1997). While we demonstrate that the erythroid maturation defect of Mtf2 null cells is cell-autonomous, this cannot rule out a role of Mtf2 in any of the non-hematopoietic supporting cells of the fetal liver microenvironment (hepatocytes, fibroblasts, etc). Creating a bone marrow or fetal liver stroma lacking Mtf2 and assessing wild-type hematopoietic cell growth and function in that microenvironment will elucidate the role of Mtf2 in supporting normal hematopoiesis.

3.3 The changing role of Polycomb accessory proteins

One unique result that has come out of this study is the changing role of Polycomb accessory proteins. Classically, work has been focused on the "core" PRC2 proteins, Suz12, Ezh2 and Eed based on their importance in ESCs and early development (Faust, Schumacher et al. 1995, O'Carroll, Erhardt et al. 2001, Pasini, Bracken et al. 2004). Accessory proteins like Jarid2, Aebp2, Pcl proteins (Phf1/Mtf2, Phf19) and ePRC48 were originally defined based on their co-immunoprecipitation association with the PRC2 core complex members (Cao and Zhang 2004, Nekrasov, Klymenko et al. 2007,

Kim, Kang et al. 2009, Peng, Valouev et al. 2009, Shen, Kim et al. 2009, Pasini, Cloos et al. 2010, Walker, Chang et al. 2010) but their role was considered minor in defining targeting to particular loci or assisting in the enhancement of methylation. In our study of Mtf2 in the hematopoietic system, we begin to define a novel role for Polycomb accessory proteins. While their "supporting" role in ESCs may be limited to "fine-tuning" PRC2 function, perhaps these accessory proteins only play their "starring" role within distinct tissues. Each Polycomb accessory protein has a more restricted expression in adult tissues compared to the ubiquitous expression of core complex members (Zhang, Morris et al. 2004).

Prospective identification of PRC2 targets in various cell types has proven difficult and the field has yet to define a molecular binding site for PRC2 in any cell type. Motif analysis on Jarid2 and Pcl3 binding sites has yielded only CpG rich regions (Peng, Valouev et al. 2009, Hunkapiller, Shen et al. 2012) and defining a classic Polycomb Response Element (PRE), as is common in flies (Simon, Chiang et al. 1993, Chan, Rastelli et al. 1994), has also proven challenging in mammalian cells (Sing, Pannell et al. 2009, Woo, Kharchenko et al. 2010). Our own motif analysis of Mtf2 binding in ESCs (Stanford lab, unpublished data) or erythroblasts failed to reveal a consensus motif. Together this suggests that PRC2 binding through accessory proteins may be loosely defined for the purpose of acting on different targets in different cell types. The addition of co-factors, including various isoforms of PRC2 core proteins, and the use of tissue specific enhancer elements, may all work together to create a wide range of transcriptional control by PRC2 in various cell types.

Based on our observations of Mtf2 in the hematopoietic system, we see post-transcriptional regulation of core complex members leading to major downstream effects. We propose that Mtf2 in hematopoietic cells function as a core PRC2 complex member and is necessary for PRC2 stability. Future biochemical studies of PRC2 complex stability, such as gel elutriation studies using proteosomal inhibitors will be integral to confirm our proposed role for Mtf2 and aid in tracing the fate of PRC2 proteins in cells deficient of Mtf2. The role for PRC2 accessory proteins in complex stability in specific tissue may not be limited to Mtf2. A recent paper investigating the role of Jarid2 in the hematopoietic system using shRNA mediated knockdown described a phenotype similar to the loss of Suz12 (Kinkel, Galeev et al. 2015). There was no change in transcript level of other PRC2 proteins after loss of Jarid2, although protein levels were not analyzed. It will be critical to determine whether other PRC2 accessory proteins also play a role in complex stabilization in particular tissues or cell lineages, a feature previously described only for core PRC2 proteins.

In data shown in this thesis, I describe unique roles for Mtf2 in hematopoietic cells that were not predicted from ESC work. In ESCs, loss of Mtf2 leads to enhanced self-renewal (Walker, Chang et al. 2010), while in HSCs we observe loss of self-renewal and exhaustion of the stem cell pool. Although the PRC2 complex is repressive in nature, its targets could easily change from cell type to cell type. For instance, without Mtf2, loss of methylation at targets that have a negative effect on self-renewal (i.e. p57) may lead to decreased self-renewal (Matsumoto, Takeishi et al. 2011). Very recently, the PRC2 field has reported a non-canonical, activating role of the PRC2 in the

hematopoietic system, based on a complex that contains Suz12 and Ezh1, but not Eed (Xu, Shao et al. 2015). It will be interesting to determine whether this secondary, activating role for this alternative PRC2 is active in other cell types, and what role accessory proteins play in this non-canonical PRC2 complex.

3.4 Using a systems biology approach to define the role of Mtf2 in development

Using next-generation sequencing techniques we have provided unique insight into the role of a poorly understood Polycomb protein in the context of hematopoietic development. While technically challenging, our analysis of Mtf2 binding in low numbers of sorted primary cells was key to fully understand the role of transcription and chromatin remodeling factors in particular cell types. The discrepancy with Mtf2 binding sites identified in ESCs prompted the need to draft cell-specific GRNs to gain insight on the functional consequences of transcriptional regulator depletion or mis-expression. This phenomenon is not globally recognized and some TFs may have a more consistent binding profile across many cells types (for example, CTCF) (Shen, Yue et al. 2012, Griffon, Barbier et al. 2015). With the abundance of publically available ChIP-seq datasets, large-scale analyses of TF binding or histone occupancy across cell types has become possible (Griffon, Barbier et al. 2015). Many factors have been shown to contribute to cell-type specific transcription factor binding, including changes in chromatin confirmation and accessibility by histone modifications (Heintzman, Hon et al. 2009, Ernst and Kellis 2013), DNA methylation status (Deaton and Bird 2011, Wiench, John et al. 2011), unique enhancer elements (Shen, Yue et al. 2012) and DNase

accessibility (Thomas, Li et al. 2011). Another key factor is the abundance of transcription factor expression in a certain cell type (Wang, Zhuang et al. 2012) or the expression of necessary cofactors. Cell type specific interactions and binding are key for delineating differential gene expression (Teng, He et al. 2014), and this integrative approach allowed us to uncover the function of Mtf2-PRC2 during hematopoietic development.

To define a gene regulatory network controlled by the Mtf2-PRC2 complex within the hematopoietic system I used a systems biology approach and integrated transcriptomic, transcription factor binding and methylation binding data. Using H3K27me3 ChIP from wild-type and *Mtf2*$^{-/-}$ erythroblasts, we identified more than 2500 genes which specifically lost H3K27me3 at regions proximal to their transcriptional start site. This list contained master regulators of differentiation including members of the Gata, Lhx and Hox families. The Gata family in particular plays a key role during erythroid maturation. A switch from high levels of Gata2 expression to Gata1 expression and change in target occupancy allows erythroid cells to terminally differentiate (Ikonomi, Rivera et al. 2000, Bresnick, Lee et al. 2010, Kaneko, Shimizu et al. 2010, Snow, Trowbridge et al. 2011, Dore, Chlon et al. 2012, Suzuki, Kobayashi-Osaki et al. 2013). A recent paper by the Orkin group (Xu, Shao et al. 2015) demonstrated that during erythroid maturation, the "Gata switch" mediates the expression of Ezh1, which allows re-occupancy of targets formerly bound by Ezh2 and binding of non-canonical PRC2 complexes, leading to gene activation. As we have shown that Mtf2 post-transcriptionally regulates core PRC2 members in the erythroid system, it likely acts as a

critical factor during this Gata activation. Further work on the binding of Mtf2-containing PRC2 complexes at erythroid-specific enhancer elements and at targets bound by either Gata1 or Gata2 will help elucidate the role of Mtf2-PRC2 in the regulation of red blood cell development.

3.5 Implications for normal hematopoietic stem-cell development

Another important finding has been the role of Mtf2 in controlling self-renewal of HSCs. In ESCs, loss of Mtf2 resulted in increased self-renewal via a feed-forward mechanism that enhances the pluripotency network controlled by Oct4 and Sox2 (Walker, Chang et al. 2010). In my thesis, I show how HSCs that lack Mtf2 eventually exhausted, resulting in a buildup of multipotent progenitors in secondary transplant recipients. These opposing roles for Mtf2 can be explained through the multiple gene regulatory networks controlled by the Polycomb Repressive complexes in various tissues. For example, PU.1 is also critical for HSC self-renewal and differentiation. While PU.1 expression is necessary for HSC self-renewal (Arinobu, Mizuno et al. 2007), expression of PU.1 is low in HSCs and increases as cells differentiate to a multi-potent progenitor stage (Iwasaki, Somoza et al. 2005). Thus, upregulation of PU.1 in *Mtf2*$^{-/-}$ LT-HSC could contribute to defective self-renewal.

One caveat to my studies is how assays were performed to assess HSC self-renewal. We performed bulk primary and secondary transplants and observed a robust phenotype. This was recapitulated in our serial 5FU transplants. Nonetheless, it is important to accurately enumerate HSC and test their individual capacity for self-

renewal. Using *in vitro* and *in vivo* limiting dilution assays (transplants and LT-CICs) would provide greater resolution in understanding the regulation of HSC self-renewal by Mtf2.

The construction of our Mtf2-PRC2 hematopoietic-specific gene regulatory network is also highly influenced by the expression levels of co-factors and Polycomb protein isotypes, by the accessibility of targets via chromatin compaction or other epigenetic modifications; all factors that are tissue and cell type specific. In ESCs, Mtf2 does not transcriptionally or post-transcriptionally regulate other PRC2 complex members, and is important for regulating H3K27me3 at a subset of targets. In contrast, the post-transcriptional control of core PRC2 members by Mtf2 and the resulting effect on global methylation may be the cause of its widespread effect on major cell functions, including stem cell self-renewal.

3.6 The role of Mtf2 in hematological diseases

The role of Mtf2 in hematopoietic differentiation is not only interesting from a development point of view, but from a clinical perspective as well. Mutations and mis-expression of multiple PRC1 and PRC2 proteins have been associated with the development of cancer, including lymphomas and leukemias (reviewed in (Sauvageau and Sauvageau 2010)). Our work with the Friend Virus leukemia model suggested that with loss of Mtf2, there is expansion of erythroid progenitor cells at the expense of LSCs. Recognizing the limitations of the FV erythroleukemia model and its distance from clinically-relevant models of leukemia, we tested our progenitor expansion hypothesis in

two other mouse models of cancer (Figure A1). Through collaboration with the Paulson lab, we knocked down Mtf2 levels in a mouse model of acute myeloid leukemia (created via expression of the MLL-AF9 fusion oncogene) and in a model of chronic myeloid leukemia (created via expression of the BCR-ABL fusion oncogene). In both models, again we observed expansion in the progenitor cells and reduction in LSCs. Re-transplanting BCR-ABL infected LSCs with reduced Mtf2 levels led to reduced white blood cell counts at 4 weeks post-infection, compared to LSCs with normal levels of Mtf2 and led to longer overall survival. We now see a common role for Mtf2 in progenitor cell expansion in 3 different models of leukemia.

These results – the increased morbidity in the FV model and the amelioration of leukemia in both an AML and a CML mouse model – suggest that a common mechanism of progenitor cell expansion can either be positive or detrimental, depending on the circumstances. During rapid expansion of leukemic blasts the risk of acquiring a mutation increases. This can be observed during the tracking of pre-leukemic clones that, due to their increased genetic instability, have an increased rate of accumulating mutations during clonal expansion (Jan, Snyder et al. 2012). If a cell first experiences a loss of PRC2, then gains a mutation driving a leukemic phenotype - as in the case of the Friend Virus model - our data suggests this would be detrimental and would exacerbate the leukemia. Instead if a cell first gained a leukemia-inducing mutation and later experienced loss of PRC2 (due to mutation or hypomethylation), data from our study and others (Neff, Sinha et al. 2012, Tanaka, Miyagi et al. 2012) suggest the secondary loss of PRC2 may ameliorate the disease. In each case, the order of mutation acquisition

may play a profound role in the future of the disease. Adopting disease models that carefully consider the timing of multiple mutations and polyclonal models of disease will help to refine our understanding of leukemia progression. And although current patient diagnostics may not be tracking mutation load, the creation of new deep-sequencing technologies at relatively low cost could track leukemic and pre-leukemic clones and use that information to dictate treatment regimes. While many prospective leukemia treatments being developed focus on eradicating LSCs (Herrmann, Blatt et al. 2012, Dos Santos, McDonald et al. 2013, Saito, Yuki et al. 2013, Guzman, Yang et al. 2014) thereby preventing recurrences, we must also consider disease in terms of tumor burden. A rapidly expanding population of leukemic progenitor cells with a reduced level of Mtf2 could create a high tumour burden that is difficult to control with current treatments. It will be critical to understand the molecular mechanisms behind expanding progenitor populations and LSC self-renewal to develop a multi-pronged approach to treating leukemias.

3.7 Future studies

The data generated from the Mtf2 null mouse model has been beneficial beyond the basic knowledge of hematopoietic stem cell and erythroid development. We have generated several avenues of future research that could be further pursued.

3.7.1 Mtf2 regulates cell cycle control in HSCs

Firstly, in trying to uncover a mechanism of action for Mtf2, our *in vivo* data suggests cell cycle regulation is affected with the loss of Mtf2. Mtf2-null cells showed increased cycling, with fewer cells in the G_0/G_1 phase and more cells in S-phase. Cell cycle regulators, such as $p16^{INK}$ and $p19^{ARF}$ are known targets of PRC2 that have been well established (Jacobs, Kieboom et al. 1999, Bracken, Kleine-Kohlbrecher et al. 2007, Kotake, Cao et al. 2007). I hypothesize that Mtf2 is acting through post-transcriptional regulation of core PRC2 proteins, thus controlling canonical PRC2-mediated H3K27me3 gene repression. We observe levels of cell cycle regulators being affected in our *Mtf2*$^{-/-}$ mice. Overexpression of some key cell cycle regulators, such as Cdk6, have been recently implicated in human HSC cycle kinetics, maintenance of the stem cell pool and control of exit from quiescence. In work from the Dick group, overexpression of Cdk6 led to a decrease in G_0 transit time, therefore increasing HSC cycling and leading to exhaustion of the stem cell pool (Laurenti, Frelin et al. 2015). Since we also observe overexpression of Cdk6 in our *Mtf2*$^{-/-}$ LT-HSCs, we proposed new experiments to test whether these cells have a decreased G_0 transit time, which could be a reason for the observed stem cell exhaustion. Due to our limitations in sorting LT-HSCs to absolute purity (Kiel, Yilmaz et al. 2005), we felt it critical to observe cycle transit times in individual HSCs. We singly sorted LT-HSCs from both wild-type and *Mtf2*$^{+/-}$ adult mice and visually observed their time to first and 2nd cell divisions over a 96hr period (Figure A2). It was critical to study cycling times within adult HSCs which follow a cell cycle

profile that includes a G_0 quiescent phase, which is not present in the rapidly expanding HSC population in the developing fetal liver (Nygren, Bryder et al. 2006, Pietras, Warr et al. 2011). The time to first cell division includes both transit time through G_0 ($t_{G0\ exit}$) plus the time for cell division ($t_{1st\ cell\ division}$), while a second cell division of LT-HSCs does not require the cell to re-enter G_0. Therefore, we can calculate the apparent resident time in G_0 by subtracting the time for first cell division from the time to 2nd cell division ($t_{G0\ exit} = t_{1st\ cell\ division} - t_{2nd\ cell\ division}$) (Laurenti, Frelin et al. 2015). Cell cycle time to 2nd cell division was not different in LT-HSCs from wild-type or *Mtf2*$^{+/-}$ mice (average time was ~ 18 hrs) but the time to first cell division was approximately 3.16 hrs shorter in *Mtf2*$^{+/-}$ LT-HSCs, although not statistically different from wild-type. Since the time for 2nd cell division is comparable between genotypes, we conclude that the difference observed in 1st cell division kinetics are due to a shortened G_0 transit time in *Mtf2*$^{+/-}$ LT-HSCs. The small sample number (n=3 per genotype) and use of HSCs expressing 50% normal levels of Mtf2, the effects observed are likely more pronounced in cells deficient in Mtf2. Nevertheless, the observation of shortened G_0 transit time follows the same trend recently reported for human LT-HSCs overexpressing Cdk6 (Laurenti, Frelin et al. 2015). The observed increase in Cdk6 in cells with reduced Mtf2 may regulate the exit of quiescence, leading to more rapid entry in to the cell cycle and eventual exhaustion of the stem cell pool. Transplanting fetal liver *Mtf2*$^{-/-}$ HSCs into the bone marrow of an adult recipient mouse will allow them to re-enter a quiescent state and could be a model to study exit of quiescence in adult HSCs deficient in Mtf2. Our observations using adult *Mtf2*$^{+/-}$ mice also provide clinical relevance to the state of HSCs in a

pathological situation, where Mtf2 levels may be reduced due to mutation or changes in promoter methylation state.

A unique feature we observed in hematopoietic cells from our *Mtf2*$^{-/-}$ mice is upregulation of *Pcgf* family transcripts, including *Bmi1*, and multiple *Cbx* proteins (Figure A3). There has been a significant amount of research describing the cross talk between PRC1 and PRC2, although transcriptional control of the Polycomb family of proteins is still poorly understood. At the functional level, the classic recruitment model of PRC2 proposes that H3K27me3 marks originally laid down by PRC2 are recognized by the Bmi1 protein in the PRC1 complex, which can mono-ubiquitinate H2A at lysine 119 (H2AK119ub1 mark) through its action of Ring1b (Wang, Wang et al. 2004). As we gain information on the complexity of Polycomb complexes in various tissues, this classic model may appear too simple and there are cases, at least in ESCs, of PRC2 targets not bound by PRC1 (Ku, Koche et al. 2008) or some PRC1 targets that are independent of PRC2 binding (Boyer, Plath et al. 2006). Some known Bmi1 regulators such as cMyc (Wang, Liu et al. 2013) and E2F1 (Nowak, Kerl et al. 2006) are also upregulated upon loss of PRC2 in particular cell types, suggesting indirect regulation, but H3K27me3 levels are also lost at PRC1 genes upon loss of Mtf2. In flies, there is direct evidence to suggest positive regulation of Cbx homologues by esc and E(z) (homologues of Eed and Ezh1/2, respectively)(Ali and Bender 2004). Our data would suggest that in mammalian cells, misregulation of PRC2 proteins leads to hypomethylation at PRC1 promoters that may lead to transcriptional activation. Similar examples are seen in primary adipocytes, where knockdown of Ezh2 increases expression of *Bmi1* (Wang, Jin et al. 2010) and in

embryonic fibroblasts, where activation of *Bmi1* is seen in cells with knockdown of Suz12 or Eed (Bracken, Dietrich et al. 2006). Bmi1 has a well-established role in controlling development and regulating senescence. When PRC1 target genes are not properly de-ubiquitinated (via loss of Mysm1, a histone 2 de-ubiquitinase), hematopoiesis was impaired, specifically in HSC function and erythroid development (Nijnik, Clare et al. 2012). Overexpression of Bmi1 can lead to many downstream changes in gene expression since Bmi1 is the rate-limiting component of PRC1 monoubiquitination controlling gene repression (Cao, Wang et al. 2002). One target of Bmi1, at least in ESCs, is p57 (Bommi, Dimri et al. 2010), a member of the CIP/KIP family of cell cycle inhibitors, which is also down-regulated in our *Mtf2*$^{-/-}$ LT-HSCs. While transcript levels of p57 did not appear different than wild-type at the CD71^{+}Ter119^{high} or CD71^{+}Ter119$^{lo/mid}$ erythroblast stages used for our RNA-seq analysis, we did observe a significant decrease in p57 in *Mtf2*$^{-/-}$ LT-HSCs.

We sought to investigate the role of Mtf2 at the early erythroblast stage (Ter119^{-}) using an *in vitro* differentiation method to determine its role in erythroid maturation and propose a mechanism of p57 control through both PRC2 and PRC1. Using transcription factor ChIP-seq for Mtf2 in our wild-type erythroblasts, we show strong binding of Mtf2 at the Bmi1 promoter (Figure A3). Ezh2 can also be found bound to the p57 promoter (Tan, Yang et al. 2007, Yang, Karuturi et al. 2009). This sets up a model with at least two repressive inputs feeding into the p57 promoter. If Mtf2 negatively regulates Bmi1 and post-transcriptionally controls the levels of Ezh2, then loss of Mtf2 may lead to both reduced Ezh2 repression at p57 and increased Bmi1

repression of p57. As with all networks with multiple inputs, we must consider timing and strength of inputs. Using our data, we propose a model where the repressive influence of increased Bmi1 may overshadow the de-repression via Ezh2 loss, resulting in overall decreased levels of p57. To test this model, we overexpressed p57 in Mtf2-null erythroblasts and tested their ability to differentiate *in vitro*. Wild-type e13.5 $Ter119^-$ erythroblasts are able to differentiate *in vitro* with the addition of Epo and turn on expression of Ter119, a critical step in terminal erythroid maturation. In contrast, most Mtf2-null e13.5 erythroblasts fail to turn on Ter119 *in vitro*, resulting in a decrease in $Ter119^+$ cells over 3 days of differentiation. When we overexpress p57 in these cells, we see an increased number of $Ter119^+$ cells at both day 2 and 3 of differentiation. Although the results were variable, we conclude that overexpression of p57 may partially rescue the erythroid differentiation defects seen with loss of Mtf2. Since we know that both Bmi1 and Ezh2 bind to the p57 promoter, we assessed levels of H3K27me3 and H2AK119ub1 at the p57 promoter as a functional consequence of Mtf2 deficiency. Interestingly, there was very little enrichment of H3K27me3 or H2AK119ub1 compared to the IgG control in either wild-type or Mtf2 null erythroblasts. Mtf2 null erythroblasts express very low levels of Mtf2 transcript due to the gene-targeted cassette but we observed an even further reduction in Mtf2 transcript in cells with p57 overexpression. This suggests a feedback loop may exist between p57 and Mtf2, potentially through other intermediaries, which may act to regulate the levels of Mtf2. This hypothesis of indirect down-regulation of a cell cycle component via upregulation

of the PRC1 may be one mechanism that explains the defect in hematopoietic self-renewal and a defect in erythroid maturation we see in Mtf2-deficient mice.

3.7.2 Identifying the role of Mtf2 in disease to improve diagnosis and therapies

The function of a protein in normal development can often provide insight into disease progression and the development of new therapies. Increased proliferation and abnormal cell cycle observed in our *Mtf2*$^{-/-}$ cells along with the association of misregulated core Polycomb proteins and cancer, restricted expression of Mtf2 in the adult hematopoietic system and our initial work with the Friend Virus erythroleukemia model, led us to hypothesize that Mtf2 expression may be correlated with the initiation or progression of leukemia in humans. Furthermore, we drafted an Mtf2-PRC2 gene signature based on data gathered from our Mtf2-knockdown ESCs (Walker, Chang et al. 2010) and compared this to publically available datasets from 10 different cancers. We observed a close relationship between the gene signature upon Mtf2 knockdown and patients with AML. This provided the rationale to further study the association between Mtf2 and AML. We are currently moving all our future studies into human hematopoietic stem and progenitor cells (HSPCs) derived from umbilical cord blood and acute myeloid leukemia (AML) samples, cell lines or AML patient bone marrow aspirates.

Using our transcriptomics and promoter binding data to identify misregulated genes in *Mtf2*$^{-/-}$erythroblasts, we observed an enrichment in genes involved in DNA damage response (Figure A4). Considering a dysfunctional DNA damage response is one

of the hallmarks of cancer (Hanahan and Weinberg 2000, Hanahan and Weinberg 2011), a potential link between Mtf2 expression and DNA damage response could be interesting in the context of developing leukemia. What this association may mean in normal and leukemic cells will be a future avenue of study.

Many studies in the cancer field have reported overexpression of Polycomb components, including Ezh2, associated with various forms of cancer (Bracken, Pasini et al. 2003, Kleer, Cao et al. 2003, Collett, Eide et al. 2006). Recently, small molecule inhibitors of Ezh2 such as DZNep (Tan, Yang et al. 2007), which inhibits Ezh2 mediated methylation, have been developed and show promise in multiple types of cancer (Puppe, Drost et al. 2009, Suva, Riggi et al. 2009, Rao, Chinnasamy et al. 2011). Some of these inhibitors have also shown promise in treating lymphomas as well (McCabe, Ott et al. 2012, Garapaty-Rao, Nasveschuk et al. 2013). But we should be critical of these inhibitors as a "magic bullet" for cancer treatment. As more and more treatments move from the bench to the bedside, it is important to look closely at the expression of all PRC2 components in a patient and the functional outcome of PRC2 misexpression. There is strong evidence that overexpression of PRC2 components can be as detrimental as loss of their expression. For instance, overexpression of Ezh and Suz12 have been associated with breast cancer, colon cancer and lymphomas (van Kemenade, Raaphorst et al. 2001, Bracken, Pasini et al. 2003, Kirmizis, Bartley et al. 2003, Martin-Perez, Piris et al. 2010). Upregulation of Phf19 has been implicated in many cancers including colon, skin, lung (Wang, Robertson et al. 2004) and medulloblastomas (Boulay, Rosnoblet et al. 2011). Recent work in our lab screening AML patients has revealed two distinct patient

groups with either low or high levels of Mtf2, both of which have poor response to current treatment strategies. Our data suggest that misregulated Mtf2 levels affect overall H3K27me3 levels via control of canonical PRC2 signaling. Therefore Mtf2 may present a novel target for controlling PRC2-mediated H3K27me3. Using Mtf2 as a treatment target would provide more specificity due to its restricted expression in the adult. Alternatively, understanding that abnormal levels of Mtf2 may be correlated with poor prognosis, we could screen additional treatment options that may be effective for this patient group. Using levels of Mtf2 as a biomarker would allow us to stratify patients and suggest more appropriate or aggressive types of treatment.

3.8 Conclusions

Building upon our knowledge of the Mtf2 protein in ESCs, we wanted to move away from a model system and understand the role of Mtf2 *in vivo*. Instead of simply taking a reductionist approach using a knockout mouse model, we used an integrative method to combine multiple facets of data to build a comprehensive story of the role of Mtf2 during hematopoietic development and disease. Relying not only on transcript expression, we used functional outcomes to assess changes in Polycomb proteins which uncovered unique roles for Mtf2, a protein previously characterized as simply a PRC2 accessory protein. The data provided in this thesis helps re-define the role of Polycomb accessory proteins and highlights the tissue-specificity of their functions. We also open the avenue for understanding the role of Mtf2 both in normal hematopoietic

development and in the context of disease. Our future work on Mtf2 will help broaden our knowledge of Polycomb proteins in leukemic development and help develop novel therapies and improved diagnostic and prognostic markers.

References

Akasaka, T., K. Tsuji, H. Kawahira, M. Kanno, K. Harigaya, L. Hu, Y. Ebihara, T. Nakahata, O. Tetsu, M. Taniguchi and H. Koseki (1997). "The role of mel-18, a mammalian Polycomb group gene, during IL-7-dependent proliferation of lymphocyte precursors." Immunity **7**(1): 135-146.

Ali, J. Y. and W. Bender (2004). "Cross-regulation among the polycomb group genes in Drosophila melanogaster." Mol Cell Biol **24**(17): 7737-7747.

Alkema, M. J., J. Jacobs, J. W. Voncken, N. A. Jenkins, N. G. Copeland, D. P. Satijn, A. P. Otte, A. Berns and M. van Lohuizen (1997). "MPc2, a new murine homolog of the Drosophila polycomb protein is a member of the mouse polycomb transcriptional repressor complex." J Mol Biol **273**(5): 993-1003.

Aloia, L., B. Di Stefano and L. Di Croce (2013). "Polycomb complexes in stem cells and embryonic development." Development **140**(12): 2525-2534.

Alon, U. (2007). "Network motifs: theory and experimental approaches." Nat Rev Genet **8**(6): 450-461.

Anderson, N. M., Z. Berberovic, E. Berndl, M. L. Bailey, A. M. Flenniken, L. R. Osborne, S. L. Adamson, J. Rossant, C. Wang, M. D. Minden, K. M. McNagny, R. F. Paulson, D. L. Barber and W. L. Stanford (2012). "Cytopenia induction by 5-fluorouracil identifies thrombopoietic mutants in sensitized ENU mutagenesis screens." Exp Hematol **40**(1): 48-60.

Antonchuk, J., G. Sauvageau and R. K. Humphries (2001). "HOXB4 overexpression mediates very rapid stem cell regeneration and competitive hematopoietic repopulation." Exp Hematol **29**(9): 1125-1134.

Aplan, P. D. (2006). "Chromosomal translocations involving the MLL gene: molecular mechanisms." DNA Repair (Amst) **5**(9-10): 1265-1272.

Arai, S. and T. Miyazaki (2005). "Impaired maturation of myeloid progenitors in mice lacking novel Polycomb group protein MBT-1." EMBO J **24**: 1863-1873.

Arinobu, Y., S. Mizuno, Y. Chong, H. Shigematsu, T. Iino, H. Iwasaki, T. Graf, R. Mayfield, S. Chan, P. Kastner and K. Akashi (2007). "Reciprocal activation of GATA-1 and PU.1 marks initial specification of hematopoietic stem cells into myeloerythroid and myelolymphoid lineages." Cell Stem Cell **1**(4): 416-427.

Ballare, C., G. Castellano, L. Gaveglia, S. Althammer, J. Gonzalez-Vallinas, E. Eyras, F. Le Dily, R. Zaurin, D. Soronellas, G. P. Vicent and M. Beato (2013). "Nucleosome-driven transcription factor binding and gene regulation." Mol Cell **49**(1): 67-79.

Beguelin, W., R. Popovic, M. Teater, Y. Jiang, K. L. Bunting, M. Rosen, H. Shen, S. N. Yang, L. Wang, T. Ezponda, E. Martinez-Garcia, H. Zhang, Y. Zheng, S. K. Verma, M. T. McCabe, H. M. Ott, G. S. Van Aller, R. G. Kruger, Y. Liu, C. F. McHugh, D. W. Scott, Y. R. Chung, N. Kelleher, R. Shaknovich, C. L. Creasy, R. D. Gascoyne, K. K. Wong, L. Cerchietti, R. L. Levine, O. Abdel-Wahab, J. D. Licht, O. Elemento and A. M. Melnick (2013). "EZH2 is required for germinal center formation and somatic EZH2 mutations promote lymphoid transformation." Cancer Cell **23**(5): 677-692.

Ben David, Y., V. R. Prideaux, V. Chow, S. Benchimol and A. Bernstein (1988). "Inactivation of the p53 oncogene by internal deletion or retroviral integration in erythroleukemic cell lines induced by Friend leukemia virus." Oncogene **3**(2): 179-185.

Benveniste, P., C. Frelin, S. Janmohamed, M. Barbara, R. Herrington, D. Hyam and N. N. Iscove (2010). "Intermediate-term hematopoietic stem cells with extended but time-limited reconstitution potential." Cell Stem Cell **6**(1): 48-58.

Berger, S. L., T. Kouzarides, R. Shiekhattar and A. Shilatifard (2009). "An operational definition of epigenetics." Genes Dev **23**(7): 781-783.

Bertrand, J. Y., N. C. Chi, B. Santoso, S. Teng, D. Y. Stainier and D. Traver (2010). "Haematopoietic stem cells derive directly from aortic endothelium during development." Nature **464**(7285): 108-111.

Blackledge, N. P., A. M. Farcas, T. Kondo, H. W. King, J. F. McGouran, L. L. Hanssen, S. Ito, S. Cooper, K. Kondo, Y. Koseki, T. Ishikura, H. K. Long, T. W. Sheahan, N. Brockdorff, B. M. Kessler, H. Koseki and R. J. Klose (2014). "Variant PRC1 complex-dependent H2A ubiquitylation drives PRC2 recruitment and polycomb domain formation." Cell **157**(6): 1445-1459.

Boisset, J. C., W. van Cappellen, C. Andrieu-Soler, N. Galjart, E. Dzierzak and C. Robin (2010). "In vivo imaging of haematopoietic cells emerging from the mouse aortic endothelium." Nature **464**(7285): 116-120.

Bommi, P. V., M. Dimri, A. A. Sahasrabuddhe, J. Khandekar and G. P. Dimri (2010). "The polycomb group protein BMI1 is a transcriptional target of HDAC inhibitors." Cell Cycle **9**(13): 2663-2673.

Boulay, G., C. Rosnoblet, C. Guerardel, P. O. Angrand and D. Leprince (2011). "Functional characterization of human Polycomb-like 3 isoforms identifies them as components of distinct EZH2 protein complexes." Biochem J **434**(2): 333-342.

Bowie, M. B., K. D. McKnight, D. G. Kent, L. McCaffrey, P. A. Hoodless and C. J. Eaves (2006). "Hematopoietic stem cells proliferate until after birth and show a reversible phase-specific engraftment defect." J Clin Invest **116**(10): 2808-2816.

Bowie, M. B., D. G. Kent, B. Dykstra, K. D. McKnight , L. McCaffrey, P. A. Hoodless and C. J. Eaves (2007). " Identification of a new intrinsically timed developmental checkpoint that reprograms key hematopoietic stem cell properties." PNAS 104(14): 5878-5882.

Boyer, L. A., K. Plath, J. Zeitlinger, T. Brambrink, L. A. Medeiros, T. I. Lee, S. S. Levine, M. Wernig, A. Tajonar, M. K. Ray, G. W. Bell, A. P. Otte, M. Vidal, D. K. Gifford, R. A. Young and R. Jaenisch (2006). "Polycomb complexes repress developmental regulators in murine embryonic stem cells." Nature **441**(7091): 349-353.

Bracken, A. P., N. Dietrich, D. Pasini, K. H. Hansen and K. Helin (2006). "Genome-wide mapping of Polycomb target genes unravels their roles in cell fate transitions." Genes Dev **20**(9): 1123-1136.

Bracken, A. P. and K. Helin (2009). "Polycomb group proteins: navigators of lineage pathways led astray in cancer." Nat Rev Cancer **9**(11): 773-784.

Bracken, A. P., D. Kleine-Kohlbrecher, N. Dietrich, D. Pasini, G. Gargiulo, C. Beekman, K. Theilgaard-Monch, S. Minucci, B. T. Porse, J. C. Marine, K. H. Hansen and K. Helin (2007). "The Polycomb group proteins bind throughout the INK4A-ARF locus and are disassociated in senescent cells." Genes Dev **21**(5): 525-530.

Bracken, A. P., D. Pasini, M. Capra, E. Prosperini, E. Colli and K. Helin (2003). "EZH2 is downstream of the pRB-E2F pathway,

essential for proliferation and amplifed in cancer." EMBO J **22**(20): 5323-5335.

Bradford, G. B., B. Williams, R. Rossi and I. Bertoncello (1997). "Quiescence, cycling, and turnover in the primitive hematopoietic stem cell compartment." Exp Hematol **25**(5): 445-453.

Brecqueville, M., N. Cervera, J. Adelaide, J. Rey, N. Carbuccia, M. Chaffanet, M. J. Mozziconacci, N. Vey, D. Birnbaum, V. Gelsi-Boyer and A. Murati (2011). "Mutations and deletions of the SUZ12 polycomb gene in myeloproliferative neoplasms." Blood Cancer J **1**(8): e33.

Bresnick, E. H., H. Y. Lee, T. Fujiwara, K. D. Johnson and S. Keles (2010). "GATA switches as developmental drivers." J Biol Chem **285**(41): 31087-31093.

Brien, G. L., E. Healy, E. Jerman, E. Conway, E. Fadda, D. O'Donovan, A. V. Krivtsov, A. M. Rice, C. J. Kearney, A. Flaus, S. S. McDade, S. J. Martin, A. McLysaght, D. J. O'Connell, S.

A. Armstrong and A. P. Bracken (2015). "A chromatin-independent role of Polycomb-like 1 to stabilize p53 and promote cellular quiescence." Genes Dev **29**(21): 2231-2243.

Cai, L., S. B. Rothbart, R. Lu, B. Xu, W. Y. Chen, A. Tripathy, S. Rockowitz, D. Zheng, D. J. Patel, C. D. Allis, B. D. Strahl, J. Song and G. G. Wang (2013). "An H3K36 methylation-engaging Tudor motif of polycomb-like proteins mediates PRC2 complex targeting." Mol Cell **49**(3): 571-582.

Cales, C., M. Roman-Trufero, L. Pavon, I. Serrano, T. Melgar, M. Endoh, C. Perez, H. Koseki and M. Vidal (2008). "Inactivation of the polycomb group protein Ring1B unveils an antiproliferative role in hematopoietic cell expansion and cooperation with tumorigenesis associated with Ink4a deletion." Mol Cell Biol **28**(3): 1018-1028.

Cancer Genome Atlas Research, N. (2013). "Genomic and epigenomic landscapes of adult de novo acute myeloid leukemia." N Engl J Med **368**(22): 2059-2074.

Cao, R., H. Wang, J. He, H. Erdjument-Bromage, P. Tempst and Y. Zhang (2008). "Role of hPHF1 in H3K27 methylation and Hox gene silencing." Mol Cell Biol **28**(5): 1862-1872.

Cao, R., L. Wang, H. Wang, L. Xia, H. Erdjument-Bromage, P. Tempst, R. S. Jones and Y. Zhang (2002). "Role of histone H3 lysine 27 methylation in Polycomb-group silencing." Science **298**(5595): 1039-1043.

Cao, R. and Y. Zhang (2004). "SUZ12 is required for both the histone methyltransferase activity and the silencing function of the EED-EZH2 complex." Mol Cell **15**(1): 57-67.

Casanova, M., T. Preissner, A. Cerase, R. Poot, D. Yamada, X. Li, R. Appanah, K. Bezstarosti, J. Demmers, H. Koseki and N. Brockdorff (2011). "Polycomblike 2 facilitates the recruitment of PRC2 Polycomb group complexes to the inactive X chromosome and to target loci in embryonic stem cells." Development **138**(8): 1471-1482.

Chan, C. S., L. Rastelli and V. Pirrotta (1994). "A Polycomb response element in the Ubx gene that determines an epigenetically inherited state of repression." EMBO J **13**(11): 2553-2564.

Cheng, T. (2000). "Hematopoietic Stem Cell Quiescence Maintained by p21cip1/waf1." Science **287**(5459): 1804-1808.

Cheshier, S. H., S. J. Morrison, X. Liao and I. L. Weissman (1999). "In vivo proliferation and cell cycle kinetics of long-term self-renewing hematopoietic stem cells." Proc Natl Acad Sci U S A **96**(6): 3120-3125.

Christophersen, N. S. and K. Helin (2010). "Epigenetic control of embryonic stem cell fate." J Exp Med **207**(11): 2287-2295.

Chu, H. C., H. Y. Lee, Y. S. Huang, W. L. Tseng, C. J. Yen, J. C. Cheng and C. P. Tseng (2014). "Erythroid differentiation is augmented in Reelin-deficient K562 cells and homozygous reeler mice." FEBS Lett **588**(1): 58-64.

Chung, S. W., L. Wolff and S. K. Ruscetti (1989). "Transmembrane domain of the envelope gene of a polycythemia-inducing retrovirus determines erythropoietin-independent growth." Proc Natl Acad Sci U S A **86**(20): 7957-7960.

Clark, A. J., K. M. Doyle and P. O. Humbert (2004). "Cell-intrinsic requirement for pRb in erythropoiesis." Blood **104**(5): 1324-1326.

Cmarik, J. and S. Ruscetti (2010). "Friend Spleen Focus-Forming Virus Activates the Tyrosine Kinase sf-Stk and the Transcription Factor PU.1 to Cause a Multi-Stage Erythroleukemia in Mice." Viruses **2**(10): 2235-2257.

Collett, K., G. E. Eide, J. Arnes, I. M. Stefansson, J. Eide, A. Braaten, T. Aas, A. P. Otte and L. A. Akslen (2006). "Expression of enhancer of zeste homologue 2 is significantly associated with increased tumor cell proliferation and is a marker of aggressive breast cancer." Clin Cancer Res **12**(4): 1168-1174.

Consortium, E. P. (2007). "Identification and analysis of functional elements in 1% of the human genome by the ENCODE pilot project." Nature **447**(7146): 799-816.

Czermin, B., R. Melfi, D. McCabe, V. Seitz, A. Imhof and V. Pirrotta (2002). "Drosophila Enhancer of Zeste/ESC Complexes Have a Histone H3 Methyltransferase Activity that Marks Chromosomal Polycomb Sites." Cell **111**: 185-196.

Deaton, A. M. and A. Bird (2011). "CpG islands and the regulation of transcription." Genes Dev **25**(10): 1010-1022.

Ding, L. and S. J. Morrison (2013). "Haematopoietic stem cells and early lymphoid progenitors occupy distinct bone marrow niches." Nature **495**(7440): 231-235.

Ding, L., T. L. Saunders, G. Enikolopov and S. J. Morrison (2012). "Endothelial and perivascular cells maintain haematopoietic stem cells." Nature **481**(7382): 457-462.

Dore, L. C., T. M. Chlon, C. D. Brown, K. P. White and J. D. Crispino (2012). "Chromatin occupancy analysis reveals genome-wide GATA factor switching during hematopoiesis." Blood **119**(16): 3724-3733.

Dos Santos, C., T. McDonald, Y. W. Ho, H. Liu, A. Lin, S. J. Forman, Y. H. Kuo and R. Bhatia (2013). "The Src and c-Kit kinase inhibitor dasatinib enhances p53-mediated targeting of human acute myeloid leukemia stem cells by chemotherapeutic agents." Blood **122**(11): 1900-1913.

Dumble, M., L. Moore, S. M. Chambers, H. Geiger, G. Van Zant, M. A. Goodell and L. A. Donehower (2007). "The impact of altered p53 dosage on hematopoietic stem cell dynamics during aging." Blood **109**(4): 1736-1742.

Duncan, I. M. (1982). "Polycomblike: A Gene That Appears to be Required for the Normal Expresion of the Bithorax and Antennapedia Gene Complexes of Drosophila Melanogaster." Genetics **102**: 49-70.

Eilken, H. M., S. Nishikawa and T. Schroeder (2009). "Continuous single-cell imaging of blood generation from haemogenic endothelium." Nature **457**(7231): 896-900.

Ernst, J. and M. Kellis (2013). "Interplay between chromatin state, regulator binding, and regulatory motifs in six human cell types." Genome Res **23**(7): 1142-1154.

Ernst, T., A. J. Chase, J. Score, C. E. Hidalgo-Curtis, C. Bryant, A. V. Jones, K. Waghorn, K. Zoi, F. M. Ross, A. Reiter, A. Hochhaus, H. G. Drexler, A. Duncombe, F. Cervantes, D. Oscier, J. Boultwood, F. H. Grand and N. C. Cross (2010). "Inactivating mutations of the histone methyltransferase gene EZH2 in myeloid disorders." Nat Genet **42**(8): 722-726.

Faderl, S., M. Talpaz, Z. Estrov, S. O'Brien, R. Kurzrock and H. M. Kantarjian (1999). "The biology of chronic myeloid leukemia." N Engl J Med **341**(3): 164-172.

Fan, A. C., D. Deb-Basu, M. W. Orban, J. R. Gotlib, Y. Natkunam, R. O'Neill, R. A. Padua, L. Xu, D. Taketa, A. E. Shirer, S. Beer, A. X. Yee, D. W. Voehringer and D. W. Felsher (2009). "Nanofluidic proteomic assay for serial analysis of oncoprotein activation in clinical specimens." Nat Med **15**(5): 566-571.

Faust, C., A. Schumacher, B. Holdener and T. Magnuson (1995). "The eed mutation disrupts anterior mesoderm production in mice." Development **121**: 273-285.

Fauvarque, M. O. and J. M. Dura (1993). "polyhomeotic regulatory sequences induce developmental regulator-dependent variegation and targeted P-element insertions in Drosophila." Genes Dev **7**(8): 1508-1520.

Fialkow, P. J., J. W. Singer, W. H. Raskind, J. W. Adamson, R. J. Jacobson, I. D. Bernstein, L. W. Dow, V. Najfeld and R. Veith (1987). "Clonal development, stem-cell differentiation, and clinical remissions in acute nonlymphocytic leukemia." N Engl J Med **317**(8): 468-473.

Fiskus, W., M. Pranpat, M. Balasis, B. Herger, R. Rao, A. Chinnaiyan, P. Atadja and K. Bhalla (2006). "Histone deacetylase inhibitors deplete enhancer of zeste 2 and associated polycomb repressive complex 2 proteins in human acute leukemia cells." Mol Cancer Ther **5**(12): 3096-3104.

Fraser, S. T., J. Isern and M. H. Baron (2007). "Maturation and enucleation of primitive erythroblasts during mouse embryogenesis is accompanied by changes in cell-surface antigen expression." Blood **109**(1): 343-352.

Friberg, A., A. Oddone, T. Klymenko, J. Muller and M. Sattler (2010). "Structure of an atypical Tudor domain in the Drosophila Polycomblike protein." Protein Sci **19**(10): 1906-1916.

Friedrich, G. and P. Soriano (1991). "Promoter traps in embryonic stem cells: a genetic screen to identify and mutate developmental genes in mice." Genes Dev **5**(9): 1513-1523.

Friend, C., W. Scher, J. G. Holland and T. Sato (1971). "Hemoglobin synthesis in murine virus-induced leukemic cells in vitro: stimulation of erythroid differentiation by dimethyl sulfoxide." Proc Natl Acad Sci U S A **68**(2): 378-382.

Gala, S., A. Marreiros, G. J. Stewart and P. Williamson (2001). "Overexpression of E2F-1 leads to cytokine-independent proliferation and survival in the hematopoietic cell line BaF-B03." Blood **97**(1): 227-234.

Gao, Z., J. Zhang, R. Bonasio, F. Strino, A. Sawai, F. Parisi, Y. Kluger and D. Reinberg (2012). "PCGF homologs, CBX proteins, and RYBP define functionally distinct PRC1 family complexes." Mol Cell **45**(3): 344-356.

Garapaty-Rao, S., C. Nasveschuk, A. Gagnon, E. Y. Chan, P. Sandy, J. Busby, S. Balasubramanian, R. Campbell, F. Zhao, L. Bergeron, J. E. Audia, B. K. Albrecht, J. C. Harmange, R. Cummings and P. Trojer (2013). "Identification of EZH2 and EZH1 small molecule inhibitors with selective impact on diffuse large B cell lymphoma cell growth." Chem Biol **20**(11): 1329-1339.

Geiduschek, J. B. and S. J. Singer (1979). "Molecular changes in the membranes of mouse erythroid cells accompanying differentiation." Cell **16**(1): 149-163.

Ghislin, S., F. Deshayes, S. Middendorp, N. Boggetto and C. Alcaide-Loridan (2012). "PHF19 and Akt control the switch between proliferative and invasive states in melanoma." Cell Cycle **11**(8): 1634-1645.

Giebel, B. and I. Bruns (2008). "Self-renewal versus differentiation in hematopoietic stem and progenitor cells: a focus on asymmetric cell divisions." Curr Stem Cell Res Ther **3**(1): 9-16.

Gieni, R. S. and M. J. Hendzel (2009). "Polycomb group protein gene silencing, non-coding RNA, stem cells, and cancer." Biochemistry and Cell Biology **87**(5): 711-746.

Gilliland, D. G. and J. D. Griffin (2002). "Role of FLT3 in leukemia." Curr Opin Hematol **9**(4): 274-281.

Gossler, A., A. L. Joyner, J. Rossant and W. C. Skarnes (1989). "Mouse embryonic stem cells and reporter constructs to detect developmentally regulated genes." Science **244**(4903): 463-465.

Greenbaum, A., Y. M. Hsu, R. B. Day, L. G. Schuettpelz, M. J. Christopher, J. N. Borgerding, T. Nagasawa and D. C. Link (2013). "CXCL12 in early mesenchymal progenitors is required for haematopoietic stem-cell maintenance." Nature **495**(7440): 227-230.

Griffiths, R. E., S. Kupzig, N. Cogan, T. J. Mankelow, V. M. Betin, K. Trakarnsanga, E. J. Massey, J. D. Lane, S. F. Parsons and D. J. Anstee (2012). "Maturing reticulocytes internalize plasma membrane in glycophorin A-containing vesicles that fuse with autophagosomes before exocytosis." Blood **119**(26): 6296-6306.

Griffon, A., Q. Barbier, J. Dalino, J. van Helden, S. Spicuglia and B. Ballester (2015). "Integrative analysis of public ChIP-seq experiments reveals a complex multi-cell regulatory landscape." Nucleic Acids Res **43**(4): e27.

Guzman, M. L., N. Yang, K. K. Sharma, M. Balys, C. A. Corbett, C. T. Jordan, M. W. Becker, U. Steidl, O. Abdel-Wahab, R. L. Levine, G. Marcucci, G. J. Roboz and D. C. Hassane (2014). "Selective activity of the histone deacetylase inhibitor AR-42 against leukemia stem cells: a novel potential strategy in acute myelogenous leukemia." Mol Cancer Ther **13**(8): 1979-1990.

Hanahan, D. and R. A. Weinberg (2000). "The hallmarks of cancer." Cell **100**(1): 57-70.

Hanahan, D. and R. A. Weinberg (2011). "Hallmarks of cancer: the next generation." Cell **144**(5): 646-674.

Hanson, R. D., J. L. Hess, B. D. Yu, P. Ernst, M. van Lohuizen, A. Berns, N. M. van der Lugt, C. S. Shashikant, F. H. Ruddle, M. Seto and S. J. Korsmeyer (1999). "Mammalian Trithorax and polycomb-group homologues are antagonistic regulators of homeotic development." Proc Natl Acad Sci U S A **96**(25): 14372-14377.

Hegde, S., P. Hankey and R. F. Paulson (2012). "Self-renewal of leukemia stem cells in Friend virus-induced erythroleukemia requires proviral insertional activation of Spi1 and hedgehog signaling but not mutation of p53." Stem Cells **30**(2): 121-130.

Hegde, S., N. Kaushal, K. C. Ravindra, C. Chiaro, K. T. Hafer, U. H. Gandhi, J. T. Thompson, J. P. van den Heuvel, M. J. Kennett, P. Hankey, R. F. Paulson and K. S. Prabhu (2011).

"Delta12-prostaglandin J3, an omega-3 fatty acid-derived metabolite, selectively ablates leukemia stem cells in mice." Blood **118**(26): 6909-6919.

Heintzman, N. D., G. C. Hon, R. D. Hawkins, P. Kheradpour, A. Stark, L. F. Harp, Z. Ye, L. K. Lee, R. K. Stuart, C. W. Ching, K. A. Ching, J. E. Antosiewicz-Bourget, H. Liu, X. Zhang, R. D. Green, V. V. Lobanenkov, R. Stewart, J. A. Thomson, G. E. Crawford, M. Kellis and B. Ren (2009). "Histone modifications at human enhancers reflect global cell-type-specific gene expression." Nature **459**(7243): 108-112.

Herrmann, H., K. Blatt, J. Shi, K. V. Gleixner, S. Cerny-Reiterer, L. Mullauer, C. R. Vakoc, W. R. Sperr, H. P. Horny, J. E. Bradner, J. Zuber and P. Valent (2012). "Small-molecule inhibition of BRD4 as a new potent approach to eliminate leukemic stem- and progenitor cells in acute myeloid leukemia AML." Oncotarget **3**(12): 1588-1599.

Huang, W., R. Loganantharaj, B. Schroeder, D. Fargo and L. Li (2013). "PAVIS: a tool for Peak Annotation and Visualization." Bioinformatics **29**(23): 3097-3099.

Hunkapiller, J., Y. Shen, A. Diaz, G. Cagney, D. McCleary, M. Ramalho-Santos, N. Krogan, B. Ren, J. S. Song and J. F. Reiter (2012). "Polycomb-like 3 promotes polycomb repressive complex 2 binding to CpG islands and embryonic stem cell self-renewal." PLoS Genet **8**(3): e1002576.

Ikonomi, P., C. E. Rivera, M. Riordan, G. Washington, A. N. Schechter and C. T. Noguchi (2000). "Overexpression of GATA-2 inhibits erythroid and promotes megakaryocyte differentiation." Exp Hematol **28**(12): 1423-1431.

Ingham, P. W. (1985). "A clonal analysis of the requirement for the trithorax gene in the diversification of segments in Drosophila." J Embryol Exp Morphol **89**: 349-365.

Isern, J., S. T. Fraser, Z. He and M. H. Baron (2010). "Dose-dependent regulation of primitive erythroid maturation and identity by the transcription factor Eklf." Blood **116**: 3972-3980.

Ivanova, N., R. Dobrin, R. Lu, I. Kotenko, J. Levorse, C. DeCoste, X. Schafer, Y. Lun and I. R. Lemischka (2006). "Dissecting self-renewal in stem cells with RNA interference." Nature **442**(7102): 533-538.

Iwama, A., H. Oguro, M. Negishi, Y. Kato, Y. Morita, H. Tsukui, H. Ema, T. Kamijo, Y. Katoh-Fukui, H. Koseki, M. van Lohuizen and H. Nakauchi (2004). "Enhanced self-renewal of hematopoietic stem cells mediated by the polycomb gene product Bmi-1." Immunity **21**(6): 843-851.

Iwasaki, H., C. Somoza, H. Shigematsu, E. A. Duprez, J. Iwasaki-Arai, S. Mizuno, Y. Arinobu, K. Geary, P. Zhang, T. Dayaram, M. L. Fenyus, S. Elf, S. Chan, P. Kastner, C. S.

Huettner, R. Murray, D. G. Tenen and K. Akashi (2005). "Distinctive and indispensable roles of PU.1 in maintenance of hematopoietic stem cells and their differentiation." Blood **106**(5): 1590-1600.

Jacobs, J. J., K. Kieboom, S. Marino, R. A. DePinho and M. van Lohuizen (1999). "The oncogene and Polycomb-group gene bmi-1 regulates cell proliferation and senescence through the ink4a locus." Nature **397**(6715): 164-168.

Jan, M., T. M. Snyder, M. R. Corces-Zimmerman, P. Vyas, I. L. Weissman, S. R. Quake and R. Majeti (2012). "Clonal evolution of preleukemic hematopoietic stem cells precedes human acute myeloid leukemia." Sci Transl Med **4**(149): 149ra118.

Janzen, C. J., S. B. Hake, J. E. Lowell and G. A. Cross (2006). "Selective di- or trimethylation of histone H3 lysine 76 by two DOT1 homologs is important for cell cycle regulation in Trypanosoma brucei." Mol Cell **23**(4): 497-507.

Jung, J., M. R. Mysliwiec and Y. Lee (2005). "Roles of JUMONJI in mouse embryonic development." Dev Dyn **232**(1): 21-32.

Kahn, T. G., P. Stenberg, V. Pirrotta and Y. B. Schwartz (2014). "Combinatorial interactions are required for the efficient recruitment of pho repressive complex (PhoRC) to polycomb response elements." PLoS Genet **10**(7): e1004495.

Kaneko, H., R. Shimizu and M. Yamamoto (2010). "GATA factor switching during erythroid differentiation." Curr Opin Hematol **17**(3): 163-168.

Kassouf, M. T., J. R. Hughes, S. Taylor, S. J. McGowan, S. Soneji, A. L. Green, P. Vyas and C. Porcher (2010). "Genome-wide identification of TAL1's functional targets: insights into its mechanisms of action in primary erythroid cells." Genome Res **20**(8): 1064-1083.

Kennison, J. A. and J. W. Tamkun (1988). "Dosage-dependent modifiers of polycomb and antennapedia mutations in Drosophila." Proc Natl Acad Sci U S A **85**(21): 8136-8140.

Khalil, A. M., M. Guttman, M. Huarte, M. Garber, A. Raj, D. Rivea Morales, K. Thomas, A. Presser, B. E. Bernstein, A. van Oudenaarden, A. Regev, E. S. Lander and J. L. Rinn (2009). "Many human large intergenic noncoding RNAs associate with chromatin-modifying complexes and affect gene expression." Proc Natl Acad Sci U S A **106**(28): 11667-11672.

Kiel, M. J., S. He, R. Ashkenazi, S. N. Gentry, M. Teta, J. A. Kushner, T. L. Jackson and S. J. Morrison (2007). "Haematopoietic stem cells do not asymmetrically segregate chromosomes or retain BrdU." Nature **449**(7159): 238-242.

Kiel, M. J., O. H. Yilmaz, T. Iwashita, O. H. Yilmaz, C. Terhorst and S. J. Morrison (2005). "SLAM family receptors distinguish hematopoietic stem and progenitor cells and reveal endothelial niches for stem cells." Cell **121**(7): 1109-1121.

Kim, H., K. Kang, M. B. Ekram, T. Y. Roh and J. Kim (2011). "Aebp2 as an epigenetic regulator for neural crest cells." PLoS One **6**(9): e25174.

Kim, H., K. Kang and J. Kim (2009). "AEBP2 as a potential targeting protein for Polycomb Repression Complex PRC2." Nucleic Acids Res **37**(9): 2940-2950.

Kim, T. G., J. C. Kraus, J. Chen and Y. Lee (2003). "JUMONJI, a critical factor for cardiac development, functions as a transcriptional repressor." J Biol Chem **278**(43): 42247-42255.

Kim, W., K. D. Klarmann and J. R. Keller (2014). "Gfi-1 regulates the erythroid transcription factor network through Id2 repression in murine hematopoietic progenitor cells." Blood **124**(10): 1586-1596.

Kingsley, P. D., J. Malik, R. L. Emerson, T. P. Bushnell, K. E. McGrath, L. A. Bloedorn, M. Bulger and J. Palis (2006). ""Maturational" globin switching in primary primitive erythroid cells." Blood **107**(4): 1665-1672.

Kingsley, P. D., J. Malik, K. A. Fantauzzo and J. Palis (2004). "Yolk sac-derived primitive erythroblasts enucleate during mammalian embryogenesis." Blood **104**(1): 19-25.

Kinkel, S. A., R. Galeev, C. Flensburg, A. Keniry, K. Breslin, O. Gilan, S. Lee, J. Liu, K. Chen, L. J. Gearing, D. L. Moore, W. S. Alexander, M. Dawson, I. J. Majewski, A. Oshlack, J. Larsson and M. E. Blewitt (2015). "Jarid2 regulates hematopoietic stem cell function by acting with polycomb repressive complex 2." Blood **125**(12): 1890-1900.

Kirmizis, A., S. M. Bartley and P. J. Farnham (2003). "Identification of the polycomb group protein SU(Z)12 as a potential molecular target for human cancer therapy." Mol Cancer Ther **2**(1): 113-121.

Kissa, K. and P. Herbomel (2010). "Blood stem cells emerge from aortic endothelium by a novel type of cell transition." Nature **464**(7285): 112-115.

Kitajima, K., M. Kojima, K. Nakajima, H. Kondo, A. Miyajima and T. Takeuchi (1999). "Definitive But Not Primitive Hematopoiesis Is Impaired in jumonji Mutant Mice." Blood **1999**(93): 87-95.

Kleer, C. G., Q. Cao, S. Varambally, R. Shen, I. Ota, S. A. Tomlins, D. Ghosh, R. G. Sewalt, A. P. Otte, D. F. Hayes, M. S. Sabel, D. Livant, S. J. Weiss, M. A. Rubin and A. M. Chinnaiyan (2003). "EZH2 is a marker of aggressive breast cancer and promotes

neoplastic transformation of breast epithelial cells." Proc Natl Acad Sci U S A **100**(20): 11606-11611.

Klose, R. J., E. M. Kallin and Y. Zhang (2006). "JmjC-domain-containing proteins and histone demethylation." Nat Rev Genet **7**(9): 715-727.

Knezevic, K., T. Bee, N. K. Wilson, M. E. Janes, S. Kinston, S. Polderdijk, A. Kolb-Kokocinski, K. Ottersbach, N. Pencovich, Y. Groner, M. de Bruijn, B. Gottgens and J. E. Pimanda (2011). "A Runx1-Smad6 rheostat controls Runx1 activity during embryonic hematopoiesis." Mol Cell Biol **31**(14): 2817-2826.

Konstantinidis, D. G., S. Pushkaran, K. Giger, S. Manganaris, Y. Zheng and T. A. Kalfa (2014). "Identification of a murine erythroblast subpopulation enriched in enucleating events by multi-spectral imaging flow cytometry." J Vis Exp(88).

Kotake, Y., R. Cao, P. Viatour, J. Sage, Y. Zhang and Y. Xiong (2007). "pRB family proteins are required for H3K27 trimethylation and Polycomb repression complexes binding to and silencing p16INK4alpha tumor suppressor gene." Genes Dev **21**(1): 49-54.

Koulnis, M., R. Pop, E. Porpiglia, J. R. Shearstone, D. Hidalgo and M. Socolovsky (2011). "Identification and analysis of mouse erythroid progenitors using the CD71/TER119 flow-cytometric assay." J Vis Exp(54): 2809.

Koury, S. T., M. J. Koury and M. C. Bondurant (1989). "Cytoskeletal distribution and function during the maturation and enucleation of mammalian erythroblasts." J Cell Biol **109**(6 Pt 1): 3005-3013.

Ku, M., R. P. Koche, E. Rheinbay, E. M. Mendenhall, M. Endoh, T. S. Mikkelsen, A. Presser, C. Nusbaum, X. Xie, A. S. Chi, M. Adli, S. Kasif, L. M. Ptaszek, C. A. Cowan, E. S. Lander, H. Koseki and B. E. Bernstein (2008). "Genomewide analysis of PRC1 and PRC2 occupancy identifies two classes of bivalent domains." PLoS Genet **4**(10): e1000242.

Kuzmichev, A., K. Nishioka, H. Erdjument-Bromage, P. Tempst and D. Reinberg (2002). "Histone methyltransferase activity associated with a human multiprotein complex containing the Enhancer of Zeste protein." Genes Dev **16**(22): 2893-2905.

Landeira, D., S. Sauer, R. Poot, M. Dvorkina, L. Mazzarella, H. F. Jorgensen, C. F. Pereira, M. Leleu, F. M. Piccolo, M. Spivakov, E. Brookes, A. Pombo, C. Fisher, W. C. Skarnes, T. Snoek, K. Bezstarosti, J. Demmers, R. J. Klose, M. Casanova, L. Tavares, N. Brockdorff, M. Merkenschlager and A. G. Fisher (2010). "Jarid2 is a PRC2 component in embryonic stem cells required for multi-lineage differentiation and recruitment of PRC1 and RNA Polymerase II to developmental regulators." Nat Cell Biol **12**(6): 618-624.

Langmead, B. and S. L. Salzberg (2012). "Fast gapped-read alignment with Bowtie 2." Nat Methods **9**(4): 357-359.

Laurenti, E., C. Frelin, S. Xie, R. Ferrari, C. F. Dunant, S. Zandi, A. Neumann, I. Plumb, S. Doulatov, J. Chen, C. April, J. B. Fan, N. Iscove and J. E. Dick (2015). "CDK6 levels regulate quiescence exit in human hematopoietic stem cells." Cell Stem Cell **16**(3): 302-313.

Lee, J. C., J. A. Gimm, A. J. Lo, M. J. Koury, S. W. Krauss, N. Mohandas and J. A. Chasis (2004). "Mechanism of protein sorting during erythroblast enucleation: role of cytoskeletal connectivity." Blood **103**(5): 1912-1919.

Lee, S. C., S. Miller, C. Hyland, M. Kauppi, M. Lebois, L. Di Rago, D. Metcalf, S. A. Kinkel, E. C. Josefsson, M. E. Blewitt, I. J. Majewski and W. S. Alexander (2015). "Polycomb repressive complex 2 component Suz12 is required for hematopoietic stem cell function and lymphopoiesis." Blood.

Leeb, M., D. Pasini, M. Novatchkova, M. Jaritz, K. Helin and A. Wutz (2010). "Polycomb complexes act redundantly to repress genomic repeats and genes." Genes Dev **24**(3): 265-276.

Lewis, E. B. (1978). "A gene complex controlling segmentation in Drosophila." Nature **276**(5688): 565-570.

Li, G., R. Margueron, M. Ku, P. Chambon, B. E. Bernstein and D. Reinberg (2010). "Jarid2 and PRC2, partners in regulating gene expression." Genes Dev **24**(4): 368-380.

Li, J. P., A. D. D'Andrea, H. F. Lodish and D. Baltimore (1990). "Activation of cell growth by binding of Friend spleen focus-forming virus gp55 glycoprotein to the erythropoietin receptor." Nature **343**(6260): 762-764.

Li, L., J. Y. Lee, J. Gross, S. H. Song, A. Dean and P. E. Love (2010). "A requirement for Lim domain binding protein 1 in erythropoiesis." J Exp Med **207**(12): 2543-2550.

Li, X., K. Isono, D. Yamada, T. A. Endo, M. Endoh, J. Shinga, Y. Mizutani-Koseki, A. P. Otte, M. Casanova, H. Kitamura, T. Kamijo, J. Sharif, O. Ohara, T. Toyada, B. E. Bernstein, N. Brockdorff and H. Koseki (2011). "Mammalian polycomb-like Pcl2/Mtf2 is a novel regulatory component of PRC2 that can differentially modulate polycomb activity both at the Hox gene cluster and at Cdkn2a genes." Mol Cell Biol **31**(2): 351-364.

Liao, S. K. and A. A. Axelrad (1975). "Erythropoietin-independent erythroid colony formation in vitro by hemopoietic cells of mice infected with friend virus." Int J Cancer **15**(3): 467-482.

Lin, Y. W., H. M. Chen and J. Y. Fang (2011). "Gene silencing by the Polycomb group proteins and associations with cancer." Cancer Invest **29**(3): 187-195.

Ling, K. W., K. Ottersbach, J. P. van Hamburg, A. Oziemlak, F. Y. Tsai, S. H. Orkin, R. Ploemacher, R. W. Hendriks and E. Dzierzak (2004). "GATA-2 plays two functionally distinct roles during the ontogeny of hematopoietic stem cells." J Exp Med **200**(7): 871-882.

Liu, J., N. Mohandas and X. An (2011). "Membrane assembly during erythropoiesis." Curr Opin Hematol **18**(3): 133-138.

Londhe, P. and J. K. Davie (2013). "Interferon-gamma resets muscle cell fate by stimulating the sequential recruitment of JARID2 and PRC2 to promoters to repress myogenesis." Sci Signal **6**(305): ra107.

Longmore, G. D. and H. F. Lodish (1991). "An activating mutation in the murine erythropoietin receptor induces erythroleukemia in mice: a cytokine receptor superfamily oncogene." Cell **67**(6): 1089-1102.

Lund, A. H. and M. van Lohuizen (2004). "Polycomb complexes and silencing mechanisms." Curr Opin Cell Biol **16**(3): 239-246.

Lynch, M. D., A. J. Smith, M. De Gobbi, M. Flenley, J. R. Hughes, D. Vernimmen, H. Ayyub, J. A. Sharpe, J. A. Sloane-Stanley, L. Sutherland, S. Meek, T. Burdon, R. J. Gibbons, D. Garrick and D. R. Higgs (2012). "An interspecies analysis reveals a key role for unmethylated CpG dinucleotides in vertebrate Polycomb complex recruitment." EMBO J **31**(2): 317-329.

Mager, D. L. and A. Bernstein (1985). "Induction of clonogenic and erythroleukemic cells by different helper virus pseudotypes of Friend spleen focus-forming virus." Virology **141**(2): 337-341.

Majewski, I. J., M. E. Blewitt, C. A. de Graaf, E. J. McManus, M. Bahlo, A. A. Hilton, C. D. Hyland, G. K. Smyth, J. E. Corbin, D. Metcalf, W. S. Alexander and D. J. Hilton (2008). "Polycomb repressive complex 2 (PRC2) restricts hematopoietic stem cell activity." PLoS Biol **6**(4): e93.

Malaterre, J., M. Carpinelli, M. Ernst, W. Alexander, M. Cooke, S. Sutton, S. Dworkin, J. K. Heath, J. Frampton, G. McArthur, H. Clevers, D. Hilton, T. Mantamadiotis and R. G. Ramsay (2007). "c-Myb is required for progenitor cell homeostasis in colonic crypts." Proc Natl Acad Sci U S A **104**(10): 3829-3834.

Malumbres, M., R. Sotillo, D. Santamaria, J. Galan, A. Cerezo, S. Ortega, P. Dubus and M. Barbacid (2004). "Mammalian cells cycle without the D-type cyclin-dependent kinases Cdk4 and Cdk6." Cell **118**(4): 493-504.

Margueron, R. and D. Reinberg (2011). "The Polycomb complex PRC2 and its mark in life." Nature **469**(7330): 343-349.

Martin-Perez, D., M. A. Piris and M. Sanchez-Beato (2010). "Polycomb proteins in hematologic malignancies." Blood **116**(25): 5465-5475.

Masuoka, H. C. and T. M. Townes (2002). "Targeted disruption of the activating transcription factor 4 gene results in severe fetal anemia in mice." Blood **99**(3): 736-745.

Matsumoto, A., S. Takeishi, T. Kanie, E. Susaki, I. Onoyama, Y. Tateishi, K. Nakayama and K. I. Nakayama (2011). "p57 is required for quiescence and maintenance of adult hematopoietic stem cells." Cell Stem Cell **9**(3): 262-271.

Matushansky, I., F. Radparvar and A. I. Skoultchi (2003). "CDK6 blocks differentiation: coupling cell proliferation to the block to differentiation in leukemic cells." Oncogene **22**(27): 4143-4149.

McCabe, M. T., H. M. Ott, G. Ganji, S. Korenchuk, C. Thompson, G. S. Van Aller, Y. Liu, A. P. Graves, A. Della Pietra, 3rd, E. Diaz, L. V. LaFrance, M. Mellinger, C. Duquenne, X. Tian, R. G. Kruger, C. F. McHugh, M. Brandt, W. H. Miller, D. Dhanak, S. K. Verma, P. J. Tummino and C. L. Creasy (2012). "EZH2 inhibition as a therapeutic strategy for lymphoma with EZH2-activating mutations." Nature **492**(7427): 108-112.

McGrath, K. E., T. P. Bushnell and J. Palis (2008). "Multispectral imaging of hematopoietic cells: where flow meets morphology." J Immunol Methods **336**(2): 91-97.

McGrath, K. E., P. D. Kingsley, A. D. Koniski, R. L. Porter, T. P. Bushnell and J. Palis (2008). "Enucleation of primitive erythroid cells generates a transient population of "pyrenocytes" in the mammalian fetus." Blood **111**(4): 2409-2417.

McLean, C. Y., D. Bristor, M. Hiller, S. L. Clarke, B. T. Schaar, C. B. Lowe, A. M. Wenger and G. Bejerano (2010). "GREAT improves functional interpretation of cis-regulatory regions." Nat Biotechnol **28**(5): 495-501.

Medyouf, H., M. Mossner, J. C. Jann, F. Nolte, S. Raffel, C. Herrmann, A. Lier, C. Eisen, V. Nowak, B. Zens, K. Mudder, C. Klein, J. Oblander, S. Fey, J. Vogler, A. Fabarius, E. Riedl, H. Roehl, A. Kohlmann, M. Staller, C. Haferlach, N. Muller, T. John, U. Platzbecker, G. Metzgeroth, W. K. Hofmann, A. Trumpp and D. Nowak (2014). "Myelodysplastic cells in patients reprogram mesenchymal stromal cells to establish a transplantable stem cell niche disease unit." Cell Stem Cell **14**(6): 824-837.

Mejetta, S., L. Morey, G. Pascual, B. Kuebler, M. R. Mysliwiec, Y. Lee, R. Shiekhattar, L. Di Croce and S. A. Benitah (2011). "Jarid2 regulates mouse epidermal stem cell activation and differentiation." EMBO J **30**(17): 3635-3646.

Mende, N., E. E. Kuchen, M. Lesche, T. Grinenko, K. D. Kokkaliaris, H. Hanenberg, D. Lindemann, A. Dahl, A. Platz, T. Hofer, F. Calegari and C. Waskow (2015). "CCND1-CDK4-mediated cell cycle progression provides a competitive advantage for human hematopoietic stem cells in vivo." J Exp Med **212**(8): 1171-1183.

Mendez-Ferrer, S., T. V. Michurina, F. Ferraro, A. R. Mazloom, B. D. Macarthur, S. A. Lira, D. T. Scadden, A. Ma'ayan, G. N. Enikolopov and P. S. Frenette (2010). "Mesenchymal and haematopoietic stem cells form a unique bone marrow niche." Nature **466**(7308): 829-834.

Merico, D., R. Isserlin and G. D. Bader (2011). "Visualizing gene-set enrichment results using the Cytoscape plug-in enrichment map." Methods Mol Biol **781**: 257-277.

Merico, D., R. Isserlin, O. Stueker, A. Emili and G. D. Bader (2010). "Enrichment map: a network-based method for gene-set enrichment visualization and interpretation." PLoS One **5**(11): e13984.

Mikkelsen, T. S., M. Ku, D. B. Jaffe, B. Issac, E. Lieberman, G. Giannoukos, P. Alvarez, W. Brockman, T. K. Kim, R. P. Koche, W. Lee, E. Mendenhall, A. O'Donovan, A. Presser, C. Russ, X. Xie, A. Meissner, M. Wernig, R. Jaenisch, C. Nusbaum, E. S. Lander and B. E. Bernstein (2007). "Genome-wide maps of chromatin state in pluripotent and lineage-committed cells." Nature **448**(7153): 553-560.

Mochizuki-Kashio, M., Y. Mishima, S. Miyagi, M. Negishi, A. Saraya, T. Konuma, J. Shinga, H. Koseki and A. Iwama (2011). "Dependency on the polycomb gene Ezh2 distinguishes fetal from adult hematopoietic stem cells." Blood **118**(25): 6553-6561.

Monroe, S. C., S. Y. Jo, D. S. Sanders, V. Basrur, K. S. Elenitoba-Johnson, R. K. Slany and J. L. Hess (2011). "MLL-AF9 and MLL-ENL alter the dynamic association of transcriptional regulators with genes critical for leukemia." Exp Hematol **39**(1): 77-86 e71-75.

Montgomery, N. D., D. Yee, A. Chen, S. Kalantry, S. J. Chamberlain, A. P. Otte and T. Magnuson (2005). "The murine polycomb group protein Eed is required for global histone H3 lysine-27 methylation." Curr Biol **15**(10): 942-947.

Moreau-Gachelin, F. (2006). "Lessons from models of murine erythroleukemia to acute myeloid leukemia (AML): proof-of-principle of co-operativity in AML." Haematologica **91**: 1644-1652.

Moreau-Gachelin, F. (2008). "Multi-stage Friend murine erythroleukemia: molecular insights into oncogenic cooperation." Retrovirology **5**: 99.

Moreau-Gachelin, F., A. Tavitian and P. Tambourin (1988). "Spi-1 is a putative oncogene in virally induced murine erythroleukaemias." Nature **331**(6153): 277-280.

Morey, L., L. Aloia, L. Cozzuto, S. A. Benitah and L. Di Croce (2013). "RYBP and Cbx7 define specific biological functions of polycomb complexes in mouse embryonic stem cells." Cell Rep **3**(1): 60-69.

Morey, L., G. Pascual, L. Cozzuto, G. Roma, A. Wutz, S. A. Benitah and L. Di Croce (2012). "Nonoverlapping functions of the Polycomb group Cbx family of proteins in embryonic stem cells." Cell Stem Cell **10**(1): 47-62.

Morin, R. D., N. A. Johnson, T. M. Severson, A. J. Mungall, J. An, R. Goya, J. E. Paul, M. Boyle, B. W. Woolcock, F. Kuchenbauer, D. Yap, R. K. Humphries, O. L. Griffith, S. Shah, H. Zhu, M. Kimbara, P. Shashkin, J. F. Charlot, M. Tcherpakov, R. Corbett, A. Tam, R. Varhol, D. Smailus, M. Moksa, Y. Zhao, A. Delaney, H. Qian, I. Birol, J. Schein, R. Moore, R. Holt, D. E. Horsman, J. M. Connors, S. Jones, S. Aparicio, M. Hirst, R. D. Gascoyne and M. A. Marra (2010). "Somatic mutations altering EZH2 (Tyr641) in follicular and diffuse large B-cell lymphomas of germinal-center origin." Nat Genet **42**(2): 181-185.

Motoyama, J., K. Kitajima, M. Kojima, S. Kondo and T. Takeuchi (1997). "Organogenesis of the liver, thymus and spleen is affected in jumonji mutant mice." Mechanisms of Development **66**: 27-37.

Mowat, M., A. Cheng, N. Kimura, A. Bernstein and S. Benchimol (1985). "Rearrangements of the cellular p53 gene in erythroleukaemic cells transformed by Friend virus." Nature **314**(6012): 633-636.

Muller, J., C. M. Hart, N. J. Francis, M. L. Vargas, A. Sengupta, B. Wild, E. L. Miller, M. B. O'Connor, R. E. Kingston and J. A. Simon (2002). "Histone methyltransferase activity of a Drosophila Polycomb group repressor complex." Cell **111**(2): 197-208.

Muntean, A. G., J. Tan, K. Sitwala, Y. Huang, J. Bronstein, J. A. Connelly, V. Basrur, K. S. Elenitoba-Johnson and J. L. Hess (2010). "The PAF complex synergizes with MLL fusion proteins at HOX loci to promote leukemogenesis." Cancer Cell **17**(6): 609-621.

Musselman, C. A., N. Avvakumov, R. Watanabe, C. G. Abraham, M. E. Lalonde, Z. Hong, C. Allen, S. Roy, J. K. Nunez, J. Nickoloff, C. A. Kulesza, A. Yasui, J. Cote and T. G. Kutateladze (2012). "Molecular basis for H3K36me3 recognition by the Tudor domain of PHF1." Nat Struct Mol Biol **19**(12): 1266-1272.

Neff, T., A. U. Sinha, M. J. Kluk, N. Zhu, M. H. Khattab, L. Stein, H. Xie, S. H. Orkin and S. A. Armstrong (2012). "Polycomb repressive complex 2 is required for MLL-AF9 leukemia." Proc Natl Acad Sci U S A **109**(13): 5028-5033.

Nekrasov, M., T. Klymenko, S. Fraterman, B. Papp, K. Oktaba, T. Kocher, A. Cohen, H. G. Stunnenberg, M. Wilm and J. Muller (2007). "Pcl-PRC2 is needed to generate high levels of H3-K27 trimethylation at Polycomb target genes." EMBO J **26**: 4078-4088.

Nekrasov, M., B. Wild and J. Muller (2005). "Nucleosome binding and histone methyltransferase activity of Drosophila PRC2." EMBO Rep **6**(4): 348-353.

Nijnik, A., S. Clare, C. Hale, C. Raisen, R. E. McIntyre, K. Yusa, A. R. Everitt, L. Mottram, C. Podrini, M. Lucas, J. Estabel, D. Goulding, F. Sanger Institute Microarray, P. Sanger Mouse Genetics, N. Adams, R. Ramirez-Solis, J. K. White, D. J. Adams, R. E. Hancock and G. Dougan (2012). "The critical role of histone H2A-deubiquitinase Mysm1 in hematopoiesis and lymphocyte differentiation." Blood **119**(6): 1370-1379.

Nikoloski, G., S. M. Langemeijer, R. P. Kuiper, R. Knops, M. Massop, E. R. Tonnissen, A. van der Heijden, T. N. Scheele, P. Vandenberghe, T. de Witte, B. A. van der Reijden and J. H. Jansen (2010). "Somatic mutations of the histone methyltransferase gene EZH2 in myelodysplastic syndromes." Nat Genet **42**(8): 665-667.

Nishigaki, K., D. Thompson, C. Hanson, T. Yugawa and S. Ruscetti (2001). "The envelope glycoprotein of friend spleen focus-forming virus covalently interacts with and constitutively activates a truncated form of the receptor tyrosine kinase Stk." J Virol **75**(17): 7893-7903.

Nord, A. S., P. J. Chang, B. R. Conklin, A. V. Cox, C. A. Harper, G. G. Hicks, C. C. Huang, S. J. Johns, M. Kawamoto, S. Liu, E. C. Meng, J. H. Morris, J. Rossant, P. Ruiz, W. C. Skarnes, P. Soriano, W. L. Stanford, D. Stryke, H. von Melchner, W. Wurst, K. Yamamura, S. G. Young, P. C. Babbitt and T. E. Ferrin (2006). "The International Gene Trap Consortium Website: a portal to all publicly available gene trap cell lines in mouse." Nucleic Acids Res **34**(Database issue): D642-648.

North, T. E., M. F. de Bruijn, T. Stacy, L. Talebian, E. Lind, C. Robin, M. Binder, E. Dzierzak and N. A. Speck (2002). "Runx1 expression marks long-term repopulating hematopoietic stem cells in the midgestation mouse embryo." Immunity **16**(5): 661-672.

Nowak, A. J., C. Alfieri, C. U. Stirnimann, V. Rybin, F. Baudin, N. Ly-Hartig, D. Lindner and C. W. Muller (2011). "Chromatin-modifying complex component Nurf55/p55 associates with histones H3 and H4 and polycomb repressive complex 2 subunit Su(z)12 through partially overlapping binding sites." J Biol Chem **286**(26): 23388-23396.

Nowak, K., K. Kerl, D. Fehr, C. Kramps, C. Gessner, K. Killmer, B. Samans, B. Berwanger, H. Christiansen and W. Lutz (2006). "BMI1 is a target gene of E2F-1 and is strongly expressed in primary neuroblastomas." Nucleic Acids Res **34**(6): 1745-1754.

Ntziachristos, P., A. Tsirigos, P. Van Vlierberghe, J. Nedjic, T. Trimarchi, M. S. Flaherty, D. Ferres-Marco, V. da Ros, Z. Tang, J. Siegle, P. Asp, M. Hadler, I. Rigo, K. De Keersmaecker, J. Patel, T. Huynh, F. Utro, S. Poglio, J. B. Samon, E. Paietta, J. Racevskis, J. M. Rowe, R. Rabadan, R. L. Levine, S. Brown, F. Pflumio, M. Dominguez, A. Ferrando and I. Aifantis (2012). "Genetic inactivation of the polycomb repressive complex 2 in T cell acute lymphoblastic leukemia." Nat Med **18**(2): 298-301.

Nygren, J. M., D. Bryder and S. E. W. Jacobsen (2006). "Prolonged Cell Cycle Transit Is a Defining and Developmentally Conserved Hemopoietic Stem Cell Property." The Journal of Immunology **177**(1): 201-208.

O'Carroll, D., S. Erhardt, M. Pagani, S. C. Barton, M. A. Surani and T. Jenuwein (2001). "The polycomb-group gene Ezh2 is required for early mouse development." Mol Cell Biol **21**(13): 4330-4336.

O'Neill, R. A., A. Bhamidipati, X. Bi, D. Deb-Basu, L. Cahill, J. Ferrante, E. Gentalen, M. Glazer, J. Gossett, K. Hacker, C. Kirby, J. Knittle, R. Loder, C. Mastroieni, M. Maclaren, T. Mills, U. Nguyen, N. Parker, A. Rice, D. Roach, D. Suich, D. Voehringer, K. Voss, J. Yang, T. Yang and P. B. Vander Horn (2006). "Isoelectric focusing technology quantifies protein signaling in 25 cells." Proc Natl Acad Sci U S A **103**(44): 16153-16158.

Ohta, H., A. Sawada, J. Y. Kim, S. Tokimasa, S. Nishiguchi, R. K. Humphries, J. Hara and Y. Takihara (2002). "Polycomb group gene rae28 is required for sustaining activity of hematopoietic stem cells." J Exp Med **195**(6): 759-770.

Padron-Barthe, L., S. Temino, C. Villa del Campo, L. Carramolino, J. Isern and M. Torres (2014). "Clonal analysis identifies hemogenic endothelium as the source of the blood-endothelial common lineage in the mouse embryo." Blood **124**(16): 2523-2532.

Palis, J., S. Robertson, M. Kennedy, C. Wall and G. Keller (1999). "Development of erythroid and myeloid progenitors in the yolk sac and embryo proper of the mouse." Development **126**(22): 5073-5084.

Palis, J. and M. C. Yoder (2001). "Yolk-sac hematopoiesis: The first blood cells of mouse and man." Exp Hematol **29**: 927-936.

Park, I., D. Qian, M. Kiel, M. W. Becker, M. Pihalja, I. Weissman, S. J. Morrison and M. F. Clarke (2003). "Bmi-1 is required for maintenance of adult self-renewing haematopoietic stem cells." Nature **423**: 302-305.

Pasini, D., A. P. Bracken, J. B. Hansen, M. Capillo and K. Helin (2007). "The polycomb group protein Suz12 is required for embryonic stem cell differentiation." Mol Cell Biol **27**(10): 3769-3779.

Pasini, D., A. P. Bracken, M. R. Jensen, E. Lazzerini Denchi and K. Helin (2004). "Suz12 is essential for mouse development and for EZH2 histone methyltransferase activity." EMBO J **23**(20): 4061-4071.

Pasini, D., P. A. Cloos, J. Walfridsson, L. Olsson, J. P. Bukowski, J. V. Johansen, M. Bak, N. Tommerup, J. Rappsilber and K. Helin (2010). "JARID2 regulates binding of the Polycomb repressive complex 2 to target genes in ES cells." Nature **464**(7286): 306-310.

Paul, R., S. Schuetze, S. L. Kozak and D. Kabat (1989). "A common site for immortalizing proviral integrations in Friend erythroleukemia: molecular cloning and characterization." J Virol **63**(11): 4958-4961.

Peng, J. C., A. Valouev, T. Swigut, J. Zhang, Y. Zhao, A. Sidow and J. Wysocka (2009). "Jarid2/Jumonji coordinates control of PRC2 enzymatic activity and target gene occupancy in pluripotent cells." Cell **139**(7): 1290-1302.

Persons, D. A., J. A. Allay, E. R. Allay, R. A. Ashmun, D. Orlic, S. M. Jane, J. M. Cunningham and A. W. Nienhuis (1999). "Enforced expression of the GATA-2 transcription factor blocks normal hematopoiesis." Blood **93**(2): 488-499.

Peschle, C., G. Migliaccio, F. Lettieri, A. R. Migliaccio, R. Ceccarelli, P. Barba, F. Titti and G. B. Rossi (1980). "Kinetics of erythroid precursors in mice infected with the anemic or the polycythemic strain of Friend leukemia virus." Proc Natl Acad Sci U S A **77**(4): 2054-2058.

Pietras, E. M., M. R. Warr and E. Passegue (2011). "Cell cycle regulation in hematopoietic stem cells." J Cell Biol **195**(5): 709-720.

Pilon, A. M., S. S. Ajay, S. A. Kumar, L. A. Steiner, P. F. Cherukuri, S. Wincovitch, S. M. Anderson, N. C. S. Center, J. C. Mullikin, P. G. Gallagher, R. C. Hardison, E. H. Margulies and D. M. Bodine (2011). "Genome-wide ChIP-Seq reveals a dramatic shift in the binding of the transcription factor erythroid Kruppel-like factor during erythrocyte differentiation." Blood **118**(17): e139-148.

Pop, R., J. R. Shearstone, Q. Shen, Y. Liu, K. Hallstrom, M. Koulnis, J. Gribnau and M. Socolovsky (2010). "A key commitment step in erythropoiesis is synchronized with the cell cycle clock through mutual inhibition between PU.1 and S-phase progression." PLoS Biol **8**(9).

Puppe, J., R. Drost, X. Liu, S. A. Joosse, B. Evers, P. Cornelissen-Steijger, P. Nederlof, Q. Yu, J. Jonkers, M. van Lohuizen and A. M. Pietersen (2009). "BRCA1-deficient mammary tumor cells are dependent on EZH2 expression and sensitive to Polycomb Repressive Complex 2-inhibitor 3-deazaneplanocin A." Breast Cancer Res **11**(4): R63.

Quang, C. T., O. Wessely, M. Pironin, H. Beug and J. Ghysdael (1997). "Cooperation of Spi-1/PU.1 with an activated erythropoietin receptor inhibits apoptosis and Epo-dependent differentiation in primary erythroblasts and induces their Kit ligand-dependent proliferation." EMBO J **16**(18): 5639-5653.

Rao, M., N. Chinnasamy, J. A. Hong, Y. Zhang, M. Zhang, S. Xi, F. Liu, V. E. Marquez, R. A. Morgan and D. S. Schrump (2011). "Inhibition of histone lysine methylation enhances cancer-testis antigen expression in lung cancer cells: implications for adoptive immunotherapy of cancer." Cancer Res **71**(12): 4192-4204.

Reddington, J. P., S. M. Perricone, C. E. Nestor, J. Reichmann, N. A. Youngson, M. Suzuki, D. Reinhardt, D. S. Dunican, J. G. Prendergast, H. Mjoseng, B. H. Ramsahoye, E. Whitelaw, J. M. Greally, I. R. Adams, W. A. Bickmore and R. R. Meehan (2013). "Redistribution of H3K27me3 upon DNA hypomethylation results in de-repression of Polycomb target genes." Genome Biol **14**(3): R25.

Reimand, J., T. Arak and J. Vilo (2011). "g:Profiler--a web server for functional interpretation of gene lists (2011 update)." Nucleic Acids Res **39**(Web Server issue): W307-315.

Reimand, J., M. Kull, H. Peterson, J. Hansen and J. Vilo (2007). "g:Profiler--a web-based toolset for functional profiling of gene lists from large-scale experiments." Nucleic Acids Res **35**(Web Server issue): W193-200.

Ringrose, L. and R. Paro (2004). "Epigenetic regulation of cellular memory by the Polycomb and Trithorax group proteins." Annu Rev Genet **38**: 413-443.

Ringrose, L. and R. Paro (2007). "Polycomb/Trithorax response elements and epigenetic memory of cell identity." Development **134**(2): 223-232.

Ringrose, L., M. Rehmsmeier, J. M. Dura and R. Paro (2003). "Genome-wide prediction of Polycomb/Trithorax response elements in Drosophila melanogaster." Dev Cell **5**(5): 759-771.

Robb, L., I. Lyons, R. Li, L. Hartley, F. Kontgen, R. P. Harvey, D. Metcalf and C. G. Begley (1995). "Absence of yolk sac hematopoiesis from mice with a targeted disruption of the scl gene." Proc Natl Acad Sci U S A **92**(15): 7075-7079.

Rosen, B., J. Schick and W. Wurst (2015). "Beyond knockouts: the International Knockout Mouse Consortium delivers modular and evolving tools for investigating mammalian genes." Mamm Genome **26**(9-10): 456-466.

Ruscetti, S. and L. Wolff (1984). "Spleen focus-forming virus: relationship of an altered envelope gene to the development of a rapid erythroleukemia." Curr Top Microbiol Immunol **112**: 21-44.

Saito, M., K. Helin, M. B. Valentine, B. B. Griffith, C. L. Willman, E. Harlow and A. T. Look (1995). "Amplification of the E2F1 transcription factor gene in the HEL erythroleukemia cell line." Genomics **25**(1): 130-138.

Saito, Y., H. Yuki, M. Kuratani, Y. Hashizume, S. Takagi, T. Honma, A. Tanaka, M. Shirouzu, J. Mikuni, N. Handa, I. Ogahara, A. Sone, Y. Najima, Y. Tomabechi, M. Wakiyama, N. Uchida, M. Tomizawa-Murasawa, A. Kaneko, S. Tanaka, N. Suzuki, H. Kajita, Y. Aoki, O. Ohara, L. D. Shultz, T. Fukami, T. Goto, S. Taniguchi, S. Yokoyama and F. Ishikawa (2013). "A pyrrolo-pyrimidine derivative targets human primary AML stem cells in vivo." Sci Transl Med **5**(181): 181ra152.

Sampath, P., D. K. Pritchard, L. Pabon, H. Reinecke, S. M. Schwartz, D. R. Morris and C. E. Murry (2008). "A hierarchical network controls protein translation during murine embryonic stem cell self-renewal and differentiation." Cell Stem Cell **2**(5): 448-460.

Sanchez, M. J., E. O. Bockamp, J. Miller, L. Gambardella and A. R. Green (2001). "Selective rescue of early haematopoietic progenitors in Scl(-/-) mice by expressing Scl under the control of a stem cell enhancer." Development **128**(23): 4815-4827.

Sanchez, M. J., A. Holmes, C. Miles and E. Dzierzak (1996). "Characterization of the first definitive hematopoietic stem cells in the AGM and liver of the mouse embryo." Immunity **5**(6): 513-525.

Santaguida, M., K. Schepers, B. King, A. J. Sabnis, E. C. Forsberg, J. L. Attema, B. S. Braun and E. Passegue (2009). "JunB protects against myeloid malignancies by limiting hematopoietic stem cell proliferation and differentiation without affecting self-renewal." Cancer Cell **15**(4): 341-352.

Sarma, K., R. Margueron, A. Ivanov, V. Pirrotta and D. Reinberg (2008). "Ezh2 requires PHF1 to efficiently catalyze H3 lysine 27 trimethylation in vivo." Mol Cell Biol **28**(8): 2718-2731.

Sasaki, D., Y. Imaizumi, H. Hasegawa, A. Osaka, K. Tsukasaki, Y. L. Choi, H. Mano, V. E. Marquez, T. Hayashi, K. Yanagihara, Y. Moriwaki, Y. Miyazaki, S. Kamihira and Y. Yamada (2011). "Overexpression of Enhancer of zeste homolog 2 with trimethylation of lysine 27

on histone H3 in adult T-cell leukemia/lymphoma as a target for epigenetic therapy." Haematologica **96**(5): 712-719.

Satijn, D. P. and A. P. Otte (1999). "RING1 interacts with multiple Polycomb-group proteins and displays tumorigenic activity." Mol Cell Biol **19**(1): 57-68.

Sauvageau, M. and G. Sauvageau (2010). "Polycomb group proteins: multi-faceted regulators of somatic stem cells and cancer." Cell Stem Cell **7**(3): 299-313.

Savla, U., J. Benes, J. Zhang and R. S. Jones (2008). "Recruitment of Drosophila Polycomb-group proteins by Polycomblike, a component of a novel protein complex in larvae." Development **135**(5): 813-817.

Schmitges, F. W., A. B. Prusty, M. Faty, A. Stutzer, G. M. Lingaraju, J. Aiwazian, R. Sack, D. Hess, L. Li, S. Zhou, R. D. Bunker, U. Wirth, T. Bouwmeester, A. Bauer, N. Ly-Hartig, K. Zhao, H. Chan, J. Gu, H. Gut, W. Fischle, J. Muller and N. H. Thoma (2011). "Histone methylation by PRC2 is inhibited by active chromatin marks." Mol Cell **42**(3): 330-341.

Serrano, M., H. Lee, L. Chin, C. Cordon-Cardo, D. Beach and R. A. DePinho (1996). "Role of the INK4a locus in tumor suppression and cell mortality." Cell **85**(1): 27-37.

Shearstone, J. R., R. Pop, C. Bock, P. Boyle, A. Meissner and M. Socolovsky (2011). "Global DNA demethylation during mouse erythropoiesis in vivo." Science **334**(6057): 799-802.

Shen, X., W. Kim, Y. Fujiwara, M. D. Simon, Y. Liu, M. R. Mysliwiec, G. C. Yuan, Y. Lee and S. H. Orkin (2009). "Jumonji modulates polycomb activity and self-renewal versus differentiation of stem cells." Cell **139**(7): 1303-1314.

Shen, Y., F. Yue, D. F. McCleary, Z. Ye, L. Edsall, S. Kuan, U. Wagner, J. Dixon, L. Lee, V. V. Lobanenkov and B. Ren (2012). "A map of the cis-regulatory sequences in the mouse genome." Nature **488**(7409): 116-120.

Shivdasani, R. A. and S. H. Orkin (1995). "Erythropoiesis and globin gene expression in mice lacking the transcription factor NF-E2." Proc Natl Acad Sci U S A **92**(19): 8690-8694.

Simon, J., A. Chiang, W. Bender, M. J. Shimell and M. O'Connor (1993). "Elements of the Drosophila bithorax complex that mediate repression by Polycomb group products." Dev Biol **158**(1): 131-144.

Sing, A., D. Pannell, A. Karaiskakis, K. Sturgeon, M. Djabali, J. Ellis, H. D. Lipshitz and S. P. Cordes (2009). "A vertebrate Polycomb response element governs segmentation of the posterior hindbrain." Cell **138**(5): 885-897.

Skarnes, W. C., B. A. Auerbach and A. L. Joyner (1992). "A gene trap approach in mouse embryonic stem cells: the lacZ reported is activated by splicing, reflects endogenous gene expression, and is mutagenic in mice." Genes Dev **6**(6): 903-918.

Skarnes, W. C., B. Rosen, A. P. West, M. Koutsourakis, W. Bushell, V. Iyer, A. O. Mujica, M. Thomas, J. Harrow, T. Cox, D. Jackson, J. Severin, P. Biggs, J. Fu, M. Nefedov, P. J. de Jong, A. F. Stewart and A. Bradley (2011). "A conditional knockout resource for the genome-wide study of mouse gene function." Nature **474**(7351): 337-342.

Smits, A. H., P. W. Jansen, I. Poser, A. A. Hyman and M. Vermeulen (2013). "Stoichiometry of chromatin-associated protein complexes revealed by label-free quantitative mass spectrometry-based proteomics." Nucleic Acids Res **41**(1): e28.

Snow, J. W., J. J. Trowbridge, K. D. Johnson, T. Fujiwara, N. E. Emambokus, J. A. Grass, S. H. Orkin and E. H. Bresnick (2011). "Context-dependent function of "GATA switch" sites in vivo." Blood **117**(18): 4769-4772.

Stanford, W. L., J. B. Cohn and S. P. Cordes (2001). "Gene-trap mutagenesis: past, present and beyond." Nat Rev Genet **2**(10): 756-768.

Struhl, G. and M. Akam (1985). "Altered distributions of Ultrabithorax transcripts in extra sex combs mutant embryos of Drosophila." EMBO J **4**(12): 3259-3264.

Su, I. H., A. Basavaraj, A. N. Krutchinsky, O. Hobert, A. Ullrich, B. T. Chait and A. Tarakhovsky (2003). "Ezh2 controls B cell development through histone H3 methylation and Igh rearrangement." Nat Immunol **4**(2): 124-131.

Subramanian, A., S. Hegde, P. Porayette, M. Yon, P. Hankey and R. F. Paulson (2008). "Friend virus utilizes the BMP4-dependent stress erythropoiesis pathway to induce erythroleukemia." J Virol **82**(1): 382-393.

Surface, L. E., S. R. Thornton and L. A. Boyer (2010). "Polycomb group proteins set the stage for early lineage commitment." Cell Stem Cell **7**(3): 288-298.

Suva, M. L., N. Riggi, M. Janiszewska, I. Radovanovic, P. Provero, J. C. Stehle, K. Baumer, M. A. Le Bitoux, D. Marino, L. Cironi, V. E. Marquez, V. Clement and I. Stamenkovic (2009). "EZH2 is essential for glioblastoma cancer stem cell maintenance." Cancer Res **69**(24): 9211-9218.

Suzuki, M., M. Kobayashi-Osaki, S. Tsutsumi, X. Pan, S. Ohmori, J. Takai, T. Moriguchi, O. Ohneda, K. Ohneda, R. Shimizu, Y. Kanki, T. Kodama, H. Aburatani and M. Yamamoto (2013). "GATA factor switching from GATA2 to GATA1 contributes to erythroid differentiation." Genes Cells **18**(11): 921-933.

Taby, R. and J. P. Issa (2010). "Cancer epigenetics." CA Cancer J Clin **60**(6): 376-392.

Takeuchi, T., Y. Yamazaki, Y. Katoh-Fukui, R. Tsuchiya, S. Kondo, J. Motoyama and T. Higashinakagawa (1995). "Gene trap capture of a novel mouse gene, jumonji, required for neural tube formation." Genes Dev **9**(10): 1211-1222.

Tambourin, P., F. Wendling and F. Moreau-Gachelin (1981). "Friend leukemia as a multiple-step disease." Blood Cells **7**(1): 133-144.

Tambourin, P. E. and F. Wendling (1975). "Target cell for oncogenic action of polycythaemia-inducing Friend virus." Nature **256**(5515): 320-322.

Tan, J., X. Yang, L. Zhuang, X. Jiang, W. Chen, P. L. Lee, R. K. Karuturi, P. B. Tan, E. T. Liu and Q. Yu (2007). "Pharmacologic disruption of Polycomb-repressive complex 2-mediated gene repression selectively induces apoptosis in cancer cells." Genes Dev **21**(9): 1050-1063.

Tanaka, S., S. Miyagi, G. Sashida, T. Chiba, J. Yuan, M. Mochizuki-Kashio, Y. Suzuki, S. Sugano, C. Nakaseko, K. Yokote, H. Koseki and A. Iwama (2012). "Ezh2 augments leukemogenicity by reinforcing differentiation blockage in acute myeloid leukemia." Blood **120**(5): 1107-1117.

Tavares, L., E. Dimitrova, D. Oxley, J. Webster, R. Poot, J. Demmers, K. Bezstarosti, S. Taylor, H. Ura, H. Koide, A. Wutz, M. Vidal, S. Elderkin and N. Brockdorff (2012). "RYBP-PRC1 complexes mediate H2A ubiquitylation at polycomb target sites independently of PRC2 and H3K27me3." Cell **148**(4): 664-678.

Teng, L., B. He, P. Gao, L. Gao and K. Tan (2014). "Discover context-specific combinatorial transcription factor interactions by integrating diverse ChIP-Seq data sets." Nucleic Acids Res **42**(4): e24.

Thomas, S., X. Y. Li, P. J. Sabo, R. Sandstrom, R. E. Thurman, T. K. Canfield, E. Giste, W. Fisher, A. Hammonds, S. E. Celniker, M. D. Biggin and J. A. Stamatoyannopoulos (2011). "Dynamic reprogramming of chromatin accessibility during Drosophila embryo development." Genome Biol **12**(5): R43.

Tokimasa, S., H. Ohta, A. Sawada, Y. Matsuda, J. Y. Kim, S. Nishiguchi, J. Hara and Y. Takihara (2001). "Lack of the Polycomb-group gene rae28 causes maturation arrest at the early B-cell developmental stage." Exp Hematol **29**(1): 93-103.

Trapnell, C., A. Roberts, L. Goff, G. Pertea, D. Kim, D. R. Kelley, H. Pimentel, S. L. Salzberg, J. L. Rinn and L. Pachter (2012). "Differential gene and transcript expression analysis of RNA-seq experiments with TopHat and Cufflinks." Nat Protoc **7**(3): 562-578.

Tsang, A. P., Y. Fujiwara, D. B. Hom and S. H. Orkin (1998). "Failure of megakaryopoiesis and arrested erythropoiesis in mice lacking the GATA-1 transcriptional cofactor FOG." Genes Dev **12**(8): 1176-1188.

van der Lugt, N. M., J. Domen, K. Linders, M. van Roon, E. Robanus-Maandag, H. te Riele, M. van der Valk, J. Deschamps, M. Sofroniew and M. van Lohuizen (1994). "Posterior transformation, neurological abnormalities, and severe hematopoietic defects in mice with a targeted deletion of the bmi-1 proto-oncogene." Genes & Development **8**(7): 757-769.

van Kemenade, F. J., F. M. Raaphorst, T. Blokzijl, E. Fieret, K. M. Hamer, D. P. Satijn, A. P. Otte and C. J. Meijer (2001). "Coexpression of BMI-1 and EZH2 polycomb-group proteins is associated with cycling cells and degree of malignancy in B-cell non-Hodgkin lymphoma." Blood **97**(12): 3896-3901.

Visser, H. P., M. J. Gunster, H. C. Kluin-Nelemans, E. M. Manders, F. M. Raaphorst, C. J. Meijer, R. Willemze and A. P. Otte (2001). "The Polycomb group protein EZH2 is upregulated in proliferating, cultured human mantle cell lymphoma." Br J Haematol **112**(4): 950-958.

Vizan, P., M. Beringer, C. Ballare and L. Di Croce (2015). "Role of PRC2-associated factors in stem cells and disease." FEBS J **282**(9): 1723-1735.

Walker, E., W. Y. Chang, J. Hunkapiller, G. Cagney, K. Garcha, J. Torchia, N. J. Krogan, J. F. Reiter and W. L. Stanford (2010). "Polycomb-like 2 associates with PRC2 and regulates transcriptional networks during mouse embryonic stem cell self-renewal and differentiation." Cell Stem Cell **6**(2): 153-166.

Walker, E., J. L. Manias, W. Y. Chang and W. L. Stanford (2011). "PCL2 modulates gene regulatory networks controlling self-renewal and commitment in embryonic stem cells." Cell Cycle **10**(1): 45-51.

Walker, E., M. Ohishi, R. E. Davey, W. Zhang, P. A. Cassar, T. S. Tanaka, S. D. Der, Q. Morris, T. R. Hughes, P. W. Zandstra and W. L. Stanford (2007). "Prediction and testing of novel transcriptional networks regulating embryonic stem cell self-renewal and commitment." Cell Stem Cell **1**(1): 71-86.

Walker, E. and W. L. Stanford (2009). Transcriptional Networks Regulating Embryonic Stem Cell Fate Decisions. Regulatory Networks in Stem Cells. V. K. Rajasekhar and M. C. Vemuri**:** 87-100.

Wang, H., L. Wang, H. Erdjument-Bromage, M. Vidal, P. Tempst, R. S. Jones and Y. Zhang (2004). "Role of histone H2A ubiquitination in Polycomb silencing." Nature **431**(7010): 873-878.

Wang, H. B., G. H. Liu, H. Zhang, S. Xing, L. J. Hu, W. F. Zhao, B. Xie, M. Z. Li, B. H. Zeng, Y. Li and M. S. Zeng (2013). "Sp1 and c-Myc regulate transcription of BMI1 in nasopharyngeal carcinoma." FEBS J **280**(12): 2929-2944.

Wang, J., J. Zhuang, S. Iyer, X. Lin, T. W. Whitfield, M. C. Greven, B. G. Pierce, X. Dong, A. Kundaje, Y. Cheng, O. J. Rando, E. Birney, R. M. Myers, W. S. Noble, M. Snyder and Z. Weng (2012). "Sequence features and chromatin structure around the genomic regions bound by 119 human transcription factors." Genome Res **22**(9): 1798-1812.

Wang, L., Q. Jin, J. E. Lee, I. H. Su and K. Ge (2010). "Histone H3K27 methyltransferase Ezh2 represses Wnt genes to facilitate adipogenesis." Proc Natl Acad Sci U S A **107**(16): 7317-7322.

Wang, S., F. He, W. Xiong, S. Gu, H. Liu, T. Zhang, X. Yu and Y. Chen (2007). "Polycomblike-2-deficient mice exhibit normal left-right asymmetry." Dev Dyn **236**(3): 853-861.

Wang, S., G. P. Robertson and J. Zhu (2004). "A novel human homologue of Drosophila polycomblike gene is up-regulated in multiple cancers." Gene **343**(1): 69-78.

Wang, S., X. Yu, T. Zhang, X. Zhang, Z. Zhang and Y. Chen (2004). "Chick Pcl2 regulates the left-right asymmetry by repressing Shh expression in Hensen's node." Development **131**(17): 4381-4391.

Warren, A. J., W. H. Colledge, M. B. Carlton, M. J. Evans, A. J. Smith and T. H. Rabbitts (1994). "The oncogenic cysteine-rich LIM domain protein rbtn2 is essential for erythroid development." Cell **78**(1): 45-57.

Waugh, R. E., A. Mantalaris, R. G. Bauserman, W. C. Hwang and J. H. Wu (2001). "Membrane instability in late-stage erythropoiesis." Blood **97**(6): 1869-1875.

Wendling, F., F. Moreau-Gachelin and P. Tambourin (1981). "Emergence of tumorigenic cells during the course of Friend virus leukemias." Proc Natl Acad Sci U S A **78**(6): 3614-3618.

Wiench, M., S. John, S. Baek, T. A. Johnson, M. H. Sung, T. Escobar, C. A. Simmons, K. H. Pearce, S. C. Biddie, P. J. Sabo, R. E. Thurman, J. A. Stamatoyannopoulos and G. L. Hager (2011). "DNA methylation status predicts cell type-specific enhancer activity." EMBO J **30**(15): 3028-3039.

Wilson, A., E. Laurenti, G. Oser, R. C. van der Wath, W. Blanco-Bose, M. Jaworski, S. Offner, C. F. Dunant, L. Eshkind, E. Bockamp, P. Lio, H. R. Macdonald and A. Trumpp (2008). "Hematopoietic stem cells reversibly switch from dormancy to self-renewal during homeostasis and repair." Cell **135**(6): 1118-1129.

Wontakal, S. N., X. Guo, B. Will, M. Shi, D. Raha, M. C. Mahajan, S. Weissman, M. Snyder, U. Steidl, D. Zheng and A. I. Skoultchi (2011). "A large gene network in immature erythroid cells is controlled by the myeloid and B cell transcriptional regulator PU.1." PLoS Genet **7**(6): e1001392.

Woo, C. J., P. V. Kharchenko, L. Daheron, P. J. Park and R. E. Kingston (2010). "A region of the human HOXD cluster that confers polycomb-group responsiveness." Cell **140**(1): 99-110.

Wu, W., Y. Cheng, C. A. Keller, J. Ernst, S. A. Kumar, T. Mishra, C. Morrissey, C. M. Dorman, K. B. Chen, D. Drautz, B. Giardine, Y. Shibata, L. Song, M. Pimkin, G. E. Crawford, T. S. Furey, M. Kellis, W. Miller, J. Taylor, S. C. Schuster, Y. Zhang, F. Chiaromonte, G. A. Blobel, M. J. Weiss and R. C. Hardison (2011). "Dynamics of the epigenetic landscape during erythroid differentiation after GATA1 restoration." Genome Res **21**(10): 1659-1671.

Xie, H., J. Xu, J. H. Hsu, M. Nguyen, Y. Fujiwara, C. Peng and S. H. Orkin (2014). "Polycomb repressive complex 2 regulates normal hematopoietic stem cell function in a developmental-stage-specific manner." Cell Stem Cell **14**(1): 68-80.

Xiong, J. W. (2008). "Molecular and developmental biology of the hemangioblast." Dev Dyn **237**(5): 1218-1231.

Xu, J., Z. Shao, D. Li, H. Xie, W. Kim, J. Huang, J. E. Taylor, L. Pinello, K. Glass, J. D. Jaffe, G. C. Yuan and S. H. Orkin (2015). "Developmental control of polycomb subunit composition by GATA factors mediates a switch to non-canonical functions." Mol Cell **57**(2): 304-316.

Yang, X., R. K. Karuturi, F. Sun, M. Aau, K. Yu, R. Shao, L. D. Miller, P. B. Tan and Q. Yu (2009). "CDKN1C (p57) is a direct target of EZH2 and suppressed by multiple epigenetic mechanisms in breast cancer cells." PLoS One **4**(4): e5011.

Ye, T., A. R. Krebs, M. A. Choukrallah, C. Keime, F. Plewniak, I. Davidson and L. Tora (2011). "seqMINER: an integrated ChIP-seq data interpretation platform." Nucleic Acids Res **39**(6): e35.

Yoder, M. C. and K. Hiatt (1997). "Engraftment of embryonic hematopoietic cells in conditioned newborn recipients." Blood **89**(6): 2176-2183.

Yoder, M. C., K. Hiatt and P. Mukherjee (1997). "In vivo repopulating hematopoietic stem cells are present in the murine yolk sac at day 9.0 postcoitus." Proc Natl Acad Sci U S A **94**(13): 6776-6780.

Yoshida, H., K. Kawane, M. Koike, Y. Mori, Y. Uchiyama and S. Nagata (2005). "Phosphatidylserine-dependent engulfment by macrophages of nuclei from erythroid precursor cells." Nature **437**(7059): 754-758.

Yu, X., J. K. Alder, J. H. Chun, A. D. Friedman, S. Heimfeld, L. Cheng and C. I. Civin (2006). "HES1 inhibits cycling of hematopoietic progenitor cells via DNA binding." Stem Cells **24**(4): 876-888.

Yuan, Y., H. Shen, D. S. Franklin, D. T. Scadden and T. Cheng (2004). "In vivo self-renewing divisions of haematopoietic stem cells are increased in the absence of the early G1-phase inhibitor, p18INK4C." Nat Cell Biol **6**(5): 436-442.

Zhang, J., M. S. Randall, M. R. Loyd, W. Li, R. L. Schweers, D. A. Persons, J. E. Rehg, C. T. Noguchi, J. N. Ihle and P. A. Ney (2006). "Role of erythropoietin receptor signaling in Friend virus-induced erythroblastosis and polycythemia." Blood **107**(1): 73-78.

Zhang, J., M. Socolovsky, A. W. Gross and H. F. Lodish (2003). "Role of Ras signaling in erythroid differentiation of mouse fetal liver cells: functional analysis by a flow cytometry-based novel culture system." Blood **102**(12): 3938-3946.

Zhang, J. A., A. Mortazavi, B. A. Williams, B. J. Wold and E. V. Rothenberg (2012). "Dynamic transformations of genome-wide epigenetic marking and transcriptional control establish T cell identity." Cell **149**(2): 467-482.

Zhang, W., Q. D. Morris, R. Chang, O. Shai, M. A. Bakowski, N. Mitsakakis, N. Mohammad, M. D. Robinson, R. Zirngibl, E. Somogyi, N. Laurin, E. Eftekharpour, E. Sat, J. Grigull, Q. Pan, W. T. Peng, N. Krogan, J. Greenblatt, M. Fehlings, D. van der Kooy, J. Aubin, B. G. Bruneau, J. Rossant, B. J. Blencowe, B. J. Frey and T. R. Hughes (2004). "The functional landscape of mouse gene expression." J Biol **3**(5): 21.

Zhang, Y., T. Liu, C. A. Meyer, J. Eeckhoute, D. S. Johnson, B. E. Bernstein, C. Nusbaum, R. M. Myers, M. Brown, W. Li and X. S. Liu (2008). "Model-based analysis of ChIP-Seq (MACS)." Genome Biol **9**(9): R137.

Zhang, Z., A. Jones, C. W. Sun, C. Li, C. W. Chang, H. Y. Joo, Q. Dai, M. R. Mysliwiec, L. C. Wu, Y. Guo, W. Yang, K. Liu, K. M. Pawlik, H. Erdjument-Bromage, P. Tempst, Y. Lee, J. Min, T. M. Townes and H. Wang (2011). "PRC2 complexes with JARID2, MTF2, and esPRC2p48 in ES cells to modulate ES cell pluripotency and somatic cell reprogramming." Stem Cells **29**(2): 229-240.

Zon, L. I., J. F. Moreau, J. W. Koo, B. Mathey-Prevot and A. D. D'Andrea (1992). "The erythropoietin receptor transmembrane region is necessary for activation by the Friend spleen focus-forming virus gp55 glycoprotein." Mol Cell Biol **12**(7): 2949-2957.

Appendix A

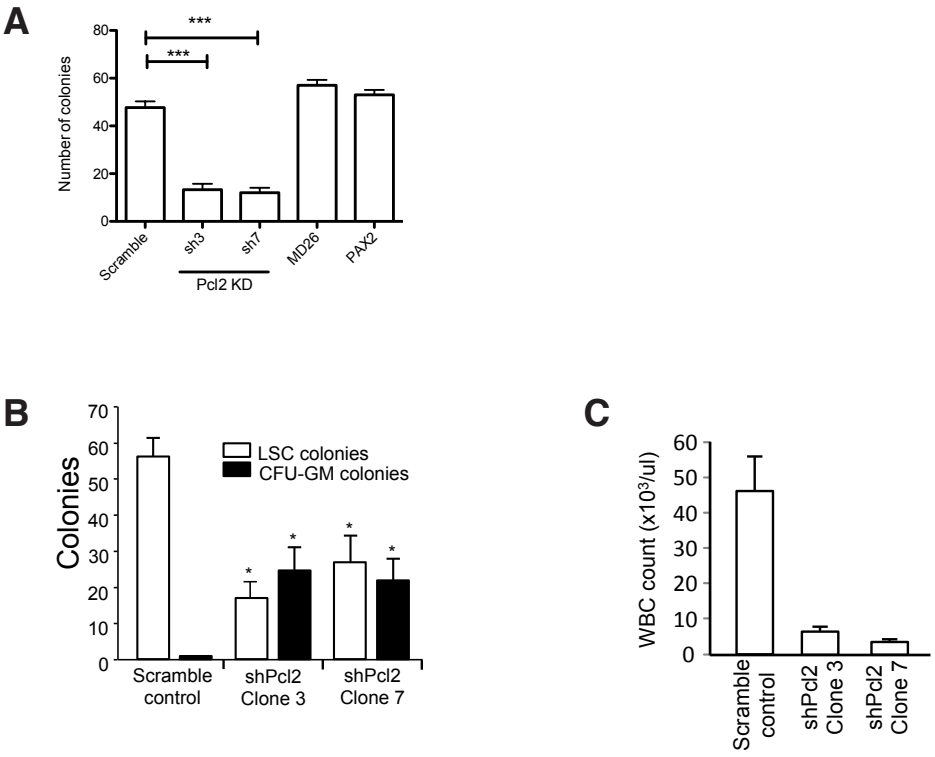

Figure A1. Reduced Mtf2 levels in other models of leukemia also leads to progenitor cell expansion. (A) In a mouse model of AML driven by the MLL-AF9 fusion protein, infected bone marrow cells with reduced Mtf2 levels produced fewer leukemic stem cells colonies. ***p<0.001 compared to scrambled control. (B) Similarly, in a mouse model of chronic myeloid leukemia (CML), driven by the BCR-ABL fusion protein, infected $CD34^{+}CD133^{+}Kit^{+}Sca1^{+}$ LSCs with reduced Mtf2 levels gave rise to more progenitor colonies (CFU-GM) at the expense of leukemic stem cell (LSC) colonies. **p<0.01, scramble shRNA control compared to shRNA clone. Data is representative of two independent experiments (C) Mice were transplanted with BCR-ABL induced LSCs with reduced Mtf2 levels. Four weeks after transplantation, mice receiving LSCs with reduced Mtf2 levels decreased peripheral white blood cell counts compared to mice infected with LSCs with normal Mtf2 levels. Data is representative of two independent experiments.

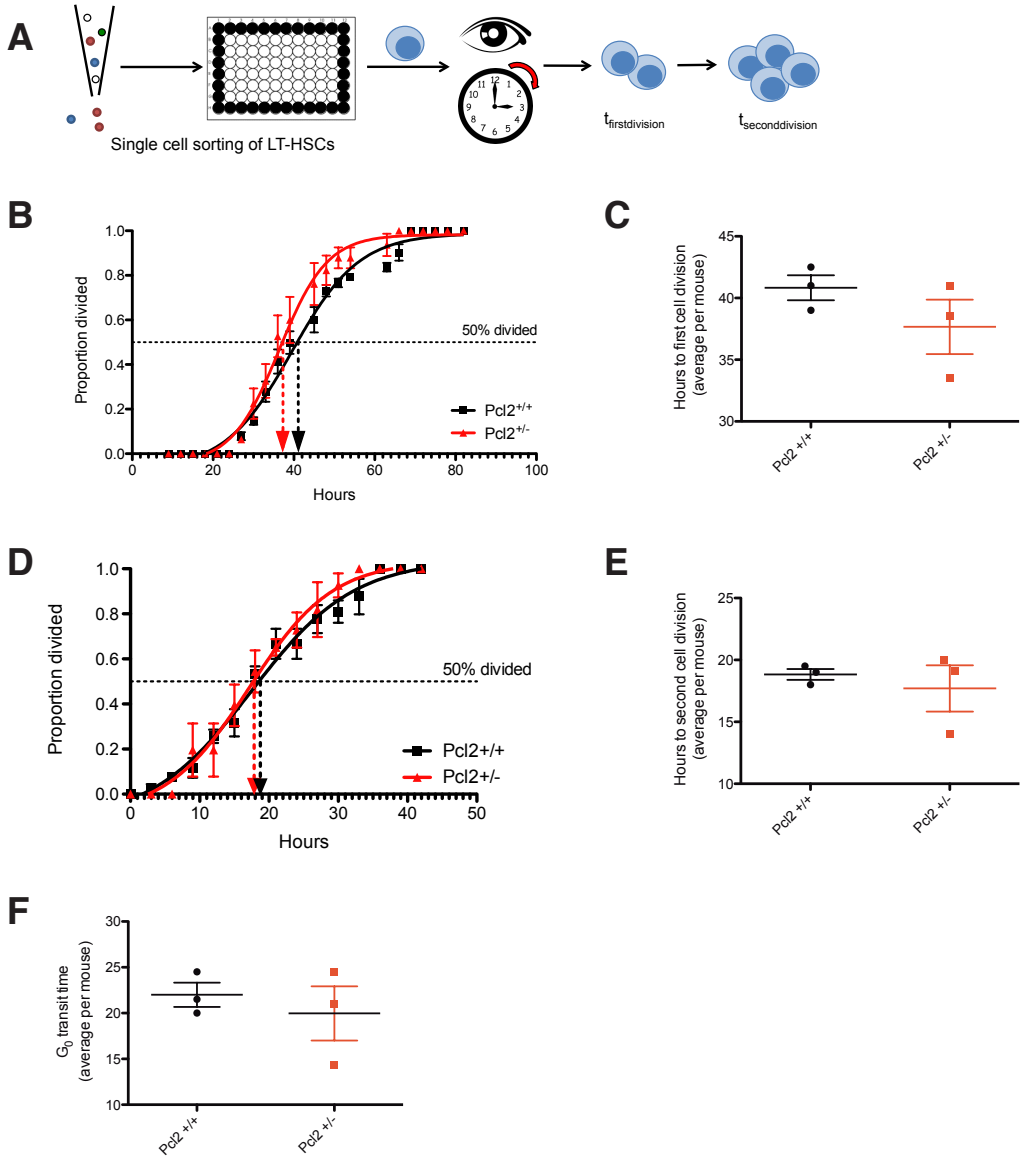

Figure A2. Isolated single *Mtf2*$^{+/-}$ HSCs have a reduced time to 1st cell division compared to wild-type LT-HSCs. (A) Schematic showing experimental design. LT-HSCs (LSK CD48^{-}CD150^{+}) were sorted from adult wild-type or *Mtf2*$^{+/-}$ mice and plated as single cells in supportive media. After 16 hrs, cells were observed every 3 hours and time to 1st and 2nd cell divisions were recorded. Cells that did not divide after 72 hrs were excluded. (B,C) The average time to first cell division was slightly shorter in *Mtf2*$^{+/-}$ LT-HSCs compared to *Mtf2*$^{+/+}$ LT-HSCs (37.7 hrs vs 40.8 hrs). (D, E) The time to 2nd cell division was similar between genotypes (approx. 17 hrs). (F) The G_0 transit time (calculated as the time difference between first cell division and 2nd cell division), is approximately 3 hours shorter in *Mtf2*$^{+/-}$ LT-HSCs.

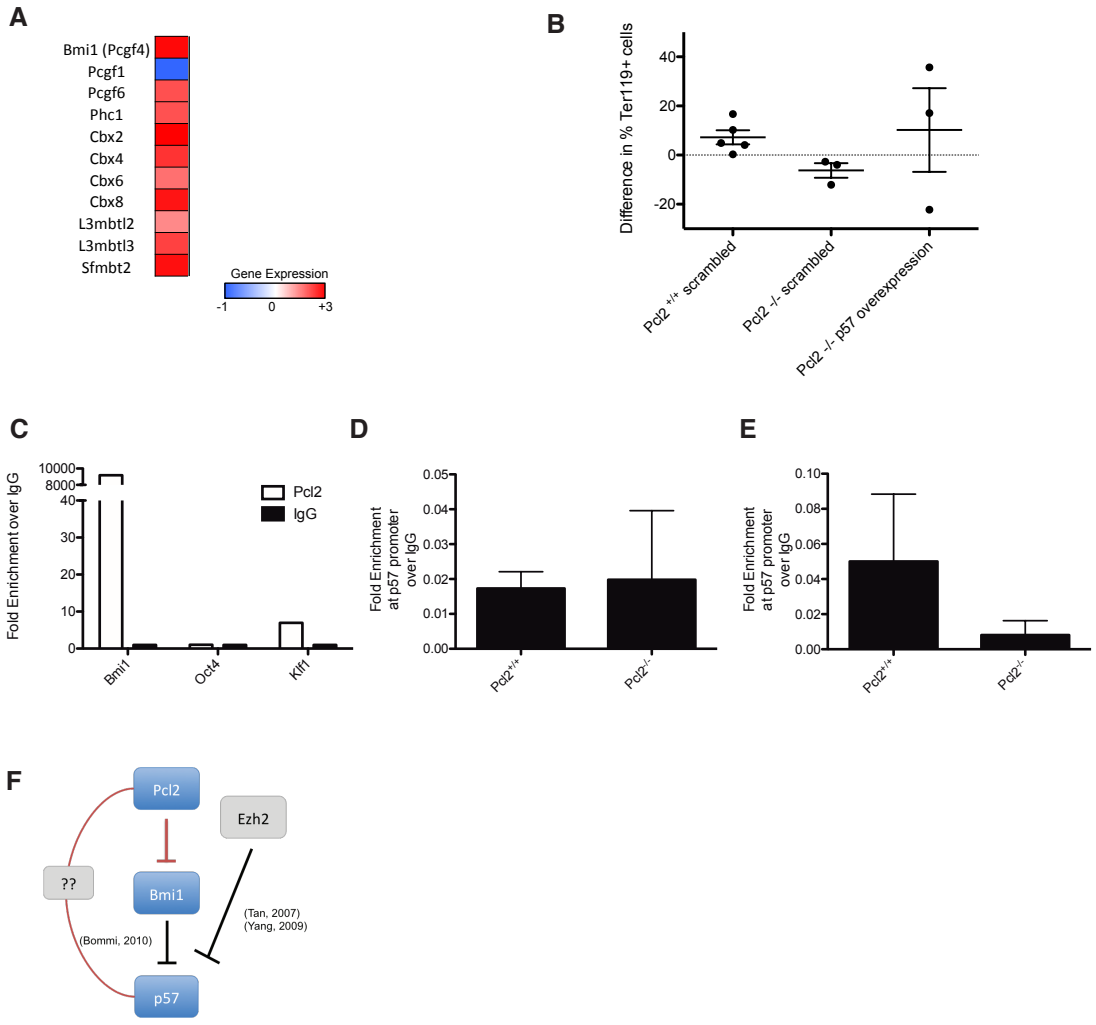

Figure A3. Overexpression of p57 can partially rescue the erythroid differentiation defect seen in *Mtf2*$^{-/-}$ erythroblasts. (A) Heatmap showing multiple PRC1 genes are significantly upregulated in *Mtf2*$^{-/-}$ Ter119^{+} cells. (B) Wild-type Ter119^{-} cells isolated from e13.5 fetal liver are able to differentiate in-vitro with addition of Epo and turn on expression of Ter119^{+}. In contrast *Mtf2*$^{-/-}$ erythroblasts fail to differentiate. Overexpression of p57 in *Mtf2*$^{-/-}$ erythroblasts partially rescues this defect and some cells begin to express Ter119. (C) Mtf2 directly binds to the Bmi1 promoter in erythroblasts. (D) H3K27me3 and (E) H2AK119ub1 levels are not significantly different at the p57 promoter in *Mtf2*$^{-/-}$ erythroblasts compared to wild-type, despite the overall changes in Ezh2 and Bmi1 levels. (F) Bmi1 and Ezh2 have been previously shown to bind the p57 promoter. Our data suggests that loss of Mtf2 decreases Ezh2, which negatively regulates p57, but also increases Bmi1 expression that negatively regulates p57. The increase in Bmi1 has a stronger effect leading to overall decrease in p57. Possible feedback loops may further control levels of Mtf2 in wild-type cells.

A

GO ID	GO Term	Gene List	p-value
GO:0000077	DNA damage checkpoint	MAPKAPK2,CRY1,CDKN1A,NEK6,TRP73,CLOCK,TIPIN,CDC14B,BRSK1,PLK5,SOX4	0.0256
GO:0042770	signal transduction in response to DNA damage	WNT1,CDKN1A,SPRED1,TRP73,TWIST1,SNAI1,HIC1,CDKN2A,BCL3,SOX4	0.00712
GO:0030330	DNA damage response, signal transduction by p53 class mediator	CDKN1A,SPRED1,TRP73,TWIST1,SNAI1,HIC1,CDKN2A,BCL3,SOX4	0.00438
GO:0008630	intrinsic apoptotic signaling pathway in response to DNA damage	HMOX1,EPHA2,CDKN1A,NFATC4,BOK,NACC2,BCL2L11,DYRK2,TRP73,PHLDA3,SNAI1,HIC1,SFN,BCL3,BCL2	0.000731
GO:0043516	regulation of DNA damage response, signal transduction by p53 class mediator	SPRED1,TWIST1,SNAI1,HIC1,CDKN2A	0.0431
GO:0006974	cellular response to DNA damage stimulus	AXIN2,HMOX1,EPHA2,MAPKAPK2,SGK1,NUAK1,CRY1,NKX3-1,BCL6,WNT1,CDKN1A,NFATC4,MMS19,CBX8, BOK,NEK6,NACC2,SPRED1,BCL2L11,ZMAT3,DYRK2,PLK3,TRP73,SPATA18,CLOCK,GGN,TIPIN,CDC14B,VAV3, EGLN3, BRSK1, SOX4, CCDC13, HSPA1A,SPDYA,YAP1,BCL3,HMGA2,BCL2,FIGN PLK5,TWIST1,PHLDA3,CCNO,SNAI1,HIC1,FOXO1,CDKN2A,SFN,	0.00367

B

	Pcl2+/+ vs Pcl2-/- Ter119high Erythroblasts	
Gene	log2FoldChange	Adj p value
BCL2	3.323	0.000196
HMGA2	2.608	0.000276
SOX4	2.533	0.000434
NEK6	1.666	0.000910
HSPA1A	2.703	0.001427
PLK3	2.312	0.002730
CBX8	2.664	0.002762
CRY1	2.380	0.003165
VAV3	1.978	0.003353
CDKN1A	1.934	0.004682
FOXO1	2.357	0.005865
DYRK2	2.344	0.006180
AXIN2	2.621	0.007181
MMS19	0.718	0.009767
EGLN3	2.232	0.009804
CDC14B	1.663	0.017196
PHLDA3	1.843	0.017399
MAPKAPK2	1.637	0.017635

Figure A4. Genes without promoter-proximal H3K27me3 marks in Mtf2-deficient erythroblasts are related to the DNA damage and repair pathways. (A) By analyzing the list of genes that have lost promoter-proximal methylation in *Mtf2*$^{-/-}$ erythroblasts (Rothberg, 2016; Table 2), we observe a significant overrepresentation of genes associated with gene ontology (GO) terms for cellular response to DNA damage. GO analysis was performed using gProfiler data and a Benjamini-Hochberg FDR statistical test. (B) Examples of genes associated with GO terms listed in Table A and their changes in expression level in *Mtf2*$^{-/-}$ Ter119^{high} erythroblasts compared to wild-type. Most genes are significantly upregulated, keeping with the role of Mtf2 as a transcriptional repressor.

Methods

Single cell HSC kinetics

Single cell cycle kinetics were analyzed based on methods outlined in (Benveniste, Frelin et al. 2010). Briefly, bone marrow was isolated from adult (8-12 wk old) *Mtf2*$^{+/+}$ and *Mtf2*$^{+/-}$ mice. After lysis using NH_4Cl, cells were lineage depleted (Stem Cell Technologies), then stained with antibodies against cKit (2B8), Sca1 (D7), CD48 (HM48-1) and CD150 (mShad150) (eBioscience). LSK $CD48^-CD150^+$ cells were sorted on a MoFlo sorter and single cells were deposited into a wells of a 96-well plate that contained 100ul of media (IMDM + 1%FBS, 0.1%BSA, IL-11 (10ng/ml), SCF (50ng/ml), Flt3 (50ng/ml); transferrin (5ug/ml), insulin (5ug/ml)). Wells containing single cells were identified using an inverted microscope (Leica) 16 hrs after plating. Wells were then visualized every 3 hours for 96 hrs and cell divisions were recorded. A minimum of 35 clones were observed per mouse. The proportion of cells divided at each time interval was plotted and fit to a sigmoid curve (Graph Pad) and time of 1st and 2nd cell divisions were calculated as the $logEC_{50}$ of each respective sigmoid curve. The time of G_0 exit is defined as $t_{G0exit} = t_{FirstDiv} – t_{SecondDiv}$, as outlined in (Laurenti, Frelin et al. 2015).

In Vitro Erythroid Differentiation

In vitro erythroid differentiation experiments were modified from an assay described previously (Zhang, Socolovsky et al. 2003). Briefly, fetal liver from e13.5 *Mtf2*$^{+/+}$ and *Mtf2*$^{-/-}$ mice was labeled with purified Ter119 antibody (eBioscience) and $Ter119^-$ cells were isolated using magnetic bead depletion according to manufacturer's instructions

(Invitrogen). Cells were transduced with lentivirus containing RFP-expressing plasmids encoding p57 cDNA or scrambled control (constructs from Applied Biological Materials). Cells were cultured on fibronectin-coated plates in erythroid maintenance media (IMDM containing 15% FBS, 1% BSA, 200g/mL holo-transferrin (Sigma), 10g/mL recombinant human insulin (Sigma), 2 mM L-glutamine, 10^{-4} M b-mercaptoethanol, and 2 U/mL Epo) for 2 days, then in erythroid differentiation media (IMDM containing 20% FBS, 2mM L-glutamine, and 10^{-4} M b-mercaptoethanol) for one day. At days 2 and 3, the percentage of $Ter119^{+}$ cells was assessed by flow cytometry.

Other leukemia models

CML was induced in C57BL/6 mice as previously described (Hegde, Kaushal et al. 2011). MLL-AF9 or CML $CD34^{+}CD133^{+}Kit^{+}Sca1^{+}$ leukemia stem cells (LSCs) from CML mice were isolated by FACS using antibodies to CD34 (Biolegend, San Diego, CA), CD133 (Millipore, Burlington, MA), cKit (Biolegend) and Sca1 (Biolegend). The cells were infected with lentiviruses expressing Mtf2 shRNAs clone 3 and clone 7 or scramble control. Infected cells were selected in puromycin containing media. For *in vitro* assays cells were plated in methylcellulose media containing Shh (200 ng/ml), GDF15 (30 ng/ml), SCF (50ng/ml) and IL-3 (10 ng/ml) for LSC colony assay or Methocult 3234 containing 10 ng/ml GM-CSF for CFU-GM assays. The cells were incubated for 7 days and colonies scored. For *in vivo* assays, lentiviral infected LSCs were transplanted into secondary recipients as previously described (Hegde, Kaushal et al. 2011). White blood cell counts were performed at 4 weeks post-transplantation. All data from MLL-AF9 and BCR-ABL mouse models is representative of two independent experiments.

Appendix B

Janet Rothberg - CV

Education

Doctor of Philosophy,
Cellular and Molecular Medicine, University of Ottawa (transfer) **Sept 2011- Present**

Doctor of Philosophy, **Sept 2009-Aug 2011**
Institute for Biomaterials and Biomedical Engineering, University of Toronto

Master of Science, Department of Physiology, Western University **Sept 2005- Aug 2007**

Bachelor of Medical Science (Hons.), **Sept 2001- April 2005**
Department of Physiology & Pharmacology, Western University

Skills & Workshops

2nd International Advanced Course on
Regenerative Medicine Manufacturing **March 2016**
Hilton Head, SC

Foundations of Project Management II **March 2014**
Mitacs, Ottawa, ON

Communication & Commercialization Workshop, **March 2013**
Stem Cell Network, Toronto, ON

Imaging Flow Cytometry (ImageStream) Training Workshop, **May 2012**
Amnis, Seattle, WA

Advanced Multi-colour Flow Cytometry, **May 2011**
Stem Cell Network, Vancouver, BC

Scholarships and Awards

Oral Presentation Award, 2nd place, Lightning Round, 2015 Till & McCulloch Meeting	2015
Ontario Graduate Scholarship	2013-2014
University of Ottawa, Excellence Scholarship	2011-2016
Oral Presentation Award, 1st place, OHRI Research Day 2013	2013
Stem Cell Network Soft Skills Workshop Bursary	2013
CIHR Banting and Best Canada Graduate Scholarship	2010-2013
Queen Elizabeth II Scholarship (declined)	2012
Oral Presentation Award, Lightning Round, 2013 Till & McCulloch Meeting	2012
University of Ottawa, CMM Seminar Award	2012
Stem Cell Network Advanced Multi-colour Flow Cytometry Course Bursary	2011
University of Toronto Barbara and Frank Milligan Scholarship	2010-2011
Ontario Graduate Scholarship (declined)	2010-2011
Ontario Graduate Scholarship	2009-2010
University of Toronto Open Fellowship	2009-2010

Peer-Reviewed Publications (as Rothberg or Manias)

Nag S, **Manias JL**, Kapadia A, Stewart DJ. Molecular changes associated with the protective effects of Angiopoietin-1 during blood-brain barrier breakdown post-injury. Molecular Neurobiology. 2016 June 22.

Julian LM, Carpenedo RL, **Rothberg JL**, Stanford WL. Formula G1: Cell cycle in the driver's seat of stem cell fate determination. Bioessays. 2016 April.

Chitilian JM, Thillainadesan G, **Manias JL**, Chang WY, Walker E, Isovic M, Stanford WL Torchia J. The p/CIP/SRC-3 oncogene is required to maintain pluripotency of embryonic stem cells. Stem Cells. 2013 Oct 1.

Chang WY, Lavoie JR, Kwon SY, **Manias JL**, Chen Z, Ling V, Stewart DJ, Stanford WL. Feeder-Independent derivation of induced-pluripotent stem cells from peripheral blood endothelial progenitor cells. Stem Cell Res. 2013 Mar;10(2):195-202.

Chang WY, Garcha K, **Manias JL**, Stanford WL. Deciphering the complexities of human diseases and disorders by coupling induced-pluripotent stem cells and systems genetics.Wiley Interdiscip Rev Syst Biol Med. 2012 Jul;4(4):339-50.

Walker E*, **Manias JL***, Chang WY* and Stanford WL. PCL2 modulates gene regulatory networks controlling self-renewal and commitment in embryonic stem cells. Cell Cycle 2011 Jan; 10(1): 45-51. *co-authors

Shuhendler AJ, Cheung RY, **Manias J**, Connor A, Rauth AM, Wu XY. A novel doxorubicin-mitomycin C co-encapsulated nanoparticle formulation exhibits anti-cancer synergy in multidrug resistant human breast cancer cells. Breast Cancer Res Treat. 2010 Jan;119(2):255-69.

Nag S, **Manias JL**, Stewart DJ. Pathology and new players in the pathogenesis of brain edema. Acta Neuropathol. 2009 Aug;118(2):197-217.

Nag S, **Manias JL**, Stewart DJ. Expression of endothelial phosphorylated caveolin-1 is increased in brain injury. Neuropathol Appl Neurobiol. 2009; 35:417-426.

Manias JL, Plante I, Gong XQ, Shao Q, Churko J, Bai D, Laird DW. Fate of connexin43 in cardiac tissue harbouring a disease-linked connexin43 mutant. Cardiovasc Res. 2008 Dec 1;80(3):385-95.

Yeung D, **Manias JL**, Stewart DJ, Nag S. Decreased junctional adhesion molecule-A expression during blood-brain barrier breakdown. Acta Neuropathol. 2008 Jun;115(6):635-42.

Langlois S, Mayer AC, **Manias JL**, Shao Q, Kidder GM, Laird DW. Connexin levels regulate keratinocyte differentiation in the epidermis. J Biol Chem. 2007 Oct 12;282(41):30171-80.

Wong HL, Rauth AM, Bendayan R, **Manias JL**, Ramaswamy M, Liu Z, Erhan SZ, Wu XY. A new polymer-lipid hybrid nanoparticle system increases cytotoxicity of doxorubicin against multidrug-resistant human breast cancer cells.
Pharm Res. 2006 Jul; 23(7):1574-85.

McLachlan E, **Manias JL**, Gong XQ, Lounsbury CS, Shao Q, Bernier SM, Bai D, Laird DW. Functional characterization of oculodentodigital dysplasia-associated Cx43 mutants. Cell Commun Adhes, 2005 Jul-Dec;12(5-6):279-92.

Conference Presentations and Publications

Manias-Rothberg JL, Maganti H, Porter CJ, Palidwor GA, Perkins TJ, Paulson R, Ito C, Stanford WL. The in vivo role of Polycomb-like 2. 2015 Till & McCulloch Annual Meeting (Lightning Round Oral Presentation, won 2nd place)

Rothberg, JL. "Presenting Your Research to a Lay Audience". Invited workshop at CALAS Annual Symposium, May 2015.

Rothberg JL, Stanford WL. Polycomb-like 2 (Pcl2/Mtf2) is required for epigenetic regulation of hematopoiesis. 2015 Ottawa Institute for Systems Biology Symposium, May 2015. (Oral Presentation)

Manias JL, Maganti H, Porter CJ, Palidwor GA, Perkins TJ, Paulson R, Ito C, Stanford WL. The in vivo role of Polycomb-like 2. 2014 Till & McCulloch Annual Meeting (Poster)

Rothberg, JL. "Presenting Your Research to a Lay Audience". Invited workshop at Trainee Poster Competition and Workshop, Arthritis Network/Canadian Arthritis Foundation, November 2013.

Rothberg (Manias) JL, Stanford WL. Polycomb-like 2 (Pcl2) is critical for normal hematopoietic development. 2013 OHRI Research Day (Oral Presentation, won 1st prize)

Manias JL, Maganti H, Porter CJ, Palidwor GA, Perkins TJ, Paulson R, Ito C, Stanford WL. The in vivo role of Polycomb-like 2. 2013 Till & McCulloch Annual Meeting (Poster)

Manias JL, Stanford WL. The in vivo role of Polycomb-like 2. 2012 Till & McCulloch Annual Meeting (Lightning Round Oral Presentation, won top PhD presentation prize)

Manias JL, Stanford WL. Review of Sing, A et al. (2009). A vertebrate Polycomb response element governs segmentation of the posterior hindbrain. Cell 138, 885–897. (F1000)

Manias JL, Kapadia A, Nag S. Detection of multiple proteins in intracerebral vessels by confocal microscopy. Methods Mol Biol. 2011;686:177-92. (Book Chapter)

Manias JL, Laird, DW. Expression and Fate of Cx43 in vivo and in Cardiac-derived Cells Harboring an Autosomal Dominant Gja1 (Cx43) Gene Mutation. American Society of Cell Biology 46th Annual Meeting. December 2006. (Poster)

Manias JL, Laird DW. The role of disease-linked connexin43 mutations in cardiac function. Canadian Student Health Research Forum, Winnipeg, MB. June 2006. (Poster)

Table S1. Genes identified as losing H3K27me3 in Mtf2-/- erythroblasts

	Mtf2+/+ vs Mtf2-/-			Mtf2+/+ vs Mtf2-/-		
	Ter119-/lo Erythroblasts			Ter119high Erythroblasts		
Gene Name	**log2FoldChange**	**Adj p value**	**Significant p<0.05**	**log2FoldChange**	**Adj p value**	**Significant p<0.05**
0610010O12Rik	2.6501	0.1643	no	2.3812	0.1211	no
1110012J17Rik	8.0000	1.0000	no	18.0000	1.0000	no
1110032F04Rik	1.6204	0.3129	no	2.2126	0.0269	yes
1110067D22Rik	0.2483	0.9997	no	1.8882	0.0119	yes
1190005I06Rik	0.6894	0.9802	no	-0.7435	1.0000	no
1300014I06Rik	2.8239	0.0042	yes	1.7044	0.0120	yes
1520402A15Rik	1.3637	0.5980	no	0.4942	0.7969	no
1600021P15Rik	1.4149	1.0000	no	1.0249	1.0000	no
1600029O15Rik	-6.0000	1.0000	no	18.0000	1.0000	no
1700001C19Rik	0.1104	1.0000	no	-1.1472	1.0000	no
1700001O22Rik	8.0000	1.0000	no	0.0000	1.0000	no
1700018A14Rik	0.0000	1.0000	no	0.0000	1.0000	no
1700019N12Rik	8.0000	1.0000	no	18.0000	1.0000	no
1700025G04Rik	2.4364	0.0554	no	0.9311	0.2099	no
1700054N08Rik	0.2353	0.9997	no	0.0622	0.9591	no
1700101E01Rik	0.4990	1.0000	no	-1.1444	1.0000	no
1810019J16Rik	1.4665	1.0000	no	18.0000	1.0000	no
1810027O10Rik	0.3497	0.5868	no	-1.1053	0.0155	yes
2010107G23Rik	2.0753	0.1591	no	3.6454	0.0599	no
2010300C02Rik	8.0000	1.0000	no	18.0000	1.0000	no
2210411K11Rik	-0.0166	0.9997	no	0.9281	0.1949	no
2310014H01Rik	NA	NA	NA	NA	NA	NA
2410017I17Rik	0.0000	1.0000	no	0.0000	1.0000	no
2410022L05Rik	0.1964	0.9997	no	2.1028	0.0223	yes
2510009E07Rik	1.5162	0.3510	no	1.2627	0.1836	no
2610017I09Rik	0.0000	1.0000	no	0.0000	1.0000	no
2610019F03Rik	-0.0283	0.9997	no	18.0000	0.0371	yes
2610109H07Rik	1.0174	1.0000	no	-12.0000	1.0000	no
2700046G09Rik	-0.5767	1.0000	no	18.0000	1.0000	no
2700086A05Rik	8.0000	1.0000	no	0.6097	1.0000	no
2810025M15Rik	0.0321	0.9997	no	1.3412	0.1249	no
2810030E01Rik	1.9018	1.0000	no	1.1522	1.0000	no
2810032G03Rik	0.0000	1.0000	no	18.0000	1.0000	no
2810055F11Rik	1.8035	0.1069	no	1.8165	0.0625	no
2810410L24Rik	8.0000	1.0000	no	1.5771	0.2475	no
2810459M11Rik	1.9963	0.0270	yes	0.6165	0.4678	no
2900092D14Rik	NA	NA	NA	NA	NA	NA
3830403N18Rik	0.6354	0.9871	no	0.1402	0.9173	no
3830431G21Rik	1.6378	0.2398	no	4.2527	1.0000	no
4430402I18Rik	-0.2461	1.0000	no	18.0000	1.0000	no
4732471D19Rik	0.1851	0.9997	no	2.3770	0.0000	yes
4833427G06Rik	0.0000	1.0000	no	0.0000	1.0000	no
4921515J06Rik	-6.0000	1.0000	no	0.0112	1.0000	no
4930412O13Rik	8.0000	1.0000	no	18.0000	1.0000	no
4930420K17Rik	1.6353	0.2730	no	1.2071	0.2149	no
4930429B21Rik	0.0000	1.0000	no	0.0000	1.0000	no
4931408A02Rik	0.9708	1.0000	no	0.0006	0.9995	no
4931429I11Rik	0.0000	1.0000	no	-12.0000	1.0000	no
4932441J04Rik	0.0221	1.0000	no	0.0000	1.0000	no
4933406I18Rik	0.0000	1.0000	no	0.0000	1.0000	no
4933421O10Rik	0.7414	0.9414	no	0.2719	1.0000	no

4933439C10Rik	0.3894	0.9765	no	2.3368	0.0087	yes
5430405G05Rik	0.0000	1.0000	no	0.0000	1.0000	no
5430407P10Rik	2.8297	0.0008	yes	1.8146	0.0099	yes
5730528L13Rik	2.8298	0.0046	yes	4.2116	0.0004	yes
5730559C18Rik	8.0000	1.0000	no	18.0000	1.0000	no
6030419C18Rik	0.0000	1.0000	no	18.0000	1.0000	no
6030429G01Rik	1.3297	1.0000	no	3.3957	1.0000	no
6230409E13Rik	8.0000	1.0000	no	18.0000	1.0000	no
6330512M04Rik	0.5750	1.0000	no	1.8167	1.0000	no
6430527G18Rik	5.0052	0.0007	yes	2.6252	0.0039	yes
6430548M08Rik	2.6617	0.0069	yes	2.4551	0.0004	yes
6430704M03Rik	-6.0000	1.0000	no	18.0000	1.0000	no
8430427H17Rik	0.3200	0.9502	no	-0.0633	0.9154	no
9030224M15Rik	0.0275	1.0000	no	1.5413	1.0000	no
9030409G11Rik	NA	NA	NA	NA	NA	NA
9030612E09Rik	0.0000	1.0000	no	0.0000	1.0000	no
9130024F11Rik	0.0000	1.0000	no	18.0000	1.0000	no
9130206I24Rik	2.9486	0.0001	yes	3.1465	0.0005	yes
9330182L06Rik	2.5231	0.0460	yes	2.3666	0.0269	yes
9430021M05Rik	0.0000	1.0000	no	0.0000	1.0000	no
9430076C15Rik	0.0000	1.0000	no	0.0000	1.0000	no
9830001H06Rik	-0.6195	0.8117	no	0.6851	0.3980	no
A330050F15Rik	-6.0000	1.0000	no	0.0000	1.0000	no
A430107O13Rik	1.4840	0.9340	no	0.1172	1.0000	no
A4galt	3.9637	1.0000	no	18.0000	1.0000	no
A530013C23Rik	0.0000	1.0000	no	18.0000	1.0000	no
A930011G23Rik	-6.0000	1.0000	no	0.0000	1.0000	no
Abca5	0.3128	0.9997	no	0.6957	1.0000	no
Abcb1b	1.6205	0.2844	no	1.9723	0.0273	yes
Abcg1	1.6980	0.1313	no	1.1503	0.1872	no
Abhd15	0.7326	0.9095	no	1.8455	0.0240	yes
Abhd6	1.0881	0.3586	no	0.4871	0.5060	no
Ablim3	-6.0000	1.0000	no	-12.0000	1.0000	no
Abtb2	1.6817	0.0982	no	-0.4138	0.6636	no
Acan	0.0000	1.0000	no	0.0000	1.0000	no
Accn1	0.0000	1.0000	no	18.0000	1.0000	no
Accn2	0.0300	1.0000	no	1.4876	1.0000	no
Accn4	-0.1368	1.0000	no	18.0000	1.0000	no
Acer2	-0.0068	0.9997	no	0.8214	0.3530	no
Acot1	1.6150	0.2447	no	0.8620	0.3819	no
Acsl6	-0.6700	0.2521	no	2.0060	0.0089	yes
Actl6b	-6.0000	1.0000	no	18.0000	1.0000	no
Actn1	1.2791	0.0093	yes	0.9980	0.0288	yes
Acvr1	1.1918	0.4116	no	1.3183	0.0767	no
Acvr1b	1.5410	0.2498	no	2.4118	0.0034	yes
Acvr2a	0.3556	0.9997	no	0.7420	0.4692	no
Acvr2b	0.0961	0.9997	no	3.0961	0.0388	yes
Adam11	8.0000	0.1243	no	0.6312	1.0000	no
Adam15	2.3720	0.0001	yes	1.4358	0.0016	yes
Adam19	1.0234	0.9311	no	-0.1966	0.8751	no
Adam23	8.0000	1.0000	no	1.9264	1.0000	no
Adamts14	8.0000	1.0000	no	1.3965	1.0000	no
Adamts2	0.5378	1.0000	no	-2.6198	1.0000	no
Adamts20	1.4991	1.0000	no	4.4149	1.0000	no
Adamts7	0.8112	1.0000	no	-0.7591	1.0000	no
Adamts8	8.0000	1.0000	no	0.0000	1.0000	no
Adap1	0.8736	0.2338	no	2.2350	0.0000	yes
Adap2	1.7085	0.0802	no	1.1653	0.0675	no

Adarb1	3.1497	0.0061	yes	-0.1490	1.0000	no
Adc	-1.1885	1.0000	no	18.0000	1.0000	no
Adcy2	1.8382	1.0000	no	0.9588	1.0000	no
Adcy3	0.0415	0.9997	no	1.2235	0.2194	no
Adcy5	1.5158	1.0000	no	0.1456	1.0000	no
Adm	3.0013	1.0000	no	0.2668	1.0000	no
Adora2b	3.8503	1.0000	no	0.0791	1.0000	no
Adra1d	-6.0000	1.0000	no	-1.5821	1.0000	no
Adra2a	8.0000	1.0000	no	2.7254	1.0000	no
Adra2c	0.0000	1.0000	no	18.0000	1.0000	no
Adrb1	2.6492	1.0000	no	-0.5701	1.0000	no
Aebp1	2.2373	0.0029	yes	1.2923	0.0474	yes
Agap1	1.0822	0.2847	no	2.6287	0.0004	yes
Agap2	0.5545	0.9300	no	2.8577	0.0003	yes
Agpat3	1.3363	0.0004	yes	1.8603	0.0000	yes
Agpat9	-0.5009	1.0000	no	0.6969	0.7752	no
Ahdc1	0.0171	0.9997	no	2.2870	0.0031	yes
Ahnak	2.6160	0.0055	yes	2.0885	0.0019	yes
AI118078	0.0000	1.0000	no	0.0000	1.0000	no
AI314831	0.0000	1.0000	no	0.0000	1.0000	no
AI646023	-0.9701	1.0000	no	-1.6321	1.0000	no
AI661453	3.7943	0.0262	yes	1.5398	1.0000	no
AI836003	0.0000	1.0000	no	0.0000	1.0000	no
Aif1l	0.0656	0.9997	no	2.0477	0.1774	no
Aim1	1.8150	0.0202	yes	2.1407	0.0023	yes
Ajap1	0.0000	1.0000	no	0.0000	1.0000	no
AK129341	0.6818	0.9706	no	2.6288	1.0000	no
Ak4	0.2649	0.9997	no	2.7676	0.0000	yes
Ak5	0.0346	1.0000	no	18.0000	1.0000	no
Akap12	1.4669	1.0000	no	0.7100	1.0000	no
Aldh1a2	1.0474	1.0000	no	0.2536	1.0000	no
Aldh5a1	2.0921	0.0756	no	1.5663	0.0852	no
Alox12	1.4359	0.2887	no	0.6508	0.4978	no
Alpl	2.4282	0.0272	yes	-0.5134	0.6208	no
Als2cl	3.0318	0.0000	yes	1.9556	0.0118	yes
Alx3	2.3298100000000(	1.0000	no	0.0000	1.0000	no
Alx4	0.0000	1.0000	no	0.0000	1.0000	no
Amigo1	0.3430	0.9997	no	1.2079	1.0000	no
Amigo2	0.3818	1.0000	no	1.0930	1.0000	no
Amn	1.0358	1.0000	no	1.5204	1.0000	no
Amotl2	2.4015	0.0310	yes	0.2897	0.8002	no
Amph	2.3500	1.0000	no	0.7877	1.0000	no
Ank1	0.2631	0.3464	no	-0.7418	0.0208	yes
Ank3	1.8462	0.0008	yes	0.8828	0.1530	no
Ankrd13b	0.3809	0.5455	no	3.5407	0.0000	yes
Ankrd33b	8.0000	1.0000	no	0.3873	1.0000	no
Ankrd34a	3.4424	1.0000	no	0.0000	1.0000	no
Ankrd34b	0.0000	1.0000	no	18.0000	1.0000	no
Ankrd44	1.4118	0.1931	no	2.4379	0.0015	yes
Ankrd56	NA	NA	NA	NA	NA	NA
Ankrd57	NA	NA	NA	NA	NA	NA
Ankrd6	-0.1892	0.9997	no	0.3900	0.7005	no
Anks1b	0.0000	1.0000	no	-12.0000	1.0000	no
Anks6	-0.0030	1.0000	no	2.3905	1.0000	no
Ano6	0.6684	0.5637	no	0.9419	0.0815	no
Ap1m2	8.0000	1.0000	no	-0.0254	1.0000	no
Apba1	2.4818	1.0000	no	2.8055	1.0000	no
Apbb2	2.6607	0.5204	no	0.9013	0.6840	no

Apc2	1.8443	1.0000	no	0.2470	1.0000	no
Apcdd1	8.0000	1.0000	no	18.0000	1.0000	no
Aqp5	0.0000	1.0000	no	0.0000	1.0000	no
Arap2	3.6203	0.1630	no	0.5453	0.5620	no
Arf3	0.2615	0.9733	no	1.6610	0.0040	yes
Arg2	0.5780	1.0000	no	1.5301	1.0000	no
Arhgap20	-6.0000	1.0000	no	-2.2346	1.0000	no
Arhgap26	4.1377	0.0000	yes	1.9621	0.0158	yes
Arhgap29	0.5708	0.6697	no	1.0607	0.0573	no
Arhgap31	1.1863	0.3255	no	1.1329	0.1269	no
Arhgef10l	1.4063	0.0611	no	1.9788	0.0002	yes
Arhgef16	1.1707	1.0000	no	1.8221	0.0174	yes
Arhgef17	1.6113	1.0000	no	1.3396	1.0000	no
Arhgef26	1.0469	1.0000	no	1.5407	1.0000	no
Arhgef37	1.9951	1.0000	no	1.2036	1.0000	no
Arhgef5	2.2534	1.0000	no	2.2635	0.0115	yes
Arhgef7	0.1827	0.9997	no	1.0119	0.1419	no
Arid3c	0.0000	1.0000	no	0.0000	1.0000	no
Arl4c	1.3514	1.0000	no	1.1113	1.0000	no
Arnt2	3.3441	1.0000	no	18.0000	1.0000	no
Arntl	-0.0152	0.9997	no	1.7633	0.0139	yes
Arpp21	0.1433	1.0000	no	3.0052	1.0000	no
Arsb	1.2231	0.3099	no	2.1767	0.0047	yes
Artn	2.4175	0.0007	yes	-0.1540	0.7967	no
Arvcf	-0.8032	0.0282	yes	0.9461	0.0401	yes
Asap2	0.7778	0.5046	no	2.2294	0.0007	yes
Asb4	2.1585	0.0792	no	1.7442	0.0577	no
Asb8	-0.1369	0.9997	no	0.2559	0.6688	no
Ascl2	1.7792	1.0000	no	3.6474	1.0000	no
Atf3	0.6742	1.0000	no	1.3707	0.2337	no
Atn1	1.4083	0.1068	no	1.4013	0.0788	no
Atoh7	0.0000	1.0000	no	0.0000	1.0000	no
Atoh8	2.8812	1.0000	no	18.0000	1.0000	no
Atp11a	0.7417	0.2848	no	1.1918	0.0539	no
Atp6v1c2	2.0836	1.0000	no	18.0000	1.0000	no
Atp8b1	0.4927	1.0000	no	1.1970	1.0000	no
Atp8b2	1.6318	0.0507	no	2.8353	0.0000	yes
Atp9a	-0.5022	0.9758	no	1.2044	0.3138	no
Atrnl1	0.0669	0.9997	no	0.7573	0.4232	no
Atxn1	0.1458	1.0000	no	0.2685	1.0000	no
AU023871	1.4523	0.6956	no	1.5350	0.1468	no
AW011738	6.3688	0.0013	yes	1.8674	0.0333	yes
AW555464	1.9808	0.0067	yes	1.7690	0.0042	yes
Axin2	1.0037	0.7835	no	2.6208	0.0072	yes
B3galnt1	0.2961	1.0000	no	0.1531	0.9097	no
B3gnt3	0.9463	0.6767	no	-0.6293	0.4978	no
B4galnt1	0.5150	0.6800	no	2.9609	0.0000	yes
B4galnt2	0.4425	0.9997	no	0.2320	1.0000	no
B4galnt3	0.4558	1.0000	no	-1.6087	0.0918	no
B4galnt4	0.5677	1.0000	no	1.4687	1.0000	no
B4galt2	0.7047	0.7422	no	0.9230	0.1398	no
B4galt4	1.7409	0.2843	no	0.4142	0.6256	no
B4galt5	1.7096	0.0119	yes	0.8500	0.0922	no
B4galt6	2.8596	0.0018	yes	2.6067	0.0007	yes
B830017H08Rik	NA	NA	NA	NA	NA	NA
B930041F14Rik	3.2564	1.0000	no	1.2439	1.0000	no
Bahcc1	0.8187	0.2468	no	2.0111	0.0029	yes
Bahd1	0.0496	0.9997	no	0.5132	0.2381	no

Bai1	0.0000	1.0000	no	0.0000	1.0000	no
Bai2	8.0000	1.0000	no	18.0000	1.0000	no
Baiap2	1.2410	0.2120	no	1.1644	0.1020	no
Baiap3	0.1934	1.0000	no	1.6951	1.0000	no
Barhl1	-6.0000	1.0000	no	0.0000	1.0000	no
Barhl2	0.0000	1.0000	no	0.0000	1.0000	no
Barx1	8.0000	1.0000	no	18.0000	1.0000	no
Barx2	0.0000	1.0000	no	0.0000	1.0000	no
Batf3	2.3747	1.0000	no	1.4309	0.2092	no
BC005764	0.4575	0.8023	no	2.0629	0.0003	yes
BC022687	1.5020	0.4068	no	1.5927	0.1238	no
BC030476	0.0000	1.0000	no	2.6076	1.0000	no
BC057022	0.0962	1.0000	no	2.6815	1.0000	no
BC061194	0.0000	1.0000	no	18.0000	1.0000	no
BC068157	1.4869	1.0000	no	1.6155	1.0000	no
Bcan	0.0000	1.0000	no	1.9286	1.0000	no
Bcar1	1.5874	0.1537	no	1.1278	0.2458	no
Bcar3	2.1267	1.0000	no	0.7253	1.0000	no
Bcl11b	2.0364	1.0000	no	0.0000	1.0000	no
Bcl2	1.0883	0.6948	no	3.3226	0.0002	yes
Bcl2l11	-0.2020	0.9997	no	0.5949	0.3199	no
Bcl3	2.3942	0.0242	yes	1.2916	0.0950	no
Bcl6	2.7756	1.0000	no	1.2875	0.1886	no
Bcr	2.1090	0.0001	yes	3.1446	0.0000	yes
Bean1	0.0000	1.0000	no	0.0000	1.0000	no
Bend4	2.5043	0.0204	yes	2.3969	0.0059	yes
Bend5	8.0000	1.0000	no	-0.5042	1.0000	no
Bend6	1.1308	1.0000	no	1.1716	1.0000	no
Bend7	2.7798	0.0292	yes	1.6561	0.0294	yes
Bfsp1	1.3897	1.0000	no	2.5546	1.0000	no
Bhlhe22	0.0000	1.0000	no	18.0000	1.0000	no
Bhlhe23	0.0000	1.0000	no	0.0000	1.0000	no
Bhlhe40	2.2738	0.2343	no	1.3214	0.1740	no
Bhlhe41	2.9811	1.0000	no	-0.0892	1.0000	no
Bicc1	1.8434	1.0000	no	1.4812	1.0000	no
Bik	1.8605	0.2983	no	3.3444	0.0185	yes
Bin1	2.0802	0.0082	yes	1.4518	0.0716	no
Blvrb	0.1085	0.9590	no	-1.0710	0.0025	yes
Bmf	1.7718	0.5709	no	0.3132	0.8059	no
Bmi1	0.7186	0.0918	no	2.8412	0.0000	yes
Bmp1	2.1962	0.0022	yes	2.0721	0.0003	yes
Bmp2	3.2571	0.0078	yes	0.4078	1.0000	no
Bmp6	-0.4013	1.0000	no	1.7076	1.0000	no
Bmp7	3.0749	1.0000	no	2.5348	1.0000	no
Bmper	8.0000	1.0000	no	0.0000	1.0000	no
Bmpr1a	1.4912	0.0679	no	1.0659	0.1245	no
Bnc1	0.0000	1.0000	no	18.0000	1.0000	no
Bnc2	0.4089	1.0000	no	1.8196	1.0000	no
Boc	8.0000	1.0000	no	-0.0658	1.0000	no
Bok	4.3562	0.0599	no	0.4461	1.0000	no
Boll	1.7206	1.0000	no	18.0000	0.0619	no
Brsk1	8.0000	1.0000	no	2.4145	1.0000	no
Brsk2	8.0000	1.0000	no	1.8979	1.0000	no
Brwd1	0.1327	0.9997	no	1.6864	0.0030	yes
Bsn	0.1138	0.9997	no	-0.0384	0.9708	no
Bspry	0.2567	1.0000	no	0.0933	1.0000	no
Bves	0.9898	1.0000	no	1.0378	1.0000	no
C030039L03Rik	1.0719	0.6000	no	-0.0784	1.0000	no

C130071C03Rik	8.0000	1.0000	no	18.0000	1.0000	no
C130074G19Rik	2.1332	0.0538	no	1.1148	0.2365	no
C1ql1	0.4417	1.0000	no	1.4941	1.0000	no
C1ql2	0.0000	1.0000	no	18.0000	1.0000	no
C1ql3	-6.0000	1.0000	no	0.0000	1.0000	no
C1ql4	0.0000	1.0000	no	0.0000	1.0000	no
C1qtnf4	1.1216	0.6707	no	-0.0839	0.9498	no
C2cd4b	1.2144	1.0000	no	18.0000	1.0000	no
C2cd4d	0.0000	1.0000	no	0.0000	1.0000	no
C530028O21Rik	8.0000	1.0000	no	0.0000	1.0000	no
C630004H02Rik	1.0742	1.0000	no	0.1135	1.0000	no
C77080	0.9243	0.7107	no	1.9351	0.0145	yes
C77370	8.0000	1.0000	no	1.0292	1.0000	no
Cables1	2.1458	0.0451	yes	2.3689	0.0029	yes
Cabp7	-0.1051	0.9997	no	0.6724	0.5206	no
Cachd1	0.8826	0.4995	no	-0.9323	0.1147	no
Cacna1a	0.9344	0.9842	no	6.9259	0.0060	yes
Cacna1b	8.0000	1.0000	no	18.0000	1.0000	no
Cacna1c	2.0186	0.0310	yes	1.9890	0.0208	yes
Cacna1g	1.7245	0.0001	yes	-0.2374	0.6182	no
Cacna1h	0.4320	0.9997	no	0.9795	1.0000	no
Cacna1i	0.0000	1.0000	no	0.0000	1.0000	no
Cacna1s	0.0000	1.0000	no	0.0000	1.0000	no
Cacna2d1	1.9878	1.0000	no	0.2418	1.0000	no
Cacna2d2	8.0000	1.0000	no	18.0000	1.0000	no
Cacna2d3	8.0000	1.0000	no	2.2414	1.0000	no
Cacnb1	0.0702	1.0000	no	1.6004	1.0000	no
Cacnb2	2.6097	1.0000	no	2.2988	0.0131	yes
Cacnb3	2.3359	1.0000	no	-2.9422	1.0000	no
Cacnb4	-1.1445	0.6494	no	-1.5953	1.0000	no
Cacng4	8.0000	1.0000	no	0.9840	1.0000	no
Cadm1	0.8570	0.7252	no	0.2199	0.7765	no
Cadm3	1.4789	0.2603	no	-1.1626	0.1599	no
Cadm4	2.6538	1.0000	no	3.1110	1.0000	no
Cadps2	-5.7389	1.0000	no	4.4998	1.0000	no
Camk1d	1.4258	0.2318	no	1.4156	0.2413	no
Camk2b	2.5263	1.0000	no	1.3275	1.0000	no
Camk2d	1.0153	0.3637	no	1.5575	0.0332	yes
Camk2n1	2.9480	0.0088	yes	1.4020	0.1406	no
Camk2n2	1.4358	1.0000	no	2.1197	1.0000	no
Camk4	0.4917	1.0000	no	0.6787	1.0000	no
Camkk1	1.4138	0.1827	no	1.7907	0.0558	no
Camkv	3.3535	1.0000	no	18.0000	1.0000	no
Capn2	2.0901	0.0155	yes	1.1439	0.1399	no
Car11	2.2149	1.0000	no	18.0000	1.0000	no
Car14	1.3187	0.4154	no	0.6099	0.5628	no
Car4	8.0000	1.0000	no	18.0000	1.0000	no
Car7	2.5383	0.0158	yes	2.0287	0.0092	yes
Card10	2.8276	0.0032	yes	2.5082	0.0000	yes
Caskin1	0.3260	1.0000	no	2.5897	1.0000	no
Casz1	3.3476	1.0000	no	2.7082	0.0005	yes
Cbfa2t3	0.1313	0.9997	no	0.6583	0.1188	no
Cbfb	1.3014	0.0180	yes	2.1506	0.0000	yes
Cbln1	0.0000	1.0000	no	0.0000	1.0000	no
Cbr3	2.8494	1.0000	no	0.7034	1.0000	no
Cbs	2.8907	0.0001	yes	2.3618	0.0002	yes
Cbx2	0.5287	0.9402	no	2.9552	0.0010	yes
Cbx4	0.8512	0.5082	no	2.2047	0.0005	yes

Cbx7	0.4804	0.8434	no	0.7664	0.1374	no
Cbx8	-1.0577	0.6086	no	2.6641	0.0028	yes
Ccdc102a	-0.1198	0.9997	no	2.3560	0.0067	yes
Ccdc109b	0.3404	0.9460	no	-0.4581	0.3735	no
Ccdc13	0.0000	1.0000	no	0.0000	1.0000	no
Ccdc136	8.0000	1.0000	no	18.0000	1.0000	no
Ccdc3	1.7546	1.0000	no	0.9641	1.0000	no
Ccdc40	-1.7674	0.0538	no	2.3124	0.0605	no
Ccdc48	2.4699	1.0000	no	0.6786	1.0000	no
Ccdc64	0.6549	0.8238	no	0.8559	0.3588	no
Ccdc85c	0.8033	0.8808	no	2.8368	0.0019	yes
Ccdc92	3.8496	0.0022	yes	2.2777	0.1309	no
Ccna1	8.0000	1.0000	no	18.0000	1.0000	no
Ccnd2	0.7751	0.0688	no	3.0731	0.0000	yes
Ccnjl	0.6137	1.0000	no	1.2790	1.0000	no
Ccno	2.0652	1.0000	no	2.1102	1.0000	no
Ccr10	-0.2280	1.0000	no	18.0000	1.0000	no
Cd109	8.0000	1.0000	no	0.5985	1.0000	no
Cd14	1.9460	1.0000	no	0.2805	0.8244	no
Cd302	1.3910	0.3019	no	0.5103	0.5968	no
Cd63	2.4591	0.0008	yes	2.0283	0.0032	yes
Cd70	0.0000	1.0000	no	0.0000	1.0000	no
Cd9	2.3728	0.0011	yes	1.3021	0.0790	no
Cdc14b	1.1300	0.0306	yes	1.6627	0.0172	yes
Cdc42bpb	0.7135	0.5955	no	1.6099	0.0390	yes
Cdc42ep1	2.5731	0.0259	yes	1.3780	0.1422	no
Cdh1	2.6332	0.0043	yes	1.7932	0.0311	yes
Cdh2	2.3616	0.0018	yes	1.4634	0.0293	yes
Cdh22	0.0000	1.0000	no	0.0000	1.0000	no
Cdh4	8.0000	1.0000	no	0.9432	1.0000	no
Cdk14	2.2097	0.0142	yes	0.9537	0.2704	no
Cdk18	1.3660	0.2610	no	1.3886	0.1428	no
Cdk5r2	8.0000	1.0000	no	18.0000	1.0000	no
Cdkl1	1.1037	0.6448	no	-1.2542	0.1319	no
Cdkn1a	2.2601	0.0062	yes	1.9337	0.0047	yes
Cdkn1c	1.6995	0.0162	yes	0.6250	0.4118	no
Cdkn2a	8.0000	1.0000	no	0.0000	1.0000	no
Cdr2l	2.2966	1.0000	no	0.8311	1.0000	no
Cds1	2.0020	0.6457	no	1.2308	0.3974	no
Cdv3	-0.1182	0.8832	no	0.7782	0.0058	yes
Cdx1	-6.0000	1.0000	no	0.0000	1.0000	no
Cdx2	0.0000	1.0000	no	0.0000	1.0000	no
Cdyl2	-0.5078	0.9997	no	0.6228	0.5665	no
Cebpa	2.6451	0.0032	yes	1.5023	0.0642	no
Cebpb	1.0553	0.5817	no	1.0875	0.2332	no
Cebpd	1.3878	0.4447	no	2.3750	0.0056	yes
Cecr6	0.0000	1.0000	no	18.0000	1.0000	no
Celsr1	3.4121	1.0000	no	3.3135	1.0000	no
Celsr2	1.0901	0.1398	no	3.3601	0.0951	no
Celsr3	3.1680	1.0000	no	2.5997	1.0000	no
Cgn	0.5384	0.7858	no	-0.8429	0.1136	no
Cgnl1	0.5915	1.0000	no	0.6142	1.0000	no
Ch25h	8.0000	1.0000	no	18.0000	1.0000	no
Chd3	1.3783	0.0002	yes	1.3414	0.0000	yes
Chd5	0.3591	1.0000	no	1.3951	1.0000	no
Chn1	0.7193	0.6873	no	0.8586	0.4048	no
Chn2	2.4578	0.0011	yes	1.7290	0.0018	yes
Chpf	0.3861	0.8867	no	3.3224	0.0000	yes

Chrd	8.0000	1.0000	no	1.0226	1.0000	no
Chrdl2	0.0000	1.0000	no	0.0000	1.0000	no
Chrm4	1.5921	0.2205	no	4.4111	1.0000	no
Chrna5	8.0000	1.0000	no	0.0000	1.0000	no
Chrnb1	2.8675	1.0000	no	18.0000	0.0756	no
Chst1	8.0000	1.0000	no	18.0000	1.0000	no
Chst15	-0.4717	0.9842	no	1.5958	0.1014	no
Chst2	1.6379	1.0000	no	1.5239	1.0000	no
Chst3	0.8011	1.0000	no	0.9091	1.0000	no
Chsy3	1.2762	1.0000	no	0.1923	1.0000	no
Cidea	8.0000	1.0000	no	0.0000	1.0000	no
Cilp2	-0.9255	1.0000	no	-12.0000	1.0000	no
Cited1	1.9461	0.0021	yes	1.0175	0.1226	no
Ckap4	2.7549	0.0000	yes	1.9651	0.0000	yes
Ckb	1.5289	0.1812	no	0.5923	0.5202	no
Clcf1	8.0000	1.0000	no	4.0350	1.0000	no
Cldn10	-1.4667	0.5060	no	-2.3321	0.0368	yes
Cldn23	8.0000	1.0000	no	0.0000	1.0000	no
Cldn3	0.2560	1.0000	no	18.0000	1.0000	no
Cldn5	1.3294	0.5942	no	0.7273	0.5070	no
Cldn6	0.0000	1.0000	no	0.0000	1.0000	no
Cldn7	8.0000	0.0430	yes	1.8830	0.2545	no
Clec2l	2.3528	1.0000	no	1.2495	1.0000	no
Clgn	1.3047	0.2603	no	1.5168	0.0074	yes
Clic6	4.7368	1.0000	no	4.9061	1.0000	no
Clip1	-0.0044	0.9997	no	0.8445	0.0008	yes
Clock	0.1352	0.9997	no	0.9178	0.0842	no
Clstn1	0.7386	0.6712	no	2.4095	0.0124	yes
Clstn2	1.0414	1.0000	no	0.0443	1.0000	no
Cmtm4	0.5697	0.9997	no	2.8912	0.0019	yes
Cmtm7	1.9118	0.0000	yes	2.5029	0.0000	yes
Cnih3	8.0000	1.0000	no	0.0000	1.0000	no
Cnn1	0.0190	1.0000	no	-0.0173	1.0000	no
Cnn2	2.3840	0.0000	yes	2.1290	0.0000	yes
Cnn3	-0.5342	0.5012	no	1.8345	0.0114	yes
Cnnm1	2.8360	0.0004	yes	18.0000	0.0001	yes
Cnr1	8.0000	1.0000	no	18.0000	1.0000	no
Cntfr	2.0889	1.0000	no	18.0000	1.0000	no
Cntnap1	3.9507	1.0000	no	2.1918	1.0000	no
Cobll1	1.8815	0.2436	no	0.6021	0.5872	no
Coch	-1.9696	1.0000	no	18.0000	1.0000	no
Col18a1	1.4751	0.0038	yes	1.0554	0.0441	yes
Col23a1	0.8086	1.0000	no	4.5081	1.0000	no
Col27a1	3.0983	0.0000	yes	1.3447	0.0170	yes
Col2a1	2.0285	1.0000	no	-2.1175	1.0000	no
Col4a2	0.7159	0.6767	no	0.6824	0.4096	no
Col5a1	-0.3694	0.8764	no	0.7454	0.2234	no
Col8a2	1.0440	1.0000	no	18.0000	1.0000	no
Col9a2	3.1174	1.0000	no	18.0000	1.0000	no
Colec12	0.6994	0.9499	no	0.6482	0.5258	no
Comp	-0.1358	1.0000	no	0.9080	1.0000	no
Copz2	3.2066	0.0560	no	0.6718	0.4226	no
Coro2a	2.5786	0.0009	yes	2.4008	0.0000	yes
Coro6	-0.8974	1.0000	no	18.0000	1.0000	no
Cox8a	-0.0684	0.9997	no	-0.0411	0.9678	no
Cpeb1	8.0000	1.0000	no	18.0000	1.0000	no
Cpeb2	1.7298	0.0108	yes	2.0987	0.0050	yes
Cpm	2.0306	0.0143	yes	1.5734	0.0444	yes

Cpne2		2.0342	0.1807	no		1.8921	0.0531	no
Cpne5		0.1675	1.0000	no		0.7615	1.0000	no
Cpne7		-0.2280	0.9997	no		2.1949	0.0002	yes
Cpxm1		4.1013	0.0081	yes		-0.7000	1.0000	no
Crabp1		8.0000	1.0000	no		18.0000	1.0000	no
Crabp2		-1.5470	1.0000	no		0.1039	1.0000	no
Crb2		-3.5931	1.0000	no		0.9279	1.0000	no
Crb3		1.5644	1.0000	no		2.7104	0.0458	yes
Crhr1		0.0000	1.0000	no		0.0000	1.0000	no
Crim1		-0.3423	0.9997	no		1.5247	0.0886	no
Crlf1		0.4047	0.9997	no		-0.5774	0.5167	no
Crmp1		1.9446	1.0000	no		0.2140	1.0000	no
Crtac1		0.0000	1.0000	no		1.9445	1.0000	no
Crtc3		-0.1371	0.9997	no		1.6180	0.0145	yes
Cry1		0.5887	0.9084	no		2.3797	0.0032	yes
Csf1		1.8489	0.0097	yes		0.4873	0.3901	no
Csnk1e		0.5869	0.5265	no		1.5790	0.0007	yes
Csrnp1		2.0040	0.1412	no		2.1822	0.0168	yes
Csrnp2		0.2602	0.9997	no		1.4923	1.0000	no
Ctbp2		0.2650	0.9712	no		2.9912	0.0000	yes
Ctgf		0.8741	1.0000	no		1.2561	1.0000	no
Cthrc1		0.0000	1.0000	no		0.0000	1.0000	no
Ctnnbip1		0.7194	0.7974	no		1.8714	0.0171	yes
Ctnnd2		2.4294	1.0000	no		2.7907	1.0000	no
Ctsf		1.8404	0.0047	yes		-0.6375	0.4106	no
Cttnbp2		0.9718	0.6523	no		-0.9151	0.2493	no
Cttnbp2nl		1.4863	1.0000	no		0.5110	1.0000	no
Cuedc1		1.3938	0.9629	no		0.1918	1.0000	no
Cul9		3.3511	1.0000	no		1.6499	1.0000	no
Cux1		0.2090	0.7786	no		0.2731	0.3912	no
Cux2		2.1370	1.0000	no		1.6917	1.0000	no
Cwh43		0.0000	1.0000	no		0.0000	1.0000	no
Cx3cl1		8.0000	1.0000	no		-0.6569	1.0000	no
Cxcr4		3.2173	0.0000	yes		2.2734	0.0000	yes
Cxcr7		8.0000	0.0161	yes		1.5841	0.0869	no
Cxxc5		2.5949	0.0143	yes		1.5688	0.0760	no
Cyfip2		0.7774	0.1669	no		2.8330	0.0000	yes
Cygb		8.0000	1.0000	no		18.0000	1.0000	no
Cyp1b1		8.0000	1.0000	no		-12.0000	1.0000	no
Cyp26a1		1.3983	1.0000	no		0.2207	1.0000	no
Cyp27b1		1.8167	1.0000	no		18.0000	1.0000	no
Cyp46a1		8.0000	1.0000	no		18.0000	1.0000	no
Cyr61		1.3675	1.0000	no		0.8921	1.0000	no
Cys1		1.4682	1.0000	no		-0.1796	1.0000	no
D030025P21Rik		0.0000	1.0000	no		0.0000	1.0000	no
D18Ertd653e		3.1807	0.0016	yes		-0.8913	0.2620	no
D19Ertd652e	NA	NA		NA	NA	NA		NA
D430041D05Rik		2.6829	1.0000	no		-2.5392	1.0000	no
D430050G20	NA	NA		NA	NA	NA		NA
D630045J12Rik		-0.2173	0.9997	no		0.2366	1.0000	no
D730039F16Rik		3.2064	0.0113	yes		2.6553	0.0043	yes
D8Ertd82e		1.7580	1.0000	no		1.0652	1.0000	no
D930020B18Rik		0.0000	1.0000	no		18.0000	1.0000	no
D930020E02Rik	NA	NA		NA	NA	NA		NA
D930048N14Rik		0.7860	1.0000	no		-1.4855	1.0000	no
Dab1		0.0000	1.0000	no		-12.0000	1.0000	no
Dab2ip		1.1650	0.3243	no		1.4167	0.0789	no
Dact1		-0.4749	1.0000	no		2.1319	1.0000	no

Dact2		3.2133	0.0129	yes	1.0904	1.0000	no
Dag1		0.0782	0.9997	no	0.8873	0.1201	no
Dapk1		0.1836	0.9997	no	0.9484	0.0598	no
Dbn1		0.7265	0.8177	no	0.6815	0.4632	no
Dbndd1		0.1391	0.9997	no	1.4486	1.0000	no
Dbndd2		0.8466	0.9170	no	1.2323	0.3347	no
Dbx1		0.0000	1.0000	no	0.0000	1.0000	no
Dcbld2		1.0739	0.0792	no	0.2381	0.7187	no
Dcdc2a		-0.9868	1.0000	no	18.0000	1.0000	no
Dchs1		1.9015	1.0000	no	1.4078	1.0000	no
Dclk2		0.5673	0.6354	no	-0.8753	0.0602	no
Ddn		4.1283	1.0000	no	0.6681	1.0000	no
Ddr1		1.5021	1.0000	no	1.9542	0.0630	no
Ddx25		1.0233	1.0000	no	2.0135	1.0000	no
Ddx43		8.0000	1.0000	no	18.0000	1.0000	no
Dennd2a		0.9162	1.0000	no	1.0091	1.0000	no
Dennd5b		1.0991	0.5341	no	1.4429	0.0960	no
Depdc7		0.9134	0.8377	no	1.7240	0.0410	yes
Dgka		1.8713	0.1627	no	2.0198	0.0231	yes
Dgki		8.0000	1.0000	no	18.0000	1.0000	no
Dhh		0.7486	1.0000	no	1.5201	1.0000	no
Dio3		8.0000	1.0000	no	18.0000	1.0000	no
Dio3os		8.0000	1.0000	no	-0.0278	1.0000	no
Dip2b		0.1840	0.9997	no	1.6596	0.0001	yes
Dip2c		0.2585	0.9997	no	1.4076	0.0167	yes
Disc1		3.4843	1.0000	no	4.2891	1.0000	no
Dkkl1		-0.2626	0.9997	no	2.3977	0.0151	yes
Dleu7		8.0000	1.0000	no	18.0000	1.0000	no
Dlg5		1.9469	0.0001	yes	1.9344	0.0034	yes
Dlgap2		0.0000	1.0000	no	0.0000	1.0000	no
Dlgap3		8.0000	1.0000	no	0.9172	1.0000	no
Dlgap4		-0.0626	0.9997	no	1.8854	0.0002	yes
Dlk2		8.0000	1.0000	no	18.0000	1.0000	no
Dll1		0.0621	1.0000	no	1.6845	1.0000	no
Dll4		0.4796	1.0000	no	0.3641	1.0000	no
Dlx1		-0.2660	1.0000	no	-1.9234	1.0000	no
Dlx2		8.0000	1.0000	no	0.0000	1.0000	no
Dlx3		0.0000	1.0000	no	18.0000	1.0000	no
Dlx4		3.7887	1.0000	no	2.7738	1.0000	no
Dlx6		0.7034	1.0000	no	-1.0347	1.0000	no
Dlx6as	NA	NA		NA	NA	NA	NA
Dmbx1		0.0000	1.0000	no	0.0000	1.0000	no
Dmrt2		1.3605	1.0000	no	4.2172	1.0000	no
Dmrt3		0.0000	1.0000	no	0.0000	1.0000	no
Dmrta1		0.0000	1.0000	no	0.0000	1.0000	no
Dmrta2		0.0937	1.0000	no	-0.1300	1.0000	no
Dmrtc2		0.0000	1.0000	no	0.0000	1.0000	no
Dmxl2		1.3134	0.0554	no	1.9557	0.0269	yes
Dnajc22		2.3063	0.0533	no	1.2468	0.1888	no
Dnajc6		3.3482	0.0066	yes	4.7874	1.0000	no
Dnm1		2.1800	0.3126	no	2.3860	0.1202	no
Dnmt3a		0.0048	0.9997	no	1.6739	0.0000	yes
Dnmt3b		0.3188	0.8177	no	2.7483	0.0000	yes
Doc2a		-0.0220	0.9997	no	1.5921	0.0575	no
Doc2b		0.0000	1.0000	no	0.0000	1.0000	no
Dock1		2.1137	0.0532	no	1.4870	0.0915	no
Dock3		0.7218	0.9997	no	2.7948	1.0000	no
Dock4		0.7296	1.0000	no	0.6849	1.0000	no

Dock7	-0.8328	0.0090	yes	1.2092	0.0008	yes
Dock9	0.1852	0.9997	no	2.0971	0.0007	yes
Dok7	8.0000	1.0000	no	2.9407	0.1788	no
Dos	1.1065	0.2468	no	0.8649	0.2992	no
Dpf1	0.3186	0.9997	no	3.3442	0.1256	no
Dpysl5	8.0000	1.0000	no	2.3493	1.0000	no
Drd4	0.0000	1.0000	no	0.0000	1.0000	no
Dscam	0.0000	1.0000	no	0.0000	1.0000	no
Dse	1.0319	0.7139	no	0.4811	0.6515	no
Dsp	1.2842	0.3225	no	0.7622	0.3657	no
Dtx4	2.3751	0.0168	yes	2.6131	0.0009	yes
Duox2	0.0000	1.0000	no	0.0000	1.0000	no
Duoxa2	0.0000	1.0000	no	0.0000	1.0000	no
Dusp14	1.7215	1.0000	no	0.1402	1.0000	no
Dusp2	0.6291	0.9423	no	4.2346	0.0000	yes
Dusp22	1.3017	0.3822	no	0.5612	0.5744	no
Dusp4	0.6375	1.0000	no	0.9267	1.0000	no
Dusp5	1.9561	0.1601	no	1.3579	0.1536	no
Dyrk2	0.2931	0.9997	no	2.3439	0.0062	yes
Dzip1	-0.4744	0.9997	no	-0.6852	0.5150	no
E130012A19Rik	2.3801	0.0152	yes	3.5525	0.0000	yes
E130201H02Rik	0.1224	1.0000	no	-0.8858	1.0000	no
E330009J07Rik	1.3270	0.3792	no	2.1749	0.0087	yes
E330016A19Rik	1.9548	0.0001	yes	3.0848	0.0000	yes
E530011L22Rik	0.0389	1.0000	no	-12.0000	1.0000	no
Ebf1	8.0000	0.3747	no	2.3975	1.0000	no
Ebf2	-0.3993	1.0000	no	-0.6260	1.0000	no
Ebf3	0.0000	1.0000	no	0.0000	1.0000	no
Ebf4	8.0000	1.0000	no	18.0000	1.0000	no
Ece2	-0.3748	0.9824	no	1.7589	0.0348	yes
Ecel1	0.0000	1.0000	no	18.0000	1.0000	no
Echdc3	1.8078	0.1609	no	1.4306	0.1444	no
Efcab4a	0.4938	0.9811	no	1.3996	0.0444	yes
Efemp2	2.9436	0.0000	yes	0.8895	0.1831	no
Efhd1	0.0000	1.0000	no	18.0000	1.0000	no
Efna1	2.4067	0.3234	no	0.5263	1.0000	no
Efna2	2.0651	0.1968	no	18.0000	1.0000	no
Efna3	8.0000	1.0000	no	0.0000	1.0000	no
Efna5	0.6051	1.0000	no	18.0000	1.0000	no
Efnb2	0.1623	1.0000	no	0.3298	1.0000	no
Efr3b	1.3496	1.0000	no	1.9718	1.0000	no
Efs	3.2741	1.0000	no	3.4529	1.0000	no
EG434280	NA	NA	NA	NA	NA	NA
Egln3	3.4800	0.0022	yes	2.2322	0.0098	yes
Egr1	1.5278	0.2888	no	1.5380	0.0919	no
Egr2	0.0000	1.0000	no	18.0000	1.0000	no
Egr3	0.0000	1.0000	no	0.0000	1.0000	no
Egr4	0.0000	1.0000	no	0.0000	1.0000	no
Eid2	1.7417	0.2152	no	2.9716	0.0011	yes
Eif2c4	2.7680	1.0000	no	1.8211	1.0000	no
Eif4e3	1.8627	0.1857	no	1.9260	0.0296	yes
Elac1	0.2219	0.9997	no	1.8970	0.0316	yes
Elavl2	4.8993	0.0065	yes	4.0294	0.0332	yes
Elavl3	8.0000	1.0000	no	2.2930	1.0000	no
Elfn1	8.0000	1.0000	no	-0.4885	1.0000	no
Elk3	1.9374	0.0021	yes	1.6225	0.0001	yes
Elovl2	2.0498	0.0407	yes	0.6519	0.5094	no
Elovl3	1.5927	1.0000	no	18.0000	1.0000	no

Elovl4	8.0000	1.0000	no	0.0000	1.0000	no
Elovl7	2.4602	1.0000	no	2.3289	1.0000	no
Emid1	2.5455	0.0002	yes	2.6298	0.0001	yes
Eml1	-0.7154	0.9820	no	0.0360	1.0000	no
Eml5	0.2469	0.9997	no	1.1912	0.1644	no
Emx1	8.0000	1.0000	no	0.0000	1.0000	no
Emx2	0.0000	1.0000	no	0.0000	1.0000	no
Emx2os	0.7818	1.0000	no	-12.0000	1.0000	no
En1	0.0000	1.0000	no	0.0000	1.0000	no
En2	0.0000	1.0000	no	0.0000	1.0000	no
Enah	2.3184	1.0000	no	1.8074	0.0323	yes
Enc1	0.7998	0.8901	no	2.3743	0.0069	yes
Eno2	8.0000	1.0000	no	1.7556	1.0000	no
Enox1	0.0000	1.0000	no	0.0000	1.0000	no
Enpp1	-0.1097	0.9997	no	1.9152	0.0006	yes
Entpd4	-0.0912	0.9997	no	1.6106	0.0379	yes
Eomes	8.0000	1.0000	no	0.0000	1.0000	no
Epas1	1.3227	0.4872	no	1.3118	1.0000	no
Epb4.1l1	2.2951	0.0000	yes	0.1483	0.7511	no
Epb4.1l4a	0.8490	1.0000	no	1.5678	1.0000	no
Epb4.1l4b	1.7977	0.0097	yes	1.6482	0.0126	yes
Epcam	8.0000	1.0000	no	1.5767	1.0000	no
Epha2	3.5909	1.0000	no	1.4828	0.1714	no
Epha4	2.1914	1.0000	no	0.8214	1.0000	no
Epha7	1.5969	1.0000	no	2.4937	0.0470	yes
Epha8	2.8167	0.0077	yes	0.6262	0.5573	no
Ephb2	4.9048	1.0000	no	1.8752	1.0000	no
Ephb3	3.7660	0.0101	yes	3.1914	1.0000	no
Ephx4	8.0000	1.0000	no	18.0000	1.0000	no
Epn2	0.3558	0.9997	no	1.9752	0.0839	no
Eps8	2.0642	0.2393	no	1.7315	0.1949	no
Erbb2	2.7864	0.0460	yes	1.4735	1.0000	no
Erbb2ip	-0.2276	0.8686	no	0.7291	0.0565	no
Erbb3	0.9606	0.7931	no	1.6724	1.0000	no
Erbb4	0.0000	1.0000	no	-12.0000	1.0000	no
Errfi1	1.8551	0.1211	no	0.9337	0.2801	no
Esam	1.4420	0.3183	no	-0.0343	0.9746	no
Espn	0.9074	0.2672	no	2.5767	0.0505	no
Esr2	8.0000	1.0000	no	0.0000	1.0000	no
Esrp1	8.0000	1.0000	no	18.0000	1.0000	no
Esrp2	0.7775	0.8014	no	0.6624	0.4113	no
Esrrb	8.0000	1.0000	no	0.7907	1.0000	no
Etv4	0.8306	1.0000	no	0.0825	1.0000	no
Etv5	0.4720	0.9295	no	0.9924	0.1956	no
Evl	1.0389	0.0502	no	1.6757	0.0013	yes
Evx2	0.0000	1.0000	no	0.0000	1.0000	no
Exoc6b	0.6203	0.6625	no	-0.2786	0.7136	no
Extl1	1.9573	1.0000	no	-0.3496	1.0000	no
F2rl1	8.0000	1.0000	no	1.2963	1.0000	no
F730043M19Rik	1.0456	0.9342	no	-0.0252	1.0000	no
Fa2h	0.0000	1.0000	no	0.0000	1.0000	no
Faah	2.1369	0.0092	yes	2.3451	0.0002	yes
Fabp3	8.0000	0.0767	no	2.1390	1.0000	no
Fam101b	1.4641	0.2658	no	2.7994	0.0004	yes
Fam102a	1.8277	0.1620	no	1.7647	0.0853	no
Fam113b	0.4195	0.9997	no	-0.5441	0.5670	no
Fam114a1	1.7525	0.0865	no	0.5428	0.6037	no
Fam123a	-1.8491	1.0000	no	18.0000	1.0000	no

Fam131a	1.1835	0.5150	no	0.8712	0.3643	no
Fam131b	-6.0000	1.0000	no	1.2213	1.0000	no
Fam131c	-0.0014	1.0000	no	0.9460	1.0000	no
Fam135a	2.6503	0.0181	yes	2.7742	0.0014	yes
Fam150b	-0.1238	0.9997	no	-0.9156	0.3705	no
Fam159a	8.0000	1.0000	no	0.0000	1.0000	no
Fam163a	8.0000	1.0000	no	0.0000	1.0000	no
Fam169a	0.1077	0.9997	no	0.1666	0.8603	no
Fam171a1	1.5210	0.0243	yes	1.6520	0.0060	yes
Fam171a2	-0.4048	0.9997	no	1.4936	0.1831	no
Fam171b	1.0194	1.0000	no	18.0000	1.0000	no
Fam174b	1.9505	0.1069	no	3.4298	0.0001	yes
Fam176b	2.3269	0.0107	yes	0.8184	0.3328	no
Fam181b	8.0000	1.0000	no	-0.6599	1.0000	no
Fam184a	-1.5060	0.9308	no	3.1717	1.0000	no
Fam189a1	0.0000	1.0000	no	18.0000	1.0000	no
Fam189a2	8.0000	1.0000	no	1.3631	1.0000	no
Fam190a	0.0000	1.0000	no	0.0000	1.0000	no
Fam19a2	-0.9284	1.0000	no	-0.0548	1.0000	no
Fam19a3	0.0000	1.0000	no	0.0000	1.0000	no
Fam19a4	0.0000	1.0000	no	0.0000	1.0000	no
Fam19a5	0.0000	1.0000	no	18.0000	1.0000	no
Fam20c	3.8558	0.0000	yes	1.0038	0.2120	no
Fam43a	2.7316	0.0135	yes	2.1743	0.0132	yes
Fam43b	0.0000	1.0000	no	0.0000	1.0000	no
Fam46b	1.0657	1.0000	no	18.0000	1.0000	no
Fam49b	-0.0495	0.9997	no	1.5451	0.0210	yes
Fam57a	-0.2600	0.9845	no	1.8945	0.0013	yes
Fam59b	8.0000	1.0000	no	18.0000	1.0000	no
Fam65a	-0.0995	0.9997	no	2.6595	0.0002	yes
Fam65b	0.2990	0.9920	no	1.8445	0.0003	yes
Fam69b	0.6716	0.9683	no	2.4825	0.0675	no
Fam69c	0.0000	1.0000	no	0.0000	1.0000	no
Fam78b	1.6573	1.0000	no	1.8097	1.0000	no
Fam83f	8.0000	1.0000	no	1.3062	1.0000	no
Fam83h	2.6140	1.0000	no	1.9878	1.0000	no
Fam89a	1.1105	0.7861	no	3.4641	0.0143	yes
Farp1	1.0028	0.6523	no	0.3713	0.7185	no
Fblim1	0.5839	1.0000	no	0.3839	0.8437	no
Fbll1	0.0000	1.0000	no	0.0000	1.0000	no
Fbn1	1.8584	1.0000	no	0.6060	1.0000	no
Fbxl16	8.0000	1.0000	no	18.0000	1.0000	no
Fbxo43	8.0000	1.0000	no	0.0085	1.0000	no
Fdx1	0.1013	0.9997	no	1.5778	0.0773	no
Fermt2	2.0704	0.0147	yes	0.6671	0.3615	no
Fes	2.9064	0.0001	yes	2.3447	0.0005	yes
Fev	0.0000	1.0000	no	0.0000	1.0000	no
Fgd1	1.2668	0.4031	no	0.6558	0.4877	no
Fgf11	3.1112	0.0034	yes	1.6377	1.0000	no
Fgf12	0.0000	1.0000	no	18.0000	1.0000	no
Fgf15	4.0343	1.0000	no	18.0000	1.0000	no
Fgf16	0.0000	1.0000	no	0.0000	1.0000	no
Fgf17	8.0000	1.0000	no	0.0000	1.0000	no
Fgf18	-6.0000	1.0000	no	18.0000	1.0000	no
Fgf2	-0.3703	0.9997	no	0.8802	1.0000	no
Fgf3	2.8168	1.0000	no	0.2973	0.8215	no
Fgf4	0.0000	1.0000	no	0.0000	1.0000	no
Fgf8	8.0000	1.0000	no	0.0000	1.0000	no

Fgf9	8.0000	1.0000	no	0.0000	1.0000	no
Fgfr1	1.6764	1.0000	no	3.4545	0.0119	yes
Fgfr3	1.4421	0.1013	no	1.6970	0.0431	yes
Fgfr4	3.7679	0.0005	yes	1.6611	0.2195	no
Fhdc1	1.1371	0.0029	yes	-0.9610	0.0006	yes
Fhl3	1.8448	0.0082	yes	2.1825	0.0001	yes
Fhod1	0.4079	0.9303	no	1.7417	0.0061	yes
Fhod3	-0.4220	0.9997	no	0.6563	1.0000	no
Fibcd1	8.0000	1.0000	no	18.0000	1.0000	no
Fign	-1.1713	1.0000	no	0.5376	1.0000	no
Filip1l	1.8140	0.1412	no	0.7458	0.4566	no
Fjx1	2.8898	0.0253	yes	2.3931	1.0000	no
Fkbp1b	1.6595	0.3119	no	2.5911	0.0103	yes
Fkbp5	0.1962	0.9997	no	1.8020	0.0011	yes
Fkbp9	0.5747	0.7772	no	1.6070	0.0500	no
Fli1	2.4666	0.0126	yes	1.8288	0.0268	yes
Flnc	0.9046	1.0000	no	1.5063	1.0000	no
Flt1	2.2184	0.0611	no	1.1344	0.1329	no
Flt3	2.4677	0.0032	yes	2.5867	0.0000	yes
Flt4	1.3876	0.3618	no	0.9383	0.3338	no
Fmnl1	2.6611	0.0000	yes	2.9821	0.0000	yes
Fmnl2	1.5884	0.0417	yes	1.1289	0.0611	no
Fmnl3	1.8767	0.0048	yes	1.6764	0.0002	yes
Fn1	2.4044	0.0000	yes	1.3974	0.0014	yes
Fnbp1	0.2701	0.9842	no	1.7435	0.0001	yes
Fnbp1l	1.1484	0.5280	no	1.4548	0.0952	no
Fndc3a	0.7277	0.3166	no	1.4720	0.0231	yes
Fndc3b	1.7151	0.1149	no	1.8449	0.0234	yes
Fndc4	2.3233	0.0054	yes	3.4144	0.0000	yes
Fndc5	1.4190	0.3881	no	0.9318	0.3497	no
Fndc8	0.2414	1.0000	no	0.9549	1.0000	no
Fosl1	0.2035	1.0000	no	1.5141	1.0000	no
Fosl2	2.7235	0.0161	yes	1.7721	0.0439	yes
Foxa1	2.1064	1.0000	no	1.2893	1.0000	no
Foxb1	0.0000	1.0000	no	0.0000	1.0000	no
Foxb2	0.0000	1.0000	no	0.0000	1.0000	no
Foxc1	8.0000	1.0000	no	18.0000	1.0000	no
Foxc2	-6.0000	1.0000	no	0.0000	1.0000	no
Foxd1	8.0000	1.0000	no	18.0000	1.0000	no
Foxd2	1.6850	1.0000	no	18.0000	1.0000	no
Foxd3	0.0000	1.0000	no	0.0000	1.0000	no
Foxd4	0.0000	1.0000	no	0.0000	1.0000	no
Foxe1	8.0000	1.0000	no	-12.0000	1.0000	no
Foxe3	0.0000	1.0000	no	0.0000	1.0000	no
Foxf1a	8.0000	1.0000	no	18.0000	1.0000	no
Foxf2	0.0000	1.0000	no	0.0000	1.0000	no
Foxg1	0.0000	1.0000	no	0.0000	1.0000	no
Foxi3	0.0000	1.0000	no	0.0000	1.0000	no
Foxj1	1.7263	1.0000	no	0.6135	1.0000	no
Foxl1	0.0000	1.0000	no	0.0000	1.0000	no
Foxl2	0.0000	1.0000	no	0.0000	1.0000	no
Foxl2os	0.0000	1.0000	no	0.0000	1.0000	no
Foxo1	0.6403	0.9558	no	2.3570	0.0059	yes
Foxo6	8.0000	1.0000	no	0.0000	1.0000	no
Foxp4	0.2062	0.9758	no	1.9211	0.0003	yes
Foxq1	8.0000	1.0000	no	18.0000	1.0000	no
Fras1	1.6098	1.0000	no	-0.7451	1.0000	no
Frem3	-2.1621	1.0000	no	-12.0000	1.0000	no

Frmd4a	0.8363	0.0005	yes	-0.5591	0.1022	no
Frmd5	0.5080	0.9712	no	0.9844	1.0000	no
Frmpd1	-0.5392	0.9997	no	1.0702	1.0000	no
Frs3	0.5636	0.9985	no	0.3004	1.0000	no
Frzb	8.0000	1.0000	no	-0.0475	1.0000	no
Fscn1	2.5962	0.0000	yes	1.5619	0.0019	yes
Fsd1l	0.1886	0.9997	no	1.1654	0.3189	no
Fst	1.5769	1.0000	no	1.9421	1.0000	no
Fstl4	0.0000	1.0000	no	0.0000	1.0000	no
Furin	1.8362	0.0002	yes	1.7415	0.0014	yes
Fzd1	2.1747	1.0000	no	-0.0099	1.0000	no
Fzd2	-6.0000	1.0000	no	1.8947	1.0000	no
Fzd3	-0.1572	1.0000	no	18.0000	0.0959	no
Fzd4	1.9947	1.0000	no	0.6686	1.0000	no
Fzd6	1.8315	0.1393	no	2.2990	0.0123	yes
Fzd8	1.3007	0.5354	no	2.5207	0.0080	yes
Fzd9	1.7934	1.0000	no	4.3743	1.0000	no
G530011O06Rik	0.6038	0.9971	no	0.4919	0.6797	no
G630025P09Rik	NA	NA	NA	NA	NA	NA
G6b	NA	NA	NA	NA	NA	NA
Gab1	-0.3651	0.7758	no	-0.0045	0.9960	no
Gabbr1	2.2689	0.0599	no	2.3071	0.0716	no
Gabbr2	-6.0000	1.0000	no	-0.0570	1.0000	no
Gabrb3	0.0000	1.0000	no	0.0000	1.0000	no
Gad1	0.0000	1.0000	no	0.0000	1.0000	no
Gad2	-1.1985	1.0000	no	-3.6398	1.0000	no
Gadd45b	2.8959	0.0241	yes	2.6836	0.0044	yes
Galnt12	3.3468	0.0062	yes	2.9104	0.0030	yes
Galnt3	2.8044	0.2811	no	2.7563	0.0220	yes
Galnt6	2.0290	0.0378	yes	1.3473	0.0509	no
Galntl1	8.0000	1.0000	no	0.0000	1.0000	no
Galr2	-0.5520	1.0000	no	2.2424	1.0000	no
Galr3	NA	NA	NA	NA	NA	NA
Gapdh	-0.1986	0.9637	no	0.8562	0.1583	no
Gas1	0.0940	1.0000	no	2.2975	1.0000	no
Gas6	2.7965	0.0147	yes	1.0357	0.2836	no
Gata2	2.2535	0.0013	yes	2.0430	0.0001	yes
Gata3	3.2781	0.0497	yes	4.2186	0.0257	yes
Gata4	1.5717	0.1285	no	0.1262	0.8918	no
Gata5	1.7700	1.0000	no	18.0000	1.0000	no
Gata6	1.7324	0.2544	no	1.0401	1.0000	no
Gbx1	2.0679	1.0000	no	18.0000	1.0000	no
Gbx2	4.1281	0.0013	yes	3.2604	1.0000	no
Gcgr	2.0446	0.0129	yes	0.8126	0.2218	no
Gcnt4	1.6986	1.0000	no	3.3227	1.0000	no
Gdf10	1.2859	1.0000	no	0.8628	1.0000	no
Gdf11	2.4184	1.0000	no	2.9519	1.0000	no
Gdf6	0.0000	1.0000	no	0.0000	1.0000	no
Gdf7	0.0000	1.0000	no	0.0000	1.0000	no
Gdnf	0.0000	1.0000	no	0.0000	1.0000	no
Gdpd5	0.3203	1.0000	no	0.7731	1.0000	no
Gfi1	2.8568	0.0000	yes	2.8741	0.0000	yes
Gfod1	1.4662	0.3099	no	1.6780	0.0563	no
Gfra1	1.5823	0.4105	no	1.7826	0.0790	no
Gfra3	0.0000	1.0000	no	0.0000	1.0000	no
Gfra4	0.0000	1.0000	no	2.3992	1.0000	no
Ggn	2.7161	1.0000	no	2.0529	1.0000	no
Ggt7	0.4089	0.9997	no	1.3398	1.0000	no

Gipc2	1.3412	0.3475	no	0.7879	0.4441	no
Gipc3	8.0000	1.0000	no	18.0000	1.0000	no
Gja3	0.0000	1.0000	no	0.0000	1.0000	no
Gjb2	-0.2928	0.9997	no	2.9885	0.0007	yes
Gjc1	8.0000	1.0000	no	18.0000	1.0000	no
Gjd3	0.0000	1.0000	no	0.0000	1.0000	no
Gkap1	1.2831	0.2114	no	3.3646	0.0000	yes
Gldc	2.0056	0.0144	yes	1.2631	0.0528	no
Gli1	-3.7740	1.0000	no	1.2532	1.0000	no
Gli3	-0.9276	1.0000	no	1.0196	1.0000	no
Glis1	-0.0107	0.9997	no	0.8309	1.0000	no
Glis2	2.5989	0.0382	yes	1.5098	0.1164	no
Glis3	1.6829	1.0000	no	3.7649	0.0098	yes
Gls2	1.4270	0.0045	yes	3.6538	0.0043	yes
Glt25d2	0.8518	1.0000	no	0.5499	1.0000	no
Gm10125	-0.3848	1.0000	no	0.5557	1.0000	no
Gm10190	0.0000	1.0000	no	0.0000	1.0000	no
Gm10345	0.4401	1.0000	no	0.3926	1.0000	no
Gm10406	8.0000	1.0000	no	18.0000	1.0000	no
Gm106	8.0000	1.0000	no	-0.0234	1.0000	no
Gm11190	0.0000	1.0000	no	0.0000	1.0000	no
Gm11529	0.0000	1.0000	no	0.0000	1.0000	no
Gm12824	8.0000	1.0000	no	18.0000	1.0000	no
Gm1337	3.9180	1.0000	no	2.7957	1.0000	no
Gm13889	-6.0000	1.0000	no	18.0000	1.0000	no
Gm14207	0.8807	1.0000	no	1.8452	1.0000	no
Gm1564	2.3978	1.0000	no	-2.3013	1.0000	no
Gm1568	8.0000	1.0000	no	18.0000	1.0000	no
Gm1673	1.4507	0.7035	no	0.7927	0.5215	no
Gm266	8.0000	1.0000	no	18.0000	1.0000	no
Gm2694	0.8671	1.0000	no	-0.6172	1.0000	no
Gm3230	NA	NA	NA	NA	NA	NA
Gm347	NA	NA	NA	NA	NA	NA
Gm4349	-0.4259	0.9997	no	0.9909	0.3256	no
Gm4980	-6.0000	1.0000	no	0.0000	1.0000	no
Gm5577	0.0871	0.9997	no	0.7750	0.4109	no
Gm581	NA	NA	NA	NA	NA	NA
Gm628	0.0000	1.0000	no	0.0000	1.0000	no
Gm6320	0.0000	1.0000	no	0.0000	1.0000	no
Gm6623	0.0000	1.0000	no	0.0000	1.0000	no
Gm6762	-0.8698	1.0000	no	0.1645	1.0000	no
Gm70	NA	NA	NA	NA	NA	NA
Gm7854	-6.0000	1.0000	no	18.0000	1.0000	no
Gm88	-0.1448	1.0000	no	-1.8602	1.0000	no
Gm8909	-4.2846	1.0000	no	2.3879	1.0000	no
Gm9880	NA	NA	NA	NA	NA	NA
Gm996	3.3685	1.0000	no	18.0000	1.0000	no
Gnai1	1.3395	1.0000	no	-0.3419	1.0000	no
Gnal	0.1653	0.9997	no	-1.2479	0.0807	no
Gnao1	-0.2796	1.0000	no	-0.1584	1.0000	no
Gnaq	1.5973	0.1334	no	2.0913	0.0088	yes
Gnas	-0.0298	0.9997	no	-0.1809	0.5450	no
Gnb4	-0.1719	0.9997	no	1.9766	0.0001	yes
Gng12	0.5833	0.3687	no	1.8623	0.0000	yes
Gng8	0.0000	1.0000	no	0.0000	1.0000	no
Gp1bb	1.5902	0.2444	no	0.2245	0.8351	no
Gp5	0.7013	0.9404	no	1.3602	0.1401	no
Gpc1	2.7434	0.0050	yes	2.5735	0.0011	yes

Gpr124		1.3749	0.4353	no		1.4170	0.1245	no
Gpr135		0.0558	1.0000	no		18.0000	1.0000	no
Gpr137c		0.0873	1.0000	no		-1.5963	1.0000	no
Gpr153		2.6975	1.0000	no		-0.9704	1.0000	no
Gpr156		0.0000	1.0000	no		0.0000	1.0000	no
Gpr160		2.0931	0.0049	yes		2.4611	0.0000	yes
Gpr162		8.0000	1.0000	no		1.5187	1.0000	no
Gpr176		0.6183	1.0000	no		18.0000	1.0000	no
Gpr25		8.0000	1.0000	no		0.0000	1.0000	no
Gpr27		8.0000	1.0000	no		18.0000	1.0000	no
Gpr3		8.0000	1.0000	no		0.0000	1.0000	no
Gpr4		2.1941	1.0000	no		1.4155	1.0000	no
Gpr45		0.0000	1.0000	no		0.0000	1.0000	no
Gpr6		0.0000	1.0000	no		0.0000	1.0000	no
Gpr62		8.0000	1.0000	no		0.0000	1.0000	no
Gpr88		0.0000	1.0000	no		18.0000	1.0000	no
Gpr98		3.9044	0.3786	no		1.2113	1.0000	no
Gprc5b		3.9329	1.0000	no		1.0579	1.0000	no
Gprc5c		1.5502	0.2028	no		1.1205	0.2133	no
Gprin1		8.0000	1.0000	no		18.0000	1.0000	no
Gpt2		0.6431	0.7822	no		1.8216	0.0039	yes
Gpx7		1.6300	1.0000	no		1.6008	0.1250	no
Grasp		3.2348	1.0000	no		2.3821	1.0000	no
Grb10		-0.0584	0.9997	no		1.0829	0.0032	yes
Greb1		3.2152	1.0000	no		2.1562	1.0000	no
Greb1l		0.5160	1.0000	no		0.3973	1.0000	no
Grhl1		0.3755	0.9971	no		-0.8204	0.2346	no
Grhl2		8.0000	1.0000	no		18.0000	1.0000	no
Grid1		1.0260	1.0000	no		-12.0000	1.0000	no
Grid2		0.0000	1.0000	no		0.0000	1.0000	no
Grik3		0.0000	1.0000	no		0.0000	1.0000	no
Grik4		3.5965	1.0000	no		0.2003	1.0000	no
Grin2c		8.0000	1.0000	no		18.0000	1.0000	no
Grin2d		1.9573	1.0000	no		-12.0000	1.0000	no
Grin3b		0.5474	0.9497	no		-0.7972	1.0000	no
Grip1		0.6912	1.0000	no		1.7205	1.0000	no
Grm8		8.0000	1.0000	no		0.0000	1.0000	no
Grwd1		-0.1244	0.9997	no		2.4230	0.0000	yes
Gsc		0.0000	1.0000	no		0.0000	1.0000	no
Gsc2		8.0000	1.0000	no		18.0000	1.0000	no
Gsg1l		1.6106	1.0000	no		0.9441	1.0000	no
Gstt3		1.4260	0.2615	no		2.2659	0.0124	yes
Gsx1		0.0000	1.0000	no		0.0000	1.0000	no
Gsx2		0.0000	1.0000	no		0.0000	1.0000	no
Gucy2e		8.0000	1.0000	no		18.0000	1.0000	no
Gxylt2		8.0000	1.0000	no		-12.0000	1.0000	no
H1f0		1.2117	0.0127	yes		1.8792	0.0086	yes
H1fx		2.1168	0.1235	no		2.0259	0.0323	yes
H2-Bl		0.3436	0.9997	no		1.5102	0.1403	no
H2-K1		0.5388	0.1972	no		1.5929	0.0000	yes
H2-Q10		2.2411	0.0010	yes		0.8336	0.2607	no
H2-Q6		0.8477	0.6669	no		1.8569	0.0145	yes
H2-Q7		1.9352	0.0090	yes		1.2614	0.0325	yes
H2-Q8	NA	NA		NA	NA	NA		NA
H2afy2		2.9113	0.0041	yes		2.6767	0.0048	yes
Hand1		0.0000	1.0000	no		18.0000	1.0000	no
Hand2		1.5263	1.0000	no		0.3415	1.0000	no
Hap1		2.1317	1.0000	no		1.1038	1.0000	no

Hapln4	0.0659	1.0000	no	18.0000	1.0000	no
Has3	-0.2533	0.9997	no	0.9265	0.2980	no
Hbegf	0.4267	1.0000	no	1.8204	0.0712	no
Hcn2	1.9478	0.0527	no	3.0355	0.0109	yes
Hcn3	-0.2907	0.8484	no	-0.5800	0.4643	no
Hcn4	0.0000	1.0000	no	18.0000	1.0000	no
Hcrtr1	-6.0000	1.0000	no	0.0000	1.0000	no
Hdac5	0.6630	0.0282	yes	0.2712	0.3876	no
Hdgfrp3	3.0959	0.0024	yes	2.2861	0.0054	yes
Hectd2	2.3139	0.0067	yes	0.6875	1.0000	no
Hecw2	0.1726	1.0000	no	3.7687	0.0024	yes
Hes1	2.0193	0.0982	no	0.8145	0.4120	no
Hes2	-6.0000	1.0000	no	18.0000	1.0000	no
Hes5	-1.5552	1.0000	no	18.0000	1.0000	no
Hes7	0.0573	1.0000	no	0.9209	1.0000	no
Hey1	0.3264	1.0000	no	-0.0183	1.0000	no
Hey2	3.8556	1.0000	no	-0.0496	0.9707	no
Heyl	2.8413	1.0000	no	18.0000	1.0000	no
Hhex	1.4071	0.1037	no	1.6008	0.0103	yes
Hic1	1.9398	1.0000	no	1.5057	1.0000	no
Hip1r	0.3744	0.8500	no	1.8619	0.0001	yes
Hivep2	2.2428	1.0000	no	0.5462	1.0000	no
Hivep3	1.7742	0.4474	no	1.8628	0.0834	no
Hlx	1.8789	0.1659	no	2.5491	0.0054	yes
Hmga2	2.4101	0.0004	yes	2.6082	0.0003	yes
Hmox1	1.5360	0.0000	yes	0.4458	0.3295	no
Hmx1	0.0000	1.0000	no	0.0000	1.0000	no
Hmx2	0.0000	1.0000	no	18.0000	1.0000	no
Hmx3	0.0000	1.0000	no	0.0000	1.0000	no
Hnf1b	1.6167	1.0000	no	2.2791	1.0000	no
Homer2	0.6837	0.5634	no	1.1800	0.1652	no
Homer3	0.1550	0.9997	no	1.1183	0.0175	yes
Hopx	0.9217	0.8245	no	3.5247	0.0028	yes
Hoxa10	8.0000	1.0000	no	0.2655	1.0000	no
Hoxa11	0.0000	1.0000	no	0.0000	1.0000	no
Hoxa11as	0.0000	1.0000	no	0.0000	1.0000	no
Hoxa13	0.0000	1.0000	no	0.0000	1.0000	no
Hoxa2	0.1766	1.0000	no	18.0000	1.0000	no
Hoxa3	0.0000	1.0000	no	0.0000	1.0000	no
Hoxa4	2.4780	1.0000	no	0.4354	1.0000	no
Hoxa5	2.8105	1.0000	no	2.6323	1.0000	no
Hoxa6	8.0000	1.0000	no	18.0000	1.0000	no
Hoxa7	8.0000	1.0000	no	2.9994	0.2412	no
Hoxa9	1.7187	0.6282	no	2.9284	0.0311	yes
Hoxb13	8.0000	1.0000	no	0.0000	1.0000	no
Hoxb4	2.0444	1.0000	no	1.4615	1.0000	no
Hoxb6	8.0000	1.0000	no	0.0000	1.0000	no
Hoxb7	8.0000	1.0000	no	0.0000	1.0000	no
Hoxb8	0.0000	1.0000	no	0.0000	1.0000	no
Hoxb9	0.0000	1.0000	no	18.0000	1.0000	no
Hoxc10	0.0000	1.0000	no	0.0000	1.0000	no
Hoxc12	0.0000	1.0000	no	0.0000	1.0000	no
Hoxc13	0.0000	1.0000	no	0.0000	1.0000	no
Hoxc5	0.0000	1.0000	no	18.0000	1.0000	no
Hoxc6	0.0148	1.0000	no	0.0000	1.0000	no
Hoxc8	0.0000	1.0000	no	0.0000	1.0000	no
Hoxc9	0.0000	1.0000	no	0.0000	1.0000	no
Hoxd1	0.0000	1.0000	no	0.0000	1.0000	no

Hoxd10	0.0000	1.0000	no	0.0000	1.0000	no
Hoxd11	0.0000	1.0000	no	0.0000	1.0000	no
Hoxd13	0.0000	1.0000	no	0.0000	1.0000	no
Hoxd8	0.0000	1.0000	no	0.0000	1.0000	no
Hoxd9	0.0000	1.0000	no	0.0000	1.0000	no
Hpca	8.0000	1.0000	no	-0.6571	1.0000	no
Hpcal4	0.0000	1.0000	no	0.0000	1.0000	no
Hpdl	0.2382	0.9997	no	3.3819	0.0171	yes
Hr	0.0078	1.0000	no	1.6531	1.0000	no
Hrh3	0.0000	1.0000	no	0.0000	1.0000	no
Hrk	0.0000	1.0000	no	0.0000	1.0000	no
Hs3st3b1	2.6672	0.0100	yes	1.2946	0.1619	no
Hs3st6	0.0000	1.0000	no	-12.0000	1.0000	no
Hs6st3	0.0000	1.0000	no	18.0000	1.0000	no
Hsd11b2	-0.0909	0.9997	no	1.0885	1.0000	no
Hsd17b1	3.4726	1.0000	no	2.8499	0.0192	yes
Hsf4	8.0000	1.0000	no	18.0000	1.0000	no
Hsf5	-6.0000	1.0000	no	-12.0000	1.0000	no
Hspa1a	1.8942	0.1157	no	2.7033	0.0014	yes
Hspa1b	1.8999	0.0497	yes	2.9063	0.0000	yes
Hspa1l	0.0161	0.9997	no	0.7307	0.4840	no
Hspa2	0.3270	0.9997	no	2.1165	0.0171	yes
Hspb1	8.0000	1.0000	no	18.0000	1.0000	no
Htr1d	0.0000	1.0000	no	0.0000	1.0000	no
Htr6	-6.0000	1.0000	no	0.0000	1.0000	no
Htr7	8.0000	1.0000	no	0.0000	1.0000	no
Htra1	0.0000	1.0000	no	-12.0000	1.0000	no
Htra4	-6.0000	1.0000	no	0.0000	1.0000	no
Hunk	1.4707	1.0000	no	1.3300	1.0000	no
Ica1	1.8396	0.0226	yes	1.3867	0.0081	yes
Ica1l	-0.1905	0.9997	no	4.0501	1.0000	no
Icam1	1.9076	0.0856	no	1.1201	0.2145	no
Icam5	0.4960	0.9997	no	-0.3747	0.7467	no
Id1	0.8523	0.6906	no	1.2047	0.1501	no
Id2	2.2498	0.0115	yes	1.4370	0.0692	no
Id3	2.2034	0.0274	yes	1.6559	0.0318	yes
Id4	8.0000	1.0000	no	0.0000	1.0000	no
Ier5l	1.2996	1.0000	no	1.8668	1.0000	no
Iffo2	1.5582	0.0753	no	0.8216	1.0000	no
Igdcc3	8.0000	1.0000	no	18.0000	1.0000	no
Igdcc4	2.0365	0.0679	no	1.3932	0.1157	no
Igf2	2.2370	0.0000	yes	1.1456	0.0001	yes
Igf2as	1.3007	0.9682	no	1.6302	0.1353	no
Igf2bp2	2.0663	0.0002	yes	3.0246	0.0000	yes
Igfbp2	2.5640	1.0000	no	-0.0377	1.0000	no
Igfbp4	2.2986	0.0000	yes	1.8797	0.0000	yes
Igfbp5	0.9743	1.0000	no	0.4923	1.0000	no
Igfbp6	8.0000	1.0000	no	1.9305	1.0000	no
Igfbp7	2.3103	0.0094	yes	0.8022	0.4515	no
Igsf11	8.0000	1.0000	no	18.0000	1.0000	no
Igsf9	0.1586	1.0000	no	2.7604	0.4515	no
Ihh	1.5857	1.0000	no	0.1548	1.0000	no
Ikzf3	0.3518	1.0000	no	2.7863	1.0000	no
Il11	0.2673	1.0000	no	0.0000	1.0000	no
Il17d	0.1355	1.0000	no	-0.2507	1.0000	no
Il17ra	0.4624	0.7883	no	1.0534	0.1627	no
Il17rd	0.8739	1.0000	no	-1.4400	1.0000	no
Il20ra	3.1992	1.0000	no	3.4704	1.0000	no

Il28ra	8.0000	1.0000	no	18.0000	1.0000	no
Il6ra	1.7809	0.1383	no	1.7342	0.0362	yes
Il6st	1.7451	0.1358	no	1.4661	0.0980	no
Ildr2	8.0000	1.0000	no	-12.0000	1.0000	no
Impdh1	0.1968	0.9997	no	2.7946	0.0000	yes
Ina	0.0590	1.0000	no	18.0000	1.0000	no
Inadl	0.6413	0.8874	no	1.2472	0.3140	no
Inf2	1.0044	0.2467	no	1.9518	0.0009	yes
Inhbb	1.6591	1.0000	no	0.7098	1.0000	no
Inppl1	1.7884	0.0390	yes	1.7313	0.0148	yes
Insl3	1.9400	0.7855	no	1.1422	0.4913	no
Insm1	0.0000	1.0000	no	0.0000	1.0000	no
Insm2	0.0000	1.0000	no	18.0000	1.0000	no
Insrr	0.0000	1.0000	no	0.0000	1.0000	no
Iqsec3	0.0000	1.0000	no	0.0000	1.0000	no
Irak3	2.0847	0.0016	yes	2.0928	0.0000	yes
Irf1	1.8716	0.0006	yes	1.4648	0.0106	yes
Irf5	-0.0612	0.9997	no	0.7485	0.2714	no
Irf6	3.0379	0.0587	no	1.8511	0.2414	no
Irs1	1.2480	1.0000	no	0.7931	1.0000	no
Irx2	8.0000	1.0000	no	0.0000	1.0000	no
Irx3	8.0000	1.0000	no	18.0000	1.0000	no
Irx4	8.0000	1.0000	no	0.0000	1.0000	no
Irx5	0.0000	1.0000	no	-0.0547	1.0000	no
Isl2	0.0000	1.0000	no	0.0000	1.0000	no
Islr2	-2.1876	1.0000	no	2.1534	1.0000	no
Ism1	0.0000	1.0000	no	18.0000	1.0000	no
Itga1	2.1640	0.0775	no	0.9202	0.3431	no
Itga3	-0.0786	0.9997	no	1.7512	1.0000	no
Itga5	0.7481	0.3535	no	2.1033	0.0042	yes
Itga6	0.8993	0.1798	no	1.7869	0.0001	yes
Itga9	1.5118	0.0228	yes	1.8398	0.0003	yes
Itgav	1.5785	0.0671	no	1.6244	0.0093	yes
Itgb4	3.0298	1.0000	no	0.7211	1.0000	no
Itgb5	1.5012	0.0602	no	1.1410	0.0505	no
Itpka	1.3578	0.4784	no	1.1196	0.2620	no
Itpr2	0.2650	0.9997	no	0.7596	0.3224	no
Itpr3	2.0819	0.0495	yes	2.1198	0.0091	yes
Itpripl2	2.0800	0.1132	no	1.5587	0.0993	no
Itsn1	1.6470	0.0000	yes	-0.7557	0.0162	yes
Jag1	1.0431	1.0000	no	1.7284	1.0000	no
Jag2	1.5450	1.0000	no	4.5636	0.0008	yes
Jakmip3	-6.0000	1.0000	no	18.0000	1.0000	no
Jazf1	8.0000	1.0000	no	1.3234	1.0000	no
Jdp2	2.6522	0.0245	yes	1.7619	0.0190	yes
Jmjd1c	-0.4714	0.2138	no	1.2575	0.0007	yes
Jph1	2.6431	1.0000	no	18.0000	1.0000	no
Jph3	0.6257	1.0000	no	18.0000	1.0000	no
Jph4	8.0000	1.0000	no	18.0000	1.0000	no
Jub	1.3260	0.5149	no	0.9259	0.3580	no
Jun	2.4242	0.0002	yes	2.5048	0.0000	yes
Kank1	1.1448	0.2735	no	1.0696	0.0960	no
Kank4	8.0000	1.0000	no	0.0000	1.0000	no
Kazald1	0.4670	1.0000	no	0.2549	1.0000	no
Kbtbd13	0.0000	1.0000	no	18.0000	1.0000	no
Kcna3	3.0789	1.0000	no	2.5677	1.0000	no
Kcna7	8.0000	1.0000	no	0.0000	1.0000	no
Kcnb1	8.0000	1.0000	no	18.0000	1.0000	no

Kcnc1	0.0000	1.0000	no	2.3765	1.0000	no
Kcnc3	3.0919	1.0000	no	18.0000	1.0000	no
Kcnc4	0.0000	1.0000	no	0.0000	1.0000	no
Kcnd3	0.0115	1.0000	no	-12.0000	1.0000	no
Kcng2	1.0178	0.7858	no	4.6252	0.0145	yes
Kcng3	8.0000	1.0000	no	18.0000	1.0000	no
Kcnh2	6.0356	0.0035	yes	1.3807	1.0000	no
Kcnh3	2.8024	1.0000	no	2.8996	1.0000	no
Kcnh4	0.0257	1.0000	no	18.0000	1.0000	no
Kcnip2	-0.3117	0.9727	no	-1.2285	0.0300	yes
Kcnip3	1.8240	1.0000	no	2.1920	1.0000	no
Kcnj2	2.5021	1.0000	no	2.4636	1.0000	no
Kcnj4	0.0000	1.0000	no	0.0000	1.0000	no
Kcnk12	5.1330	0.0161	yes	2.4416	0.0110	yes
Kcnk13	1.5043	1.0000	no	0.9338	1.0000	no
Kcnk3	8.0000	1.0000	no	0.0000	1.0000	no
Kcnk4	8.0000	1.0000	no	-0.0649	1.0000	no
Kcnk6	1.6538	0.1313	no	0.9103	0.3402	no
Kcnk9	0.0000	1.0000	no	0.0000	1.0000	no
Kcnma1	0.0000	1.0000	no	0.0000	1.0000	no
Kcnmb4	1.7573	0.1966	no	0.7230	0.7185	no
Kcnq1	0.0117	1.0000	no	18.0000	1.0000	no
Kcnq2	-1.1785	0.5002	no	-0.1830	1.0000	no
Kcnq4	0.3684	1.0000	no	18.0000	1.0000	no
Kcnq5	0.9319	1.0000	no	3.5543	1.0000	no
Kcns3	0.1111	1.0000	no	-12.0000	1.0000	no
Kcnt1	0.0000	1.0000	no	0.0000	1.0000	no
Kcp	5.0391	0.0000	yes	2.1191	0.0960	no
Kctd1	1.9679	0.0116	yes	3.4217	0.0001	yes
Kctd12	2.1166	0.0243	yes	1.3105	0.1052	no
Kctd17	2.4995	0.0094	yes	1.1316	0.1221	no
Kdelc2	1.7708	0.2158	no	1.8636	0.0379	yes
Kdelr3	3.2233	0.0223	yes	2.4470	0.0277	yes
Kdr	2.0588	0.0301	yes	0.5848	0.5314	no
Kif13a	-0.0240	0.9997	no	2.3497	0.0000	yes
Kif17	2.6664	1.0000	no	1.5078	1.0000	no
Kif1b	0.7713	0.2035	no	1.6513	0.0001	yes
Kif1c	0.9179	0.1197	no	1.3999	0.0101	yes
Kif21a	0.5088	0.7366	no	2.3102	0.0000	yes
Kif26a	0.9568	1.0000	no	0.8211	1.0000	no
Kif26b	0.0233	1.0000	no	0.0000	1.0000	no
Kif3c	-0.1158	0.9997	no	0.2295	0.8058	no
Kif5a	8.0000	1.0000	no	18.0000	1.0000	no
Kif5c	-2.0920	0.6578	no	0.0658	1.0000	no
Kifc3	2.1954	0.0039	yes	1.3509	0.0265	yes
Klc2	0.2609	0.9965	no	2.0543	0.0003	yes
Klf14	0.0000	1.0000	no	0.0000	1.0000	no
Klf2	1.9751	0.1519	no	1.3569	0.1536	no
Klf4	2.7754	0.2247	no	1.4613	0.1413	no
Klf5	1.5445	0.2976	no	2.2069	0.0137	yes
Klhdc8a	1.0511	1.0000	no	0.0000	1.0000	no
Klhl14	8.0000	1.0000	no	-12.0000	1.0000	no
Klhl2	-0.1164	0.9997	no	1.3868	0.1143	no
Klhl21	-0.0559	0.9997	no	0.4385	0.6358	no
Klhl22	-0.1817	0.9997	no	1.3898	0.0066	yes
Klhl29	8.0000	1.0000	no	0.0000	1.0000	no
Klhl35	8.0000	1.0000	no	18.0000	1.0000	no
Klhl8	0.4580	0.9997	no	1.2320	0.1291	no

Klrg2		2.3037	1.0000	no		18.0000	1.0000	no
Kras		0.0562	0.9997	no		0.0197	0.9707	no
Kremen1		-0.1669	0.9997	no		2.3073	0.0069	yes
Kremen2		8.0000	1.0000	no		18.0000	1.0000	no
Ksr2		8.0000	1.0000	no		0.7071	1.0000	no
L3mbtl	NA	NA		NA	NA	NA		NA
L3mbtl3		0.4221	0.9441	no		2.0054	0.0008	yes
Lad1		0.0000	1.0000	no		0.0000	1.0000	no
Lama5		3.2049	0.0489	yes		2.7342	0.0556	no
Lamc1		0.6382	0.3739	no		2.5036	0.0000	yes
Laptm4b		2.5452	0.0225	yes		1.4007	0.1296	no
Lass1		8.0000	1.0000	no		18.0000	1.0000	no
Lass6		2.2677	0.0121	yes		2.2563	0.0010	yes
Lats2		0.2104	0.9997	no		0.6474	0.3201	no
Lbx1		0.0000	1.0000	no		0.0000	1.0000	no
Lbx2		8.0000	1.0000	no		18.0000	1.0000	no
Ldlrad3		1.7688	0.1416	no		2.4817	0.0007	yes
Lef1		1.9972	1.0000	no		1.5785	1.0000	no
Lemd1		0.0000	1.0000	no		0.0000	1.0000	no
Lepre1		0.4017	0.8177	no		1.7481	0.0001	yes
Leprel2		2.3022	0.0449	yes		0.2445	1.0000	no
Leprel4		1.9040	0.6563	no		-0.1543	0.9313	no
Lgi2		3.5263	1.0000	no		5.4051	1.0000	no
Lgi3		0.0000	1.0000	no		18.0000	1.0000	no
Lgr4		0.3051	0.9997	no		0.5440	0.3729	no
Lgr6		0.0000	1.0000	no		0.0000	1.0000	no
Lhfp		1.1214	1.0000	no		0.3696	1.0000	no
Lhfpl2		-0.6177	0.7911	no		1.7362	0.0337	yes
Lhfpl3		0.0000	1.0000	no		0.0000	1.0000	no
Lhx1		8.0000	1.0000	no		3.3453	1.0000	no
Lhx2		2.2236	0.4788	no		2.1441	1.0000	no
Lhx3		-6.0000	1.0000	no		0.0000	1.0000	no
Lhx4		0.0000	1.0000	no		0.0000	1.0000	no
Lhx6		1.5525	1.0000	no		0.2669	1.0000	no
Lhx8		0.0000	1.0000	no		0.0000	1.0000	no
Lhx9		8.0000	1.0000	no		0.0000	1.0000	no
Lif		8.0000	1.0000	no		4.6341	1.0000	no
Lifr		2.3830	0.0002	yes		0.6510	0.2745	no
Limd2		2.5496	0.0000	yes		2.0365	0.0000	yes
Lingo3		3.2249	1.0000	no		18.0000	1.0000	no
Lipg		8.0000	1.0000	no		-12.0000	1.0000	no
Lix1l		1.0188	0.7404	no		1.8089	0.0474	yes
Lmo7		0.5351	0.9997	no		2.1297	0.0070	yes
Lmtk3		1.1762	1.0000	no		18.0000	1.0000	no
Lmx1a		5.2270	1.0000	no		2.3022	0.0105	yes
Lmx1b		0.0000	1.0000	no		0.0000	1.0000	no
LOC100034739	NA	NA		NA	NA	NA		NA
LOC100045653	NA	NA		NA	NA	NA		NA
Lor		0.0000	1.0000	no		0.0000	1.0000	no
Loxl2		1.6126	0.2195	no		1.6555	0.0590	no
Lpar1		1.1580	1.0000	no		-1.1071	1.0000	no
Lpar3		0.0000	1.0000	no		0.0000	1.0000	no
Lpgat1		1.8791	0.0014	yes		2.2627	0.0007	yes
Lphn1		0.3531	0.9476	no		2.0304	0.0004	yes
Lpp		1.5675	1.0000	no		0.9052	1.0000	no
Lrfn1		0.8135	1.0000	no		1.5702	0.0890	no
Lrfn4		0.3770	0.9871	no		1.8796	0.0059	yes
Lrig1		0.2348	0.9997	no		0.1290	0.9091	no

Lrp11		1.0115	0.6751	no		2.7959	0.0748	no
Lrp2		0.0000	1.0000	no		18.0000	1.0000	no
Lrp3		1.2259	1.0000	no		2.1011	1.0000	no
Lrp4		1.6661	1.0000	no		2.8345	1.0000	no
Lrp5		0.8475	0.1786	no		2.3562	0.0000	yes
Lrp6		-0.0072	0.9997	no		0.9507	0.2086	no
Lrrc1		-0.6109	0.6618	no		0.9064	0.1415	no
Lrrc10b		2.0844	1.0000	no		18.0000	1.0000	no
Lrrc15		8.0000	1.0000	no		18.0000	1.0000	no
Lrrc16a		3.1868	0.0220	yes		1.5756	0.0389	yes
Lrrc26		0.0000	1.0000	no		0.0000	1.0000	no
Lrrc4		1.9855	1.0000	no		0.3726	1.0000	no
Lrrc4b		-6.0000	1.0000	no		0.0000	1.0000	no
Lrrc8d		-0.0041	0.9997	no		1.0087	0.0492	yes
Lrrk1		0.3337	0.9552	no		2.4673	0.0000	yes
Lrrn2		0.0000	1.0000	no		18.0000	1.0000	no
Ltb4r2		8.0000	1.0000	no		-0.1056	1.0000	no
Ltbp2		1.2211	0.6823	no		-0.6558	0.4423	no
Ltbp3		1.4770	1.0000	no		0.5763	1.0000	no
Ltbp4		1.3028	0.5461	no		0.4723	0.7057	no
Ltk		2.9027	1.0000	no		2.2761	1.0000	no
Luzp1		1.5276	0.0029	yes		1.8029	0.0324	yes
Ly6g6c		0.0000	1.0000	no		0.0079	1.0000	no
Ly6h		0.0000	1.0000	no		18.0000	1.0000	no
Lypd6b		-6.0000	1.0000	no		18.0000	1.0000	no
Lysmd2		1.9275	0.1548	no		2.0034	0.0433	yes
Mab21l2		0.0000	1.0000	no		18.0000	1.0000	no
Madd		0.4382	0.6664	no		0.5633	0.0979	no
Maf		1.5903	0.0376	yes		0.4067	0.5941	no
Mafa		0.0000	1.0000	no		0.0000	1.0000	no
Mafb		1.5612	0.3158	no		0.3987	0.7281	no
Maff		2.0633	0.0682	no		2.2718	0.0348	yes
Magi3		0.5125	0.8853	no		1.1003	0.0753	no
Man1c1		1.9470	0.0002	yes		1.5974	0.0008	yes
Man2a2		1.1728	0.2427	no		2.4321	0.0002	yes
Maneal		0.0000	1.0000	no		0.0000	1.0000	no
Map3k10		-0.0612	0.9997	no		1.2840	0.0284	yes
Map3k3		0.3841	0.7732	no		1.1817	0.0020	yes
Map3k5		0.6984	0.7372	no		2.4499	0.0047	yes
Map3k9		4.3403	1.0000	no		2.2142	1.0000	no
Map4k3		0.8681	0.8177	no		1.3995	0.1274	no
Map4k4		0.9985	0.0113	yes		1.8096	0.0000	yes
Map6d1		2.6189	1.0000	no		-0.0310	1.0000	no
Mapk11		3.9676	1.0000	no		3.9151	1.0000	no
Mapk12		1.7732	1.0000	no		0.9735	1.0000	no
Mapk13		3.1904	0.0023	yes		2.6514	0.0012	yes
Mapk4		8.0000	1.0000	no		-0.3361	1.0000	no
Mapk8ip1		2.3983	1.0000	no		2.2217	1.0000	no
Mapkapk2		0.3383	0.9127	no		1.6366	0.0176	yes
Mapre3		1.6325	0.6342	no		0.5777	1.0000	no
Mapt		0.0403	0.9997	no		1.2274	1.0000	no
Mar11	NA	NA		NA	NA	NA		NA
Mar9	NA	NA		NA	NA	NA		NA
Marcks		1.6610	0.0426	yes		0.4258	0.6373	no
Marcksl1		0.3178	0.9845	no		1.9652	0.0080	yes
Mark1		4.2079	1.0000	no		2.4623	1.0000	no
Marveld1		1.4763	0.3119	no		2.1740	0.0108	yes
Mast1		0.6742	0.9308	no		0.5504	0.5830	no

Mast4	0.0813	0.9997	no	1.6939	0.1253	no
Mboat2	0.7789	0.3491	no	0.3575	0.5238	no
Mcam	0.8178	0.8671	no	0.7611	0.4114	no
Mcc	1.7466	1.0000	no	1.0144	1.0000	no
Mcmbp	-0.1250	0.9997	no	1.1286	0.0006	yes
Mctp1	2.0573	0.0059	yes	2.1843	0.0000	yes
Mdga1	0.3623	0.9682	no	-0.1925	0.7033	no
Mecom	0.5878	1.0000	no	1.3030	1.0000	no
Med12l	1.9852	1.0000	no	2.0495	1.0000	no
Megf10	8.0000	1.0000	no	18.0000	1.0000	no
Megf11	1.5117	1.0000	no	0.9122	1.0000	no
Megf6	-0.1494	1.0000	no	-1.3665	1.0000	no
Megf8	0.6359	0.5150	no	2.6760	0.0000	yes
Mei1	0.0000	1.0000	no	0.0000	1.0000	no
Meis1	2.0751	0.0025	yes	1.9384	0.0002	yes
Meis2	1.9362	0.4541	no	-0.7180	0.7059	no
Mesp1	0.0000	1.0000	no	0.0000	1.0000	no
Mest	1.4148	0.0073	yes	0.6448	0.3245	no
Metrnl	0.9767	0.8113	no	-0.0303	1.0000	no
Mettl1	0.1642	0.9997	no	2.6698	0.0000	yes
Mex3b	0.1712	0.9997	no	2.0258	0.0305	yes
Mfap3l	2.8110	1.0000	no	1.9443	1.0000	no
Mfhas1	1.4025	0.0058	yes	0.4854	0.4675	no
Mfsd4	-0.0098	0.9997	no	0.2452	0.7563	no
Mfsd6	1.9146	0.0535	no	1.5500	0.0343	yes
Mgat3	2.0199	1.0000	no	0.9431	1.0000	no
Mgat5b	0.0000	1.0000	no	0.0000	1.0000	no
Miat	8.0000	1.0000	no	18.0000	1.0000	no
Micall1	0.3269	0.9997	no	2.5256	0.0020	yes
Mier3	0.0000	1.0000	no	-0.0918	0.9091	no
Mir10b	0.0000	1.0000	no	0.0000	1.0000	no
Mir1199	0.0000	1.0000	no	0.0000	1.0000	no
Mir1247	0.0000	1.0000	no	0.0000	1.0000	no
Mir124a-1	2.3298299999999	1.0000	no	2.3361600000000	1.0000	no
Mir124a-3	0.0000	1.0000	no	0.0000	1.0000	no
Mir132	0.0000	1.0000	no	0.0000	1.0000	no
Mir152	0.0000	1.0000	no	0.0000	1.0000	no
Mir1900	2.3298399999999	1.0000	no	2.3360499999999	1.0000	no
Mir1901	0.0000	1.0000	no	0.0000	1.0000	no
Mir193	0.0000	1.0000	no	0.0000	1.0000	no
Mir196b	2.3298100000000	1.0000	no	2.33614e-310	1.0000	no
Mir212	0.0000	1.0000	no	0.0000	1.0000	no
Mir3078	2.3298299999999	1.0000	no	2.3361600000000	1.0000	no
Mir3093	0.0000	1.0000	no	0.0000	1.0000	no
Mir34b	0.0000	1.0000	no	0.0000	1.0000	no
Mir34c	0.0000	1.0000	no	0.0000	1.0000	no
Mir449c	0.0000	1.0000	no	0.0000	1.0000	no
Mir574	0.0000	1.0000	no	0.0000	1.0000	no
Mir615	0.0000	1.0000	no	0.0000	1.0000	no
Mir9-1	NA	NA	NA	NA	NA	NA
Mir9-3	0.0000	1.0000	no	0.0000	1.0000	no
Mir92b	0.0000	1.0000	no	0.0000	1.0000	no
Mixl1	0.0546	1.0000	no	-0.0370	1.0000	no
Mkx	4.4096	1.0000	no	0.2147	1.0000	no
Mllt4	1.4328	0.1400	no	0.5484	0.6489	no
Mllt6	1.0564	0.5690	no	1.1546	0.2426	no
Mmp11	8.0000	1.0000	no	3.0659	1.0000	no
Mmp14	1.5684	0.1306	no	1.4231	0.1032	no

Mmp15	2.0554	1.0000	no	0.6429	1.0000	no
Mmp17	2.0159	0.0850	no	3.3456	0.0006	yes
Mmp23	3.5359	1.0000	no	0.7712	1.0000	no
Mmp24	-0.2255	0.9997	no	1.2490	1.0000	no
Mmp25	8.0000	1.0000	no	3.3370	1.0000	no
Mmp28	2.6691	0.2398	no	2.5490	0.0035	yes
Mms19	0.1306	0.9997	no	0.7180	0.0098	yes
Mn1	3.4413	1.0000	no	1.8245	1.0000	no
Mnx1	0.0000	1.0000	no	0.0000	1.0000	no
Mocos	1.9651	1.0000	no	2.1720	0.0216	yes
Mos	0.0454	1.0000	no	-12.0000	1.0000	no
Moxd1	8.0000	1.0000	no	0.0000	1.0000	no
Mpp3	2.3471	1.0000	no	3.7823	1.0000	no
Mpp6	0.0669	0.9997	no	1.9214	0.0000	yes
Mpped2	0.9596	0.6451	no	2.1554	0.2192	no
Mras	0.1553	0.9997	no	3.3947	0.0874	no
Mrc2	-2.1255	1.0000	no	-2.1136	1.0000	no
Mreg	1.4900	0.4068	no	1.9953	0.0389	yes
Msi1	0.1710	1.0000	no	-0.4873	0.7739	no
Msrb3	1.5326	1.0000	no	0.5643	0.6609	no
Msx1	0.0000	1.0000	no	0.0000	1.0000	no
Msx3	0.0000	1.0000	no	0.0000	1.0000	no
Mtag2	0.0000	1.0000	no	0.0000	1.0000	no
Mtap1a	1.1574	1.0000	no	1.9600	1.0000	no
Mtap1b	1.1832	1.0000	no	-0.2649	1.0000	no
Mtap6	0.0000	1.0000	no	18.0000	1.0000	no
Mtap7	-0.2904	0.9997	no	2.2931	0.0003	yes
Mtap7d2	0.4136	1.0000	no	18.0000	1.0000	no
Mtmr7	-0.1102	1.0000	no	0.8764	1.0000	no
Mtss1l	1.1986	0.4610	no	1.9321	0.0117	yes
Mtus1	3.0887	0.0004	yes	2.3425	0.0000	yes
Mtus2	-1.4361	0.4790	no	2.2432	1.0000	no
Muc1	0.0000	1.0000	no	-3.4962	1.0000	no
Mxra7	0.0345	1.0000	no	-0.4530	1.0000	no
Myb	-0.0954	0.9997	no	2.6736	0.0000	yes
Mybl1	0.3759	0.9997	no	-1.1718	0.0709	no
Mycl1	2.3617	1.0000	no	18.0000	1.0000	no
Mycn	2.0476	0.2823	no	2.4598	0.0104	yes
Myo10	0.8315	0.6236	no	1.5239	0.0405	yes
Myo1b	1.9660	0.0596	no	0.4415	0.6428	no
Myo1e	2.6188	0.0249	yes	2.9649	0.0009	yes
Myo5a	1.4650	0.0001	yes	2.1515	0.0000	yes
Myo5b	0.7883	0.6838	no	0.5256	0.5733	no
Mypop	0.7261	1.0000	no	2.5957	1.0000	no
Myrip	-6.0000	1.0000	no	18.0000	1.0000	no
Myst4	-0.1364	0.9997	no	0.0436	0.9699	no
N28178	2.0425	1.0000	no	-0.3571	1.0000	no
N4bp3	1.4095	0.4537	no	1.5619	0.1059	no
Nab1	0.4294	0.8339	no	1.8557	0.0001	yes
Nab2	2.0422	0.3451	no	1.6871	0.1663	no
Nacad	0.6183	0.9637	no	-1.2668	0.0844	no
Nacc2	0.1944	0.9997	no	1.3290	0.1598	no
Nags	0.3963	0.8177	no	2.2552	0.0000	yes
Nanos1	0.9847	0.5923	no	-0.2424	0.8342	no
Nat8l	3.3095	1.0000	no	2.3921	0.0079	yes
Nav1	1.5169	1.0000	no	1.9387	1.0000	no
Nav2	1.8182	1.0000	no	2.1765	1.0000	no
Nbea	1.2596	0.1552	no	2.4026	0.0001	yes

Nbl1		-0.0210	1.0000	no		-0.6259	1.0000	no
Ncald		2.2931	0.1954	no		1.0466	1.0000	no
Ncoa1		0.8566	0.6098	no		1.7930	0.0374	yes
Ncoa2		-0.2707	0.9284	no		0.4733	0.3047	no
Ncoa3		0.7760	0.1493	no		1.6321	0.0006	yes
Ncs1		1.4340	0.5468	no		2.6484	0.0036	yes
Ndrg1		2.3894	0.0003	yes		1.1511	0.0304	yes
Necab2		-1.3254	1.0000	no		18.0000	1.0000	no
Nedd4l		0.5419	0.8219	no		2.0146	0.0026	yes
Nefh		1.3646	0.1719	no		4.0218	1.0000	no
Nefm		0.0000	1.0000	no		0.0000	1.0000	no
Nek6		0.2016	0.9997	no		1.6657	0.0009	yes
Neo1		2.6009	0.0115	yes		1.1302	1.0000	no
Nes		2.3627	0.0002	yes		1.7660	0.0012	yes
Neurl1a		1.4436	1.0000	no		0.9703	1.0000	no
Neurl1b		8.0000	1.0000	no		1.5217	1.0000	no
Neurod2		0.0000	1.0000	no		0.0000	1.0000	no
Neurog1		0.0000	1.0000	no		0.0000	1.0000	no
Neurog2		0.0000	1.0000	no		0.0000	1.0000	no
Nexn		1.0194	1.0000	no		1.8093	1.0000	no
Nfatc1		0.7852	0.3141	no		2.3896	0.0000	yes
Nfatc4		1.2525	1.0000	no		2.5713	1.0000	no
Nfe2l3		-1.0909	1.0000	no		-0.6649	1.0000	no
Nfia		2.5378	0.0035	yes		3.2250	0.0831	no
Nfib		0.3084	1.0000	no		1.8675	1.0000	no
Nfic		2.1886	0.0030	yes		1.9505	0.0042	yes
Nfil3		3.1706	0.0065	yes		2.6033	0.0026	yes
Nfix		0.8156	0.2868	no		-0.1209	0.8995	no
Nfkb1		-0.0645	0.9997	no		2.0818	0.0000	yes
Nfkbiz		0.7585	0.8463	no		1.4559	0.0877	no
Ngef		3.1078	0.0046	yes		1.1898	1.0000	no
Ngfr		0.6299	1.0000	no		-0.0698	1.0000	no
Nhlrc1		0.8242	1.0000	no		3.9709	1.0000	no
Nin		0.4763	0.3439	no		2.4846	0.0000	yes
Nkain1		3.0040	0.0045	yes		4.5446	0.0001	yes
Nkain2		0.0000	1.0000	no		0.0000	1.0000	no
Nkd1		1.1736	1.0000	no		1.9753	1.0000	no
Nkpd1		1.0653	1.0000	no		18.0000	1.0000	no
Nkx1-2		8.0000	1.0000	no		18.0000	1.0000	no
Nkx2-1		0.0000	1.0000	no		0.0000	1.0000	no
Nkx2-2		0.0000	1.0000	no		0.0000	1.0000	no
Nkx2-3		8.0000	1.0000	no		-12.0000	1.0000	no
Nkx2-4		0.0000	1.0000	no		0.0000	1.0000	no
Nkx2-5		0.0000	1.0000	no		0.0000	1.0000	no
Nkx3-1		8.0000	1.0000	no		0.0000	1.0000	no
Nkx3-2		0.0000	1.0000	no		0.0000	1.0000	no
Nkx6-1		0.0000	1.0000	no		18.0000	1.0000	no
Nkx6-2		1.0546	1.0000	no		0.5586	1.0000	no
Nlgn2		1.0473	0.2413	no		3.2475	0.0001	yes
Nlrp6		2.2909	0.0164	yes		1.0604	0.0899	no
NM_001145974	NA	NA		NA	NA	NA		NA
NM_001172117	NA	NA		NA	NA	NA		NA
Nod1		0.9962	0.5535	no		0.4315	0.6230	no
Nodal		0.0400	1.0000	no		18.0000	1.0000	no
Nog		8.0000	1.0000	no		18.0000	1.0000	no
Nol3		0.6738	1.0000	no		2.2016	1.0000	no
Nos1ap		2.6665	0.0011	yes		0.1427	0.8458	no
Notch1		1.5830	0.4186	no		1.5922	0.0177	yes

Notch3		0.7682	1.0000	no		0.4960	1.0000	no
Notum		8.0000	1.0000	no		18.0000	1.0000	no
Nova1		1.5937	0.2719	no		2.4762	1.0000	no
Npas1		-1.0031	0.7974	no		0.7988	1.0000	no
Npas3		0.0000	1.0000	no		-1.0551	1.0000	no
Npdc1		2.5173	0.1241	no		1.5170	0.1246	no
Npnt		1.2386	1.0000	no		0.6551	1.0000	no
Nppc		0.0000	1.0000	no		0.0000	1.0000	no
Npr1		1.4324	0.1149	no		1.4597	0.0089	yes
Npr2		1.1721	0.6563	no		0.3232	0.8186	no
Nptx1		0.0000	1.0000	no		0.0000	1.0000	no
Nptxr		8.0000	1.0000	no		18.0000	1.0000	no
Npw		2.6200	1.0000	no		18.0000	1.0000	no
Npy		0.0000	1.0000	no		0.0000	1.0000	no
NR_003258	NA	NA	NA	NA	NA	NA	NA	NA
NR_027352	NA	NA	NA	NA	NA	NA	NA	NA
NR_028280	NA	NA	NA	NA	NA	NA	NA	NA
NR_029460	NA	NA	NA	NA	NA	NA	NA	NA
NR_033135	NA	NA	NA	NA	NA	NA	NA	NA
NR_036582	NA	NA	NA	NA	NA	NA	NA	NA
NR_036665	NA	NA	NA	NA	NA	NA	NA	NA
Nr2e1		0.0000	1.0000	no		0.0000	1.0000	no
Nr2f1		2.6386	1.0000	no		1.8251	1.0000	no
Nr2f2		1.9104	0.2278	no		0.9236	0.3119	no
Nr2f6		0.9683	0.1416	no		1.0572	0.0481	yes
Nr4a2		0.7264	0.6491	no		2.7732	1.0000	no
Nr4a3		-0.5555	1.0000	no		18.0000	1.0000	no
Nr6a1		-0.4612	0.9539	no		2.0709	0.0442	yes
Nrarp		-0.1395	0.9997	no		1.9463	0.0220	yes
Nrbp2		1.9504	0.0714	no		1.9226	0.0269	yes
Nrg2		2.4110	0.1596	no		3.4830	0.0003	yes
Nrg3		0.0000	1.0000	no		0.0000	1.0000	no
Nrip3		2.8730	0.0032	yes		1.0504	0.2087	no
Nrp2		1.7397	1.0000	no		0.6521	1.0000	no
Nrtn		1.3622	0.4746	no		0.7262	0.5052	no
Nrxn2		8.0000	1.0000	no		1.9157	1.0000	no
Nsg1		-0.0412	1.0000	no		1.0980	1.0000	no
Nt5c1a		0.0000	1.0000	no		0.0000	1.0000	no
Nt5c2		-0.4121	0.4055	no		1.0512	0.0425	yes
Ntf5		8.0000	1.0000	no		18.0000	1.0000	no
Ntn1		2.0503	1.0000	no		-12.0000	1.0000	no
Ntn4		1.3406	0.2604	no		2.3020	0.0715	no
Ntng2		3.0453	0.3460	no		18.0000	0.0015	yes
Ntrk1		8.0000	1.0000	no		1.5033	1.0000	no
Nuak1		0.1033	1.0000	no		1.1597	0.5109	no
Nuak2		2.5790	0.0122	yes		1.8448	0.0145	yes
Nxph3		0.0000	1.0000	no		0.0000	1.0000	no
Nxph4		0.0000	1.0000	no		18.0000	1.0000	no
Obsl1		2.8216	0.0000	yes		1.5703	0.0442	yes
Ociad2		0.0506	0.9997	no		1.0141	0.2810	no
Ocln		1.0336	0.7863	no		1.7470	0.0066	yes
Odf3b		1.3297	0.5144	no		3.1323	0.0296	yes
Odz4		0.1357	1.0000	no		-0.8314	1.0000	no
Olfm1		2.2292	0.0082	yes		3.1809	0.0000	yes
Olfm2		8.0000	1.0000	no		-0.0502	1.0000	no
Olfml2b		2.2977	1.0000	no		1.5807	0.0954	no
Olig2		0.0000	1.0000	no		0.0000	1.0000	no
Onecut1		1.7715	1.0000	no		0.8361	1.0000	no

Onecut2		2.9497	1.0000	no		1.7484	1.0000	no
Onecut3		8.0000	1.0000	no		-12.0000	1.0000	no
Oprd1		0.0000	1.0000	no		-12.0000	1.0000	no
Osbpl6		8.0000	1.0000	no		1.5291	1.0000	no
Osr2		8.0000	1.0000	no		18.0000	1.0000	no
Otop1		2.0398	1.0000	no		0.0000	1.0000	no
Otp		0.0000	1.0000	no		0.0000	1.0000	no
OTTMUSG000000101	NA	NA		NA	NA	NA		NA
Otud1		1.3697	0.4361	no		0.4624	0.6809	no
Otud7a		8.0000	1.0000	no		0.0000	1.0000	no
Otx1		8.0000	1.0000	no		0.0000	1.0000	no
Otx2		0.0000	1.0000	no		0.0000	1.0000	no
Ovol1		0.2508	1.0000	no		-0.4940	1.0000	no
Ovol2		0.0000	1.0000	no		18.0000	1.0000	no
Oxr1		-0.0908	0.9997	no		0.7254	0.2156	no
Oxt		8.0000	1.0000	no		0.0000	1.0000	no
P2rx5		-1.1960	1.0000	no		18.0000	1.0000	no
P2rx6		-1.3132	1.0000	no		0.0000	1.0000	no
P2ry2		1.5000	0.3882	no		2.9675	0.0015	yes
P4ha2		1.7834	0.0477	yes		1.1947	0.4158	no
P4ha3		0.5144	1.0000	no		1.5094	1.0000	no
Pacsin1		8.0000	1.0000	no		18.0000	1.0000	no
Pacsin3		1.1395	0.5358	no		0.5161	0.4678	no
Pak6		0.9748	0.2447	no		1.9684	0.0070	yes
Panx2		0.0000	1.0000	no		0.0000	1.0000	no
Papolb		0.0000	1.0000	no		18.0000	1.0000	no
Paqr4		0.6282	0.6566	no		0.5886	0.5207	no
Paqr8		1.2054	1.0000	no		1.4670	0.1862	no
Paqr9		2.3418	0.0000	yes		2.0693	0.0051	yes
Pard3		0.8309	0.7943	no		0.3500	0.6746	no
Pard6b		0.6187	0.9590	no		1.4733	0.1104	no
Parp12		1.2128	0.3452	no		0.6604	0.4376	no
Parp14		0.7474	0.6751	no		1.0933	0.1996	no
Parp8		3.3500	0.0000	yes		2.6480	0.0000	yes
Pawr		0.7063	0.8515	no		1.9908	0.0077	yes
Pax2		0.0000	1.0000	no		0.0000	1.0000	no
Pax6		-0.2159	0.9997	no		0.6991	0.4988	no
Pax6os1		0.0000	1.0000	no		0.0000	1.0000	no
Pax9		0.5244	1.0000	no		-0.9986	1.0000	no
Pcdh1		2.5060	0.0092	yes		1.9691	0.0042	yes
Pcdh12		1.1316	1.0000	no		0.5447	1.0000	no
Pcdh7		0.3119	1.0000	no		2.5281	1.0000	no
Pcdh8		8.0000	1.0000	no		0.0000	1.0000	no
Pcdhac2	NA	NA		NA	NA	NA		NA
Pcdhgc3	NA	NA		NA	NA	NA		NA
Pcgf2		0.3590	0.9997	no		1.1453	0.1046	no
Pcnx		0.9440	0.1132	no		2.1885	0.0000	yes
Pcolce2		3.6216	0.0080	yes		2.7660	0.0100	yes
Pcp4l1		3.3260	1.0000	no		0.8087	1.0000	no
Pcsk6		2.7766	0.0000	yes		3.9664	0.0000	yes
Pcsk9		2.1313	0.0033	yes		1.2542	0.1080	no
Pde10a		3.1184	1.0000	no		0.5509	1.0000	no
Pde2a		1.5006	0.0078	yes		1.8914	0.0009	yes
Pde3b		0.0379	0.9997	no		2.3823	0.0001	yes
Pde4a		0.2045	0.9997	no		2.8870	0.0000	yes
Pde4dip		0.3567	0.9970	no		1.0995	0.0956	no
Pde5a		1.4593	0.3115	no		1.6672	0.0587	no
Pde8a		2.3699	0.0019	yes		2.7581	0.0002	yes

Pde8b	0.3568	1.0000	no	0.3384	1.0000	no
Pdgfa	4.3582	1.0000	no	18.0000	0.0086	yes
Pdgfb	2.3161	0.0876	no	0.9203	0.3698	no
Pdgfra	2.6146	1.0000	no	-0.6892	1.0000	no
Pdlim4	1.7573	0.1511	no	1.6537	0.0478	yes
Pdp1	0.1178	0.9997	no	0.2207	0.8060	no
Peli2	2.7516	1.0000	no	1.8454	0.0374	yes
Perp	1.8348	0.1501	no	1.2183	0.1837	no
Pfkfb3	2.1807	0.0011	yes	2.6398	0.0000	yes
Pfn2	2.5847	0.1378	no	-1.0533	0.3908	no
Pgbd5	0.1007	1.0000	no	0.0000	1.0000	no
Phactr2	0.6785	0.7931	no	1.7414	0.0095	yes
Phc2	-0.1714	0.9916	no	0.6933	0.2427	no
Phf13	0.4987	0.9741	no	-0.5956	0.5223	no
Phf15	0.0309	0.9997	no	1.1068	0.0842	no
Phf21b	2.1035	0.3439	no	6.1688	0.0082	yes
Phlda1	2.2612	0.1119	no	4.1689	1.0000	no
Phlda3	0.4654	0.9585	no	1.8427	0.0174	yes
Phldb1	1.6715	0.0024	yes	2.4551	0.0029	yes
Phldb2	1.1617	0.2542	no	0.4722	0.5064	no
Phox2a	0.7773	1.0000	no	0.9228	1.0000	no
Phyhip	-0.0219	0.9997	no	0.5825	0.5724	no
Phyhipl	8.0000	1.0000	no	18.0000	1.0000	no
Pigz	4.0465	0.0918	no	-0.0597	1.0000	no
Pik3c2b	1.1338	1.0000	no	2.0724	1.0000	no
Pik3ip1	0.7628	0.8725	no	2.5227	0.0298	yes
Pitpnm1	1.7102	0.0000	yes	2.1662	0.0000	yes
Pitpnm3	0.0000	1.0000	no	0.0000	1.0000	no
Pitx1	0.0000	1.0000	no	0.0000	1.0000	no
Pitx2	0.0000	1.0000	no	18.0000	1.0000	no
Pitx3	0.0000	1.0000	no	0.0000	1.0000	no
Pkd2	3.3043	0.0002	yes	2.9148	0.0007	yes
Pkdcc	2.2555	0.0005	yes	1.9947	0.0037	yes
Pkdrej	0.9441	1.0000	no	2.1534	1.0000	no
Pknox2	2.9889	1.0000	no	18.0000	1.0000	no
Pkp1	8.0000	1.0000	no	0.3791	1.0000	no
Pkp2	1.2128	0.5552	no	1.4049	0.1299	no
Pkp4	-0.0006	0.9999	no	0.9213	0.0069	yes
Plagl1	1.6346	0.1258	no	0.0818	0.9336	no
Plbd1	1.8360	0.0739	no	1.4460	0.0312	yes
Plcg1	0.4408	0.8517	no	2.0847	0.0001	yes
Plcl1	8.0000	1.0000	no	2.5805	1.0000	no
Pld2	-0.3167	0.9997	no	1.6086	0.3743	no
Plec	0.9221	0.0041	yes	2.0199	0.0000	yes
Plekha1	2.3673	0.0000	yes	1.2019	0.0215	yes
Plekha2	2.9472	0.0004	yes	2.0627	0.0005	yes
Plekha5	0.8260	0.3200	no	2.2400	0.0000	yes
Plekhg1	1.2138	1.0000	no	-0.1504	1.0000	no
Plekhg3	3.2341	0.0001	yes	1.8978	0.0162	yes
Plekhg6	1.8970	1.0000	no	2.7619	1.0000	no
Plekhh1	0.3711	0.9997	no	1.8287	0.0249	yes
Plekhh2	2.6022	1.0000	no	1.5834	1.0000	no
Plekhh3	1.5630	1.0000	no	-0.5861	1.0000	no
Plekho1	1.3245	0.0209	yes	1.3148	0.0166	yes
Plk2	1.8615	0.1827	no	1.0442	0.2944	no
Plk3	1.5628	0.0127	yes	2.3118	0.0027	yes
Plk5	8.0000	1.0000	no	18.0000	1.0000	no
Pllp	1.6313	1.0000	no	-1.6191	1.0000	no

Pls1	1.6572	0.3724	no	1.2982	0.1869	no
Pltp	0.4822	0.9811	no	0.2855	0.6742	no
Plxdc1	-0.8990	0.6767	no	3.0896	0.0012	yes
Plxna1	-0.0567	0.9997	no	2.6018	0.0008	yes
Plxna4	0.4526	1.0000	no	-0.1944	1.0000	no
Plxnb1	1.8613	0.2069	no	1.4283	0.1020	no
Plxnb2	2.0272	0.0000	yes	1.1630	0.0089	yes
Plxnc1	0.2299	0.9997	no	1.4926	0.0427	yes
Plxnd1	2.0193	0.0031	yes	1.9122	0.0055	yes
Pm20d2	1.7772	0.3106	no	3.6342	1.0000	no
Pmepa1	8.0000	1.0000	no	18.0000	1.0000	no
Pnma2	8.0000	1.0000	no	0.0000	1.0000	no
Pnmal2	-6.0000	1.0000	no	18.0000	1.0000	no
Podn	1.0033	0.3923	no	0.0771	0.9387	no
Podxl2	8.0000	0.1849	no	0.5952	0.7090	no
Pom121l2	0.0000	1.0000	no	0.0000	1.0000	no
Popdc3	2.9735	1.0000	no	-1.0258	1.0000	no
Pou2f3	0.0000	1.0000	no	0.0000	1.0000	no
Pou3f1	0.0000	1.0000	no	0.0000	1.0000	no
Pou3f2	0.0000	1.0000	no	0.0000	1.0000	no
Pou3f3	8.0000	1.0000	no	0.0000	1.0000	no
Pou4f1	2.2867	0.4324	no	18.0000	1.0000	no
Pou4f2	0.0000	1.0000	no	0.0000	1.0000	no
Pou4f3	8.0000	1.0000	no	0.0000	1.0000	no
Ppapdc1a	0.0000	1.0000	no	0.0000	1.0000	no
Ppapdc2	0.7497	0.9285	no	1.7790	0.0508	no
Pparg	3.3904	0.0028	yes	1.3657	0.0965	no
Ppargc1b	0.4076	0.9997	no	3.2227	0.0003	yes
Ppfia3	0.2757	0.9997	no	2.1522	0.1607	no
Ppig	-0.0373	0.9997	no	0.4608	0.1296	no
Ppl	2.6053	1.0000	no	1.1737	1.0000	no
Ppm1e	0.0375	0.9997	no	0.0576	0.9498	no
Ppm1h	1.6260	0.0336	yes	2.3985	0.0012	yes
Ppm1j	2.2046	1.0000	no	18.0000	1.0000	no
Ppm1n	0.0362	1.0000	no	0.0000	1.0000	no
Ppp1r16b	0.8226	1.0000	no	0.9327	1.0000	no
Ppp1r1b	8.0000	1.0000	no	0.0000	1.0000	no
Ppp2r2c	8.0000	1.0000	no	18.0000	1.0000	no
Ppp3cc	1.8854	0.0540	no	1.7772	0.0201	yes
Ppp4r1	0.1018	0.9997	no	0.6836	0.1033	no
Ppp4r4	1.9418	1.0000	no	2.0910	0.0294	yes
Ppy	0.0000	1.0000	no	0.0000	1.0000	no
Prdm12	0.0000	1.0000	no	0.0000	1.0000	no
Prdm13	0.0000	1.0000	no	0.0000	1.0000	no
Prdm14	0.0000	1.0000	no	0.0000	1.0000	no
Prdm16	1.1964	0.3680	no	1.7183	0.2409	no
Prdm6	0.0000	1.0000	no	0.0000	1.0000	no
Prdm9	0.2579	0.9997	no	1.1749	0.1760	no
Prkaa2	8.0000	1.0000	no	18.0000	1.0000	no
Prkar2a	0.7502	0.2334	no	2.2854	0.0015	yes
Prkca	1.0554	0.0759	no	1.2289	0.0082	yes
Prkce	0.5880	0.9765	no	0.1682	1.0000	no
Prkch	2.0834	0.1255	no	1.1960	0.2019	no
Prkcz	0.7987	0.7835	no	1.1094	0.3664	no
Prkd3	0.0410	0.9997	no	1.6493	0.0000	yes
Prkg1	1.6375	1.0000	no	18.0000	1.0000	no
Prkg2	8.0000	1.0000	no	-12.0000	1.0000	no
Prox1	2.5207	0.0122	yes	1.2198	0.1361	no

Prph	8.0000	1.0000	no	18.0000	1.0000	no
Prr18	8.0000	1.0000	no	18.0000	1.0000	no
Prr7	1.5217	1.0000	no	1.7662	1.0000	no
Prrt1	8.0000	1.0000	no	18.0000	1.0000	no
Prrt4	-0.9551	1.0000	no	18.0000	1.0000	no
Prrx2	2.6635	1.0000	no	0.0000	1.0000	no
Prrxl1	0.0000	1.0000	no	0.0000	1.0000	no
Prss12	0.4663	1.0000	no	-1.3997	1.0000	no
Prss16	3.2540	0.0517	no	2.0544	0.0201	yes
Prss23	-0.9784	1.0000	no	0.9833	1.0000	no
Prtg	8.0000	1.0000	no	0.9723	1.0000	no
Psd	-0.0187	0.9997	no	-0.6033	0.5109	no
Pstpip2	2.0673	0.0005	yes	1.9989	0.0000	yes
Ptch2	-0.0448	0.9997	no	0.5201	1.0000	no
Ptger3	1.8315	0.0016	yes	2.8564	0.0000	yes
Ptgfrn	2.5661	1.0000	no	1.9749	1.0000	no
Pth1r	1.5589	0.3822	no	0.7823	0.4678	no
Pth2	0.0000	1.0000	no	0.0000	1.0000	no
Ptms	2.2667	0.0011	yes	1.2063	0.0650	no
Ptpn14	-0.0617	0.9997	no	1.5986	1.0000	no
Ptpn21	0.7836	0.7179	no	2.1525	0.0064	yes
Ptpn3	2.8687	1.0000	no	-0.4199	0.8440	no
Ptpn5	0.0000	1.0000	no	18.0000	1.0000	no
Ptpn9	0.3444	0.9997	no	1.9373	0.0181	yes
Ptprf	2.7050	0.0003	yes	1.2299	0.0237	yes
Ptprg	2.4918	0.1185	no	1.0488	0.5762	no
Ptprj	0.2348	0.9997	no	1.2434	0.0715	no
Ptprn	0.0387	1.0000	no	18.0000	1.0000	no
Ptprs	1.1340	0.0115	yes	2.2694	0.0000	yes
Ptprt	8.0000	1.0000	no	-2.0362	1.0000	no
Ptpru	1.3925	0.0001	yes	1.3417	0.0089	yes
Ptrf	0.1427	0.9997	no	1.7266	0.0423	yes
Pura	0.3670	0.9770	no	1.4667	0.0744	no
Pus3	-0.3768	0.9105	no	1.1703	0.0369	yes
Pvrl1	2.1138	0.0792	no	2.0142	0.0257	yes
Pvrl3	0.8330	0.8859	no	1.8344	0.0327	yes
Pygo1	-6.0000	1.0000	no	18.0000	1.0000	no
Pyy	0.0000	1.0000	no	0.0000	1.0000	no
Rab11fip3	1.4937	0.0159	yes	1.8490	0.0013	yes
Rab11fip4	3.0225	0.3439	no	2.0154	0.0508	no
Rab15	-0.5979	1.0000	no	18.0000	1.0000	no
Rab19	3.0029	1.0000	no	-0.2407	1.0000	no
Rab20	2.0588	0.1643	no	0.0939	0.9447	no
Rab27b	1.2518	0.2675	no	0.8242	0.2481	no
Rab31	2.6457	0.0073	yes	1.8510	0.0251	yes
Rab34	0.3391	0.9997	no	1.1179	0.0536	no
Rab6b	2.6040	1.0000	no	2.9795	1.0000	no
Rac3	0.3981	0.9997	no	1.9257	0.0467	yes
Radil	3.8468	0.0406	yes	1.0747	1.0000	no
Ralgds	1.9946	0.0765	no	1.2530	0.0952	no
Ralgps2	0.0831	0.9997	no	0.6838	0.3995	no
Ralyl	0.0000	1.0000	no	0.0000	1.0000	no
Ramp2	2.1275	0.0115	yes	0.8904	0.1680	no
Ranbp9	-0.0349	0.9997	no	0.2897	0.6316	no
Rap1gap2	2.0172	0.0314	yes	1.4964	0.3456	no
Rap2a	0.5118	0.9705	no	1.5038	0.0187	yes
Rapgef3	2.3119	0.0016	yes	1.1245	0.2446	no
Rapgef4	3.7811	0.0000	yes	0.6155	0.1522	no

Rapgefl1	1.2437	1.0000	no	18.0000	1.0000	no
Raph1	1.9270	0.0015	yes	0.8812	0.0749	no
Rara	2.0469	0.0012	yes	1.4805	0.1257	no
Rarg	2.0318	0.1163	no	1.7119	0.0522	no
Rarres1	1.0206	1.0000	no	0.1183	1.0000	no
Rasa2	0.3408	0.9985	no	2.5811	0.0005	yes
Rasal2	0.2984	0.9997	no	0.9085	0.3402	no
Rasd1	1.8306	1.0000	no	1.3062	1.0000	no
Rasd2	8.0000	1.0000	no	2.8509	1.0000	no
Rasgef1c	0.0000	1.0000	no	18.0000	1.0000	no
Rasgrp2	2.5309	0.0000	yes	1.9062	0.0000	yes
Rasip1	1.4027	0.0989	no	0.8976	0.1476	no
Rasl10a	8.0000	1.0000	no	-12.0000	1.0000	no
Rasl10b	1.6948	1.0000	no	1.4002	1.0000	no
Rasl11a	1.4039	0.4675	no	2.8557	0.0522	no
Rasl11b	0.9261	1.0000	no	1.7358	1.0000	no
Rassf5	1.6729	0.1380	no	1.9711	0.0140	yes
Raver2	2.1607	1.0000	no	1.4750	1.0000	no
Rax	0.0000	1.0000	no	0.0000	1.0000	no
Rbfox2	2.0014	0.0013	yes	1.2258	0.0162	yes
Rbfox3	8.0000	1.0000	no	-0.8871	1.0000	no
Rbm20	-1.8860	1.0000	no	0.5646	1.0000	no
Rbm24	0.0606	1.0000	no	18.0000	1.0000	no
Rbm46	0.0000	1.0000	no	0.0000	1.0000	no
Rbm47	1.1678	0.9856	no	1.5276	0.0865	no
Rbms1	0.1604	0.9997	no	-0.5330	0.1095	no
Rbpms	2.2871	0.0018	yes	1.4983	0.0067	yes
Rbpms2	2.9021	0.0115	yes	1.5251	0.0604	no
Rcor2	0.9891	0.2712	no	3.0147	0.0021	yes
Rcsd1	2.3501	0.0000	yes	1.8201	0.0021	yes
Reep1	0.4741	0.9997	no	1.7376	0.0534	no
Reep2	0.8236	1.0000	no	0.6503	1.0000	no
Rel	2.9101	0.0240	yes	2.4890	0.0094	yes
Relb	1.2237	0.3676	no	1.2882	0.1056	no
Reln	3.3317	0.0000	yes	0.0000	1.0000	no
Rem1	0.0000	1.0000	no	1.5791	1.0000	no
Rem2	0.0000	1.0000	no	0.0000	1.0000	no
Ret	2.5537	1.0000	no	18.0000	1.0000	no
Rftn1	0.4382	0.9502	no	2.6407	0.0000	yes
Rfx4	0.0000	1.0000	no	0.0000	1.0000	no
Rgl1	1.8944	0.0241	yes	0.4117	0.5772	no
Rgl3	8.0000	1.0000	no	18.0000	1.0000	no
Rgma	-6.0000	1.0000	no	-12.0000	1.0000	no
Rgmb	3.7309	1.0000	no	1.2039	1.0000	no
Rgnef	-0.2578	1.0000	no	3.7094	1.0000	no
Rgs6	-6.0000	1.0000	no	0.5960	1.0000	no
Rgs7bp	1.0314	1.0000	no	1.1034	1.0000	no
Rhbdf1	4.0770	0.0000	yes	3.3521	0.0000	yes
Rhbdl3	8.0000	1.0000	no	-0.0726	1.0000	no
Rhobtb1	-0.0594	0.9997	no	1.3113	0.1676	no
Rhobtb3	0.9825	0.4232	no	2.1855	0.0076	yes
Rhoc	2.2530	0.0078	yes	0.5765	0.3814	no
Rhod	1.5415	0.5149	no	-0.3154	0.7455	no
Rhoq	1.1559	0.5625	no	1.6691	0.0394	yes
Rhou	3.1124	0.0146	yes	2.0278	0.0180	yes
Rhpn1	8.0000	1.0000	no	0.0661	1.0000	no
Rilpl1	0.5114	0.9997	no	0.8922	0.3860	no
Rimkla	8.0000	1.0000	no	0.0000	1.0000	no

Rimklb	0.0000	1.0000	no	18.0000	1.0000	no
Rims2	8.0000	1.0000	no	18.0000	1.0000	no
Rims4	2.6076	1.0000	no	0.6839	1.0000	no
Rin3	3.4593	0.0000	yes	2.1257	0.0000	yes
Ripply3	0.8252	0.9068	no	0.8771	1.0000	no
Rln1	0.0000	1.0000	no	-12.0000	1.0000	no
Rnd2	0.2702	0.9997	no	2.6018	0.0001	yes
Rnf130	0.5006	0.7523	no	2.0415	0.0014	yes
Rnf144a	2.2545	0.0002	yes	3.3994	0.0001	yes
Rnf144b	2.7952	0.0021	yes	1.9051	0.0189	yes
Rnf150	0.8064	1.0000	no	1.2267	1.0000	no
Rnf152	8.0000	1.0000	no	2.0090	1.0000	no
Rnf157	0.5358	0.8957	no	0.6807	0.5750	no
Rnf165	2.0218	1.0000	no	-0.0064	1.0000	no
Rnf182	-1.0942	1.0000	no	18.0000	1.0000	no
Rnf208	0.8121	0.7246	no	2.6451	0.0162	yes
Rnf216	-0.1490	0.9997	no	0.4059	0.6331	no
Rnf217	2.4634	0.0975	no	2.1608	0.0275	yes
Rnf220	-0.3281	0.8035	no	1.0009	0.0092	yes
Rnf39	2.4986	1.0000	no	18.0000	1.0000	no
Rpp25	1.6120	1.0000	no	-12.0000	1.0000	no
Rps6ka1	0.3972	0.3698	no	0.0905	0.8497	no
Rragd	2.7722	0.0000	yes	0.7080	0.2363	no
Rras2	0.4544	0.9997	no	1.6331	0.0623	no
Rspo1	8.0000	1.0000	no	18.0000	1.0000	no
Rspo3	0.0430	1.0000	no	0.2672	1.0000	no
Rspo4	8.0000	1.0000	no	0.0000	1.0000	no
Rsrc1	-0.3884	0.6658	no	1.4799	0.0003	yes
Rtbdn	-0.1178	0.9997	no	-0.2812	0.8164	no
Rtkn	1.6173	0.1036	no	1.2048	0.0643	no
Rtn1	-0.1442	0.9997	no	1.8797	0.0410	yes
Rtn2	-0.4130	0.9997	no	0.5904	0.4615	no
Rtn4r	1.0566	1.0000	no	2.6288	1.0000	no
Rtn4rl1	1.2751	1.0000	no	1.3272	1.0000	no
Rtn4rl2	0.0000	1.0000	no	0.0000	1.0000	no
Rufy4	2.0149	1.0000	no	0.3398	1.0000	no
Rundc3a	1.6189	0.0374	yes	-0.4585	0.4034	no
Rundc3b	0.1601	1.0000	no	4.1316	1.0000	no
Runx1t1	1.4872	0.0375	yes	-1.4284	0.0004	yes
Runx2	4.7315	0.0911	no	2.4758	0.0806	no
Rusc1	0.1036	0.9997	no	1.5248	0.0798	no
Rusc2	1.1991	0.9028	no	-1.5097	0.3010	no
Ryr2	1.3451	1.0000	no	-1.0098	1.0000	no
S1pr5	8.0000	1.0000	no	18.0000	1.0000	no
Sall1	3.3501	1.0000	no	3.6118	1.0000	no
Sall3	0.0000	1.0000	no	18.0000	1.0000	no
Sall4	2.7713	0.0589	no	0.4773	0.7991	no
Samd10	1.1123	0.3568	no	2.3390	0.0031	yes
Samd4	2.4194	1.0000	no	-0.2558	1.0000	no
Samd5	8.0000	1.0000	no	18.0000	1.0000	no
Sap30l	0.2499	0.9997	no	0.0494	0.9666	no
Sarm1	8.0000	1.0000	no	18.0000	1.0000	no
Satb1	2.2710	0.0000	yes	2.0584	0.0001	yes
Satb2	1.4710	1.0000	no	4.1518	1.0000	no
Sbf2	1.6375	0.0155	yes	0.8090	0.1723	no
Sbk1	1.1925	0.5659	no	3.3546	0.0002	yes
Scamp5	1.2181	0.5698	no	0.4380	0.6964	no
Scarf2	2.0222	1.0000	no	0.6394	1.0000	no

Sccpdh		1.2297	0.2951	no		2.0548	0.0005	yes
Scn1b		2.1264	1.0000	no		0.9598	1.0000	no
Scn5a		-6.0000	1.0000	no		18.0000	1.0000	no
Scn8a		8.0000	1.0000	no		-2.3425	1.0000	no
Scrn1		8.0000	1.0000	no		18.0000	1.0000	no
Scrt1		0.4073	1.0000	no		0.0000	1.0000	no
Scrt2		0.0000	1.0000	no		0.0000	1.0000	no
Sct		8.0000	1.0000	no		18.0000	1.0000	no
Scube1		-0.7628	1.0000	no		1.1814	1.0000	no
Scube2		-0.5917	1.0000	no		18.0000	1.0000	no
Scube3		1.6925	1.0000	no		0.9293	1.0000	no
Sdc1		0.5603	0.3693	no		2.1214	0.0000	yes
Sdc3		1.1346	0.0870	no		0.6618	0.3717	no
Sdk1		0.7065	1.0000	no		-0.2756	1.0000	no
Sdk2		3.7314	1.0000	no		1.0988	1.0000	no
Sec14l2		1.1189	0.0510	no		1.8355	0.0020	yes
Sec24d		2.0482	0.0486	yes		1.7089	0.0412	yes
Sel1l3		0.0000	1.0000	no		0.0000	1.0000	no
Sema3f		1.7449	1.0000	no		1.3871	1.0000	no
Sema4c		1.0197	0.4478	no		1.2214	0.0416	yes
Sema4f		8.0000	1.0000	no		18.0000	1.0000	no
Sema4g		2.7252	0.0000	yes		1.7967	0.0015	yes
Sema5b		0.0428	1.0000	no		-12.0000	1.0000	no
Sema6a		2.4879	1.0000	no		0.1472	1.0000	no
Sema6b		0.7614	0.8177	no		1.8471	0.0102	yes
Sema6d		1.4971	0.1954	no		0.5212	0.4758	no
Sema7a		3.1985	1.0000	no		2.3959	1.0000	no
Sepn1		-0.2659	0.9997	no		1.7956	0.0160	yes
Sept10	NA	NA		NA	NA	NA		NA
Sept3	NA	NA		NA	NA	NA		NA
Sept5	NA	NA		NA	NA	NA		NA
Serinc2		5.2975	0.0000	yes		4.5953	0.0000	yes
Serp2		0.1025	0.9997	no		0.1780	1.0000	no
Serpine2		3.6088	0.0021	yes		3.0143	0.0004	yes
Sertad4		0.5000	1.0000	no		0.2134	1.0000	no
Sesn3		2.5761	1.0000	no		2.5182	1.0000	no
Sestd1		1.6274	1.0000	no		3.0973	0.0025	yes
Setbp1		4.4091	1.0000	no		18.0000	1.0000	no
Sez6		-6.0000	1.0000	no		0.0000	1.0000	no
Sfmbt1		-0.1724	0.9682	no		0.1557	0.7185	no
Sfmbt2		2.2252	0.3325	no		2.7402	0.0426	yes
Sfn		0.9811	0.7974	no		3.1182	1.0000	no
Sfrp1		1.5020	1.0000	no		-0.5370	1.0000	no
Sfrp2		8.0000	1.0000	no		1.7163	1.0000	no
Sfrp5		0.0556	1.0000	no		18.0000	1.0000	no
Sgcb		1.2909	0.1709	no		2.1745	0.0008	yes
Sgk1		0.5143	0.9272	no		0.2931	0.7080	no
Sgk3		0.1078	0.9997	no		-1.0020	0.0311	yes
Sgms1		0.2684	0.9997	no		-0.9280	0.0638	no
Sh2d5		2.3250	0.0239	yes		1.6157	0.0082	yes
Sh3bp4		1.0813	1.0000	no		0.1471	1.0000	no
Sh3bp5		1.7497	0.0133	yes		1.4124	0.0206	yes
Sh3d20	NA	NA		NA	NA	NA		NA
Sh3pxd2a		0.1264	0.9997	no		0.2106	0.7993	no
Sh3pxd2b		0.4773	0.9997	no		1.8774	0.0299	yes
Sh3rf1		1.0112	0.7131	no		2.5751	0.0042	yes
Sh3rf3		0.0000	1.0000	no		18.0000	1.0000	no
Shank3		-0.1556	0.9997	no		2.7951	0.0002	yes

Shc2	8.0000	1.0000	no	2.6556	1.0000	no
Shc3	0.0000	1.0000	no	0.0000	1.0000	no
She	1.6086	1.0000	no	1.0937	1.0000	no
Shisa2	8.0000	1.0000	no	1.7169	1.0000	no
Shisa3	0.0888	1.0000	no	0.4390	0.7054	no
Shisa6	-1.3715	1.0000	no	0.0000	1.0000	no
Shisa7	0.0000	1.0000	no	18.0000	1.0000	no
Shisa9	8.0000	1.0000	no	0.0000	1.0000	no
Shox2	8.0000	1.0000	no	18.0000	1.0000	no
Shroom1	2.6615	1.0000	no	1.2455	1.0000	no
Shroom3	-0.8778	1.0000	no	-1.2101	1.0000	no
Siah2	0.5029	0.9142	no	1.9855	0.0003	yes
Sim1	0.0000	1.0000	no	0.0000	1.0000	no
Sim2	-6.0000	1.0000	no	0.0000	1.0000	no
Sirpa	1.7750	0.0001	yes	1.3049	0.0000	yes
Six1	-6.0000	1.0000	no	18.0000	1.0000	no
Six2	0.0000	1.0000	no	18.0000	1.0000	no
Six3	0.0000	1.0000	no	0.0000	1.0000	no
Six3os1	0.0000	1.0000	no	0.0000	1.0000	no
Six4	8.0000	1.0000	no	18.0000	1.0000	no
Six5	1.2102	0.5455	no	2.2097	0.0168	yes
Six6	0.0000	1.0000	no	0.0000	1.0000	no
Skap1	2.2786	0.1992	no	1.1907	1.0000	no
Ski	0.4893	0.2313	no	1.8882	0.0000	yes
Skor1	0.0000	1.0000	no	0.0000	1.0000	no
Slain1	2.0699	0.0345	yes	3.7889	0.0001	yes
Slain2	0.0604	0.9997	no	2.2676	0.0000	yes
Slc10a4	0.0000	1.0000	no	18.0000	1.0000	no
Slc12a2	0.1093	0.9997	no	2.0713	0.0107	yes
Slc16a11	0.8289	0.8132	no	-0.7517	0.2904	no
Slc16a12	2.0916	0.0963	no	1.1067	0.2573	no
Slc16a9	8.0000	1.0000	no	1.4464	1.0000	no
Slc17a7	2.0477	1.0000	no	18.0000	1.0000	no
Slc18a3	NA	NA	NA	NA	NA	NA
Slc22a15	1.5183	1.0000	no	3.3779	0.0000	yes
Slc22a17	2.2771	0.0891	no	1.8178	0.0195	yes
Slc23a2	0.0889	0.9997	no	2.2043	0.0009	yes
Slc25a23	0.2339	0.9997	no	1.8804	0.0062	yes
Slc25a33	0.2645	0.9997	no	2.1623	0.0115	yes
Slc26a10	0.4770	0.9583	no	2.9330	0.0001	yes
Slc26a4	0.0000	1.0000	no	0.0000	1.0000	no
Slc27a2	2.2162	0.0002	yes	0.6833	0.2426	no
Slc29a4	1.0425	1.0000	no	1.5034	1.0000	no
Slc2a13	1.6351	1.0000	no	18.0000	1.0000	no
Slc30a2	8.0000	1.0000	no	1.1473	1.0000	no
Slc30a3	1.6389	1.0000	no	1.5156	1.0000	no
Slc30a4	2.3429	0.0611	no	2.2856	0.0084	yes
Slc32a1	2.0534	1.0000	no	-1.0058	1.0000	no
Slc35d3	4.3764	0.0005	yes	1.2727	0.1834	no
Slc35e4	1.6385	1.0000	no	18.0000	1.0000	no
Slc37a3	0.3263	0.9962	no	0.9916	0.1052	no
Slc38a3	1.9987	0.0862	no	0.5833	0.5633	no
Slc41a2	8.0000	1.0000	no	0.9793	1.0000	no
Slc44a1	0.3794	0.9098	no	0.5626	0.4599	no
Slc44a5	0.4341	0.9997	no	0.4254	0.6887	no
Slc45a3	2.3038	0.0476	yes	2.4126	0.0051	yes
Slc47a2	0.0000	1.0000	no	-0.0314	1.0000	no
Slc4a11	3.4589	1.0000	no	18.0000	1.0000	no

Slc4a4		3.8996	1.0000	no		0.7809	1.0000	no
Slc4a8		4.0384	1.0000	no		3.3671	0.0546	no
Slc5a5		0.0435	1.0000	no		1.5110	1.0000	no
Slc6a17		0.0000	1.0000	no		0.0000	1.0000	no
Slc6a20a		2.4717	0.0002	yes		0.6562	0.4472	no
Slc6a4		1.8576	1.0000	no		1.5173	1.0000	no
Slc7a10		8.0000	1.0000	no		-1.9757	1.0000	no
Slc7a8		1.8834	0.0551	no		1.0291	0.2160	no
Slc9a2		0.0000	1.0000	no		0.0000	1.0000	no
Slc9a3		0.0000	1.0000	no		18.0000	1.0000	no
Slc9a3r2		2.5079	0.0020	yes		1.4875	0.0493	yes
Slc9a5		1.4807	1.0000	no		3.0623	1.0000	no
Slco3a1		3.3423	0.0204	yes		2.5389	0.0001	yes
Slmo1		1.0743	0.7157	no		1.5019	1.0000	no
Smad1		2.7367	0.0116	yes		1.7885	0.0426	yes
Smad4		0.3278	0.8886	no		1.7450	0.0000	yes
Smad6		2.0217	0.0352	yes		0.9587	0.2897	no
Smad7		1.4776	0.4611	no		1.9418	0.0113	yes
Smad9		2.2010	1.0000	no		1.3728	1.0000	no
Smagp		1.1088	0.5040	no		1.2964	0.1495	no
Smarca2		1.4121	0.0000	yes		2.1858	0.0000	yes
Smarcd3		0.1658	0.9997	no		0.8920	0.2991	no
Smo		0.1505	0.9997	no		2.4160	0.0016	yes
Smok2a		0.0000	1.0000	no		0.0000	1.0000	no
Smpdl3b		2.6091	1.0000	no		-0.7364	1.0000	no
Smtnl1		1.9435	1.0000	no		-1.0292	1.0000	no
Smurf1		1.2332	0.3812	no		2.2536	0.0072	yes
Snai1		1.2456	1.0000	no		0.4364	1.0000	no
Snai3		8.0000	1.0000	no		18.0000	1.0000	no
Snap91		0.0000	1.0000	no		18.0000	1.0000	no
Sncaip		2.0194	1.0000	no		1.1430	1.0000	no
Sncb		0.0000	1.0000	no		0.0000	1.0000	no
Snhg11		3.3865	1.0000	no		1.3162	1.0000	no
Snn		1.4213	0.4660	no		0.7879	0.4528	no
Snph		0.0000	1.0000	no		0.0000	1.0000	no
Snta1		1.3727	0.4017	no		0.2983	0.8044	no
Sntb2		0.8114	0.8519	no		2.6156	0.0057	yes
Snx10		2.0239	0.0133	yes		0.9751	0.1082	no
Snx18		0.2581	0.9997	no		1.4293	0.0823	no
Snx21		0.7978	0.2307	no		-0.2087	0.7523	no
Snx24		1.7613	0.0679	no		0.5441	0.5584	no
Sobp		0.0000	1.0000	no		18.0000	1.0000	no
Socs1		3.2627	1.0000	no		2.1869	1.0000	no
Socs2		0.8593	0.3072	no		1.7636	0.0079	yes
Socs3		2.8829	0.0000	yes		-0.4010	0.4792	no
Sort1		1.5612	0.0047	yes		2.3539	0.0000	yes
Sox1	NA	NA		NA	NA	NA		NA
Sox11		2.4161	1.0000	no		-1.0960	1.0000	no
Sox13		2.7202	0.0007	yes		2.4833	0.0004	yes
Sox18		1.3282	0.5595	no		0.9846	0.3615	no
Sox2		0.0000	1.0000	no		0.0000	1.0000	no
Sox21		0.0000	1.0000	no		18.0000	1.0000	no
Sox30		0.0000	1.0000	no		0.0000	1.0000	no
Sox4		0.5768	0.8917	no		2.5332	0.0004	yes
Sox6		0.6446	0.0040	yes		-0.7765	0.0081	yes
Sox7		3.0319	1.0000	no		0.1286	1.0000	no
Sox8		0.0400	1.0000	no		0.0000	1.0000	no
Sp5		0.0000	1.0000	no		0.0000	1.0000	no

Sp7	0.0000	1.0000	no	18.0000	1.0000	no
Sp9	-0.0198	0.9997	no	-0.7585	0.4242	no
Spata18	8.0000	1.0000	no	18.0000	1.0000	no
Spats2	0.0733	0.9997	no	1.6646	0.0485	yes
Spats2l	3.5254	0.0021	yes	3.2295	0.0674	no
Spdya	-0.0221	0.9997	no	1.4352	0.1536	no
Speg	1.3377	0.4004	no	0.0649	0.9507	no
Spint1	8.0000	1.0000	no	18.0000	1.0000	no
Spint2	0.2076	0.9997	no	2.1909	0.0003	yes
Spna2	1.9678	0.0001	yes	1.8196	0.0000	yes
Spnb2	1.4026	0.0005	yes	1.8098	0.0004	yes
Spnb3	0.9276	1.0000	no	0.1375	1.0000	no
Spnb4	2.2342	1.0000	no	1.9966	0.4057	no
Spns2	0.5329	0.2425	no	2.8712	0.0000	yes
Spock2	-0.2127	1.0000	no	3.0837	1.0000	no
Spred1	-0.1330	0.9997	no	1.4978	0.0670	no
Spred3	1.2748	1.0000	no	1.4296	1.0000	no
Spsb1	2.4325	0.4727	no	18.0000	1.0000	no
Spsb4	2.0608	1.0000	no	1.5374	1.0000	no
Src	0.5719	0.9997	no	2.0134	0.1245	no
Srcin1	-0.3751	1.0000	no	18.0000	1.0000	no
Srgap1	1.7130	1.0000	no	0.6502	1.0000	no
Srms	1.1607	1.0000	no	1.8530	1.0000	no
Srsf13b	NA	NA	NA	NA	NA	NA
St14	2.9581	0.1609	no	0.6245	0.5670	no
St8sia6	8.0000	1.0000	no	4.4008	1.0000	no
Stac2	2.0353	1.0000	no	18.0000	1.0000	no
Stat5b	-0.4129	0.5520	no	1.4041	0.0182	yes
Stau2	0.8972	0.1941	no	2.8653	0.0000	yes
Steap2	1.6828	0.0782	no	1.8868	0.0018	yes
Stk33	0.0000	1.0000	no	0.0000	1.0000	no
Stk39	1.9893	0.0023	yes	1.4564	0.0582	no
Stmn3	8.0000	1.0000	no	0.0000	1.0000	no
Stox1	1.0395	1.0000	no	0.5553	1.0000	no
Stox2	1.3928	1.0000	no	1.2814	1.0000	no
Stx3	-0.3375	0.9997	no	1.0177	0.0780	no
Stxbp5l	0.0000	1.0000	no	0.0000	1.0000	no
Sulf2	2.0587	1.0000	no	3.9124	0.0001	yes
Susd3	1.4372	0.4309	no	0.9896	0.3067	no
Susd5	0.0000	1.0000	no	0.0000	1.0000	no
Sv2c	-1.0079	1.0000	no	-12.0000	1.0000	no
Syde2	0.4847	0.9997	no	3.7340	0.0000	yes
Syn2	8.0000	1.0000	no	-1.5129	1.0000	no
Sync	0.0271	0.9997	no	-0.9620	0.1675	no
Syncrip	-0.1672	0.8122	no	1.2236	0.0000	yes
Syne2	0.9177	0.6767	no	1.0454	0.1875	no
Syngr3	-6.0000	1.0000	no	-0.0588	1.0000	no
Synj2	2.0476	0.0030	yes	1.8729	0.1725	no
Synm	0.4944	1.0000	no	2.2242	1.0000	no
Synpo	0.3264	1.0000	no	2.5559	1.0000	no
Sypl2	8.0000	1.0000	no	-12.0000	1.0000	no
Syt12	0.7034	1.0000	no	1.9838	1.0000	no
Syt13	8.0000	1.0000	no	1.9574	1.0000	no
Syt2	-0.7630	1.0000	no	2.8012	1.0000	no
Syt7	1.4851	1.0000	no	1.2957	1.0000	no
Syt9	1.1197	1.0000	no	0.0000	1.0000	no
T	0.0000	1.0000	no	18.0000	1.0000	no
Tanc1	1.1448	0.7065	no	2.2226	1.0000	no

Tbc1d16		0.6216	0.9997	no		1.8112	0.0333	yes
Tbc1d30		1.4406	1.0000	no		3.5436	1.0000	no
Tbc1d9		-0.1900	0.9997	no		-0.2461	0.7705	no
Tbkbp1		2.2964	0.0206	yes		1.8786	0.0003	yes
Tbr1		0.0000	1.0000	no		0.0000	1.0000	no
Tbx1		8.0000	1.0000	no		0.0000	1.0000	no
Tbx15		2.6089	1.0000	no		18.0000	1.0000	no
Tbx18		0.0000	1.0000	no		0.0000	1.0000	no
Tbx2		1.1771	1.0000	no		-0.5923	1.0000	no
Tbx20		0.0407	1.0000	no		18.0000	1.0000	no
Tbx21		0.0000	1.0000	no		18.0000	1.0000	no
Tbx3		2.3629	0.1366	no		0.7776	0.4161	no
Tbx4		0.0000	1.0000	no		0.0000	1.0000	no
Tcea3		1.1933	0.5200	no		0.9935	0.2846	no
Tcf15		0.7115	1.0000	no		1.5056	1.0000	no
Tcf7		2.1559	0.0097	yes		2.1809	0.0001	yes
Tcf7l1		2.9356	0.0325	yes		2.4907	0.0236	yes
Tcf7l2		0.2999	0.9275	no		-1.1973	0.0003	yes
Tcfap2a	NA	NA	NA	NA	NA	NA	NA	NA
Tcfap2c	NA	NA	NA	NA	NA	NA	NA	NA
Tcfap2e	NA	NA	NA	NA	NA	NA	NA	NA
Tcfeb	NA	NA	NA	NA	NA	NA	NA	NA
Tcfl5		8.0000	1.0000	no		18.0000	1.0000	no
Tcp11l1		1.0898	0.6641	no		2.0600	0.0092	yes
Tcte2		0.1526	1.0000	no		-0.9817	1.0000	no
Tdrd5		1.4640	1.0000	no		1.6029	1.0000	no
Tead1		2.0864	1.0000	no		0.0712	1.0000	no
Tead2		1.1469	0.4231	no		0.6823	0.4869	no
Tead4		1.4031	1.0000	no		-0.4951	1.0000	no
Tec		2.4836	0.0005	yes		1.8132	0.0000	yes
Tesc		4.1693	0.2498	no		1.8730	0.1720	no
Tex14		-1.7018	1.0000	no		2.7877	1.0000	no
Tgfa		2.6408	0.0383	yes		1.6213	1.0000	no
Tgfb2		1.0265	1.0000	no		0.7218	1.0000	no
Tgif1		0.7698	0.3306	no		2.3726	0.0000	yes
Thpo		2.0840	1.0000	no		1.3686	0.1948	no
Thrb		0.5532	1.0000	no		0.2814	1.0000	no
Tiam2		-0.4161	0.9997	no		1.3013	1.0000	no
Timp3		1.2304	0.4912	no		1.4611	0.1145	no
Tipin		-0.2916	0.8222	no		-0.2250	0.8084	no
Tjp1		1.6121	0.0008	yes		2.8937	0.0000	yes
Tjp2		0.8272	0.2837	no		1.8180	0.0047	yes
Tle2		2.0273	0.0729	no		0.5835	0.5159	no
Tll1		0.0000	1.0000	no		0.0000	1.0000	no
Tlx1		0.0000	1.0000	no		0.0000	1.0000	no
Tlx2		8.0000	1.0000	no		2.2131	1.0000	no
Tlx3		0.0000	1.0000	no		0.0000	1.0000	no
Tm6sf1		2.6985	0.0000	yes		1.8131	0.0000	yes
Tmcc3		2.3295	0.0101	yes		0.9398	0.4020	no
Tmed8		-0.1787	0.9997	no		2.5128	0.0025	yes
Tmeff1		1.2266	0.5239	no		1.6530	0.1262	no
Tmem102		2.6302	1.0000	no		3.5486	1.0000	no
Tmem108		3.2010	1.0000	no		2.3469	1.0000	no
Tmem117		8.0000	1.0000	no		18.0000	1.0000	no
Tmem121		1.0559	1.0000	no		2.5056	1.0000	no
Tmem132b		0.0000	1.0000	no		0.0000	1.0000	no
Tmem132e		1.1064	1.0000	no		1.6576	1.0000	no
Tmem145		0.0000	1.0000	no		18.0000	1.0000	no

Tmem150a	1.7118	0.1659	no	1.4789	0.0948	no
Tmem150c	0.8651	1.0000	no	4.1651	1.0000	no
Tmem151a	-1.9901	1.0000	no	18.0000	1.0000	no
Tmem151b	0.0000	1.0000	no	18.0000	1.0000	no
Tmem158	0.7097	0.9504	no	2.5162	0.0085	yes
Tmem163	8.0000	1.0000	no	3.9164	1.0000	no
Tmem22	1.0268	1.0000	no	0.0057	1.0000	no
Tmem229a	3.5182	1.0000	no	0.5107	1.0000	no
Tmem229b	1.5544	0.0108	yes	2.1329	0.0000	yes
Tmem28	8.0000	1.0000	no	0.0000	1.0000	no
Tmem30b	4.1409	1.0000	no	0.5037	1.0000	no
Tmem44	1.0228	0.3980	no	2.9047	1.0000	no
Tmem54	8.0000	0.0561	no	2.3684	0.3454	no
Tmem59l	8.0000	1.0000	no	18.0000	1.0000	no
Tmem8	0.4735	0.9300	no	1.9281	0.0184	yes
Tmem90a	0.0000	1.0000	no	0.9494	1.0000	no
Tmem91	0.0401	0.9997	no	-0.1240	1.0000	no
Tmem98	1.6449	0.1843	no	1.8342	0.0395	yes
Tmie	2.3006	1.0000	no	1.1212	1.0000	no
Tmod2	8.0000	1.0000	no	18.0000	1.0000	no
Tmtc1	1.3924	1.0000	no	0.6615	1.0000	no
Tnfrsf11a	1.3016	1.0000	no	0.6822	1.0000	no
Tnfsf11	0.0350	1.0000	no	2.0260	1.0000	no
Tnrc18	0.7859	0.3455	no	-0.0480	0.9512	no
Tns1	-0.7740	0.0208	yes	0.0689	0.9272	no
Tns3	0.9531	0.3556	no	1.7684	0.0123	yes
Tnxb	2.2087	1.0000	no	18.0000	1.0000	no
Tpbg	8.0000	1.0000	no	18.0000	1.0000	no
Tpd52	0.7535	0.1719	no	1.3732	0.0002	yes
Tpm1	-0.0903	0.9985	no	-0.5244	0.0191	yes
Tpm2	1.5900	0.0986	no	1.9761	0.0021	yes
Tpm4	1.5253	0.0138	yes	0.8811	0.1270	no
Tppp	0.6104	0.9997	no	1.7348	0.4061	no
Trank1	8.0000	1.0000	no	18.0000	1.0000	no
Trib1	1.8995	1.0000	no	0.4855	0.6662	no
Tril	8.0000	1.0000	no	0.9202	1.0000	no
Trim14	1.8271	0.0414	yes	1.1692	0.0755	no
Trim36	0.7026	1.0000	no	2.2831	1.0000	no
Trim47	1.6263	0.0409	yes	-0.2790	0.7305	no
Trim62	0.9407	1.0000	no	4.4291	1.0000	no
Trim67	0.0000	1.0000	no	-12.0000	1.0000	no
Trim7	-0.0282	0.9997	no	0.7103	0.4988	no
Trim71	2.6705	1.0000	no	1.2321	1.0000	no
Trio	1.0561	0.4216	no	2.0283	0.0114	yes
Triobp	0.3826	0.8484	no	-0.0287	0.9611	no
Trnp1	0.0000	1.0000	no	2.2092	1.0000	no
Trp53i11	2.4617	0.0787	no	0.9526	0.3250	no
Trp73	0.3476	1.0000	no	18.0000	1.0000	no
Trpc1	0.8407	1.0000	no	1.6240	1.0000	no
Trpc3	8.0000	1.0000	no	2.2707	1.0000	no
Trpm8	0.0000	1.0000	no	0.0000	1.0000	no
Trps1	1.3862	1.0000	no	1.6030	1.0000	no
Tsc22d1	-0.2027	0.9774	no	-0.3646	0.5515	no
Tshr	8.0000	1.0000	no	1.9351	1.0000	no
Tshz3	2.6013	1.0000	no	0.5395	1.0000	no
Tsku	1.7139	1.0000	no	1.1077	1.0000	no
Tspan18	0.9376	0.4343	no	0.7831	0.2567	no
Tspan2	2.2905	0.0204	yes	2.1914	0.0029	yes

Tspan5		-0.2826	0.9629	no		1.8219	0.0030	yes
Ttbk1		0.0000	1.0000	no		18.0000	1.0000	no
Ttc34		0.0000	1.0000	no		0.0000	1.0000	no
Ttc39c		2.2772	0.2269	no		2.2471	0.0009	yes
Ttc9		8.0000	1.0000	no		18.0000	1.0000	no
Ttc9b		0.0000	1.0000	no		0.0000	1.0000	no
Ttll11		0.2325	1.0000	no		0.0784	1.0000	no
Ttpa		1.1803	0.4472	no		0.3817	0.7286	no
Ttyh1		0.2971	1.0000	no		0.0863	1.0000	no
Tub		8.0000	1.0000	no		18.0000	1.0000	no
Tubb2b		0.2012	0.9997	no		0.0135	0.9908	no
Tubb6		1.9084	0.0792	no		0.7921	0.4042	no
Tulp1		2.6859	0.1971	no		-12.0000	1.0000	no
Tulp4		-0.2309	0.9606	no		1.7243	0.0028	yes
Twist1		2.0415	1.0000	no		-0.6401	1.0000	no
Txndc16		0.9746	0.4365	no		0.7242	0.2359	no
Tyro3		3.4878	0.0004	yes		1.4939	0.2554	no
Uap1l1		1.3929	0.0338	yes		1.1532	0.0131	yes
Ube2j1		-0.0254	0.9997	no		-0.2173	0.7073	no
Ube2ql1		8.0000	1.0000	no		0.4645	1.0000	no
Ubl3		0.1460	0.9997	no		1.5010	0.0021	yes
Ubtd1		1.3837	0.4513	no		1.4890	0.1042	no
Ubtd2		0.2630	0.9997	no		1.6035	0.0827	no
Ucn		0.0000	1.0000	no		0.0000	1.0000	no
Ucp1		0.0000	1.0000	no		18.0000	1.0000	no
Ulk2		0.2732	0.9997	no		0.7939	0.1655	no
Unc13b		0.2499	0.9997	no		3.0889	0.0017	yes
Unc5a		3.5823	0.1236	no		4.9207	0.0022	yes
Unc5b		3.2344	1.0000	no		0.1776	1.0000	no
Unc80		8.0000	1.0000	no		0.0000	1.0000	no
Uncx		0.0000	1.0000	no		0.0000	1.0000	no
Usp2		0.2353	0.9997	no		1.7416	0.1799	no
Usp35		-0.5305	1.0000	no		18.0000	1.0000	no
Usp43		0.0000	1.0000	no		18.0000	1.0000	no
Ust		0.9268	1.0000	no		0.5889	1.0000	no
Utf1		8.0000	1.0000	no		0.0000	1.0000	no
Vangl1		0.1518	0.9997	no		-0.8807	0.1110	no
Vash1		2.2048	0.0068	yes		1.4875	0.0319	yes
Vash2		1.3524	1.0000	no		2.3810	1.0000	no
Vat1		0.9605	0.3249	no		1.7114	0.0226	yes
Vav2		0.2897	0.9997	no		1.2468	0.1015	no
Vav3		1.3969	0.2961	no		1.9778	0.0034	yes
Vax1		8.0000	1.0000	no		0.0000	1.0000	no
Vax2		8.0000	1.0000	no		0.0000	1.0000	no
Vax2os1		0.0000	1.0000	no		0.0000	1.0000	no
Vax2os2		0.0000	1.0000	no		0.0000	1.0000	no
Vgf		4.2903	1.0000	no		1.7947	1.0000	no
Vgll3		-6.0000	1.0000	no		-12.0000	1.0000	no
Vim		2.5133	0.0000	yes		2.1227	0.0000	yes
Vipr1		8.0000	1.0000	no		3.0527	0.0618	no
Vldlr		2.4213	1.0000	no		2.0883	1.0000	no
Vmn1r90		0.3381	1.0000	no		2.5845	1.0000	no
Vmn2r-ps14	NA	NA		NA	NA	NA		NA
Vrtn		8.0000	1.0000	no		0.0000	1.0000	no
Vsig10		2.0012	1.0000	no		1.7823	1.0000	no
Vstm2l		0.0000	1.0000	no		0.0000	1.0000	no
Vsx1		0.0000	1.0000	no		0.0000	1.0000	no
Vsx2		0.0000	1.0000	no		0.0000	1.0000	no

Vwa2	0.0000	1.0000	no	0.0000	1.0000	no
Vwa5b2	1.3821	0.0762	no	3.3639	1.0000	no
Wasf1	1.3242	1.0000	no	4.2401	1.0000	no
Wasf3	8.0000	1.0000	no	18.0000	1.0000	no
Wdfy3	0.2597	0.9186	no	0.5411	0.1274	no
Wdr8	-0.1080	0.9997	no	0.4623	0.4330	no
Wdr86	0.0989	1.0000	no	1.0462	1.0000	no
Whrn	4.5019	1.0000	no	1.9204	1.0000	no
Wipf1	0.0179	0.9997	no	1.6434	0.0001	yes
Wnk2	0.3937	1.0000	no	1.0601	1.0000	no
Wnt1	0.0000	1.0000	no	0.0000	1.0000	no
Wnt10a	0.0000	1.0000	no	0.0000	1.0000	no
Wnt10b	8.0000	1.0000	no	18.0000	1.0000	no
Wnt11	0.0000	1.0000	no	-1.2277	1.0000	no
Wnt2b	1.0390	1.0000	no	-0.8780	1.0000	no
Wnt3	0.0000	1.0000	no	0.0000	1.0000	no
Wnt3a	0.0447	1.0000	no	-1.3327	1.0000	no
Wnt4	0.3885	1.0000	no	-0.4004	1.0000	no
Wnt5b	1.0412	1.0000	no	-0.0565	1.0000	no
Wnt6	0.0000	1.0000	no	18.0000	1.0000	no
Wnt7a	0.0000	1.0000	no	0.0000	1.0000	no
Wnt7b	0.0000	1.0000	no	0.0000	1.0000	no
Wnt9a	0.0000	1.0000	no	18.0000	1.0000	no
Wnt9b	8.0000	1.0000	no	18.0000	1.0000	no
Wscd2	0.0000	1.0000	no	0.0000	1.0000	no
Wt1	1.9087	1.0000	no	18.0000	1.0000	no
Wtip	3.6916	0.0001	yes	1.7556	0.0324	yes
Wwc1	3.9352	0.0010	yes	0.4952	0.8041	no
Wwtr1	1.5569	1.0000	no	1.6008	1.0000	no
X99384	1.1521	0.6016	no	0.8638	0.3754	no
Xkr4	0.0000	1.0000	no	0.0000	1.0000	no
Xkr6	1.4478	1.0000	no	2.2365	1.0000	no
Xkr7	0.0000	1.0000	no	18.0000	1.0000	no
Xlr	-1.5189	0.1346	no	-2.2148	0.0044	yes
Xylt1	0.2733	0.9997	no	2.7980	0.0074	yes
Yap1	1.6879	0.7515	no	1.0253	0.2335	no
Ybx2	5.3486	0.0982	no	-0.0813	0.9494	no
Yes1	0.9767	0.3351	no	1.0466	0.1282	no
Ypel1	0.2264	0.9997	no	0.2402	0.8319	no
Zar1	0.0000	1.0000	no	0.0000	1.0000	no
Zbed3	1.2349	0.5420	no	2.4447	0.0044	yes
Zbtb10	0.9741	0.4171	no	2.8972	0.0016	yes
Zbtb16	0.8229	1.0000	no	2.8928	0.0013	yes
Zbtb42	1.0350	0.7491	no	3.0242	0.0095	yes
Zbtb7c	8.0000	1.0000	no	-0.9677	1.0000	no
Zbtb8b	4.4052	1.0000	no	-2.0184	1.0000	no
Zc3h12c	0.5871	0.9986	no	2.6470	1.0000	no
Zcchc14	1.2225	0.2838	no	0.9146	1.0000	no
Zdbf2	2.8345	1.0000	no	-2.4303	1.0000	no
Zdhhc2	0.4627	0.8201	no	1.1353	0.0151	yes
Zdhhc23	1.3753	0.4746	no	18.0000	1.0000	no
Zdhhc8	1.5866	0.2362	no	2.5079	0.0031	yes
Zfp105	1.5297	0.2579	no	2.3056	0.0144	yes
Zfp277	-0.1297	0.9997	no	1.1541	0.0221	yes
Zfp318	0.4440	0.7683	no	1.1938	0.0714	no
Zfp358	0.1520	0.9997	no	2.1327	0.0170	yes
Zfp385b	0.5622	1.0000	no	1.0479	0.3932	no
Zfp395	-0.0899	0.9997	no	1.6408	0.0427	yes

Zfp423	8.0000	1.0000	no	-5.0401	1.0000	no
Zfp503	1.8497	1.0000	no	1.2548	1.0000	no
Zfp516	2.7142	0.0082	yes	2.0475	0.0126	yes
Zfp521	1.1573	1.0000	no	4.3944	1.0000	no
Zfp580	2.0377	0.1736	no	1.5439	0.1489	no
Zfp608	1.0979	0.5650	no	2.4060	0.0034	yes
Zfp618	1.7337	1.0000	no	1.2698	1.0000	no
Zfp623	0.2969	0.9997	no	2.2148	0.0126	yes
Zfp651	2.3413	1.0000	no	0.7186	1.0000	no
Zfp664	-0.0226	0.9997	no	0.6678	0.1900	no
Zfp703	0.9104	0.6778	no	1.3956	0.0779	no
Zfp704	0.1288	0.9997	no	1.7142	0.0289	yes
Zfp710	1.0425	0.3321	no	1.8713	0.0008	yes
Zfp777	-0.1112	0.9997	no	2.7284	0.0000	yes
Zfp810	-0.1420	0.9997	no	1.6521	0.1078	no
Zfp827	1.5315	0.0307	yes	2.5775	0.0026	yes
Zfp964	2.3274	1.0000	no	18.0000	1.0000	no
Zfpm2	0.2006	1.0000	no	-0.4280	1.0000	no
Zfyve28	0.5803	1.0000	no	3.1112	1.0000	no
Zhx2	-0.1910	0.9997	no	-9.1172	1.0000	no
Zic1	0.0000	1.0000	no	0.0000	1.0000	no
Zic2	0.0000	1.0000	no	0.0000	1.0000	no
Zic5	0.0000	1.0000	no	18.0000	1.0000	no
Zkscan16	8.0000	1.0000	no	0.0000	1.0000	no
Zkscan17	0.2589	0.9871	no	1.4054	0.0184	yes
Zkscan2	3.3912	1.0000	no	18.0000	1.0000	no
Zmat3	0.0257	0.9997	no	1.1631	0.4398	no
Zmiz1	0.9519	0.0374	yes	1.6725	0.0007	yes
Zmynd11	-0.2611	0.8177	no	0.8412	0.0065	yes
Znrf4	0.0000	1.0000	no	18.0000	1.0000	no
Zswim5	1.5850	1.0000	no	3.7505	1.0000	no
Zswim6	1.1000	0.6767	no	1.1740	0.2157	no
Zyg11a	-0.9673	1.0000	no	2.1595	1.0000	no

Table S2. Genes contained in the Mtf2-PRC2 gene regulatory network

Genes have H3K27me3 ChIP peaks in Mtf2+/+ erythroblasts but not in Mtf2 -/- erythroblasts AND gene expression is significantly misregulated in Mtf2-/- erythroblasts compared to Mtf2 +/+ erythroblasts

Gene Name	Loss of H3K27me3 signal in Mtf2 -/- erythroblasts	Mtf2 ChIP peak	log2 Fold Change	Adj p value
6430548M08Rik	yes		2.6617	0.0069
9330182L06Rik	yes	yes	2.5231	0.0460
Abca13	yes	yes	3.5966	0.0002
Abca8b	yes		2.6681	0.0043
Actn1	yes	yes	1.2791	0.0093
Adamtsl5	yes		1.7395	0.0295
Adra2b	yes		1.2893	0.0011
Agmo	yes	yes	2.2832	0.0437
Agtr1a	yes	yes	3.4401	0.0022
Aim1	yes		1.8150	0.0202
Alox15	yes		2.0557	0.0152
Arhgap26	yes	yes	4.1377	0.0000
Arvcf	yes	yes	-0.8032	0.0282
Bank1	yes	yes	1.9538	0.0170
C8a	yes	yes	2.0084	0.0091
Ccdc92	yes		3.8496	0.0022
Cd37	yes		0.8390	0.0126
Cd84	yes	yes	1.6849	0.0185
Celf2	yes	yes	2.9006	0.0000
Cfh	yes	yes	1.6342	0.0248
Col27a1	yes		3.0983	0.0000
Coro2a	yes		2.5786	0.0009
Ctsf	yes		1.8404	0.0047
Dusp8	yes		1.3975	0.0076
Epb4.1l4b	yes		1.7977	0.0097
F13a1	yes	yes	2.7502	0.0000
Fgr	yes		3.7689	0.0001
Furin	yes		1.8362	0.0002
Gata2	yes		2.2535	0.0013
Gc	yes	yes	2.2977	0.0012
Gfi1	yes		2.8568	0.0000
Gldc	yes		2.0056	0.0144
Hdac9	yes	yes	1.8393	0.0100
Hs3st3b1	yes		2.6672	0.0100
Hs6st2	yes	yes	5.5807	0.0001
Hspa1b	yes	yes	1.8999	0.0497
Ica1	yes	yes	1.8396	0.0226
Igfbp7	yes	yes	2.3103	0.0094
Itga9	yes		1.5118	0.0228
Jak3	yes		0.8161	0.0167
Jdp2	yes		2.6522	0.0245

Kcnk12	yes	yes	5.1330	0.0161
Lrrc33	yes	yes	0.9150	0.0158
Lrrfip1	yes	yes	2.1828	0.0038
Man1c1	yes	yes	1.9470	0.0002
Mgst2	yes		1.6350	0.0187
Napsa	yes		3.4120	0.0000
Neo1	yes		2.6009	0.0115
Nos1ap	yes		2.6665	0.0011
Paqr9	yes		2.3418	0.0000
Pbx1	yes		3.4298	0.0000
Pfkfb3	yes		2.1807	0.0011
Pitpnm1	yes		1.7102	0.0000
Pla2g12b	yes		3.5790	0.0003
Pld1	yes	yes	1.5242	0.0345
Plxnb2	yes		2.0272	0.0000
Plxnd1	yes		2.0193	0.0031
Prox1	yes		2.5207	0.0122
Pstpip2	yes		2.0673	0.0005
Ptprk	yes	yes	1.6161	0.0386
Rapgef3	yes		2.3119	0.0016
Reln	yes	yes	3.3317	0.0000
Rhbdf1	yes		4.0770	0.0000
Rin3	yes	yes	3.4593	0.0000
Rnf144b	yes	yes	2.7952	0.0021
Runx1t1	yes		1.4872	0.0375
Sgsh	yes	yes	-1.2894	0.0451
Siglec5	yes	yes	2.9548	0.0002
Smad6	yes		2.0217	0.0352
Socs3	yes		2.8829	0.0000
Tbc1d4	yes	yes	1.3015	0.0171
Tcf7l1	yes		2.9356	0.0325
Tjp1	yes		1.6121	0.0008
Tmem154	yes		2.5805	0.0227
Trak2	yes	yes	0.7916	0.0064
Trem1	yes	yes	2.2844	0.0118
Trim14	yes	yes	1.8271	0.0414
Zfp516	yes		2.7142	0.0082

GO Term
GO:0016477: cell migration
GO:0006464: cellular protein modification process
GO:1903506: regulation of nucleic acid-templated
GO:0006355: regulation of transcription, DNA-templated
GO:0001568: blood vessel development
GO:0030154: cell differentiation

Gene within Term
HDAC9,PROX1,GATA2,PTPRK,RHBDF1,RAPGEF3,PSTPIP2,PLD1,EPB4.1L4B,FGR,PLXND FURIN,JAK3,PLXNB2,ITGA9,TREM1,RELN,AGTR1A
HDAC9,PROX1,GATA2,ALOX15,PTPRK,RAPGEF3,TRAK2,FGR,GFI1,JAK3,JDP2,PLXNB2, SMAD6,MAN1C1,DUSP8,BANK1,RNF144B,NOS1AP,F13A1,RELN,AGTR1A,SOCS3, ADRA2B,HS3ST3B1
HDAC9,RUNX1T1,PROX1,GATA2,ACTN1,PTPRK,RAPGEF3,TRAK2,LRRFIP1,GFI1,JAK3, NEO1,JDP2,SMAD6,TRIM14,RELN,PBX1,TCF7L1,ZFP516
HDAC9,RUNX1T1,PROX1,GATA2,PTPRK,RAPGEF3,TRAK2,LRRFIP1,GFI1,JAK3,NEO1, JDP2,SMAD6,TRIM14,RELN,PBX1,TCF7L1,ZFP516
HDAC9,PROX1,GATA2,RAPGEF3,PLXND1,SMAD6,AGTR1A,SOCS3,ADRA2B
HDAC9,RUNX1T1,PROX1,GATA2,ACTN1,PTPRK,RAPGEF3,FGR,GFI1,PLXND1,TJP1,JAK3 NEO1,JDP2,PLXNB2,SMAD6,RELN,COL27A1,PBX1,SOCS3,TCF7L1,ADRA2B,ZFP516

Table S3. Genes expression changes during erythroblast differentiation

GROUP A (Blue Circles in Fig 6E)
Genes that are significantly downregulated as either
Mtf2+/+ or Mtf2-/- erythroblasts differentiate from
Ter119-/lo to Ter119high

		Mtf2+/+ Erythroblasts				Mtf2-/- Erythroblasts			
		Ter119-/lo --> Ter119high				Ter119-/lo --> Ter119high			
Gene ID	**Gene Name**	**log2FoldChange**	**Adj p value**	**-log10 (Adj p value)**	**Significant p<0.05**	**log2FoldChange**	**Adj p value**	**-log10 (Adj p value)**	**Significant p<0.05**
ENSMUSG00000021111	Papola	-0.83184	0.01272	1.89567	yes	-0.32303	0.04368	1.35975	yes
ENSMUSG00000052752	Traf7	-0.71623	0.01824	1.73903	yes	-0.32539	0.01785	1.74848	yes
ENSMUSG00000020680	Taf15	-0.96908	0.01155	1.93756	yes	-0.32736	0.03866	1.41272	yes
ENSMUSG00000039205	Ciz1	-0.87498	0.00572	2.24238	yes	-0.32967	0.03333	1.47717	yes
ENSMUSG00000060261	Gtf2i	-1.79521	0.00000	7.98630	yes	-0.33015	0.04628	1.33465	yes
ENSMUSG00000022884	Eif4a2	-1.53542	0.00000	7.84877	yes	-0.33057	0.00480	2.31845	yes
ENSMUSG00000042520	Ubap2l	-1.12292	0.00106	2.97532	yes	-0.33071	0.01425	1.84626	yes
ENSMUSG00000054766	Set	-2.36145	0.00000	9.65456	yes	-0.34015	0.03008	1.52179	yes
ENSMUSG00000032423	Syncrip	-1.73363	0.00000	7.72020	yes	-0.34285	0.02319	1.63477	yes
ENSMUSG00000069565	Dazap1	-0.76099	0.04154	1.38154	yes	-0.34567	0.00929	2.03185	yes
ENSMUSG00000005610	Eif4g2	-0.67856	0.01891	1.72340	yes	-0.34645	0.00118	2.92660	yes
ENSMUSG00000028614	Tmem48	-1.32630	0.00291	2.53627	yes	-0.34750	0.04566	1.34048	yes
ENSMUSG00000025613	Cct8	-1.45813	0.00000	6.96788	yes	-0.34972	0.00128	2.89411	yes
ENSMUSG00000025428	Atp5a1	-1.01321	0.01348	1.87029	yes	-0.35811	0.01979	1.70361	yes
ENSMUSG00000020929	Eftud2	-0.93189	0.01644	1.78411	yes	-0.36247	0.02221	1.65343	yes
ENSMUSG00000021870	Slmap	-1.53202	0.00000	5.78238	yes	-0.36559	0.04542	1.34274	yes
ENSMUSG00000059291	Rpl11	-0.71721	0.03805	1.41970	yes	-0.36904	0.00360	2.44414	yes
ENSMUSG00000043962	Thrap3	-0.82396	0.03657	1.43689	yes	-0.36922	0.03721	1.42932	yes
ENSMUSG00000015120	Ube2i	-0.80685	0.04368	1.35972	yes	-0.37172	0.02432	1.61406	yes
ENSMUSG00000020453	Patz1	-2.41045	0.00000	14.00000	yes	-0.37318	0.03339	1.47634	yes
ENSMUSG00000045983	Eif4g1	-1.49600	0.00000	8.53756	yes	-0.37417	0.00014	3.85900	yes
ENSMUSG00000009585	Apobec3	-1.96166	0.00000	9.68460	yes	-0.37535	0.01636	1.78615	yes
ENSMUSG00000030795	Fus	-1.03585	0.01537	1.81330	yes	-0.37629	0.02970	1.52719	yes
ENSMUSG00000039176	Polg	-0.96285	0.00655	2.18360	yes	-0.38255	0.04107	1.38647	yes
ENSMUSG00000026669	Mcm10	-0.83905	0.01996	1.69978	yes	-0.38263	0.00754	2.12243	yes
ENSMUSG00000002718	Cse1l	-1.04357	0.00599	2.22287	yes	-0.38420	0.02592	1.58638	yes
ENSMUSG00000070425	Trpc2	-0.67124	0.03363	1.47328	yes	-0.38528	0.02886	1.53968	yes
ENSMUSG00000022191	Drosha	-1.46878	0.00001	4.94133	yes	-0.38833	0.00661	2.17975	yes
ENSMUSG00000059796	Eif4a1	-1.39763	0.00010	4.01406	yes	-0.38842	0.00453	2.34392	yes
ENSMUSG00000052337	Immt	-0.77605	0.00741	2.13025	yes	-0.39263	0.00099	3.00286	yes
ENSMUSG00000032604	Qars	-1.45552	0.00014	3.86693	yes	-0.39851	0.01340	1.87275	yes
ENSMUSG00000020402	Vdac1	-1.84201	0.00000	6.96788	yes	-0.39958	0.00994	2.00252	yes
ENSMUSG00000033392	Clasp2	-0.99194	0.04631	1.33431	yes	-0.40048	0.03180	1.49753	yes
ENSMUSG00000027423	Snx5	-1.84816	0.00000	5.40381	yes	-0.40068	0.01022	1.99059	yes
ENSMUSG00000062203	Gspt1	-1.85455	0.00000	6.52798	yes	-0.40590	0.01507	1.82177	yes
ENSMUSG00000023118	Sympk	-1.38018	0.00007	4.15890	yes	-0.40616	0.00764	2.11684	yes
ENSMUSG00000027889	Ampd2	-1.09829	0.00449	2.34748	yes	-0.40624	0.03078	1.51177	yes
ENSMUSG00000041375	Ccdc9	-0.93104	0.01050	1.97869	yes	-0.40625	0.04330	1.36353	yes
ENSMUSG00000038900	Rpl12	-1.08587	0.02059	1.68627	yes	-0.40754	0.01066	1.97210	yes
ENSMUSG00000028760	Eif4g3	-1.47684	0.00031	3.50888	yes	-0.40759	0.04968	1.30384	yes
ENSMUSG00000014195	Dnajc7	-1.52461	0.00008	4.07352	yes	-0.40950	0.01869	1.72832	yes
ENSMUSG00000020372	Gnb2l1	-1.06013	0.02483	1.60505	yes	-0.41185	0.01198	1.92137	yes
ENSMUSG00000024949	Sf1	-1.07786	0.00404	2.39373	yes	-0.41506	0.00323	2.49124	yes
ENSMUSG00000038084	Opa1	-1.47569	0.00001	5.21347	yes	-0.42487	0.00435	2.36124	yes
ENSMUSG00000023944	Hsp90ab1	-2.52284	0.00000	10.67625	yes	-0.42546	0.00402	2.39533	yes
ENSMUSG00000001909	Trmt1	-2.22225	0.00000	8.21609	yes	-0.42619	0.01381	1.85970	yes
ENSMUSG00000005899	Smpd4	-1.33051	0.00000	8.57828	yes	-0.42816	0.00012	3.93448	yes
ENSMUSG00000058799	Nap1l1	-1.56470	0.00138	2.86089	yes	-0.43083	0.01920	1.71667	yes
ENSMUSG00000000384	Tbrg4	-1.91139	0.00000	10.95443	yes	-0.43084	0.00215	2.66840	yes
ENSMUSG00000025967	Eef1b2	-1.24394	0.00089	3.04870	yes	-0.43190	0.00178	2.74849	yes
ENSMUSG00000031985	Gnpat	-1.69209	0.00008	4.09128	yes	-0.43257	0.03009	1.52158	yes
ENSMUSG00000022698	Naa50	-1.34852	0.00687	2.16295	yes	-0.43277	0.03009	1.52156	yes
ENSMUSG00000021660	Btf3	-1.16911	0.04507	1.34611	yes	-0.43332	0.05001	1.30093	yes
ENSMUSG00000033021	Gmppa	-1.32484	0.00017	3.77202	yes	-0.43422	0.03057	1.51474	yes
ENSMUSG00000030316	1500001M20Rik	-2.53164	0.00000	8.52184	yes	-0.43523	0.04159	1.38105	yes
ENSMUSG00000031575	Ash2l	-1.61451	0.00068	3.16882	yes	-0.43792	0.02650	1.57680	yes
ENSMUSG00000041164	Zmiz2	-1.92452	0.00000	8.20130	yes	-0.43838	0.00142	2.84721	yes
ENSMUSG00000028622	Mrpl37	-1.32077	0.02210	1.65567	yes	-0.43900	0.04354	1.36109	yes
ENSMUSG00000001052	Sec24b	-1.12183	0.00588	2.23050	yes	-0.43912	0.04268	1.36973	yes
ENSMUSG00000000568	Hnrnpd	-0.85650	0.04487	1.34801	yes	-0.43943	0.00573	2.24190	yes
ENSMUSG00000026701	Prdx6	-1.92042	0.00000	5.73236	yes	-0.44196	0.00571	2.24343	yes
ENSMUSG00000022255	Mtdh	-2.11054	0.00000	8.25811	yes	-0.44362	0.00561	2.25117	yes
ENSMUSG00000037742	Eef1a1	-1.40561	0.00668	2.17499	yes	-0.44550	0.01605	1.79440	yes
ENSMUSG00000030714	Ccdc101	-1.04635	0.01323	1.87847	yes	-0.44616	0.04853	1.31396	yes
ENSMUSG00000003528	Slc25a1	-2.53989	0.00000	8.06870	yes	-0.44686	0.01828	1.73792	yes
ENSMUSG00000052997	Uba2	-1.25337	0.01818	1.74034	yes	-0.44728	0.04222	1.37451	yes
ENSMUSG00000003438	Timm50	-1.47371	0.00059	3.23107	yes	-0.44856	0.02792	1.55414	yes
ENSMUSG00000020156	Mum1	-1.01220	0.00354	2.45128	yes	-0.45036	0.00563	2.24944	yes
ENSMUSG00000061479	Snrpa	-2.21868	0.00000	10.67625	yes	-0.45414	0.00278	2.55623	yes
ENSMUSG00000032279	Idh3a	-2.01216	0.00028	3.55016	yes	-0.45846	0.04700	1.32795	yes
ENSMUSG00000039262	Prrc2b	-1.44042	0.00223	2.65213	yes	-0.45971	0.03786	1.42179	yes
ENSMUSG00000015165	Hnrnpl	-1.00005	0.01574	1.80288	yes	-0.46052	0.00607	2.21663	yes
ENSMUSG00000061032	Rrp1	-1.90135	0.00000	7.19725	yes	-0.46081	0.00126	2.90119	yes
ENSMUSG00000078619	Smarcd2	-0.92394	0.01612	1.79258	yes	-0.46197	0.00339	2.46929	yes
ENSMUSG00000039130	Zc3hc1	-1.21261	0.00800	2.09669	yes	-0.46216	0.03654	1.43728	yes
ENSMUSG00000027752	Exosc8	-1.29096	0.00234	2.63128	yes	-0.46456	0.01358	1.86718	yes
ENSMUSG00000038685	Rtel1	-1.00224	0.00038	3.42109	yes	-0.46484	0.00138	2.85974	yes
ENSMUSG00000059070	Rpl18	-1.32370	0.01974	1.70462	yes	-0.46595	0.03288	1.48309	yes
ENSMUSG00000021595	Nsun2	-2.23555	0.00000	6.12224	yes	-0.46648	0.00585	2.23283	yes
ENSMUSG00000014355	Anapc1	-1.06204	0.02874	1.54151	yes	-0.46982	0.03100	1.50866	yes
ENSMUSG00000040945	Rcc2	-1.66126	0.00150	2.82259	yes	-0.47015	0.03466	1.46021	yes
ENSMUSG00000022962	Gart	-2.44928	0.00002	4.60741	yes	-0.47057	0.04268	1.36973	yes
ENSMUSG00000089832	Shkbp1	-1.88846	0.00002	4.71609	yes	-0.47125	0.03839	1.41577	yes
ENSMUSG00000015656	Hspa8	-2.11504	0.00000	5.44690	yes	-0.47323	0.00584	2.23379	yes

ENSMUSG00000027108	Ola1	-1.65468	0.00010	4.00241	yes	-0.47522	0.00536	2.27067	yes
ENSMUSG00000028423	Nfx1	-1.31115	0.00568	2.24577	yes	-0.47529	0.04720	1.32608	yes
ENSMUSG00000027466	Rbck1	-1.40337	0.00068	3.16943	yes	-0.47553	0.00870	2.06072	yes
ENSMUSG00000001855	Nup214	-1.16579	0.00597	2.22412	yes	-0.47573	0.01651	1.78232	yes
ENSMUSG00000007029	Vars	-1.27569	0.00003	4.58858	yes	-0.47603	0.00007	4.18523	yes
ENSMUSG00000071644	Eef1g	-1.81700	0.00002	4.68956	yes	-0.47613	0.00172	2.76449	yes
ENSMUSG00000061878	Sphk1	-1.25241	0.00076	3.11637	yes	-0.48041	0.00224	2.65048	yes
ENSMUSG00000007739	Cct4	-1.69094	0.00000	5.35136	yes	-0.48049	0.00066	3.17900	yes
ENSMUSG00000031657	Heatr3	-2.77424	0.00000	7.18345	yes	-0.48175	0.02494	1.60309	yes
ENSMUSG00000031388	Naa10	-1.68521	0.00044	3.36034	yes	-0.48205	0.03078	1.51171	yes
ENSMUSG00000031403	Dkc1	-1.88566	0.00000	5.84324	yes	-0.48368	0.00486	2.31317	yes
ENSMUSG00000024561	Mbd1	-1.06994	0.02512	1.59992	yes	-0.48401	0.00661	2.17975	yes
ENSMUSG00000030688	Stard10	-1.35372	0.00217	2.66288	yes	-0.48691	0.01336	1.87408	yes
ENSMUSG00000015714	Lass2	-1.39962	0.00418	2.37893	yes	-0.48752	0.01609	1.79339	yes
ENSMUSG00000053907	Mat2a	-1.81387	0.00246	2.60959	yes	-0.48834	0.04501	1.34670	yes
ENSMUSG00000017478	Zc3h18	-1.11381	0.00140	2.85346	yes	-0.49239	0.00462	2.33497	yes
ENSMUSG00000021645	Smn1	-2.00919	0.00000	5.56832	yes	-0.49267	0.04656	1.33198	yes
ENSMUSG00000024213	Nudt3	-2.12107	0.00000	5.68518	yes	-0.49283	0.03062	1.51393	yes
ENSMUSG00000038241	Cep250	-1.00195	0.04924	1.30768	yes	-0.49373	0.02103	1.67712	yes
ENSMUSG00000039844	Rapgef1	-1.64642	0.00031	3.50592	yes	-0.49413	0.00494	2.30601	yes
ENSMUSG00000037851	Iars	-1.63353	0.00015	3.82267	yes	-0.49476	0.01043	1.98176	yes
ENSMUSG00000020739	Nup85	-1.02700	0.00370	2.43194	yes	-0.49508	0.00018	3.73355	yes
ENSMUSG00000021144	Mta1	-1.92064	0.00003	4.58858	yes	-0.49650	0.00146	2.83645	yes
ENSMUSG00000024493	Lars	-1.45892	0.02282	1.64161	yes	-0.49690	0.02361	1.62682	yes
ENSMUSG00000038812	Trmt112	-1.86054	0.00021	3.67013	yes	-0.49831	0.03320	1.47884	yes
ENSMUSG00000047824	Pygo2	-1.45975	0.00488	2.31173	yes	-0.49866	0.02886	1.53971	yes
ENSMUSG00000029388	Eif2b1	-2.30109	0.00001	5.14842	yes	-0.50190	0.04037	1.39393	yes
ENSMUSG00000052446	Zfp961	-0.93992	0.01102	1.95800	yes	-0.50440	0.02264	1.64517	yes
ENSMUSG00000006728	Cdk4	-2.35740	0.00000	10.94996	yes	-0.50478	0.00011	3.94932	yes
ENSMUSG00000038762	Abcf1	-1.33302	0.01112	1.95397	yes	-0.50513	0.01963	1.70707	yes
ENSMUSG00000046598	Bdh1	-2.25916	0.00001	4.98821	yes	-0.50721	0.04093	1.38797	yes
ENSMUSG00000023110	Prmt5	-2.60674	0.00000	5.72362	yes	-0.50748	0.04048	1.39272	yes
ENSMUSG00000041264	Uspl1	-1.28631	0.00017	3.75715	yes	-0.50756	0.00032	3.49644	yes
ENSMUSG00000022471	Xrcc6	-1.53757	0.00149	2.82691	yes	-0.50848	0.02480	1.60548	yes
ENSMUSG00000061904	Slc25a3	-1.77781	0.00003	4.51853	yes	-0.51090	0.00164	2.78570	yes
ENSMUSG00000027668	Mfn1	-1.50416	0.00006	4.20912	yes	-0.51138	0.01605	1.79452	yes
ENSMUSG00000028693	Nasp	-1.61310	0.00228	2.64131	yes	-0.51326	0.00463	2.33423	yes
ENSMUSG00000027804	Ppid	-1.95874	0.00125	2.90248	yes	-0.51348	0.04528	1.34414	yes
ENSMUSG00000020444	Guk1	-1.44043	0.00572	2.24238	yes	-0.51391	0.01882	1.72533	yes
ENSMUSG00000022407	Adsl	-2.66105	0.00000	8.70815	yes	-0.51528	0.00269	2.56995	yes
ENSMUSG00000004897	Hdgf	-1.19813	0.01444	1.84045	yes	-0.51535	0.00525	2.28010	yes
ENSMUSG00000000168	Dlat	-1.99423	0.00033	3.47642	yes	-0.51690	0.02551	1.59328	yes
ENSMUSG00000027810	Eif2a	-1.61060	0.00015	3.82253	yes	-0.52060	0.00230	2.63821	yes
ENSMUSG00000040415	Dtx3	-1.21418	0.01423	1.84675	yes	-0.52069	0.03885	1.41060	yes
ENSMUSG00000030689	Ino80e	-2.15225	0.00000	5.98598	yes	-0.52280	0.01224	1.91237	yes
ENSMUSG00000029247	Paics	-1.23347	0.01586	1.79971	yes	-0.52313	0.00596	2.22476	yes
ENSMUSG00000025374	Obfc2b	-1.46836	0.00422	2.37476	yes	-0.52318	0.02610	1.58343	yes
ENSMUSG00000022822	Abcc5	-1.57742	0.00002	4.78988	yes	-0.52619	0.01938	1.71265	yes
ENSMUSG00000024414	Mrpl27	-1.10917	0.04488	1.34791	yes	-0.52628	0.03602	1.44350	yes
ENSMUSG00000001056	Nhp2	-2.24283	0.00005	4.29739	yes	-0.52678	0.01963	1.70707	yes
ENSMUSG00000005354	Txn2	-1.45017	0.00408	2.38898	yes	-0.52829	0.00870	2.06072	yes
ENSMUSG00000028898	Trnau1ap	-1.97511	0.00000	7.77523	yes	-0.52931	0.01131	1.94648	yes
ENSMUSG00000025995	Wdr75	-2.38748	0.00000	6.65191	yes	-0.53071	0.00832	2.07994	yes
ENSMUSG00000021270	Hsp90aa1	-1.69888	0.00056	3.25472	yes	-0.53117	0.00450	2.34645	yes
ENSMUSG00000032547	Ryk	-1.71401	0.00282	2.54963	yes	-0.53258	0.02319	1.63477	yes
ENSMUSG00000068921	Dap3	-1.24681	0.00004	4.44060	yes	-0.53297	0.00001	4.90315	yes
ENSMUSG00000006005	Tpr	-1.00426	0.02080	1.68202	yes	-0.53376	0.00285	2.54588	yes
ENSMUSG00000037936	Scarb1	-1.01759	0.01734	1.76101	yes	-0.53379	0.00358	2.44610	yes
ENSMUSG00000037275	Gemin5	-2.59222	0.00000	7.51604	yes	-0.53526	0.00486	2.31317	yes
ENSMUSG00000038976	Ppp1r9b	-1.03560	0.04054	1.39211	yes	-0.53596	0.00545	2.26349	yes
ENSMUSG00000049550	Clip1	-1.38487	0.00001	4.87208	yes	-0.53599	0.00061	3.21653	yes
ENSMUSG00000027067	Ssrp1	-1.12091	0.03794	1.42088	yes	-0.53626	0.00252	2.59783	yes
ENSMUSG00000015176	Nolc1	-2.94888	0.00000	5.42710	yes	-0.53760	0.04062	1.39127	yes
ENSMUSG00000060288	Ppih	-1.11069	0.01586	1.79971	yes	-0.53781	0.01051	1.97841	yes
ENSMUSG00000038845	Phb	-1.64476	0.00407	2.38997	yes	-0.53830	0.01885	1.72461	yes
ENSMUSG00000018068	Ints2	-1.75757	0.00220	2.65669	yes	-0.53900	0.04283	1.36821	yes
ENSMUSG00000024231	Cul2	-1.12933	0.02974	1.52670	yes	-0.53919	0.02633	1.57958	yes
ENSMUSG00000002845	Tmem39a	-1.01266	0.00777	2.10977	yes	-0.53925	0.01010	1.99566	yes
ENSMUSG00000020413	Hus1	-2.13131	0.00002	4.78598	yes	-0.53935	0.03206	1.49407	yes
ENSMUSG00000030826	Bcat2	-2.94186	0.00000	11.93436	yes	-0.53983	0.00080	3.09800	yes
ENSMUSG00000067367	Lyar	-2.97485	0.00000	11.94800	yes	-0.54066	0.00036	3.43786	yes
ENSMUSG00000026036	Nif3l1	-1.96356	0.00016	3.79701	yes	-0.54372	0.01785	1.74848	yes
ENSMUSG00000034211	Mrps17	-1.16543	0.01486	1.82808	yes	-0.54423	0.01295	1.88763	yes
ENSMUSG00000011658	Fuz	-1.05389	0.03900	1.40896	yes	-0.55031	0.03378	1.47129	yes
ENSMUSG00000019777	Hdac2	-1.45205	0.00552	2.25786	yes	-0.55169	0.00906	2.04308	yes
ENSMUSG00000027367	Stard7	-1.44244	0.00233	2.63187	yes	-0.55213	0.00712	2.14777	yes
ENSMUSG00000025962	Fastkd2	-2.50105	0.00000	7.07526	yes	-0.55313	0.02401	1.61956	yes
ENSMUSG00000018446	C1qbp	-3.05341	0.00000	5.79728	yes	-0.55553	0.04314	1.36511	yes
ENSMUSG00000030609	Aen	-2.39633	0.00058	3.23753	yes	-0.55647	0.03150	1.50171	yes
ENSMUSG00000026694	Mettl13	-3.29241	0.00000	10.32658	yes	-0.55801	0.02319	1.63477	yes
ENSMUSG00000021131	Erh	-1.74611	0.00748	2.12603	yes	-0.55978	0.04851	1.31421	yes
ENSMUSG00000024130	Abca3	-1.45785	0.00008	4.08156	yes	-0.55996	0.00020	3.69390	yes
ENSMUSG00000018654	Ikzf1	-1.51591	0.00056	3.25170	yes	-0.56037	0.00482	2.31719	yes
ENSMUSG00000057541	Pus7	-3.31357	0.00000	14.00000	yes	-0.56142	0.00376	2.42479	yes
ENSMUSG00000029208	Guf1	-1.94593	0.00002	4.64989	yes	-0.56157	0.00439	2.35800	yes
ENSMUSG00000042303	Sgsm3	-2.27626	0.00000	9.00196	yes	-0.56296	0.00268	2.57185	yes
ENSMUSG00000027405	Nop56	-2.08125	0.00000	14.00000	yes	-0.56367	0.00000	7.22452	yes
ENSMUSG00000030779	Rbbp6	-1.50439	0.00044	3.35287	yes	-0.56424	0.00223	2.65178	yes
ENSMUSG00000022160	Mettl3	-1.01570	0.00046	3.33333	yes	-0.56590	0.00013	3.87283	yes
ENSMUSG00000020471	Pold2	-1.48308	0.00498	2.30251	yes	-0.56647	0.01577	1.80223	yes
ENSMUSG00000029246	Ppat	-2.37724	0.00002	4.63723	yes	-0.56873	0.01381	1.85970	yes
ENSMUSG00000029174	Tbc1d1	-1.93198	0.00001	5.20783	yes	-0.56955	0.02797	1.55336	yes
ENSMUSG00000020280	Pus10	-1.73830	0.00005	4.32390	yes	-0.57048	0.00556	2.25517	yes
ENSMUSG00000038425	Poli	-1.27947	0.00270	2.56860	yes	-0.57100	0.01963	1.70707	yes

ENSMUSG00000025223	Ldb1	-1.06878	0.01927	1.71513	yes	-0.57177	0.00059	3.22591	yes
ENSMUSG00000032078	Zfp259	-2.26436	0.00000	5.48272	yes	-0.57177	0.03300	1.48149	yes
ENSMUSG00000030881	Arfip2	-2.41403	0.00000	7.55466	yes	-0.57205	0.01077	1.96786	yes
ENSMUSG00000057388	Mrpl18	-1.18242	0.02906	1.53672	yes	-0.57441	0.01115	1.95258	yes
ENSMUSG00000002343	Armc6	-1.41397	0.00275	2.56138	yes	-0.57471	0.01594	1.79739	yes
ENSMUSG00000010554	Mettl16	-1.82263	0.00018	3.73954	yes	-0.57553	0.01132	1.94618	yes
ENSMUSG00000036932	Aifm1	-1.48954	0.02688	1.57053	yes	-0.57677	0.04093	1.38797	yes
ENSMUSG00000028292	Rars2	-1.97327	0.00047	3.33096	yes	-0.57735	0.03457	1.46128	yes
ENSMUSG00000027185	Nat10	-3.24981	0.00000	12.70623	yes	-0.57737	0.00594	2.22649	yes
ENSMUSG00000020744	Slc25a19	-1.51592	0.00133	2.87509	yes	-0.58123	0.01409	1.85111	yes
ENSMUSG00000004264	Phb2	-2.48491	0.00000	8.23127	yes	-0.58302	0.00030	3.51833	yes
ENSMUSG00000036285	Noa1	-2.99671	0.00000	9.04406	yes	-0.58486	0.00607	2.21662	yes
ENSMUSG00000054226	Tprkb	-1.52828	0.00185	2.73216	yes	-0.58631	0.02543	1.59473	yes
ENSMUSG00000057113	Npm1	-3.02224	0.00000	12.43928	yes	-0.58899	0.00017	3.76959	yes
ENSMUSG00000042719	Naa25	-2.18724	0.00000	6.41306	yes	-0.59013	0.00134	2.87415	yes
ENSMUSG00000028700	Pomgnt1	-2.09882	0.00007	4.13965	yes	-0.59686	0.04866	1.31284	yes
ENSMUSG00000022972	1110004E09Rik	-1.78033	0.00015	3.81359	yes	-0.59697	0.01414	1.84969	yes
ENSMUSG00000058809	Gm12141	-3.26958	0.00000	6.67855	yes	-0.59707	0.01882	1.72540	yes
ENSMUSG00000039826	Trub2	-1.29125	0.00858	2.06626	yes	-0.59814	0.01820	1.73988	yes
ENSMUSG00000062590	Armc9	-1.98531	0.00002	4.70898	yes	-0.59914	0.00460	2.33714	yes
ENSMUSG00000039356	Exosc2	-2.24664	0.00307	2.51227	yes	-0.60080	0.03430	1.46471	yes
ENSMUSG00000030844	Rgs10	-1.61258	0.00177	2.75219	yes	-0.60092	0.00509	2.29356	yes
ENSMUSG00000039046	Usp6nl	-1.18975	0.02741	1.56204	yes	-0.60208	0.01409	1.85121	yes
ENSMUSG00000030888	Rrp8	-2.13080	0.00007	4.12652	yes	-0.60267	0.02539	1.59541	yes
ENSMUSG00000025899	Alkbh8	-1.59136	0.00008	4.09205	yes	-0.60561	0.00063	3.20134	yes
ENSMUSG00000032113	Chek1	-1.04746	0.03527	1.45257	yes	-0.60594	0.00501	2.29995	yes
ENSMUSG00000009073	Nf2	-1.44605	0.00026	3.58671	yes	-0.60737	0.00289	2.53847	yes
ENSMUSG00000071041	Gm15210	-2.33450	0.00002	4.70776	yes	-0.60930	0.01135	1.94489	yes
ENSMUSG00000017774	Myo1c	-1.59708	0.00072	3.13980	yes	-0.61071	0.00047	3.32995	yes
ENSMUSG00000031959	Wdr59	-1.96016	0.00131	2.88306	yes	-0.61395	0.03602	1.44342	yes
ENSMUSG00000061474	Mrps36	-1.07677	0.04081	1.38925	yes	-0.61572	0.01414	1.84969	yes
ENSMUSG00000029389	Ddx55	-1.63968	0.00328	2.48381	yes	-0.61760	0.01428	1.84522	yes
ENSMUSG00000054280	C330019G07Rik	-1.38941	0.01758	1.75497	yes	-0.61861	0.02319	1.63477	yes
ENSMUSG00000017286	Glod4	-1.79153	0.00084	3.07678	yes	-0.61933	0.01963	1.70707	yes
ENSMUSG00000027002	Nckap1	-1.17920	0.03753	1.42564	yes	-0.61954	0.02376	1.62422	yes
ENSMUSG00000029145	Eif2b4	-1.09970	0.03115	1.50650	yes	-0.62010	0.00634	2.19802	yes
ENSMUSG00000013629	Cad	-3.17746	0.00000	9.94679	yes	-0.62018	0.00482	2.31736	yes
ENSMUSG00000044221	Grsf1	-1.55466	0.00006	4.23792	yes	-0.62361	0.00007	4.16218	yes
ENSMUSG00000060279	Ap2a1	-1.08460	0.00050	3.30007	yes	-0.62525	0.00000	7.18036	yes
ENSMUSG00000024436	Mrps18b	-3.03552	0.00000	6.96904	yes	-0.62757	0.01372	1.86262	yes
ENSMUSG00000021666	Gfm2	-1.18169	0.04109	1.38622	yes	-0.62832	0.01089	1.96291	yes
ENSMUSG00000028910	Mecr	-1.88263	0.00011	3.95906	yes	-0.62850	0.00429	2.36730	yes
ENSMUSG00000022474	Pmm1	-1.46071	0.00845	2.07317	yes	-0.63017	0.00285	2.54582	yes
ENSMUSG00000021048	Mthfd1	-3.08126	0.00000	5.94460	yes	-0.63094	0.00396	2.40222	yes
ENSMUSG00000006599	Gtf2h1	-1.77423	0.00022	3.65728	yes	-0.63193	0.00333	2.47801	yes
ENSMUSG00000028799	Zfp362	-2.42240	0.00003	4.48833	yes	-0.63212	0.04369	1.35965	yes
ENSMUSG00000029657	Hsph1	-2.65597	0.00000	14.00000	yes	-0.63438	0.00000	6.02729	yes
ENSMUSG00000040174	Alkbh3	-1.24767	0.00858	2.06626	yes	-0.63774	0.00934	2.02969	yes
ENSMUSG00000028741	Mrto4	-2.41085	0.00000	6.20456	yes	-0.63778	0.00201	2.69666	yes
ENSMUSG00000092203	1110038B12Rik	-2.42057	0.00000	7.47411	yes	-0.63816	0.00010	4.01878	yes
ENSMUSG00000022394	L3mbtl2	-1.54363	0.00015	3.81322	yes	-0.63839	0.00434	2.36251	yes
ENSMUSG00000033294	Noc4l	-2.28305	0.00000	5.42843	yes	-0.63955	0.00061	3.21421	yes
ENSMUSG00000006732	Mettl1	-3.14740	0.00000	6.42225	yes	-0.64185	0.01577	1.80223	yes
ENSMUSG00000020366	Mapk9	-2.08208	0.00001	5.09677	yes	-0.64358	0.00179	2.74705	yes
ENSMUSG00000053332	Gas5	-1.59177	0.00000	5.51518	yes	-0.64395	0.00000	8.28172	yes
ENSMUSG00000062175	Tgif2	-2.29696	0.00237	2.62482	yes	-0.64469	0.03299	1.48168	yes
ENSMUSG00000021694	Ercc8	-1.82124	0.00580	2.23673	yes	-0.64699	0.02315	1.63550	yes
ENSMUSG00000027198	Ext2	-2.37410	0.00056	3.25464	yes	-0.64747	0.03639	1.43899	yes
ENSMUSG00000034194	R3hcc1	-1.98972	0.00013	3.89391	yes	-0.64791	0.03983	1.39977	yes
ENSMUSG00000035311	Gnptab	-2.67862	0.00000	10.88959	yes	-0.64797	0.00008	4.12154	yes
ENSMUSG00000051169	Rpusd3	-1.45875	0.03446	1.46264	yes	-0.65070	0.04004	1.39746	yes
ENSMUSG00000000861	Bcl11a	-2.22722	0.00002	4.68341	yes	-0.65109	0.00240	2.61985	yes
ENSMUSG00000028796	Phc2	-1.51673	0.03990	1.39901	yes	-0.65195	0.03269	1.48555	yes
ENSMUSG00000085385	9430008C03Rik	-2.57792	0.00000	6.97872	yes	-0.65213	0.00797	2.09845	yes
ENSMUSG00000036281	Snapc4	-2.53851	0.00000	6.77179	yes	-0.65278	0.00893	2.04909	yes
ENSMUSG00000028010	Gar1	-3.29062	0.00000	7.41843	yes	-0.65299	0.02483	1.60503	yes
ENSMUSG00000031671	Setd6	-2.46298	0.00000	7.42393	yes	-0.65352	0.00886	2.05261	yes
ENSMUSG00000030188	Magohb	-1.75578	0.00030	3.51890	yes	-0.65694	0.04617	1.33561	yes
ENSMUSG00000020549	Elac2	-2.35653	0.00000	10.99156	yes	-0.65798	0.00001	5.04710	yes
ENSMUSG00000034175	Rhbdd3	-1.27260	0.00543	2.26534	yes	-0.65924	0.00204	2.68960	yes
ENSMUSG00000048696	Mex3d	-1.92386	0.00529	2.27663	yes	-0.66157	0.04701	1.32778	yes
ENSMUSG00000030400	Ercc2	-1.94071	0.00000	6.35841	yes	-0.66163	0.00062	3.20743	yes
ENSMUSG00000027999	Pla2g12a	-2.11425	0.00035	3.45254	yes	-0.66191	0.01564	1.80567	yes
ENSMUSG00000033728	Lrrc14	-1.81706	0.00008	4.07523	yes	-0.66247	0.00376	2.42479	yes
ENSMUSG00000027374	Mrps5	-1.68251	0.00312	2.50597	yes	-0.66478	0.00578	2.23807	yes
ENSMUSG00000023883	Phf10	-1.39485	0.00068	3.16632	yes	-0.66596	0.00004	4.40153	yes
ENSMUSG00000068874	Selenbp1	-2.21722	0.00185	2.73225	yes	-0.66635	0.04261	1.37054	yes
ENSMUSG00000020899	Pfas	-2.25769	0.00000	5.32194	yes	-0.67120	0.00285	2.54514	yes
ENSMUSG00000032892	Rangrf	-3.23099	0.00000	5.83190	yes	-0.67241	0.02827	1.54866	yes
ENSMUSG00000018995	Nars2	-1.20336	0.00845	2.07317	yes	-0.67282	0.00339	2.47036	yes
ENSMUSG00000025980	Hspd1	-3.26513	0.00000	6.32653	yes	-0.67313	0.00681	2.16703	yes
ENSMUSG00000038902	Pogz	-0.82994	0.04316	1.36490	yes	-0.67375	0.00143	2.84375	yes
ENSMUSG00000004100	Ppan	-2.30848	0.00027	3.57486	yes	-0.67419	0.00656	2.18303	yes
ENSMUSG00000015217	Hmgb3	-1.52197	0.00001	5.24253	yes	-0.67859	0.00000	7.30534	yes
ENSMUSG00000039804	Ncoa5	-1.59565	0.01132	1.94627	yes	-0.68005	0.03716	1.42993	yes
ENSMUSG00000033857	Engase	-2.49393	0.00000	9.56302	yes	-0.68388	0.00224	2.65048	yes
ENSMUSG00000024855	Pacs1	-2.26362	0.00006	4.24496	yes	-0.68744	0.00172	2.76449	yes
ENSMUSG00000022325	Pop1	-2.86804	0.00000	5.30786	yes	-0.68883	0.02145	1.66866	yes
ENSMUSG00000086290	Snhg12	-2.45612	0.00000	9.19663	yes	-0.69038	0.00052	3.28491	yes
ENSMUSG00000085241	Snhg3	-1.59542	0.00308	2.51105	yes	-0.69163	0.00906	2.04308	yes
ENSMUSG00000034032	Rpap1	-2.04329	0.00001	4.83660	yes	-0.69202	0.00006	4.23391	yes
ENSMUSG00000019810	Fuca2	-1.77405	0.00115	2.93820	yes	-0.69675	0.00518	2.28597	yes
ENSMUSG00000042632	Pla2g6	-1.40538	0.00101	2.99574	yes	-0.69994	0.00091	3.04159	yes
ENSMUSG00000058756	Thra	-1.92791	0.00000	6.52798	yes	-0.70355	0.00010	3.98172	yes

ENSMUSG00000028617	Lrrc42	-1.58646	0.00213	2.67240	yes	-0.71997	0.00884	2.05362	yes
ENSMUSG00000033762	Recql4	-1.71475	0.03862	1.41314	yes	-0.72172	0.01684	1.77358	yes
ENSMUSG00000025007	Aldh18a1	-2.77844	0.00000	10.76208	yes	-0.72202	0.00005	4.25991	yes
ENSMUSG00000026811	St6galnac6	-2.22455	0.00009	4.04313	yes	-0.72561	0.00420	2.37688	yes
ENSMUSG00000023942	Slc29a1	-1.09797	0.00057	3.24181	yes	-0.72644	0.00000	9.87141	yes
ENSMUSG00000027533	Fabp5	-1.91080	0.01462	1.83511	yes	-0.72937	0.00710	2.14862	yes
ENSMUSG00000048217	Nags	-2.59483	0.00097	3.01377	yes	-0.73592	0.02333	1.63206	yes
ENSMUSG00000049957	Ccdc137	-2.21672	0.00024	3.62341	yes	-0.73675	0.00587	2.23173	yes
ENSMUSG00000046982	Tshz1	-2.12357	0.00407	2.38992	yes	-0.74351	0.01634	1.78668	yes
ENSMUSG00000074578	1500012F01Rik	-1.66351	0.00053	3.27936	yes	-0.74421	0.00005	4.33985	yes
ENSMUSG00000021235	Coq6	-1.32551	0.00142	2.84717	yes	-0.74696	0.00137	2.86276	yes
ENSMUSG00000073433	Arhgdig	-1.76449	0.00013	3.87954	yes	-0.74701	0.00016	3.78455	yes
ENSMUSG00000039345	Mettl22	-1.98875	0.00167	2.77760	yes	-0.75472	0.01645	1.78387	yes
ENSMUSG00000062110	Scfd2	-2.18798	0.00023	3.63898	yes	-0.76734	0.00612	2.21326	yes
ENSMUSG00000026837	Col5a1	-1.88476	0.01574	1.80288	yes	-0.76994	0.03089	1.51012	yes
ENSMUSG00000025816	Sec61a2	-1.16369	0.00625	2.20399	yes	-0.77741	0.00094	3.02721	yes
ENSMUSG00000033257	Ttll4	-2.35984	0.00000	8.46908	yes	-0.78190	0.00011	3.94738	yes
ENSMUSG00000023571	Fam132a	-2.66302	0.00000	6.01668	yes	-0.78481	0.00158	2.80257	yes
ENSMUSG00000038838	Vars2	-2.42196	0.00000	9.49138	yes	-0.78861	0.00000	5.88965	yes
ENSMUSG00000056268	Dennd1b	-1.66745	0.01857	1.73115	yes	-0.78876	0.03396	1.46898	yes
ENSMUSG00000014873	Surf2	-2.65819	0.00000	14.00000	yes	-0.80775	0.00000	6.84924	yes
ENSMUSG00000041329	Atp1b2	-2.46561	0.00000	5.86645	yes	-0.80831	0.00003	4.51853	yes
ENSMUSG00000041966	Dcaf17	-2.19772	0.00000	5.98049	yes	-0.80876	0.00051	3.29156	yes
ENSMUSG00000030264	Thumpd3	-1.51070	0.00264	2.57790	yes	-0.80891	0.00013	3.88223	yes
ENSMUSG00000027381	Bcl2l11	-1.61877	0.01171	1.93139	yes	-0.82189	0.02952	1.52993	yes
ENSMUSG00000033065	Pfkm	-2.02210	0.02232	1.65136	yes	-0.82760	0.01283	1.89168	yes
ENSMUSG00000026791	Slc2a8	-1.66024	0.02064	1.68527	yes	-0.83012	0.02231	1.65141	yes
ENSMUSG00000025665	Rps6ka6	-2.98134	0.00000	8.29615	yes	-0.83222	0.00215	2.66840	yes
ENSMUSG00000017386	Traf4	-1.46268	0.04631	1.33431	yes	-0.84155	0.00224	2.65048	yes
ENSMUSG00000055322	Tns1	-1.69257	0.01506	1.82215	yes	-0.84968	0.00330	2.48149	yes
ENSMUSG00000006494	Pdk1	-2.23927	0.00000	6.93516	yes	-0.85126	0.00000	5.69250	yes
ENSMUSG00000046959	Slc26a1	-2.33680	0.00348	2.45789	yes	-0.86740	0.00563	2.24944	yes
ENSMUSG00000048351	2010305A19Rik	-2.39730	0.00001	4.87208	yes	-0.86943	0.00282	2.54942	yes
ENSMUSG00000006567	Atp7b	-2.59169	0.00748	2.12585	yes	-0.87063	0.02785	1.55521	yes
ENSMUSG00000030031	Kbtbd8	-1.69377	0.00749	2.12560	yes	-0.87606	0.00955	2.01992	yes
ENSMUSG00000031137	Fgf13	-2.23467	0.01911	1.71872	yes	-0.88498	0.02560	1.59177	yes
ENSMUSG00000017765	Slc12a4	-1.53379	0.02380	1.62334	yes	-0.89637	0.00228	2.64253	yes
ENSMUSG00000075028	Prdm11	-3.87367	0.00000	8.13467	yes	-0.90197	0.00853	2.06920	yes
ENSMUSG00000022386	Trmu	-1.54278	0.00017	3.76668	yes	-0.90473	0.00012	3.90396	yes
ENSMUSG00000055491	Pprc1	-2.61946	0.00000	14.00000	yes	-0.90589	0.00000	7.16251	yes
ENSMUSG00000086968	4933431E20Rik	-3.18219	0.00000	7.11515	yes	-0.90810	0.00118	2.92866	yes
ENSMUSG00000022747	St3gal6	-1.49085	0.00017	3.75964	yes	-0.91163	0.00000	6.13357	yes
ENSMUSG00000034796	Cpne7	-3.34731	0.00000	5.32618	yes	-0.92442	0.01607	1.79388	yes
ENSMUSG00000038930	Rccd1	-2.09157	0.00001	4.86652	yes	-0.92669	0.00077	3.11387	yes
ENSMUSG00000029101	Rgs12	-1.45104	0.00009	4.05324	yes	-0.93130	0.00000	6.63029	yes
ENSMUSG00000089989	Flt3l	-3.72081	0.00000	14.00000	yes	-0.93730	0.00003	4.53070	yes
ENSMUSG00000020486	Sept4	-3.83485	0.00000	12.59006	yes	-0.93786	0.00038	3.41666	yes
ENSMUSG00000042155	Klhl23	-2.58306	0.00005	4.28865	yes	-0.93927	0.00308	2.51204	yes
ENSMUSG00000022843	Clcn2	-0.99946	0.04086	1.38872	yes	-0.95830	0.00000	8.12770	yes
ENSMUSG00000025608	Podxl	-4.18561	0.00000	7.24055	yes	-1.03557	0.00022	3.65715	yes
ENSMUSG00000029122	Evc	-3.13883	0.00009	4.03300	yes	-1.07341	0.00935	2.02920	yes
ENSMUSG00000040726	Hesx1	-2.78194	0.00923	2.03503	yes	-1.09683	0.03533	1.45186	yes
ENSMUSG00000015659	Serac1	-1.85918	0.01496	1.82494	yes	-1.09957	0.02874	1.54149	yes
ENSMUSG00000021234	Fam161b	-1.98117	0.00140	2.85470	yes	-1.10039	0.00443	2.35388	yes
ENSMUSG00000053091	Lins	-2.10380	0.00001	5.15367	yes	-1.11272	0.00127	2.89594	yes
ENSMUSG00000025956	Mettl21a	-2.10240	0.00264	2.57899	yes	-1.12723	0.00697	2.15658	yes
ENSMUSG00000041734	Kirrel	-3.10140	0.01080	1.96651	yes	-1.13735	0.01205	1.91897	yes
ENSMUSG00000044005	Gls2	-3.36787	0.01384	1.85892	yes	-1.14109	0.00117	2.93098	yes
ENSMUSG00000053746	Ptrh1	-2.59626	0.01797	1.74534	yes	-1.14255	0.04222	1.37451	yes
ENSMUSG00000047990	C2cd4a	-4.79984	0.00001	4.95921	yes	-1.22024	0.00986	2.00601	yes
ENSMUSG00000051890	Klhdc1	-2.10667	0.03303	1.48112	yes	-1.30133	0.04442	1.35246	yes
ENSMUSG00000031075	Ano1	-2.48121	0.00001	5.25107	yes	-1.35202	0.00000	10.00571	yes
ENSMUSG00000074923	Pak6	-2.42200	0.00805	2.09438	yes	-1.42840	0.00301	2.52130	yes